NEW MEXICO BUREAU OF GEOLOGY AND MINERAL RESOURCES
Bulletin 165 2023

Quaternary and Archaeological Geology of the Mescalero Plain, Southeastern New Mexico

Stephen A. Hall
Ronald J. Goble

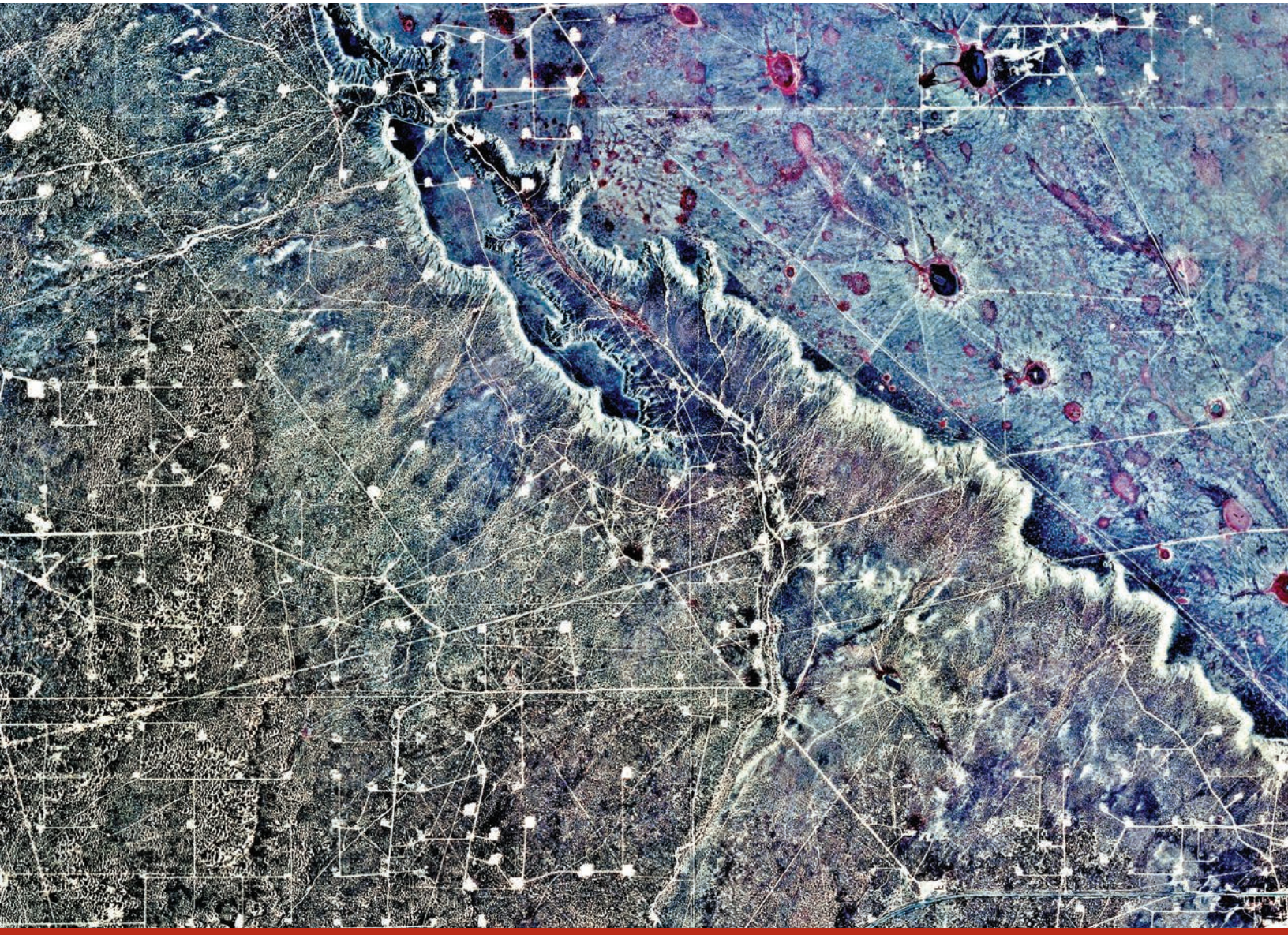

GEOLOGY

Quaternary and Archaeological Geology of the Mescalero Plain, Southeastern New Mexico

Stephen A. Hall
Ronald J. Goble

Bulletin 165
February 2023

New Mexico Bureau of Geology and Mineral Resources
A Research Division of New Mexico Institute of Mining and Technology

Bulletin 165—Quaternary and Archaeological Geology of the Mescalero Plain, Southeastern New Mexico

Stephen A. Hall and Ronald J. Goble

New Mexico Bureau of Geology and Mineral Resources
A research division of New Mexico Institute of Mining and Technology

Science Editor: Shari Kelley

Design: Lauri Logan

Layout: Marianne E. Lara Canto

Publications Program Manager: Barbara J Horowitz

Cover Photograph:
Color infrared aerial photograph of northeast Eddy and west-central Lea counties. The Mescalero Plain west of the Caprock Escarpment has mesquite coppice dunes and patches of thin sand without dunes. Farther west, the eolian sand thickens and parabolic dunes are common in this view. US Hwy. 82 and Maljamar occur in the lower right corner. USGS National High Altitude Photography (NHAP) 2, 493-200, July 30, 1986.

Suggested Citation:
Hall, S.A., and Goble, R.J., 2023, Quaternary and archaeological geology of the Mescalero Plain, southeastern New Mexico: New Mexico Bureau of Geology and Mineral Resources Bulletin 165, 216 p.
https://doi.org/10.58799/B-165

CONTENTS

Figures

Tables

EXECUTIVE SUMMARY

The Mescalero Plain of southeastern New Mexico is an undulating landscape of low relief developed on eroded Permian and Triassic red beds west of the Caprock escarpment of the Ogallala Formation and east of the Pecos River. The Mescalero Sands encompass a broad area of sheet sands and dunes extending 20,400 sq. km (7880 sq. mi.) across the plain and into adjacent Texas. Numerous investigations during the past nineteen years have addressed all aspects of the surficial geology of the Mescalero Plain in southeastern New Mexico, especially the Mescalero Sands and the occurrence and preservation of archaeological sites:

1. Stratigraphy, sedimentology, and geochronology
2. Paleosol development
3. Geology and past climate
4. Prehistoric archaeology

Stratigraphy, Sedimentology, and Geochronology

The Mescalero Sands are one of three extensive sand sheets and associated dunes in the northern Chihuahuan Desert. The other two are the Bolson sand sheet in the southern Tularosa Basin and the Hueco Bolson east of El Paso, and the Strauss sand sheet, which lies southwest of Las Cruces and west of El Paso in south-central New Mexico and northern Chihuahua, Mexico.

Sheet Sand and Dunes

The Mescalero Sands are eolian complexes that accumulated during six separate episodes of eolian sand deposition beginning at 90 ka. Two sheet sands accumulated during the late Pleistocene and three sheet sands formed during the Holocene. The sixth and last episode of eolian activity began 300 years ago, forming the numerous dunes that today are prominent features of the sand sheet. Coppice dunes formed where mesquite shrubs are present and parabolic and transverse dunes are found where sheet sand is thick. A high-resolution chronology of the eolian sand and related deposits is based on 177 optically stimulated luminescence (OSL) and 54 AMS radiocarbon dates (Table A).

Table A. Summary of episodes of eolian activity and stratigraphy, Mescalero sand sheet, southeastern New Mexico

Episodes	Stratigraphy	OSL Age
VI	Cover sand	A.D. 1784 to present
	Coppice dunes	A.D. 1745 to present
	Parabolic dunes	A.D. 1734 to present
(caps IV & V)	Eddy paleosol	2 ka to 0.3 ka (A.D. 1 to 1700)
V	Late Holocene eolian sand	6 ka to 2 ka
IV	Holocene eolian sand	12 ka to 2 ka
III	Upper eolian sand	18 ka to 5 ka
II	Middle eolian sand	33 ka to 20 ka
I	Lower eolian sand	90 ka to 50 ka
Underlies sands	Mescalero paleosol	135 ka to 100 ka

Sedimentology

The Mescalero Sands are dominated by fine-grained sand. The oldest sand, the Lower unit, is the finest textured, probably reflecting multiple distant sources across the plain. The parabolic dunes are the coarsest textured, forming locally with the finer sand being carried away. Many sequences have uniform texture, bottom to top. Some fine upwards, others coarsen upwards, perhaps reflecting changes at the sand source.

Multiple OSL dates from stratigraphic sections have provided sediment accumulation rates for eolian sand units. The Lower, Middle, Upper, Holocene, and Late Holocene sheet sands have average accumulation rates of 0.063, 0.053, 0.086, 0.107, and 0.228 mm per year, respectively. In sharp contrast, parabolic and coppice dunes have order-of-magnitude greater sedimentation rates of 6.85 and 18.3 mm per year, respectively. The sedimentation rates of the Mescalero sand sheet are similar to the rates that we found at the Bolson and Strauss sand sheets, although in comparison, the accumulation of the Late Holocene sheet sand is atypically high. The increased rate of sediment accumulation into the Holocene may be related to greater amounts of sand availability at the sources. OSL dating of the cumulic Eddy paleosol (post-Holocene sheet sands) indicate that it accumulated at an average rate of 0.41 mm per year.

Sources of Eolian Sand

All of the eolian sand on the plain is derived from stream beds that carry sand across the plain from the eroding escarpment of the Ogallala Formation. A few, but not all, large playas supply sand to the east (downwind) side of the basins, where it accumulates locally as thin eolian deposits and, in some cases, lunette dunes. Erosion of older sand units and redeposition of sand to form younger units, a process reported elsewhere, did not occur in the Mescalero Sands. An exception is the episode of erosion that began 300 years ago and resulted in deflation of Holocene sands and the formation of local parabolic and coppice dunes and cover sand deposits.

Chemical Signatures

A secondary feature of OSL dating is the measurement of radioisotopes that provides a chemical signature of the dated sand; the measured isotopes are potassium oxide (K_2O), uranium (U), and thorium (Th). Isotope signatures are an index to sand sources. In our study, dissimilar signatures from the Mescalero Sands and Pecos River alluvium indicate that the Pecos River was not the source of the eolian sands.

A widely occurring shift in radioisotope signatures during the last glacial maximum (26.5 ka to 20–19 ka) was a consequence of increased fluvial activity and the rejuvenation of stream beds across the plain at that time. Fresh sand with a different chemistry was incorporated into stream beds. The fluvial sand was the source for downwind eolian deposits, and the change in chemistry shows up in eolian stratigraphic sequences.

Paleosol Development

In the Mescalero Plain, soil development is dependent upon climate and time, whether wet or dry on a millennial scale. The long-dry climate of the Sangamon Interglaciation produced the calcic Mescalero paleosol, OSL dated 135 ka to 100 ka; this paleosol underlies the Mescalero Sands across the region. Subsequently, the long-wet climate of the middle Wisconsin resulted in the development of the non-calcic argillic Berino paleosol that formed at the top of the Lower eolian sand unit during a period 32,000 to 17,000 years ago, depending on the chronology of the overlying sand. Much later, the cumulic Eddy A horizon topsoil formed on Holocene sand and alluvium across the plain from 2.0 to 0.3 ka. The younger cumulic Loco Hills paleosol dated 500 to 200 years ago formed in eolian sand and alluvium in the northern area of Eddy County and is often found beneath coppice dunes. The equivalent of the Loco Hills paleosol is also found at the Bolson and Strauss sand sheets in New Mexico.

Geology and Past Climate

Eolian geology on the Mescalero Plain is indirectly related to past climatic conditions, which may have affected sand sources. The two Pleistocene sheet sands, the Lower and Middle units, formed under wetter conditions than found today, contrary to a conventional view that eolian deposits are to be equated with aridity. The Middle unit accumulated during the last glacial maximum; its formation may be related to a source of abundant sand (active stream beds) and strong westerly winds (southward position of the jet stream) across the plain.

Three different packages of eolian sand were deposited in the Holocene. Deposition of the Upper sand (episode III) ended at 5 ka, and the Late Holocene sand (episode V) began accumulating ca. 5–6 ka. Both events occurred in the arid middle Holocene and may have been in response to changes in the supply of sand, the supply ending for the Upper sand and beginning for the Late Holocene sand. The Holocene sand (episode IV) began to form in the latest Pleistocene and continued to accumulate through the arid middle Holocene, until the shift to the cumulic Eddy soil.

At 2,000 years ago, a change in the region resulted in the shift from sheet sand accumulation to the formation of the cumulic Eddy paleosol A horizon (topsoil) during the following 1,700 years, up until 300 years ago when deflation became dominant. The Eddy formed on late Holocene eolian sand and alluvium with grassland-shrub and shrub-grassland vegetation during the late Holocene wet period (the wettest time since the late Pleistocene). The cause of the deflation across the plain is uncertain. Deflation began about A.D. 1700 at the peak of the Little Ice Age and continued through to the end of the short-term cool wet period into the twentieth century.

Preservation of Prehistoric Sites

Prehistoric people have inhabited the Mescalero Plain for at least the past 11,000 years, from Paleoindian to Historic times, with a total of 6,182 recorded sites. Radiocarbon dated sites show a peak in prehistoric occupation of the plain at A.D. 775 (Fig. A). A big increase in population is related to the late Holocene wet climate with abundant surface water and plant and animal resources. During the Medieval Warm Period (A.D. 900 to 1300), the plain was largely by-passed for dwindling habitation in favor of the nearby Pecos River and higher elevations of the mountain slopes to the west. After the warm period, the population declined further on the plain, the river corridor, and mountain slope alike.

Most of the sites in the region (76%) occur in the topsoil of the Eddy paleosol (dated 2.0 ka to 0.3 ka). The slow sedimentation rate of the paleosol (0.41 mm/yr) leads to poor preservation of prehistoric sites along with high susceptibility to disturbance, mixing of artifacts, and erosion. Most shallow sites in the Mescalero Sands have been eroded and deflated during the recent period of widespread erosion that began only 300 years ago and is ongoing today.

Even though sedimentation rates are slow and it takes decades for sites to become buried, older sites have a potential to be entirely buried at depth in eolian sand with no indication at the surface that they are there. The potential presence of sites buried in the subsurface is related to the age of the surficial deposit. The deposits must be of the right age to incorporate archaeology, which in our case, is latest Pleistocene or Holocene or episodes III, IV, V, and the Eddy paleosol. Although the eroded landscape is highly variable, comparatively deep sand of the right age to contain archaeology is in most cases mantled by the Eddy paleosol, shinnery oak vegetation, or parabolic dunes. Elsewhere, coppice dunes are found on thin sand deposits that may have some buried-site potential; in most cases erosion between dunes will have exposed any archaeology that was buried in the shallow sand. In various situations, it appears that some prehistoric sites may have been eroded prior to the formation of coppice dunes.

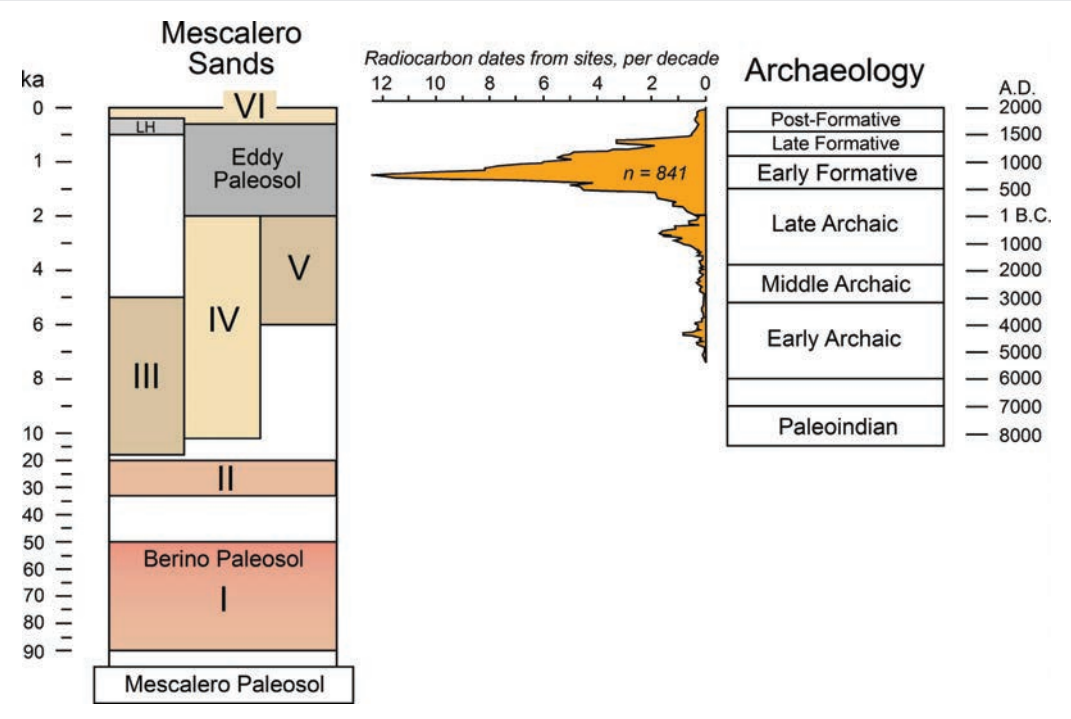

Figure A. Summary of Quaternary geology and archaeology of the Mescalero Sands, New Mexico; numbers are episodes of eolian activity (see Table A); LH = Loco Hills paleosol; scale changes at 2 and 10 ka.

In Conclusion and Going Forward

Our field approach to the study of the Quaternary and archaeological geology of the Mescalero Plain has been (i) to trench the deposits down to the base of the sheet sands, generally marked by caliche of the Mescalero paleosol, (ii) to define the stratigraphic units that make up the deposits, (iii) to close-interval sample units for sedimentology, and (iv) to sample horizons from each unit for OSL dating; from our investigations of surficial geology, we have found that the single most important, essential attribute of a deposit is its geochronology, once the stratigraphy has been determined. This successful field and laboratory method, fundamental to geological science, was applied at numerous places throughout the plain and has revealed patterns of deposition, erosion, and soil development that in turn relate to regional geologic and paleoclimatic history as well as to the occurrence and preservation of prehistoric sites. We are confident that future geologic and archaeologic investigations will benefit from the method of study that we have found to be successful in our research: the integration of stratigraphy, sedimentology, and geochronology.

Figure B. Stephen Hall (left) and Ronald Goble (right) at the type section of the Berino paleosol, Loc. 1, Eddy County, New Mexico; photograph June 12, 2016 by Edith Goble.

INTRODUCTION

The investigations reported herein had their beginning in the year 2000 with a one-year grant from the State of New Mexico Historic Preservation Division (HPD) and the Bureau of Land Management (BLM) to study the geology of the Mescalero Sands as related to the presence and condition of archaeological sites. The project was overseen by Glenna Dean, state archaeologist of New Mexico, and Stephen Fosberg, BLM archaeologist. The fieldwork was initiated in December 2000, focusing on the Loco Hills area of northern Eddy County. At that time, much of the Permian Basin oil field activity was in that area, and the BLM and HPD were looking for help with the numerous prehistoric sites that were being impacted. After a few days in the field, it became clear that the eolian sands must be dated if they are to be related to archaeology. Professor Ronald Goble of the Department of Geosciences, University of Nebraska, Lincoln, was contacted and he agreed to provide OSL dates of the eolian sands. Since that initial time, 177 OSL dates have been obtained from the Mescalero Sands, resulting in one of the better-dated sand sheets.

A requirement of the grant was to write a report on the findings suitable for use by the archaeology community. To be included in the report were (1) field tests for identifying the archaeology-related sand units and paleosols and (2) a comparison of the geology of the Mescalero Sands with the southern Tularosa Basin at Fort Bliss. The 67-page report was titled *"Field Guide to the Geoarchaeology of the Mescalero Sands, southeastern New Mexico,"* printed on October 30, 2002. For many years the report was available on the BLM Carlsbad Field Office website.

In addition to the report, it was stipulated that a field conference be conducted in southeastern New Mexico to teach the findings on archaeology-related geology to professional archaeologists who work in the area. A two-day conference was held November 2–3, 2002 at the Carlsbad Field Office, a half-day of lectures and a day and a half field trip. A 23-page handout was prepared for the participants, *"Guidebook, First Geoarchaeology Field Course: Mescalero Sands, southeastern New Mexico;"* it was a summary of the Field Guide with nine stops in the Loco Hills area.

Another two-day workshop was conducted April 19–20, 2013, out of the BLM Carlsbad Field Office; the 32-page guidebook, *"Second Workshop: Archaeological Geology of the Permian Basin, southeastern New Mexico,"* was provided along with a bibliography on a CD. The geology and archaeology of the Maroon Cliffs was a primary stop, and Doug Boggess helped with the trip and guidebook; the second workshop focused on localities in southern Eddy County.

Each year, continuing oil and gas development in the Permian Basin promoted new archaeological projects in southeastern New Mexico along with new opportunities to expand our geologic information on the Mescalero Sands. With HPD and BLM blessing, archaeologists were urged to budget for OSL and radiocarbon dating and sediment analysis. At one point, the BLM stipulated that trenches should be dug off-site, in addition to on-site, in order to facilitate geologic studies, with the idea that the site occupation itself might have disturbed the geology.

One of the larger projects with some impact on archaeological geology in southeastern New Mexico was *Adaptive Management and Planning Models for Cultural Resources in Oil and Gas Fields in New Mexico and Wyoming*, funded for three years, 2003–2005, by the Department of Energy through Gnomon, Inc., Carson City, Nevada, and referred to as PUMP III. One focus of the project was the Loco Hills area of northern Eddy County for which a detailed map of the surficial geology was produced across eight 7.5 minute quadrangles; areas with thick Holocene sands were mapped as having a strong buried-site potential.

The 2005 PUMP III project stimulated thought about producing a map that could accurately pin point areas where buried-site potential was strong versus areas where buried-site potential was weak or non-existent. Such a map would be valuable to cultural resource management, showing areas where sites might be buried and, therefore, needed special attention in land use decisions.

Two further attempts to produce a practical, working archaeological geologic map failed. A project in 2006 utilized the unpublished surficial geologic map of southeastern New Mexico on file with the New Mexico Bureau of Geology and Mineral Resources. Sixty-six map units were reduced to five that had likely archaeology-related ages. In retrospect, none of the 66 map units had actually been dated, and the attempt to relate them to the archeology record was not possible. In 2013, another attempt to produce a buried-site potential map utilized pre-existing county soil maps. It too failed; as it turned out, none of the soils had been dated. At present, an archeological geologic map of southeastern New Mexico, while desirable, has not been forth-coming.

Regardless of the absence of an archeological geologic map of the region, we found that buried-site potential can be estimated in the field. The presence of buried sites is related to the presence of comparatively thick sequences of Holocene eolian sand that can be identified by the presence of shinnery oak (*Quercus havardii*) and parabolic dunes.

In 2016, we compiled a 170-page summary of our investigations in southeastern New Mexico for the BLM Carlsbad Field Office, *"Quaternary and Archaeological Geology of Southeastern New Mexico."* The 2016 report is available through the CFO website. Since then, new studies have been completed. The present contribution is an up-to-date compilation of all of our work on the Mescalero Plain along with new expanded discussions and interpretations. In this bulletin, we summarize the results from 41 study localities (Table 1.1); each locality has its own story that can be found in publications and in technical reports on file with the appropriate state and federal agencies (Table 1.2).

Stephen A. Hall
Red Rock Geological Enterprises
Santa Fe, New Mexico

Ronald J. Goble
Department of Earth and Atmospheric Sciences
University of Nebraska, Lincoln

I. QUATERNARY GEOLOGY

The study of Quaternary geology differs from the investigation of rocks from earlier geologic periods. This is especially true for the Late Pleistocene and Holocene where the application of numerous dating methods has provided a high-resolution geochronology that cannot be matched for older rocks. As a consequence, a fine chronology promotes detailed assessment of Quaternary deposits, especially the timing of deposition and erosion, correlation of geologic units, connections with the regional paleoclimatic record, and, in this research, the relationship of the geologic units to local prehistoric archaeology.

The Mescalero Plain is a diverse complex of eolian sand, alluvium, colluvium, paleosols, and spring and pond deposits. The geologic units exhibit a vast array of physical and chemical properties that are summarized for each unit and, in separate chapters, are discussed in more detail, as well as collectively, in the context of their history through geologic time. In order to facilitate their discussion, some of the various stratigraphic units described herein are given informal names.

Mescalero Plain

The Mescalero Plain of southeastern New Mexico is an undulating landscape of low relief that developed on eroded Permian and Triassic red beds west of the Caprock escarpment of the Southern High Plains (Ogallala Formation) and east of the Pecos River. The Gatuña Formation is a comparatively thin, discontinuous sequence of alluvial and eolian deposits that formed locally on the Mescalero Plain and is capped by caliche of the late Pleistocene Mescalero paleosol (Powers and Holt, 1993; this bulletin). Numerous investigations during the past nineteen years have addressed most aspects of the surficial geology of the Mescalero Plain, especially the Mescalero Sands and the occurrence and preservation of archaeological sites (Tables 2.1, 2.2, 2.3).

On the 1965 *Geologic Map of New Mexico*, the plain was mapped as a generalized unit Qab, "alluvium and bolson deposits and other surficial deposits" (Dane and Bachman, 1965). The more recent *Geologic Map of New Mexico* (NMBGMR, 2003) (Fig. 1.1) differentiates the geology of the plain as Qep or "eolian and piedmont deposits" of Holocene to middle Pleistocene along with discontinuous outcrops of piedmont alluvium (Qp), old alluvium (Qoa), Ogallala Formation (To), and Triassic rocks of the Upper Chinle Group (TRcu). A useful geologic map that shows a fairly accurate representation of the surficial geology of the Mescalero Plain of New Mexico is the Hobbs Sheet of the Geologic Atlas of Texas (Barnes, 1976). The predominant map unit across the plain is "sand sheets, dunes, and dune ridges undivided" (Qsu) with "sand and silt in sheets" (Qs) in smaller areas, especially in the south part of Eddy and Lea counties.

Other regional geologic studies that deal with the Mescalero Plain include the report on Eddy County by Hendrickson and Jones (1952), which focuses on ground-water with a bedrock geologic map without surficial deposits. The geology of the southeastern corner of Lea County, New Mexico, was mapped by Nicholson and Clebsch (1961). Although wind-deposited sand was recognized as occurring around topographic depressions, the broad Mescalero Plain was mapped as Quaternary alluvium. However, in a discussion of the geography of southern Lea County, these authors pointed out that the surficial geology of much of the area is eolian sand: "The topography of the Pecos Valley section [Mescalero Plain] is [characterized] by vast areas of both stabilized and drifting dune sand. Sand covers perhaps 80 percent of southern Lea County" (Nicholson and Clebsch, 1961, p. 7). Other regional geologic studies include an overview of bedrock geology along the broad valley of the Pecos River of southern New Mexico, which touches upon the western portion of the Mescalero Plain where "blow sand and dunes" (Qe) were distinctive in the field east of Carlsbad and were mapped (Kelley, 1971).

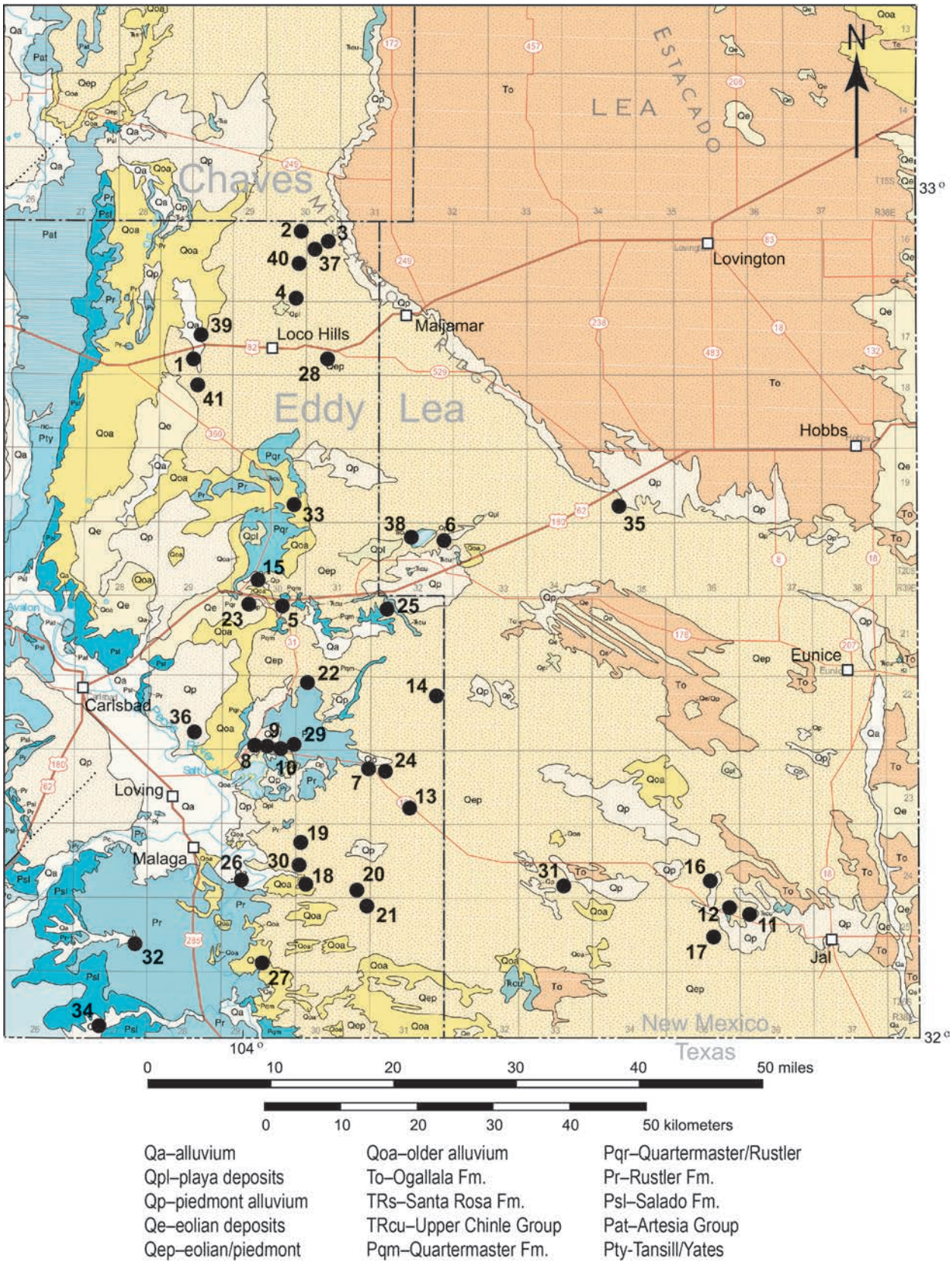

Figure 1.1. Geologic map of southeastern New Mexico with study localities 1 through 41 cited herein. Geologic information about the study localities is presented in Table 1.1. The base map is from the *Geologic Map of New Mexico* (2003, New Mexico Bureau of Geology and Mineral Resources, Socorro).

Table 1.1. Study localities cited herein (see Fig. 1.3)

Loc.	Geology		Stratigraphy										References
								Paleosols*			Dunes*		
	Eolian	Alluv.	Lower sand unit	Middle sand unit	Upper sand unit	Holo. sand unit	Late Holo. unit	B	E	LH	P	C	
1	x		x							x		x	1,2,3,4,12
2	x				x					x	x		1,2,3,4
3	x	x								x		x	1,2,3,4
4	x											x	1,2,5
5	x		x		x			x				x	6,7
6	x		x				x	x			x		8
7	x		x				x	x			x		7,9
8	x				x				x			x	9,10
9	x				x				x			x	9,10
10	x	x			x							x	9,10
11	x				x								11
12	x	x		x	x		x		x			x	11
13	x						x				x		11
14	x					x			x			x	13
15	x			x		x			x			x	8
16	x		x	x		x			x		x		18
17	x						x		x		x		18
18	x						x		x			x	14
19	x			x		x						x	15
20	x			x		x					x	x	16
21	x			x		x			x		x		17
22	x		x	x		x		x	x		x		19
23	x						x			x	x	x	20
24	x						x				x		8
25	x			x	x							x	10,21
26		x			Holocene alluvium							x	8
27	x		x	x	x				x			x	22
28	x	x			Holocene colluvium							x	23
29	x		Solution pipe fill										9
30	Gatuña Fm.							Mescalero				x	24
31	x						x		x			x	25
32		x	Pleist. alluvium		Holocene alluvium								26
33				x			x		x		x		27
34		x			Holocene alluv./colluv.				x			x	28
35	x						x		x			x	29
36	x			x			x		x			x	30
37		x			Holocene alluvium								31
38		x			Lacustrine/alluvium								32
39	x		x							x		x	33
40		x	Pleist. spring									x	1,2
41	x									x		x	1,2

* Paleosols are B = Berino, E = Eddy, LH = Loco Hills; Dunes are P = parabolic, C = coppice.
Loc. = Location, Holo. = Holocene, Pleist. = Pleistocene

Table 1.2. References cited in Table 1.1

Ref. No.	Reference	Ref. No.	Reference	Ref. No.	Reference
1	Hall, 2002a	12	Hall & Goble, 2012	23	Hall & Goble, 2015b
2	Hall, 2002b	13	Hall & Goble, 2015c	24	Hall & Goble, 2016g
3	Hall & Goble, 2006	14	Hall, 2010b	25	Hall & Kettler, 2019
4	Hall & Goble, 2008	15	Hall, 2007	26	Hall, 2016
5	Hall, Goble, & Jeter, 2003	16	Hall & Goble, 2016e	27	Hall & Goble, 2017
6	Hall, 2010a	17	Hall & Goble, 2016f	28	Hall, 2017a
7	Hall & Goble, 2011a	18	Hall & Goble, 2016d	29	Hall, 2017b
8	Hall & Goble, 2015a	19	Hall & Goble, 2016b	30	Hall, 2017c
9	Hall & Goble, 2016a	20	Hall, 2010c	31	Brown, 2011
10	Hall & Boggess, 2013	21	Hall, 2013	32	Brown, 2010
11	Hall & Goble, 2011b	22	Hall & Goble, 2016c	33	Condon et al., 2008

The U.S. Atomic Energy Commission (AEC) supported a number of geologic investigations for the Project Gnome experiment located about 25 miles southeast of Carlsbad in Eddy County (Vine, 1963; Gard, 1968). "Gnome was the first nuclear detonation within the continental limits of the United States outside of the Nevada Test Site since the Trinity shot in 1945 " (Gard, 1968, p. 1); a large literature dealt with the experiment. The geologic mapping by Vine (1963) noted "windblown sand deposits" (Qsd) and "conspicuous dunes" (Qs), but the units were not differentiated stratigraphically. Subsequently, the AEC further supported numerous geologic studies in Eddy County for the proposed construction of the Waste Isolation Pilot Plant (WIPP) about 26 miles east of Carlsbad. Among the many studies and reports, those by George Bachman (1976, 1980, 1981, 1984) were especially helpful to our investigations, providing information on the Mescalero and Berino paleosols, as well as associated eolian sands.

Mescalero Sands

The surface geology of the Mescalero Plain is dominated by wind-deposited sand and low dunes of the Mescalero sand sheet, locally called the Mescalero Sands. The eolian sands were named in N. H. Darton (1928, p. 59): "On the east side of the Pecos Valley in southern New Mexico there are very extensive sand hills formed of deposits known as the 'Mescalero Sands,' which are doubtless of Quaternary age and may represent deposits of an early stage of Pecos River that have been more or less rearranged by the wind" (although recent work reported herein suggests other sources for the eolian sands).

The Mescalero Sands form a broad area of sheet sands and dunes extending 20,400 sq. km (7880 sq. mi.) across the plain and into adjacent Texas (Fig. 1.2). The eolian sand deposits that make up the Mescalero Sands are discontinuous in New Mexico and Texas, and the deposits themselves are, for the most part, rather thin and have been described as a veneer and patchy. In large and small areas alike, eolian sand is absent and the surface geology is instead Permian and Triassic red beds, Ogallala Formation, caliche, alluvium, colluvium, or playa deposits. However, in the few areas where sheet sand is thick and parabolic and transverse dunes have formed, the sand and high dunes can extend up to about 9 m (30 ft) above caliche.

The sand sheet of the Mescalero Sands has been extensively dated by OSL. It formed during the past 90 ka and consists of a series of five sheet sands, two that are Pleistocene and three that are largely Holocene in age. The coppice and parabolic dune fields are more recent, forming in the past 300 years. The details of the results of our research are presented and discussed throughout this bulletin. For an overview of the geomorphology of the Mescalero Sands, we recommend our earlier paper, Hall and Goble (2006), even though the stratigraphy has been revised with more recent findings.

Table 1.3. Geographic Coordinates of Study Localities; geographic coordinates taken by handheld GPS, Magellan eXplorist 300; Latitude-Longitude (WGS84) and UTM (NAD83); *OSL-dated locality

Loc. no.	Latitude - North	Longitude - West	UTM - easting	UTM - northing	Zone	Elev. (ft)
1*	32° 48' 19.66"	104° 04' 19.97"	586861	3630102	13	3562
2*	32° 57' 15.63"	103° 55' 31.83"	600429	3646738	13	3952
3	32° 56' 35.10"	103° 51' 51.85"	606154	3645549	13	4166
4*	32° 52' 06.57"	103° 55' 40.62"	600297	3637217	13	3729
5*	32° 30' 48.33"	103° 57' 09.00"	598389	3597831	13	3440
6*	32° 35' 15.67"	103° 42' 15.60"	621600	3606320	13	3566
7*	32° 19' 10.31"	103° 49' 25.08"	610730	3576462	13	3304
8*	32° 20' 27.59"	103° 59' 56.08"	594209	3578674	13	3025
9*	32° 20' 31.52"	103° 59' 43.75"	594530	3758798	13	3013
10*	32° 20' 34.09"	103° 59' 16.14"	595251	3578884	13	3001
11*	32° 08' 35.52"	103° 18' 27.79"	659606	3557563	13	3184
12*	32° 08' 52.47"	103° 19' 29.08"	657992	3558060	13	3213
13*	32° 16' 34.74"	103° 46' 30.77"	615343	3571722	13	3391
14*	32° 22' 47.75"	103° 43' 23.94"	620094	3583266	13	3611
15*	32° 33' 05.32"	103° 58' 28.73"	596268	3602029	13	3378
16*	32° 10' 46.98"	103° 21' 36.12"	654610	4561535	13	3281
17*	32° 07' 16.11"	103° 21' 36.50"	654699	3555041	13	3237
18*	32° 10' 48.42"	103° 55' 17.62"	601667	3560910	13	3199
19*	32° 15' 12.49"	103° 55' 21.71"	601479	3569041	13	3211
20*	32° 10' 09.38"	103° 49' 58.90"	610027	3559795	13	3442
21	32° 09' 33.45"	103° 49' 19.47"	611072	3558700	13	3375
22*	32° 25' 36.24"	103° 54' 44.55"	602256	3588258	13	3253
23*	32° 30' 37.41"	130° 59' 37.14"	594527	3597457	13	3480
24*	32° 18' 45.53"	103° 48' 43.24"	611833	3575711	13	3334
25*	32° 30' 06.67"	103° 48' 02.23"	612670	3596698	13	3483
26*	32° 10' 50.46"	103° 59' 46.28"	594631	3560905	13	2918
27*	32° 05' 31.86"	103° 57' 43.12"	597951	3551125	13	2994
28*	32° 48' 26.88"	103° 53' 48.07"	603293	3630482	13	3670
29*	32° 20' 52.75"	103° 57' 34.78"	597895	3579484	13	2975
30*	32° 12' 03.05"	103° 55' 33.59"	601226	3563204	13	3133
31A*	32° 10' 18.44"	103° 33' 05.52"	636567	3560396	13	3494
31B*	32° 10' 15.61"	103° 32' 56.82"	636796	3560312	13	3514
31C*	32° 10' 01.39"	103° 32' 34.40"	637389	3559882	13	3499
32	32° 06' 37.32"	104° 08' 43.47"	580626	3552988	13	3019
33*	32° 38' 10.10"	103° 56' 14.85"	599666	3611449	13	3274
34	32° 00' 44.77"	104° 11' 50.74"	575799	3542095	13	3157
35	32° 37' 45.73"	103° 28' 14.68"	643459	3611232	13	3740
36	32° 21' 30.66"	104° 04' 12.97"	587477	3580555	13	3081
37	32° 56' 12.56"	103° 53' 05.47"	604250	3644834	13	4043
38	32° 35' 27.80"	103° 46' 05.00"	615616	3606622	13	3440
39*	32° 49' 35.74"	104° 03' 37.07"	587957	3632454	13	3567
40	32° 55' 36.31"	103° 54' 14.47"	602470	3643699	13	3953
41	32° 44' 58.32"	104° 03' 49.32"	587714	3623908	13	3479

Loc. No.=Location number; Elev.=Elevation

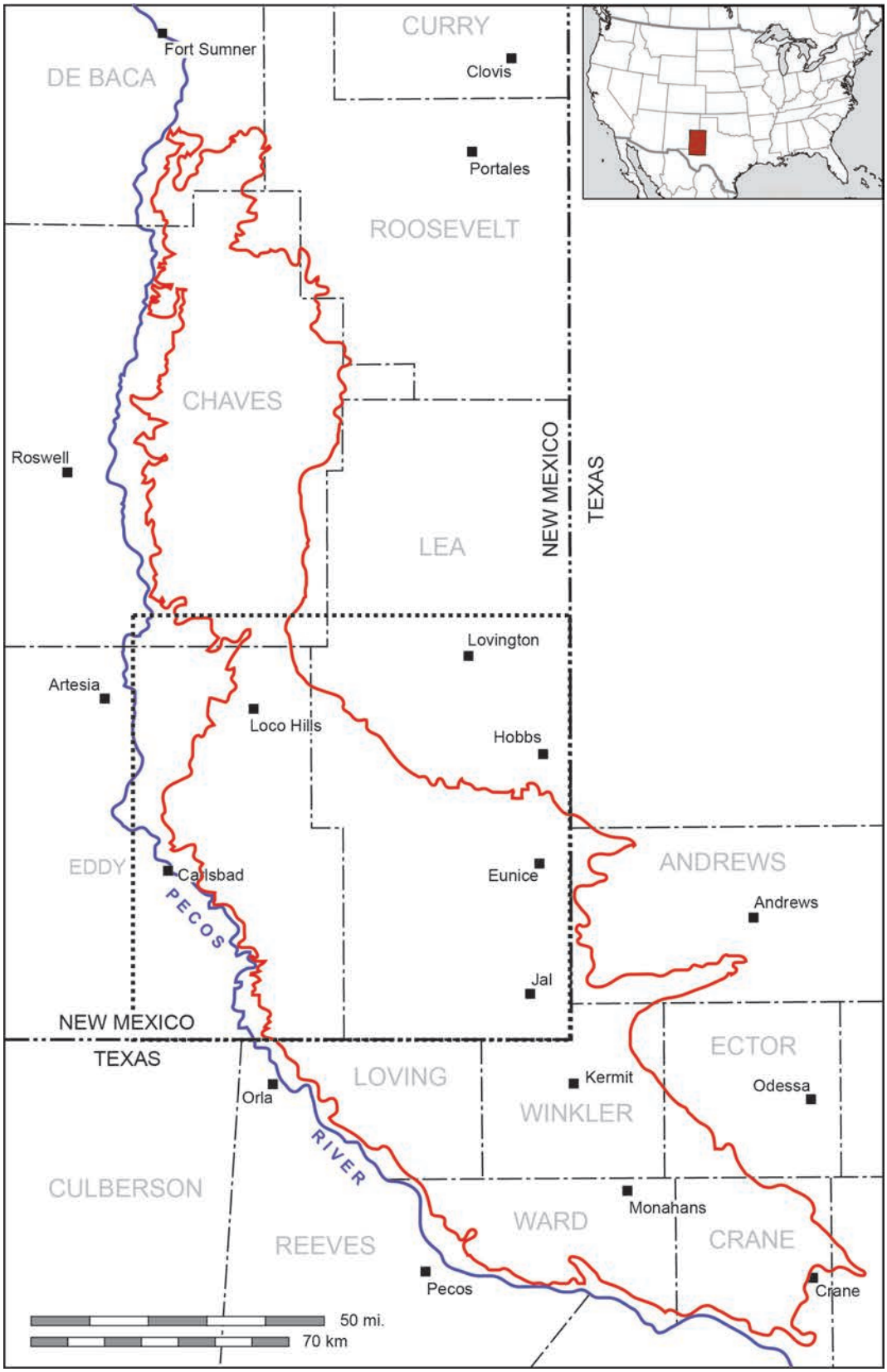

Figure 1.2. Sketch map of the Mescalero Sands in New Mexico and Texas encompassing about 20,400 square kilometers (7,880 square miles, red line); the Texas portion is called the Monahans Sandhills; our investigations are focused on the central region of the sands outlined by the dotted black line in eastern Eddy and southern Lea counties in the southeast corner of New Mexico, excluding the Southern High Plains.

Sand Shinnery Oak

A thorough review of the natural history of plants and animals of the Mescalero Sands is presented by Peterson and Boyd in their 1998 monograph "Ecology and Management of Sand Shinnery Communities: A Literature Review." The ecology of shinnery oak (*Quercus havardii*) plays an important role in the development of the sand sheet. The low-growing shin-oak forms a cover that collects wind-transported sand and facilitates the buildup and stability of sheet sands. The oak also masks the surface of the sand, hiding prehistoric artifacts and features from view. The growth and behavior of shin-oak contribute to the overall geologic condition of the sand sheets. In some areas, the thick growth of shin-oak is regarded as undesirable for agriculture and livestock grazing. Land management has been devoted to oak eradication, which as a consequence, destabilizes loose sandy soils, resulting in soil erosion.

Monahans Sandhills

Nearly a third of the area of the Mescalero Sands extends into Texas, where it has been called the Monahans Sandhills; the Monahans Sandhills State Park features active dunes and is located just northeast of the town of Monahans in Ward County. The geomorphology at the state park has been described by Machenberg (1984), who recognized coppice, wind-shadow, transverse, aklé, barchan, and parabolic dunes.

The geology and stratigraphy of the Monahans dune area were reported by Green (1961). The Monahans sands were not included in our investigations, although the stratigraphic sequence described by Green appears to have some parallels with the Mescalero Sands in New Mexico. According to Green (1961, p. 22):

> Previous work on the geology and stratigraphy of the Quaternary deposits of the Monahans Dunes area is essentially limited to a report by Huffington and Albritton (1941). In their paper the authors recognize and named two separate formations, primarily on the basis of lithology. The older of the two formations, a reddish-brown massive sand, was designated as the Judkins formation, and the younger, lighter colored sands as the Monahans formation.
>
> The formational names were later applied to predominantly eolian deposits at the Scharbauer Site south of Midland, and approximately 50 miles to the east of the type locality (Wendorf, Krieger and Albritton, 1955, p. 13). [Sharbauer is now known as the Midland site.] At this site the Judkins formation has been extended to include lacustrine sediments which contain a Late Pleistocene vertebrate fauna. The Monahans formation at the Scharbauer Site was considered to be essentially the same as the type section with an older part represented by stable or fixed dunes and a younger phase in the form of active dunes (*ibid*., p. 33).
>
> At the beginning of the field work for this project, an attempt was made to follow the nomenclature of Judkins and Monahans but this was unsuccessful for several reasons. First, the sand dune stratigraphy was found to be extremely complex, both locally and areally…Secondly, the stratigraphic picture is further complicated by the variable nature of source beds within the eolian deposits.

Green (1961, p. 41) went on to discuss the Monahans dunes, summarizing the geology in a sequence of nine stratigraphic units. Green did not accept the revised interpretation of the Judkins Formation by Wendorf et al. (1955) that included lacustrine beds in the formation. Green's (1961) new sequence included seven distinct beds that are post-Judkins and pre-Monahans formations, outlined below (Fig. 1.3).

The brick red sand of the Judkins Formation in the south area of the High Plains was regarded by Frye and Leonard (1957) as part of their Cover sands: "It seems certain that the Judkins Formation sands belong within the complex called "Cover sands," although they may be only one phase of this more extensive unit" (p. 28).

After the formal naming of the Blackwater Draw Formation by Reeves (1976) to include the "Cover sands" of Frye and Leonard (1957), the Judkins Formation in the south has also been regarded as an equivalent of the Blackwater Draw (Holliday, 1997, p. 11, 133; Muhs and Holliday, 2001, p. 84; Holliday, 2001, p. 101). There has been a tendency to refer to all red sands in the Southern High Plains as Blackwater Draw Formation. We have suggested

that some red sand deposits in the region, such as the Lower eolian sand and Middle eolian sand units in the Mescalero Sands in southeastern New Mexico (described in detail later), are post-Blackwater Draw (Hall and Goble, 2020).

Comparing the Monahans Dunes described by Green (1961) and our Mescalero Sands, there are some differences and some similarities. First, the Judkins Formation and the Lower sand occupy a similar position as the basal unit in the area of their occurrence; however, their lithology diverges and these sands may have different local origins and different ages. Second, the presence of late Pleistocene lacustrine deposits is similar but is more related to the broad regional cool, wet climate of the times. Third, Green's eolian sand VII capped by a soil and the eolian sand VIII with clayey laminae could be phases of the Upper sand in the Mescalero Sands in New Mexico.

Six OSL dates from eolian sands associated with the Monahans dunes range in age from 204 ka to 0.07 ka (Rich and Stokes, 2011). The stratigraphy of the dated sand and its relationship to Green's (1961) work are not known. However, as discussed later (chapter 7), the radioisotope signatures of the Monahans sand tend to cluster outside of or at the edge of the Mescalero Sands, indicating that the Monahans dunes may have had different sources of sand than the Mescalero Sands.

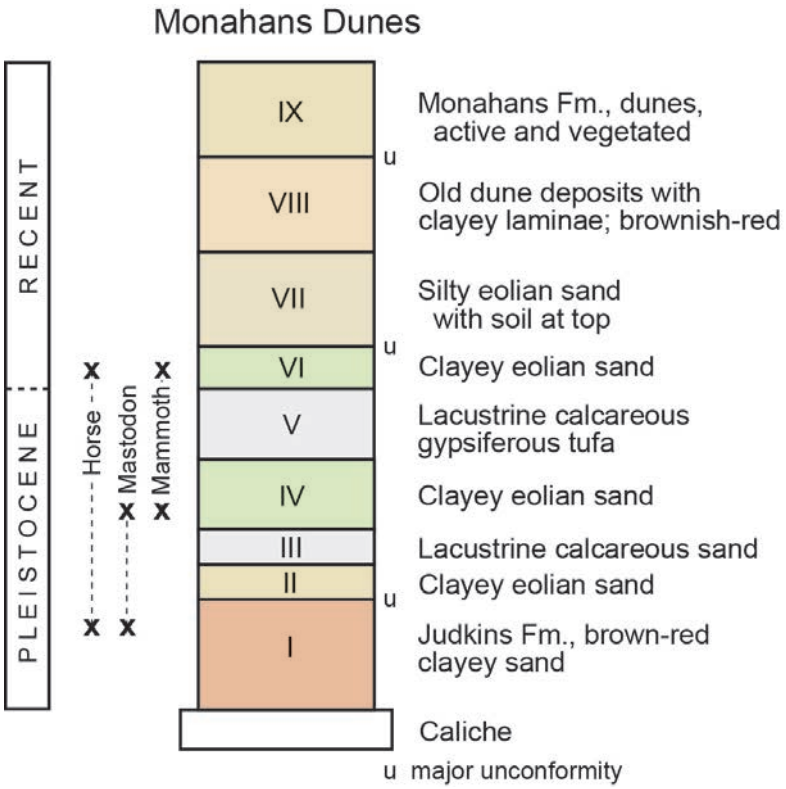

Figure 1.3. Composite of post-Pliocene strata in the Monahans Dunes area (Green, 1961, p. 41); the Judkins Formation rests directly on the caprock caliche at the top of the Ogallala Formation; vertebrate fossils were recovered from Judkins and some overlying units (x); major unconformities are shown (u).

II. DATING SEDIMENTARY DEPOSITS

In our science, a reliable chronology is vital. Without a good chronology for a stratigraphic sequence, there is little to say that has lasting value. In our research, geochronology has been the one link that ties together the diverse surficial geologic units. Thus, the lengthy discussions of the many facets of the complex geologic history of the Mescalero Plain commence with geochronology.

Optically Stimulated Luminescence Dating (OSL)

OSL is an off-shoot of thermoluminescence (TL) dating. It was first developed in 1985 and has largely replaced TL as the method of choice for dating sedimentary deposits. Since the year 2001, OSL dating has provided a fresh geochronology of the eolian sands and associated prehistoric sites in southeastern New Mexico.

Field Methods in OSL Dating

***Stratigraphy*—**The reader should take note of our field methods as related to OSL dating. Following fundamental procedures in field geology, the stratigraphy of a deposit is determined by its sedimentary properties, unconformities, paleosols, and lateral continuity. After a stratigraphic unit has been determined in a study area, samples are collected from the unit for OSL dating. Ideally, we collect samples from near the base, middle, and top of a unit, but avoiding contacts with other units where sand grains may be turbated or reworked. Three or more OSL dates from a stratigraphic unit define its period of deposition; the net sedimentation rate of the unit can also be determined. A firm dating of superimposed stratigraphic units also provides information about unconformities that represent periods of non-deposition, landscape stability, soil development, and erosion.

Our field methodology differs from that of some other researchers as has been reported in the literature. In contrast to our methods, some field workers have not determined or do not know the stratigraphy of the deposits that they sample for OSL dating. Instead, each OSL date is regarded as an independent "depositional event" that has no stratigraphic context. In other cases, an assemblage of similar OSL ages from different places is assumed to represent a single stratigraphic unit. Almost needless to say, these approaches are contrary to the very foundation and principles of stratigraphic geology.

***Field Sampling*—**The following procedure has evolved from many years of field and laboratory experience and is taken largely from Hall and Rittenour (2010):

1. Clean off the outcrop. Hammer into outcrop an opaque metal pipe or tube with a removable pounding cap at one end; we use a 1/8-in. aluminum tube, 2.0 x 7.0 inches. Place duct tape around the cap to keep it in place; a Styrofoam plug may be placed in the end entering the sediment to ensure that it is kept packed tightly during sampling. PCV and other plastic pipes or tubing are not recommended because they vibrate during pounding (mixing the sample) and some are not completely opaque.
2. Hammer the tube all the way into the outcrop. The tube must be full of sediment and packed tightly to avoid mixing during transport. If a root, pebble, or rodent burrow is encountered, thoroughly clean out the tube and relocate to another spot.
3. Sample the sediment immediately around the tube for moisture content using an airtight container. Make a note of evidence for vadose moisture or groundwater such as sediment mottling or iron staining, and describe the expected history of the water content of the sampled deposit. Label the container.

4. Sample the sediment from a 10-cm radius around the tube for environmental doserate (for K, U, Th analysis). Place the sediment in a one-quart zip-locked plastic bag, filling it half-full or more, and label the bag.
5. Extract the tube carefully to avoid loss of sediment. With the open end of tube pointed up, pack any extra space with more sediment, tamping it down lightly. If more than one centimeter needs to be added, use duct tape, paper, or plastic to fill the tube firmly, not sediment that could be mistaken for real sample; make a note of this on sample sheet. (In the laboratory, the ends of the sediment in the sampling tube are discarded because they have been exposed to light during sampling.)
6. Seal the end of the tube with at least two layers of duct tape. If the sediment in the tube rattles upon shaking, it is a ruined sample and should be discarded; start over.
7. The OSL sample is actually three samples: (a) the sediment-bearing tube from which the OSL age is determined, (b) the moisture sample, and (c) the doserate (chemistry) sample. All three should have the same identifying label; keep labels simple, but avoid sample numbers OSL-1, OSL-2, etc.; clear tape should be placed over the labels if there is a chance of the labels being rubbed off during transport.
8. Place the tube, moisture, and doserate samples in a large bag for orderly transport.
9. Document the sample: (a) depth of burial below the landform surface; if there has been recent erosion or removal of sediment, estimate the original depth; the depth of burial is needed to calculate cosmic doserate; (b) note details of the stratigraphy, both vertical and lateral, with a measured section, including sedimentology, soil horizons, and unconformities, and where the sample fits into the section; (c) relationship of the sample to other samples in the series; (d) UTM or latitude-longitude, and elevation of the sample; (e) date that the sample was collected. Finally, photograph the stratigraphic section with a meter scale in place, before and after sampling. A "before" photograph that shows the stratigraphy is useful for publication since sampling disturbs the outcrop.

***OSL Dating and Archaeological Sites*—**The field worker should also be especially cautious about sampling archaeological sites for OSL dating. Prehistoric and historic inhabitants disturb the soil and substrate, resulting in a site footprint of mixed sediment that may produce optical ages that are spurious for both the surficial geology and the site itself. In most of our studies in southeastern New Mexico, wherever possible, geologic trenching and OSL dating was conducted off site, especially at larger sites of occupation where prehistoric cultural activity was brisk.

Laboratory Methods in OSL Dating

In our studies in this region, OSL analyses were carried out by Dr. Goble, Luminescence Geochronology Laboratory, Department of Earth and Atmospheric Sciences, University of Nebraska, Lincoln (Fig. B); a later study was conducted by Dr. Richard Kettler at the same laboratory. The dated material in nearly all cases has been quartz sand grains in the 0.090 to 0.150 mm size range, or very fine- to fine-grained sand. The optical signal in the sand grains is a product of the surrounding natural radiation that is derived from radioactive components of minerals in a sedimentary deposit. Most of the radiation is produced by potassium oxide ($^{40}K_2O$), uranium (U), and thorium (Th); of these, the greatest amount of the radiation concentration is from ^{40}K (except for one location for which cosmic rays were dominant because of very low K, U, and Th). Radioactive decay of these components produces high-energy particles that dislodge electrons within the quartz (or feldspar) mineral grains. The dislodged electrons are trapped in defects in the crystal structure of the grains. With the passage of time, more electrons are dislodged and trapped.

In nature, the luminescence signal is zeroed out and lost by a few seconds exposure to light. Eolian sand is well suited for OSL dating because the quartz sand grains are exposed to sunlight and the luminescence signal is reset before being deposited and buried. In other words, the luminescence signal gives us the time of burial of the sand grains in a deposit.

In the laboratory, under amber-light conditions, the OSL sample is subjected to light of a specific wavelength (typically blue-green or green). The

trapped electrons are energized by the light, causing them to be evicted from their traps and give off energy in the form of short wavelength light as they fall into a lower energy state. The intensity of the light signal given off by a prepared sample is measured. The intensity corresponds to the number of trapped electrons; the greater the luminescence, the greater radiation exposure a sample has had and the older the sample. In our recent work in southeastern New Mexico, OSL ages are generally based on the measurement of fifty or more subsamples (aliquots).[1]

Specific laboratory preparations carried out by Dr. Goble on OSL samples from the Mescalero Sands area are outlined below (from Hall and Goble, 2017). Sample preparation was carried out under amber-light conditions. Samples were wet sieved to extract the 90–150 µm fraction, and then treated with HCl to remove carbonates and with hydrogen peroxide to remove organics. Quartz and feldspar grains were extracted by flotation using a 2.7 gm/cm^3 sodium polytungstate solution, then treated for 75 minutes in 48% HF, followed by 30 minutes in 47% HCl. The sample was then resieved and the <90 µm fraction discarded to remove residual feldspar grains. The etched quartz grains were mounted on the innermost 2 mm or 5 mm of 1 cm aluminum disks using Silkospray.

Chemical analyses were carried out using a high-resolution gamma spectrometer. Dose-rates were calculated using the method of Aitken (1998) and Adamiec and Aitken (1998). The cosmic contribution to the dose-rate was determined using the techniques of Prescott and Hutton (1994).

Optically stimulated luminescence analyses were carried out on Riso Automated OSL Dating System Models TL/OSL-DA-15B/C and TL/OSL-DA-20, equipped with blue and infrared diodes, using the Single Aliquot Regenerative Dose (SAR) technique (Murray and Wintle, 2000). Early background subtraction (Ballarini et al., 2007; Cunningham and Wallinga, 2010) was used. Preheat and cutheat temperatures were based upon preheat plateau tests between 180° and 280°C. Dose-recovery and thermal transfer tests were conducted (Murray and Wintle, 2003). Growth curves were examined to determine whether the samples were below saturation (D/Do <2; Wintle and Murray, 2006). Optical ages are based upon a minimum of 50 aliquots (Rodnight, 2008). Individual aliquots were monitored for insufficient count-rate, poor quality fits (i.e. large error in the equivalent dose, De), poor recycling ratio, strong medium versus fast component (Durcan and Duller, 2011), and detectable feldspar. Aliquots deemed unacceptable based upon these criteria were discarded from the data set prior to averaging. Calculation of sample De values was carried out using the Central Age Model (Galbraith et al., 1999), unless the De distribution (asymmetric distribution; decision table of Bailey and Arnold, 2006) indicated that the Minimum Age Model (Galbraith et al., 1999) was more appropriate. The Minimum Age Model calculates the minimum age for a partially bleached sample.

OSL Dates—OSL ages are in calendar years and by convention are listed with a 1-σ error, similar to radiocarbon dates. Ages are in years before the sample was collected in the field. As yet, there is no "zero" age for OSL ages, such as A.D. 1950 that serves as the "present" in "years before present (BP)" in radiocarbon dating. Instead, if an OSL sample is collected in 2016 and its age is 100 ± 14 years, it would be A.D. 1916 (± 14) in calendar years. In our work in the region, the earliest OSL age we have obtained is 169,800 ± 12,700 years and the youngest age is 71 ± 6 years (A.D. 1943) (Table 2.1).

Table 2.1. Time-frequency distribution of 177 OSL dates from the Mescalero Plain, New Mexico (Appendix A)

OSL Ages (years)	Number of Dates	OSL Ages (years)	Number of Dates	OSL Ages (years)	Number of Dates
0–500	41	5000–6000	6	15,000–20,000	4
500–1000	12	6000–7000	5	20,000–30,000	11
1000–2000	19	7000–8000	6	30,000–40,000	6
2000–3000	13	8000–9000	4	40,000–50,000	1
3000–4000	7	9000–10,000	8	50,000–100,000	10
4000–5000	11	10,000–15,000	10	>100,000	3

[1] The above three paragraphs are quoted directly or paraphrased from Hall and Rittenour (2010, p. 101).

Chemical Signatures—A side benefit of OSL dating is the measurement of the amount of potassium oxide (K_2O), uranium (U), and thorium (Th) that are present in the dated sediment (Fig. 2.1; Table 2.2). These values are a chemical signature of the sediment that can provide information on the source of the eolian sand in the dated deposit and whether the sand at different study sites came from the same or different sources. We should point out that the use of K_2O-U-Th signatures is a new application developed in our studies in southeastern New Mexico and has not been pursued by other luminescence laboratories. We discuss chemical signatures further in chapter 7.

Infrared Stimulated Luminescence Dating (IRSL)

IRSL dating of feldspar can provide a greater range of ages than conventional OSL dating of quartz and is capable of dating older material. In order to appraise the relationship between the well-dated Lower eolian sand unit of the Mescalero Sands with the Blackwater Draw Formation on the Southern High Plains, IRSL dating was carried out near the formation's type section north of Lubbock, Texas. The IRSL age was determined on potassium feldspar; the laboratory methodology differs somewhat from that involving quartz and is described below (from Hall and Goble, 2020, p. 32-34). IRSL dating may become more prominent in Quaternary geochronology in the future.

The material that was IRSL dated was collected from 40 to 50 cm below the top of the Blackwater Draw Formation where local slope erosion was minimal. Because of the induration of the clayey sediment, the material was chopped out of a fresh exposure in a block; the material was wrapped in tinfoil in the field.

In the laboratory, the outer portion of the sample was removed and the preparation was carried out under amber-light conditions. The sample was wet sieved to extract the 90–150 µm fraction, and then treated with hydrochloric acid (HCl) to remove carbonates and with hydrogen peroxide to remove organics. Quartz and K-feldspar grains were extracted by flotation using a 2.7 gm/cc sodium polytungstate solution. The portion used for quartz optically stimulated luminescence (OSL) was then treated for 75 minutes in 48% hydrofluoric acid (HF), followed by 30 minutes in 47% HCl. This

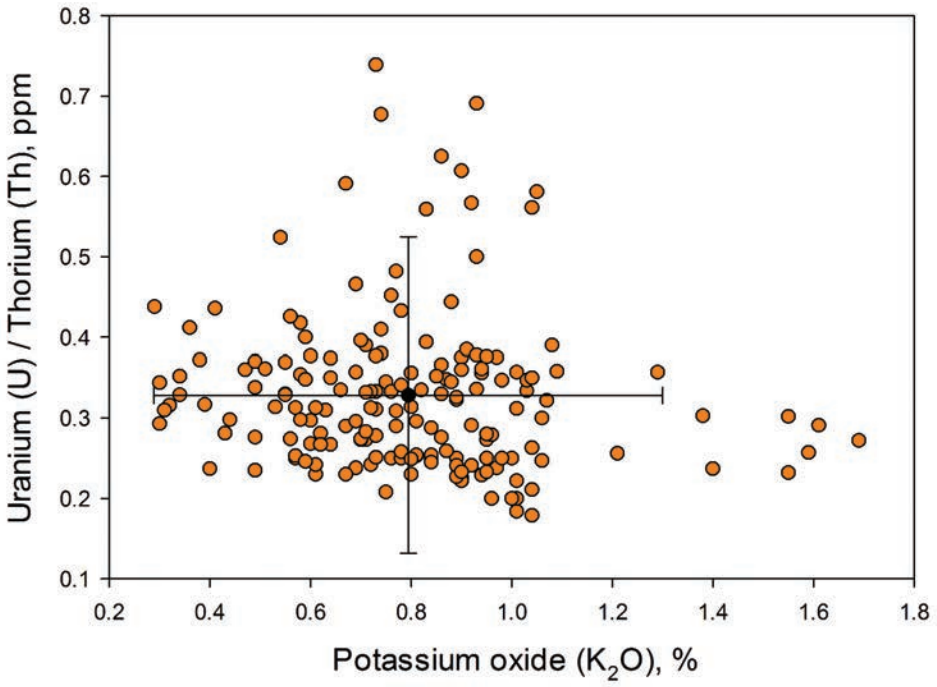

Figure 2.1. Isotope chemistry of the Mescalero Sands, southeastern New Mexico; 172 samples, the mean values with a 2 standard deviation (Table 2.2) (Appendix A); the outlying points of high values of K_2O are from the Maroon Cliff (Loc. 25) and Middle eolian sand beds; the outlying points of U/Th are mostly from Loc. 18 in the Pierce Canyon area at the western edge of the Mescalero Plain.

Table 2.2. Summary isotope measurements from optical dating samples, Mescalero Sands; 171 samples (Appendix A) (excludes samples from Pecos River alluvium, the Blackwater Draw Formation, and published material by others; these data are discussed later)

Isotopes	Mean	1 Standard Deviation	Minimum measurement	Maximum measurement
Potassium oxide (K_2O)	0.794 %	0.253	0.290 %	1.690 %
Uranium (U)	0.877 ppm	0.330	0.390 ppm	2.120 ppm
Thorium (Th)	2.721 ppm	0.798	1.000 ppm	5.960 ppm
Uranium/Thorium	0.328 ppm	0.0983	0.179 ppm	0.739 ppm

portion was then re-sieved and the <90 µm fraction discarded to remove residual feldspar grains. The etched quartz grains were mounted on the innermost 5 mm of 1 cm aluminum disks using Silkospray. The portion used for potassium feldspar infrared stimulated luminescence (IRSL) consisted of grains separated by an additional flotation using a 2.58 gm/cc sodium polytungstate solution, then treated for 40 minutes in 10% HF to etch and remove the outer alpha-irradiated layer from the rims, followed by 30 minutes in 47% HCl.

Chemical analyses were carried out using a high-resolution gamma spectrometer. The feldspar dose-rate was calculated using an assumed K_2O content of 16.9% (pure potassium feldspar). Dose-rates were calculated using the method of Aitken (1998) and Adamiec and Aitken (1998) and the updated dose rate conversion factors of Guerin et al. (2011). The cosmic contribution to the dose-rate was determined using the techniques of Prescott and Hutton (1994).

Luminescence analyses were carried out on Rise Automated OSL Dating System Models TL/OSL-DA-15B/C and TL/OSL-DA-20, equipped with blue and infrared diodes, using the Single Aliquot Regenerative Dose (SAR) technique for quartz (Murray and Wintle, 2000). Early background subtraction (Ballarini and others, 2007; Cunningham and Wallinga, 2010) was used. Preheat and cutheat temperatures of 240°C/10s and 220°C/10s were used for the quartz OSL measurements. Growth curves showed that the sample was above saturation (D/Do >2; Wintle and Murray, 2006), above which uncertainty in signal estimation results in larger, and asymmetrical uncertainty in equivalent dose estimation (Murray and Funder, 2003; Murray et al., 2002). Typical growth curves observed from single aliquots of the sample during blue OSL, 50°C IRSL, and 290°C post-IR IRSL are shown in Hall and Goble (2020, p. 34, fig. 3). Signal data have been arbitrarily scaled to 100% maximum. The blue OSL curve saturates on a plateau at a much lower applied dose than do the two superimposed IRSL curves. Blue OSL signal data from an aliquot of quartz plot at approximately 320 Gy (98% of full saturation) on the upper curve, whereas IRSL and post-IR IRSL data plot at approximately 600 Gy and 770 Gy, respectively, on the lower curve, well below saturation. Although the feldspar signal saturates at a much higher level than does the quartz signal, anomalous fading, a decrease in signal level with time, is an inherent problem for which correction must be made. Recent attempts to minimize the effect has led to several newer measurement techniques that utilize an initial IRSL measurement at 50°C, followed by a subsequent measurement at 225°C or 290°C (post-IR IRSL) (Thiel et al., 2011; Buylaert et al., 2009); 290°C post-IR IRSL was used for the Blackwater Draw sample.

Measurements for 50°C IRSL and 290°C post-IR IRSL were carried out on feldspars using the dating protocol outlined by Thiel and others (2011). Data for skew, kurtosis, and overdispersion (shown in Table 1, Hall and Goble, 2020, p. 35) indicate that the central age model (Galbraith et al., 1999) is appropriate for equivalent dose calculations (Bailey and Arnold, 2006; Galbraith, 2005). Equivalent doses were corrected for residual dose of 7.59 ± 0.55 Gy (50°C IRSL) and 31.61 ± 1.40 Gy (290°C post-IR IRSL). Fading corrections were determined over a 5 month period and applied using the methods outlined by Huntley and Lamothe (2001) and Auclair and others (2003). Fading corrected ages are 294 ± 32 ka (50°C IRSL) and 347 ± 40 ka (225°C post-IR IRSL).

The rounded IRSL age of the upper Blackwater Draw Formation is 300 to 350 ka. The Middle Pleistocene age of the formation is consistent with the mature argillic paleosol and secondary carbonate overprint. It is considerably older than the Late Pleistocene Lower eolian sand unit (90 to 50 ka) on

the Mescalero sand sheet (Hall and Goble, 2020). Although the Mescalero Sands and the Blackwater Draw Formation are both eolian in origin, they are unrelated to each other, the Mescalero Sands having formed more than 200,000 years after the deposition of the Blackwater Draw Formation ended (this is discussed further later).

Radiocarbon Dating

Radiocarbon dating is one of the more important methods of age control and is applied worldwide. The method was developed in the late 1940s by Willard F. Libby, who received a Nobel Prize in Chemistry in 1960 in recognition for his primary role in developing radiocarbon dating. All of the radiocarbon ages used on our geologic work in the region are derived from the accelerator mass spectrometry (AMS) method, developed after 1976. The AMS method has advantages over conventional radiocarbon dating because it requires only 1 mg or less of carbon and can date small amounts of humates from topsoils.

In our studies, we have obtained 54 AMS radiocarbon ages, especially from soil A horizons in stratigraphic context (Appendix B). In most cases, we instructed the laboratory (Beta Analytic, Inc.) to date only the soluble humic acids or humate fraction, separating out and not including charcoal or other solid humus in the dated material. The reasoning here is that charred particles in the dated material may have originated from prehistoric cultural activity. In these cases, we wanted a radiocarbon age of the soil, not the archaeology.

$\delta^{13}C$ Values

In radiocarbon dating, the $\delta^{13}C$ value of the material is measured in order to correct the radiocarbon age for isotopic fractionation of carbon during photosynthesis. As a side benefit, when applied to humates from a soil A horizon, the $\delta^{13}C$ value tells us whether the vegetation that produced the humates was predominantly C4 grasses or C3 woody shrubs or a combination of both. We have used this information to evaluate the paleovegetation in southeastern New Mexico, discussed later in chapter 14.

Radiocarbon and Calendar Years

Radiocarbon is the only dating method that produces ages that are not in calendar years. Consequently, radiocarbon ages are calibrated to calendar years by the use of ever-refined datasets of AMS-dated annual growth rings of trees and corals. IntCal13 is one of the more current calibration datasets and extends back 50,000 years; it is available on the Internet (Reimer et al., 2013). We routinely use 2σ calibrated radiocarbon ages to obtain calendar years B.P. (cal yr BP). Both radiocarbon years and calibrated radiocarbon calendar years are pegged at A.D. 1950, referred to as the "before present" or "BP."

Weighted Average Probability Distributions of Radiocarbon Ages

Radiocarbon ages can have multiple calendar equivalents. This is because the Earth's atmosphere and plants on the Earth's surface hold a changing, non-linear amount of ^{14}C through time. When a measured radiocarbon date produces more than one age from a calibration dataset, we use a technique called a weighted average of the probability distributions in order to normalize multiple calibrated ages to a single age value (Telford et al., 2004). Weighted averages are used where a single age is necessary, such as in comparison with OSL ages and when calculating sedimentation rates.

Radiocarbon and OSL Ages Compared

Radiocarbon and OSL ages in calendar years are different from each other and can be misleading when comparing recent ages. As stated previously, a radiocarbon age is in years before A.D. 1950, and an OSL age is in years before the sample was collected in the field. If, for example, we had an object that formed and was buried A.D. 1000, its radiocarbon age would be 950 cal yr BP. If the object was collected in the field in 2015, its OSL age would be 1015 years. The only way to normalize the two different ages for accurate comparison is to convert both of them to calendar years A.D. or B.C. We have done this in a few cases below where we have compared matched AMS and OSL ages from the same horizon.

III. STRATIGRAPHY

The stratigraphy of the surficial deposits on the Mescalero Plain, as applied in the field, is best defined by a quote from the *Glossary of Geology* (Neuendorf et al., 2005, p. 633): "Stratigraphy is the science of rock strata. It is concerned not only with the original succession and age relations of rock strata but also with their form, distribution, lithologic composition, fossil content, geophysical and geochemical properties, indeed, with all characters and attributes of rocks as strata; and their interpretation in terms of environment or mode of origin, and geologic history." Nearly all of the different units of surficial deposits, including eolian sand, that occur on the Mescalero Plain qualify as rock strata. Rules and guidelines for the definition and nomenclature of stratigraphic formations are presented in the *North American Stratigraphic Code* (North American Commission on Stratigraphic Nomenclature, 2005).

One of the challenges of stratigraphic studies of surficial deposits in the field is deciding what a discrete unit versus something else is. Generally, in our experience, a sedimentary unit will have (a) moderately uniform color, (b) texture, (c) bedding, (d) structures, (e) clearly marked lower and upper boundaries, and (f) some lateral continuity across the landscape. The presence of paleosols can be helpful in the recognition of unit tops and the lateral continuity of a unit. Unit thickness may be variable due either to primary deposition or post-depositional erosion. Ideally, a unit should have properties that can be recognized and mapped on a 7.5-minute topographic quadrangle. In practice, however, surficial units may be restricted to the subsurface and seldom exposed except in study trenches; the late Pleistocene Middle eolian sand unit, for example, is known only from trenches. Recent wind-transported cover sand often obscures the surface geology.

Eolian Stratigraphy: Episodes of Eolian Activity

Wind-blown sand deposits of the Mescalero sand sheet dominate the geology of the Mescalero Plain. However, the eolian sands are not uniform and are absent from many areas where Permian-Triassic bedrock and Pleistocene caliche are exposed at the surface of the plain. The transition from a bedrock-dominated terrain to the presence of thick deposits of Holocene eolian sand and large parabolic dunes can occur within a distance of only a few hundred feet.

Overall, based on our investigations during the past nineteen years, we have identified six episodes of eolian activity and sand deposition on the Mescalero Plain (Table 3.1). Two stratigraphic units of Pleistocene sands and four units of Holocene sands were deposited across the plain during the past 90,000 years. The sixth and most recent episode of eolian sand deposition occurred during the past 300 years and has resulted in the formation of parabolic and coppice dunes and related cover sand. All of these sand deposits make up the Mescalero sand sheet.

From a practical viewpoint, the concept of episodes of eolian activity introduced herein is a convenient means to bring together and discuss in an organized manner a considerable amount of diverse stratigraphic information from vastly different geologic sequences and topographic settings. Because of the geomorphic variability across 4,100 square miles of the Mescalero Plain, there is no one location or package of eolian deposits that can be singled out as typical. Some localities have only one stratigraphic unit of eolian sand above caliche. Other localities have as many as four superimposed stratigraphic units, each unit with different ages and sediment properties that represent different episodes of local or regional eolian activity. And, as to be expected, some deposits have been partly or completely removed by erosion, especially the two units of late Pleistocene age.

Table 3.1. Summary of episodes of eolian activity and stratigraphy, Mescalero sand sheet, southeastern New Mexico

Episodes	Stratigraphy	Age	Notes	Study Localities†
VI	Cover sand	A.D. 1784 to present	Non-dune surficial sand	6,23,25
	Coppice dunes	A.D. 1745 to present	Most mesquite dunes are probably 20th century	4,15,26,27
	Parabolic dunes	A.D. 1734 to present	Episode VI began ca. 300 years ago, ca. A.D. 1700	16,17,20,22,24
-	Eddy paleosol	2 ka to 0.3 ka, A.D. 1 to A.D. 1700	Caps Holocene (IV) & Late Holocene (V) sands	9,10,11,12,14, 15,16,18,21,25, 27,31,33
V	Late Holocene eolian sand	6 ka to 2 ka	Mantled by Eddy paleosol	7,18,23,24
IV	Holocene eolian sand	12 ka to 2 ka	Mantled by Eddy paleosol	14,15,16,17,20,22
III	Upper eolian sand	18 ka to 5 ka	Capped by paleosol Bw horizon with Bk below	2,5,8,9,11,12
II	Middle eolian sand	33 ka to 20 ka	Capped by paleosol Bt horizon	15,16,19,20,22,33
I	Lower eolian sand	90 ka to 50 ka	Capped by Berino paleosol	1,5,6,7,16,27

† Study localities listed in Table 1.1

Episode I

The first episode of eolian activity initiated the formation of the Mescalero sand sheet. The deposition of the Lower eolian sand unit on the weathered eroded surface of the caliche of the Mescalero paleosol began about 90,000 years ago and continued until about 50,000 years ago (the Mescalero and other paleosols are defined later in chapter 9). This time interval correlates with the post-Sangamon and pre-Early Wisconsin that has been called the Eowisconsin in North America and continues through the Early Wisconsin into the Middle Wisconsin, correlating as well with the late 5 and into the early 3 marine isotope stages (MIS) (Šibrava et al., 1986; Lisiecki and Raymo, 2005).

Lower Eolian Sand Unit (90–50 ka)—The first report on the archaeological geology of the Mescalero Sands focused on the area around Loco Hills and northern Eddy County, New Mexico. The sand sheet in that area is made up of two principal deposits of eolian sand. At first, we called the older deposit Unit 1 (Hall, 2002a, b); later, the nomenclature was revised and the unit is called the Lower eolian sand (Hall and Goble, 2006, 2008). The younger deposit was initially called Unit 2 and was revised and is called the Upper eolian sand. (Later studies in southern Eddy and Lea counties documented the presence of three additional bodies of sheet sand, all discussed below.)

The Lower sand occurs throughout northern Eddy County and crops out at the surface in much of that area. This deposit rests directly on the Mescalero paleosol. It has a red to dark red color (2.5YR 3-4/6-8) owing to the presence of the clayey argillic Berino paleosol at the top of the unit (Fig. 3.1). In most places, the Lower sand is thin, less than 1 meter thick, and the red Berino paleosol extends down to caliche, completely enveloping the Lower sand. In the field, it is commonly referred to as the red sand. West of the Loco Hills area, archaeological sites occur on the top eroded surface of the Lower unit and archaeological site features intrude it (Fig. 3.2).

Where Holocene sands are present, the Lower unit is buried beneath them (Fig. 3.1). However, many trenches cut to caliche at a number of places on the plain do not encounter the Lower sand, suggesting that it either was not deposited everywhere, or it has been removed from wide areas by Pleistocene erosion; we suspect the latter (Fig. 3.3).

Age of the Lower Eolian Sand Unit—OSL dating has provided eleven ages for the Lower sand from seven localities, ranging from 90.7 to 51.1 ka; one age is >87.0 ka (Fig. 3.4). In various recent summaries, the age of the Lower eolian sand unit is given as 90 to 50 ka (Hall and Goble, 2016g).

Lower Eolian Sand Unit and the Blackwater Draw Formation—A mix of isolated optical ages without stratigraphic context has been reported from red eolian sands in far southeastern New Mexico (Rich and Stokes, 2011). The dated sands fall within the range of or are close to the published chronology of the Lower sand and the Berino paleosol on the Mescalero Plain (Hall and Goble, 2006). Instead of

correlating their isolated records with the Lower sand, however, Rich and Stokes (2011) have correlated their red sand with the Blackwater Draw Formation of the Southern High Plains. They are apparently following Holliday (2001), who has described a number of stratigraphic sections of eolian deposits across the Southern High Plains. Red sand occurs below Holocene- and Paleoindian-age deposits at many localities and has been correlated with the Blackwater Draw Formation (Holliday, 1997). However, the Lower sand of the Mescalero Plain and the Blackwater Draw of the High Plains are two distinct and separate eolian deposits with nothing in common and should not be confused as the same.

We visited the type section of the Blackwater Draw Formation north of Lubbock, Texas. The section occurs in a deep gully that is partly filled-in now, but an excellent exposure is located one km (0.6 mile) to the east. The argillic paleosol that characterizes the upper Blackwater Draw Formation is thicker and much more mature than the Berino paleosol. Our infrared stimulated luminescence (IRSL) age on potassium feldspar for the upper part of the Blackwater Draw is 294 ± 32 ka (50°C IRSL) and 347 ± 40 ka (225°C post-IR IRSL) and averaged 350 to 300 ka (Hall and Goble, 2020). In contrast, the age of the Lower eolian sand of the Mescalero sand sheet is 90 to 50 ka, much younger than the Blackwater Draw (IRSL methodology is described in chapter 2).

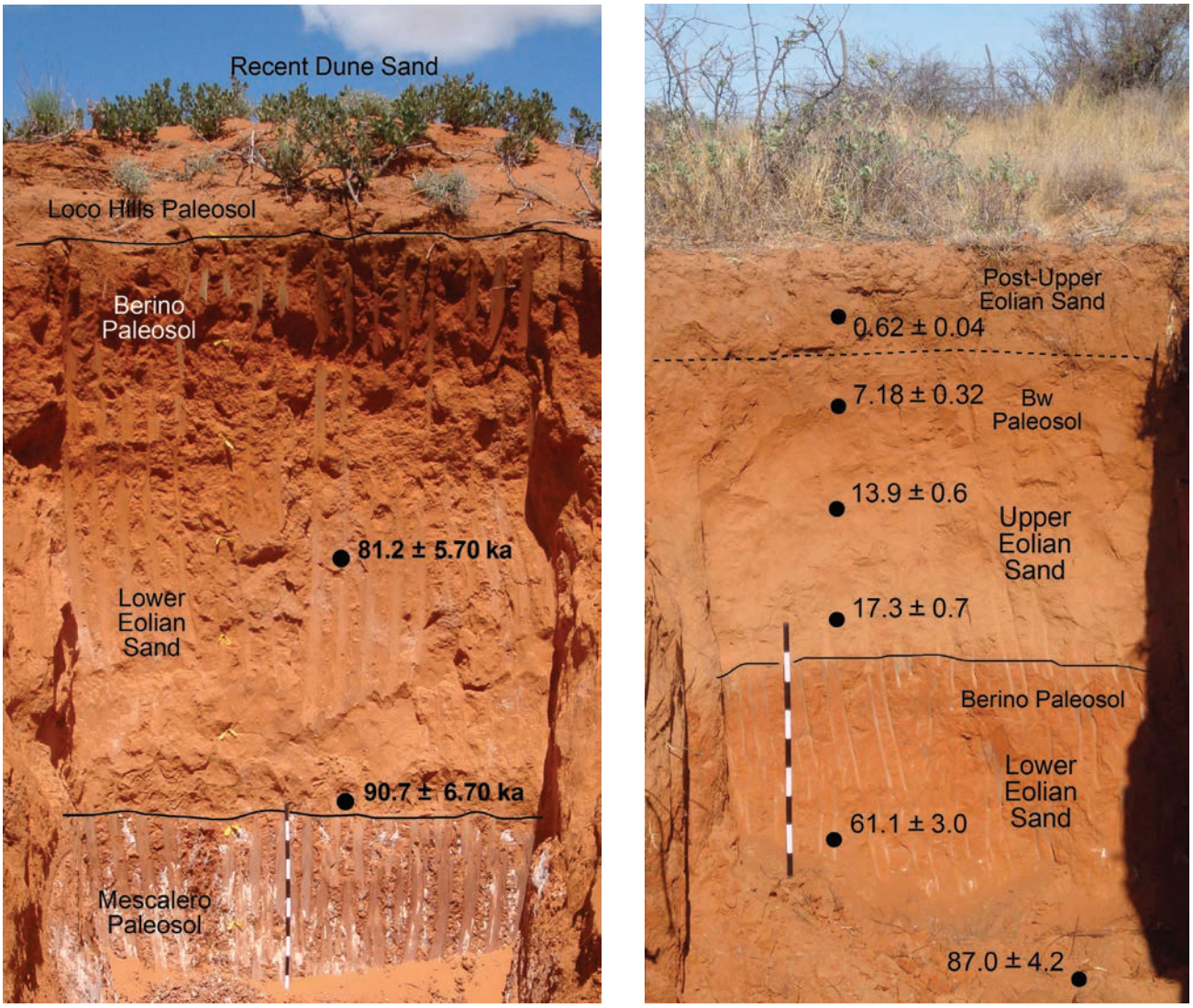

Figure 3.1. Episode I sands. (left) Lower eolian sand unit with Berino paleosol at Loc. 1; this is the type section for the Berino paleosol as a formal pedostratigraphic unit (Hall and Goble, 2012). (right) Lower and Upper eolian sand units at the Intrepid Potash-NM solar pond near the junction of U.S. Highway 62 and NM Highway 31 (Loc. 5); 1-m scale in photos.

Figure 3.2. Prehistoric hearth intruding into the Lower sand unit near Loco Hills; the hearth was originally dug into the red Lower eolian sand (dated 90 to 50 ka) and lined with dense caliche rocks; the feature is now exposed by erosion.

We conclude that the Blackwater Draw Formation does not occur in the area of the Mescalero sand sheet of southeastern New Mexico. We are also of the opinion that not all red sands in the Southern Great Plains are the Blackwater Draw Formation and that, instead, younger red eolian sand bodies are present, representing post-Blackwater Draw deposits.

Episode II

Identification of the second episode of eolian activity is based on several occurrences of reddish sand that are preserved at scattered localities across the Mescalero Plain. The episode of sand accumulation was initiated after 17,000 years of stability, soil development, and erosion of the Lower eolian sand. OSL ages verify that the sand, representing episode II, was deposited during the full-glacial cool, wet climate of the Late Wisconsinan, a time characterized by continental glaciers in Canada and the United States and alpine glaciers in the high southwestern U.S. mountains (Clark et al., 2009). The episode of eolian activity during the last glacial maximum alters the dogma that wind-deposited sands invariably represent periods of aridity; in reality, only wind and a supply of available sand are necessary for the development of eolian deposits.

***Middle Eolian Sand Unit (33–20 ka)*—**The Middle sand has been documented at six localities across the sand sheet (Fig. 3.3). This sand was called the "Late Wisconsin" unit in an earlier report (Hall and Goble, 2016g). The sand is 8 to 83 cm thick and rests directly on caliche in most cases (Fig. 3.5), except at Loc. 16, where it is exceptionally thick and overlies the Lower sand unit (Fig. 3.6). The deposit is a red (2.5YR 4/6-8) fine- to medium- and fine- to very fine-grained quartz sand with 16 to 21 percent clay and up to 0.9 percent iron (Fe). The elevated percentages of clay and iron in the eolian sand are interpreted as an argillic Bt horizon of an unnamed paleosol. The thinness of the unit indicates that it is an erosional remnant. Its rare occurrence and absence from most localities also suggest that it has been largely removed from the region by erosion, probably during the Pleistocene–Holocene transition from cool-wet to warm-dry conditions.

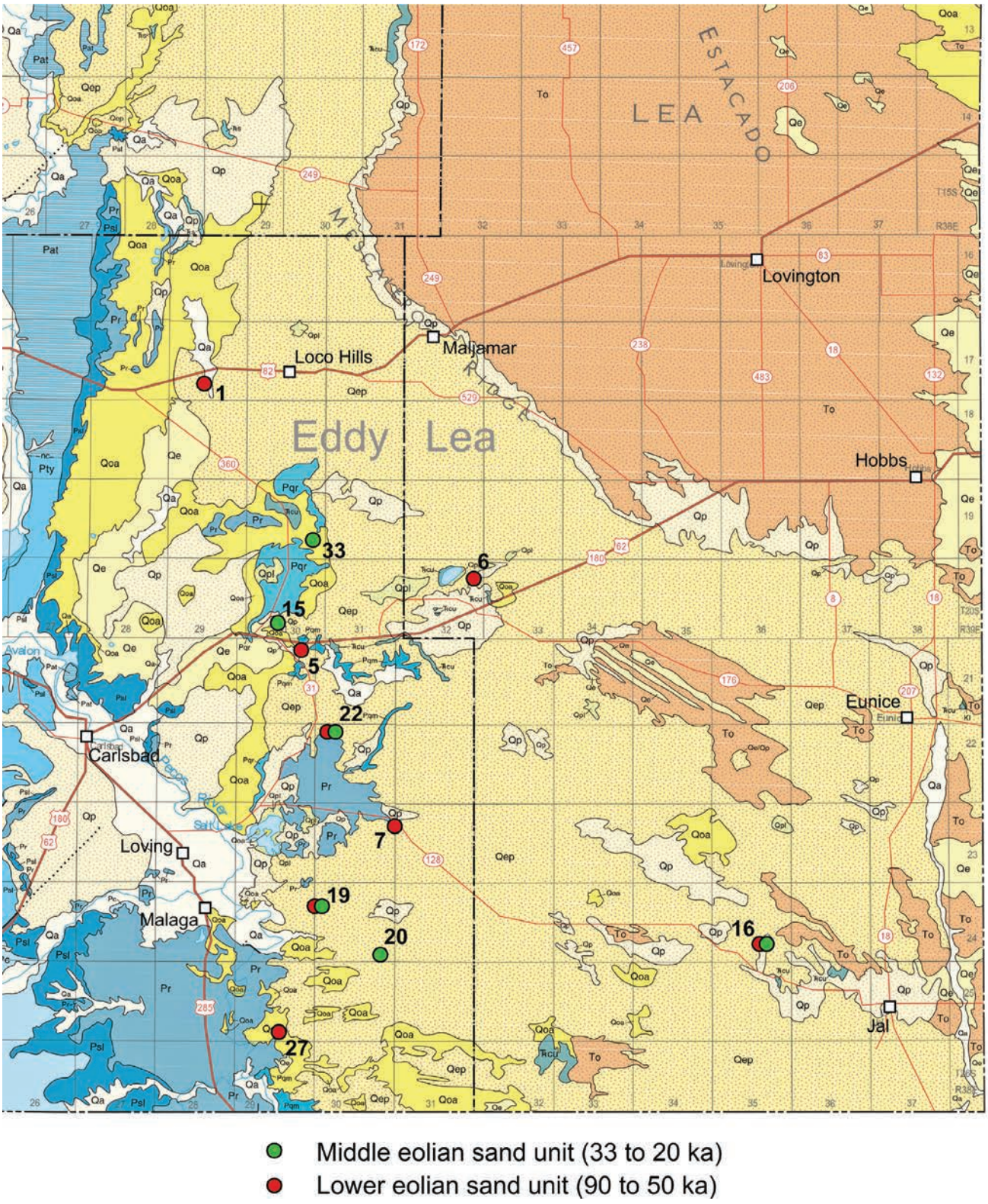

Figure 3.3. Distribution of the Late Pleistocene eolian sand units. Numbered localities are listed in Table 1.1; scale bar and description of geologic units in legend for Figure 1.1.

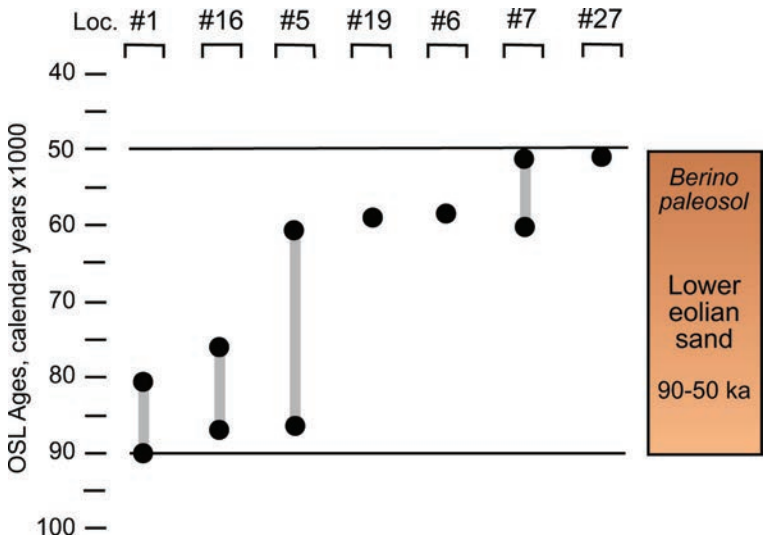

Figure 3.4. Episode I correlation chart. The Lower eolian sand unit representing the first episode of eolian activity has been OSL dated at seven localities (the vertical grey bars are simply a visual aid); in each of these records, the Lower sand rests directly on the Mescalero paleosol and is capped by the Berino paleosol. The Lower sand also occurs at Loc. 22, but was too thin to sample for OSL dating.

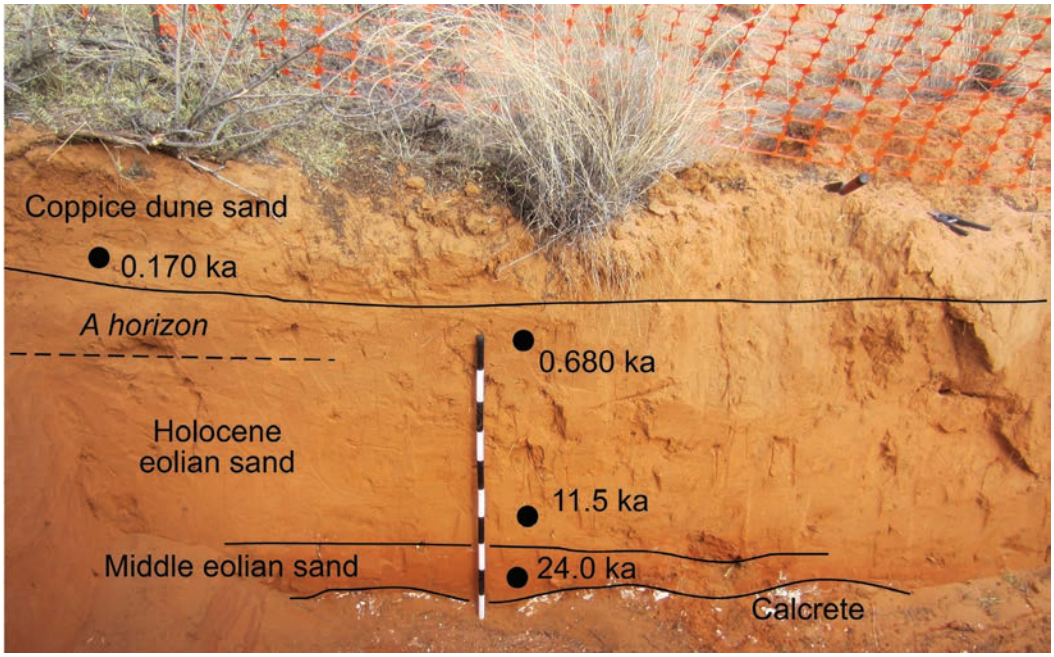

Figure 3.5. A rare occurrence of the Middle eolian sand on calcrete at Loc. 15, dated 24.0 ± 1.2 ka and overlain by Holocene eolian sand with a weak A horizon; 1-m scale. The weak A horizon is preserved beneath the coppice dune but is eroded elsewhere at this locality; it is a weakly developed facies of the Eddy paleosol. This is one of the early records for a coppice dune in the region; the OSL age is 170 ± 30 years (A.D. 1844).

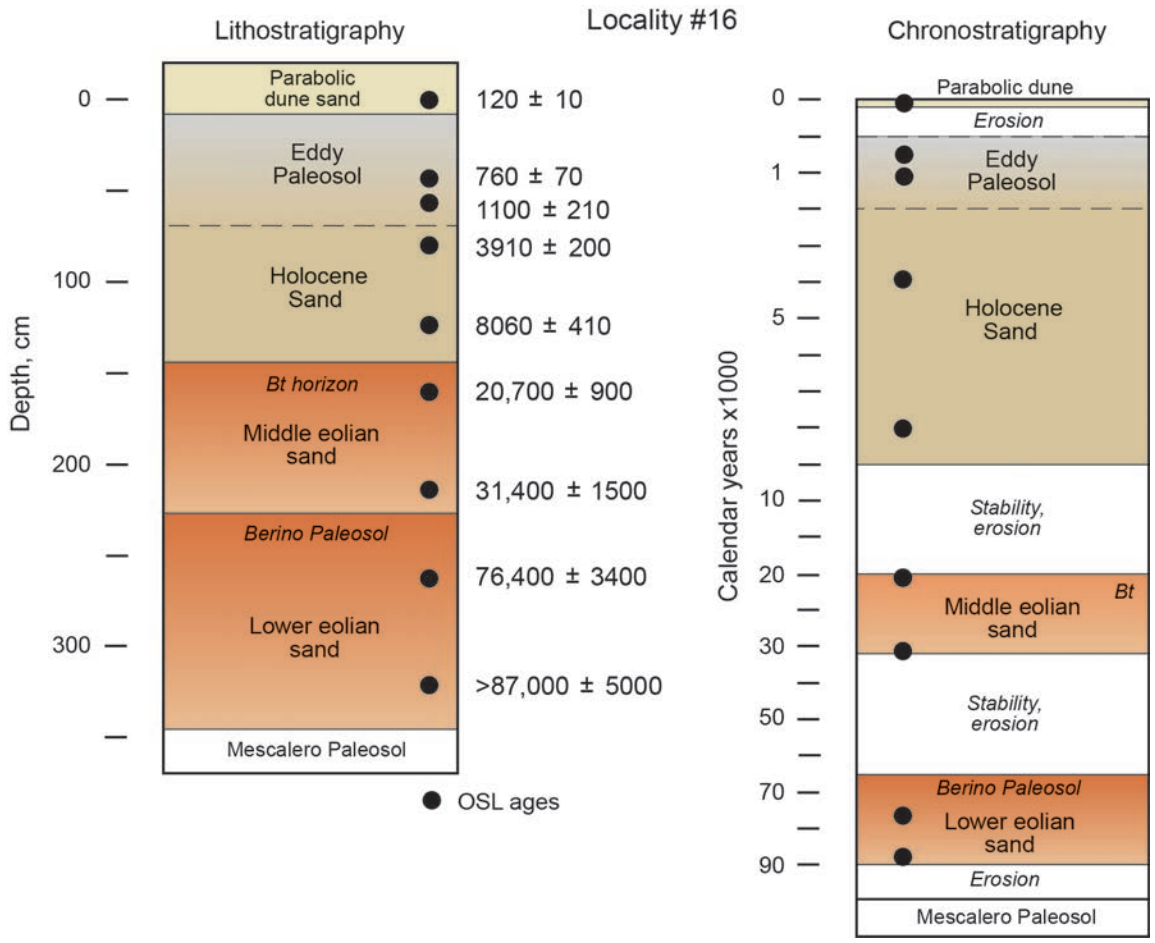

Figure 3.6. Rock and time stratigraphy at Loc. 16 northwest of Jal. This locality is the thickest record of the Middle eolian sand and the only case where it overlies the Lower eolian sand and Berino paleosol. In most other places, the Middle sand rests directly on caliche of the Mescalero paleosol. The Berino paleosol is less well developed at this locality because the deposition of the Middle sand sealed off the Lower eolian sand from soil development during the wet Late Wisconsinan. The Eddy paleosol is well-developed at this locality. The OSL age from near the base of parabolic dune sand is 120 ± 10 years (A.D. 1895). Scale changes at 1, 10, and 30 ka.

Age of the Middle Eolian Sand Unit—The Middle sand was deposited during the last glacial maximum. Worldwide, the growth of ice sheets to their maximum positions occurred during the period between 33.0 to 26.5 ka. Nearly all ice sheets were at their maximum positions from 26.5 to 20–19 ka; Northern Hemisphere deglaciation began 20–19 ka (Clark et al., 2009).

Eight OSL ages from the thin red eolian sand at six different localities range from 32.7 ± 1.7 ka to 20.7 ± 0.9 ka (Fig. 3.7). Overall, the OSL age of the red Middle sand extends from 33 to 20 ka, correlating with the growth of ice sheets and the glacial maximum of the Late Wisconsin stage of the late Pleistocene. The Late Wisconsin age of the Middle sand is consistent with the argillic Bt paleosol that caps the sand; argillic, non-calcic soil development occurred in the region during the time of wetter climate.

During the period of episode II, a thick eolian sand (locally called unit 3; Hall and Goble, 2011b) was being deposited at the eastern margin of the plain, Locs. 11 and 12, near Jal. The 160-cm thick sand is coarse-textured but poorly sorted with a large silt and clay component, characteristics that diverge from the Middle sand at nearby Loc. 16 and elsewhere. The OSL ages from the unit are 38.8, 23.4, and 19.8 ka. Future studies may find that this sand has equivalents east and south in the Texas region of the Mescalero Sands.

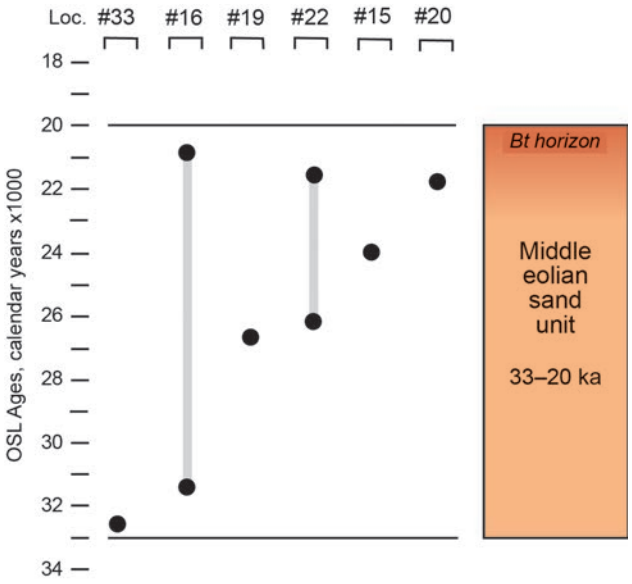

Figure 3.7. Episode II correlation chart; eight OSL ages from six localities of the Middle eolian sand unit. The sand is capped by an unnamed argillic paleosol.

Episode III

The third episode of eolian activity was initiated during the period of climatic warming at the end of the Pleistocene and the beginning of the Holocene. The beginning of sand deposition does not appear to have been instantaneous across the plain but instead occurred over a span of several thousand years from about 18 to 10 ka. However, a characteristic of Episode III is that sand accumulation appears to have ended abruptly about 5,000 years ago, bringing the episode to a close. Specifically why sand accumulation ended may be related to the depletion or shutting down of some sand sources at that time.

Upper Eolian Sand Unit (18 to 5 ka)—The Upper sand was first described, along with the Lower unit, from northern Eddy County (Hall, 2002a; Hall and Goble, 2006). Subsequently, eolian sand deposits correlating with the Upper unit have been reported throughout the Mescalero Plain. Younger, post-Upper eolian sands have also been found and dated in many places. The younger deposits are described later.

North of Loco Hills, the Upper sand exposed in deep blowouts of large parabolic dunes in the core of the sand sheet is unusually thick, up to 4.5 meters. At the margins of the sand sheet, the Upper sand is less than 1.0 meter in thickness. The sand is reddish yellow (5YR 6/6) fine- to very fine-grained quartz sand; at one section, the sand texture coarsens upwards. Overall, the sand is well sorted and does not contain coarse or very coarse grains. The grains are subround to round. The sand contains less than 1 percent silt and less than 3 percent clay. This unit is largely non-calcareous. The thick sands are massive without structures or bedding. Soil horizons or paleosols have not been found in association with the thick Upper sands north of Loco Hills.

The Upper sand is characterized by a 1.2-m-thick zone of clay bands that occur in the middle of the sand deposit between about 1.5 and 3.0 m depth (Fig. 3.8). The bands are yellowish red (5YR 5/8), slightly darker in color than the reddish yellow color of the surrounding sand. Each band is about 5 mm thick. The bands are discontinuous and extend laterally no more than about one meter. In one analysis, they contain 6.6 percent clay compared to 2.0 to 2.5 percent clay in surrounding sand. Clay bands are found only in the thick Upper sand. Elsewhere on the sand sheet where the Upper sands are comparatively thin, clay bands are absent.

The Upper sand south of Loco Hills is much thinner, about 0.8 to 1.1 m (Fig. 3.9). The sand is yellowish red to reddish brown (5YR 4/4-6), fine- to medium-grained quartz sand. The texture fines upwards slightly; grains are subround to subangular. The sand is massive without bedding. Silt content is 4 to 8 percent, and clay is 6 to 14 percent.

The Upper sand is capped by a soil Bw or AB horizon in different places. This is the only sand unit in the Mescalero Sands, in this study region, with a Bw horizon. A calcic Bk horizon commonly occurs below 40 to 50 cm depth. The soil horizons are described in detail in chapter 9 on paleosols.

Age of the Upper Eolian Sand—Sixteen OSL ages from six localities define the age of the Upper sand (Figs. 3.10–3.12). The basal ages indicating the beginning of deposition of the unit range from 17,300 ± 700 to 9,190 ± 460 years. An explanation for the wide range in ages for the initial deposition of the sand is not evident. The youngest age of the Upper sand is 4,990 ± 370 years. The deposition of the Upper sand does not continue after 5 ka. The end of sand accumulation may be a result of the depletion of the reservoir of sand at their sources. Overall, the age of the unit is summarized as 18 to 5 ka.

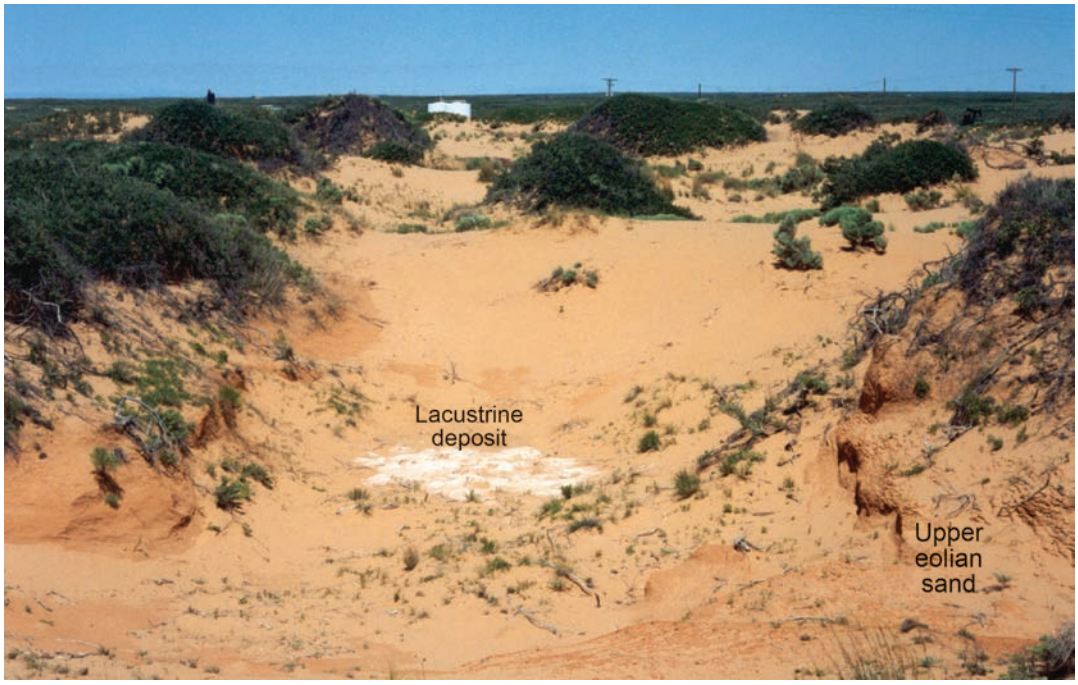

Figure 3.8. Blowout exposing the Upper eolian sand along Booger Langston Road, northern Eddy County at Loc. 2; the Upper sand has clay bands in this area; this is the locality where the (revised) OSL ages 9.39 ± 0.67 ka and 5.82 ± 0.41 ka were obtained (Hall, 2002a; Hall and Goble, 2012); photograph July 3, 2001. A lacustrine deposit is exposed in the floor of the blowout; it contains shells of land and freshwater snails and is probably Late Pleistocene in age. The 9.39 ka basal age for the Upper sand at this locality was collected about 5 cm above the pond deposit. The mounds of sand along the edges of the blowouts are erosional pillars of Upper sand, protected by shinnery oak. Since 2013, this blowout has been partly filled with sand and the lacustrine deposit may not be exposed today.

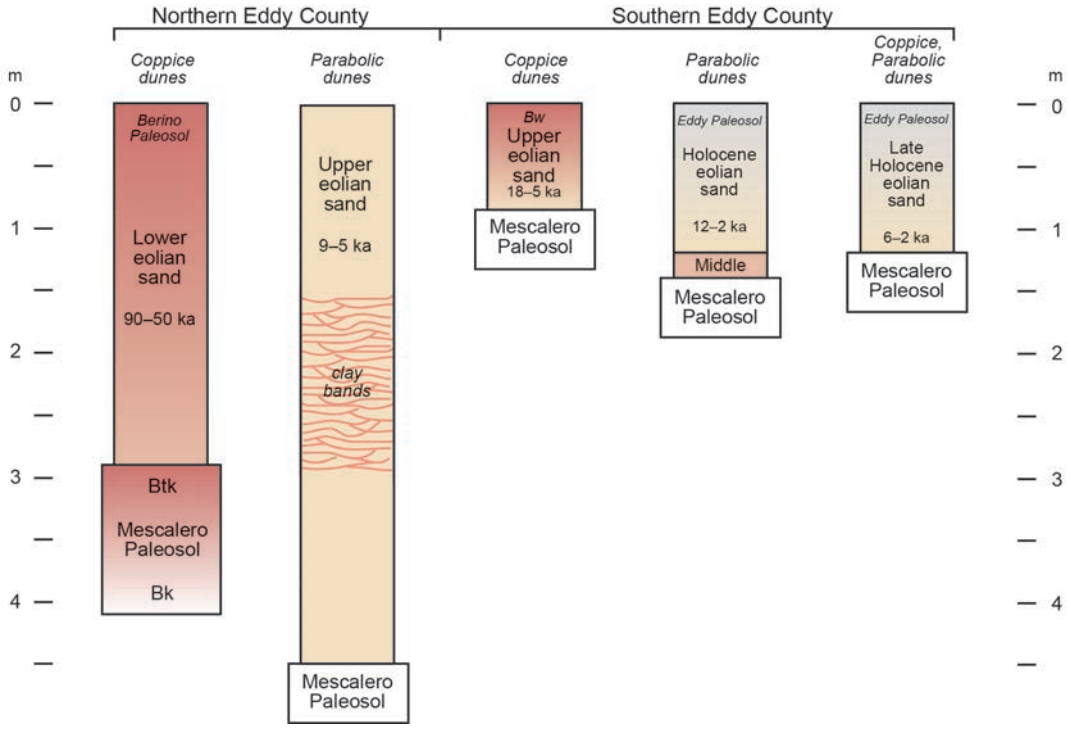

Figure 3.9. Contrasting sequences of eolian sand in northern and southern Eddy County; the Lower and Upper sand units can be much thicker in the north around Loco Hills; to the south, the units are thin. The Holocene and Late Holocene units appear to be more common in the south.

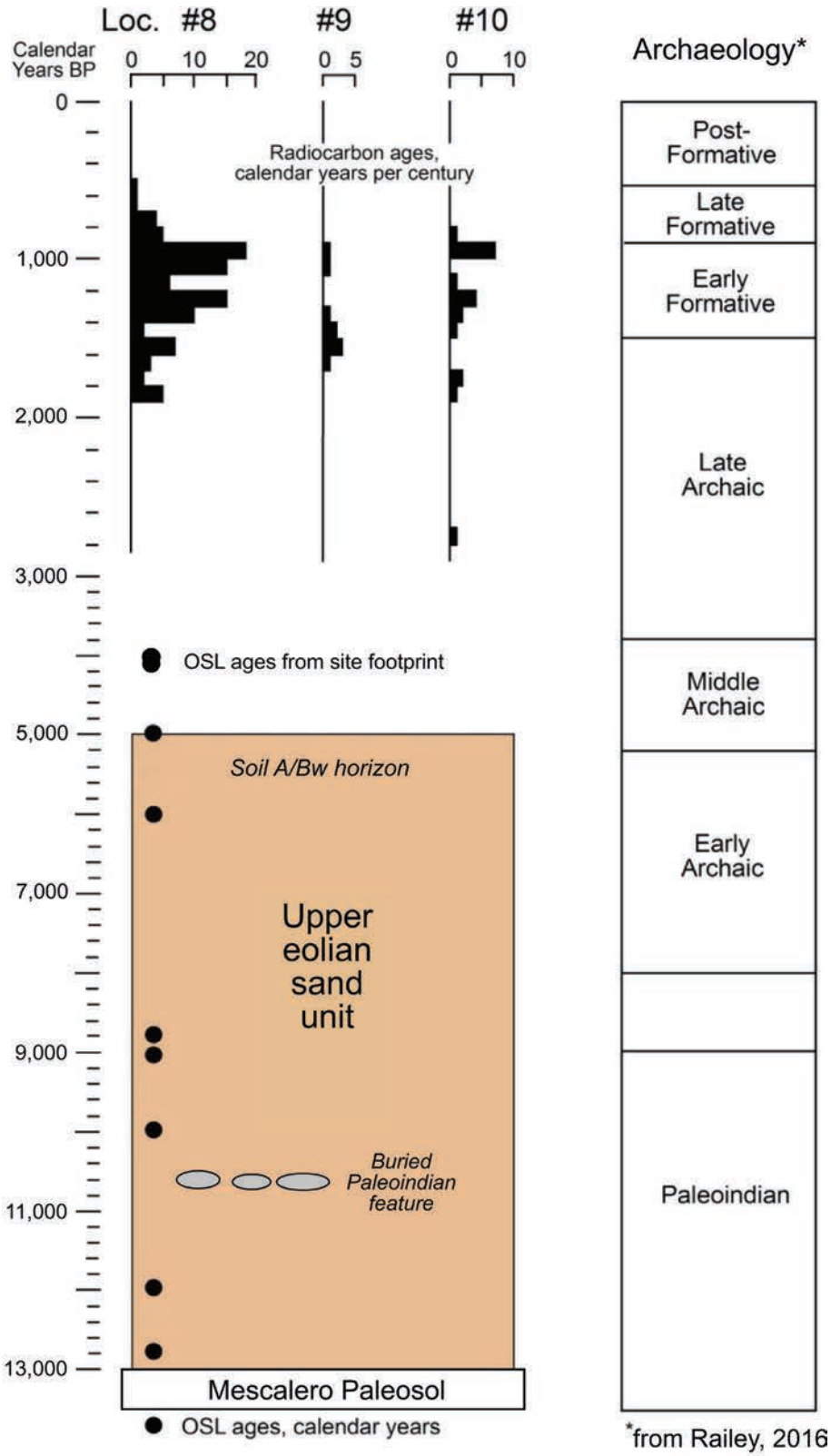

Figure 3.10. Chronostratigraphy of OSL-dated Upper eolian sand unit with AMS radiocarbon-dated archaeological features of three sites (Locs. 8, 9, 10), western Mescalero Plain (modified from Hall and Goble, 2016a). The sites are located on and intrude into the stable surface of the Upper eolian sand. The OSL ages shown are a composite from Locs. 8 and 9.

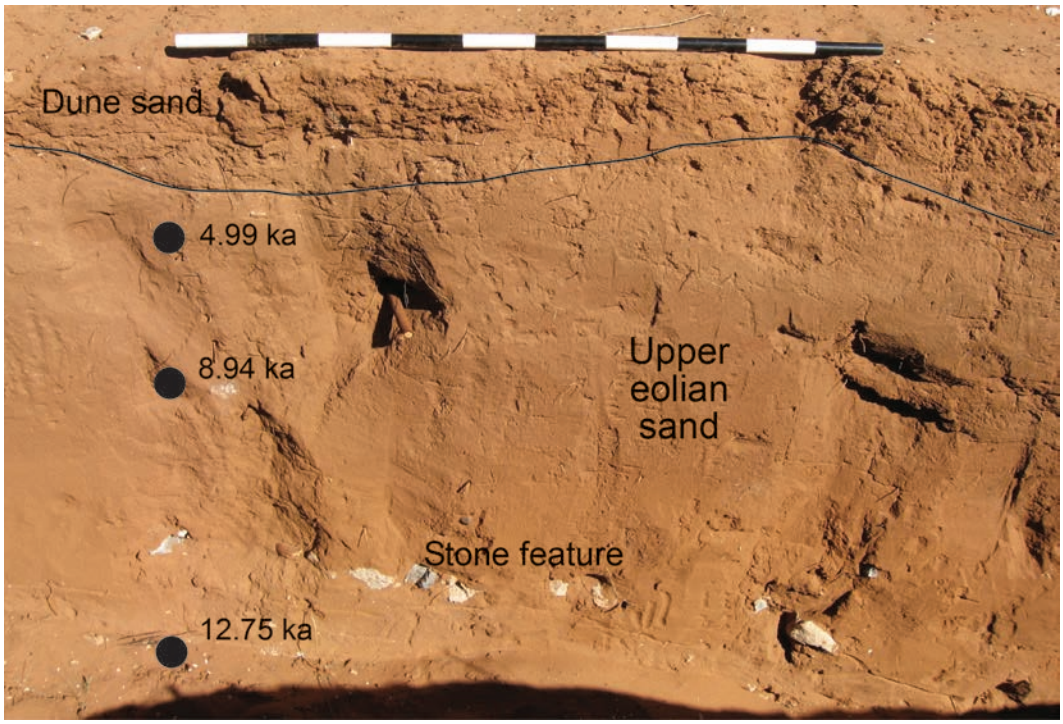

Figure 3.11. Upper eolian sand unit at Loc. 8 along NM 128 near the junction with NM 31 with an in situ archaeological stone feature buried at 58 cm depth; 1-m scale. OSL ages are from a column to the left of this view but are shown here in correct stratigraphic position; interpolated age of the feature is 10.6 ka, correlating with the Late Paleoindian period. Artifacts were not recovered from the stone feature. However, the archaeology at the surface of the Upper eolian sand is Late Archaic and Early Formative. The discovery of the Late Paleoindian feature in the trench was a surprise; there was no surface indication that the feature was present in the subsurface (modified from Hall and Goble, 2016a).

The sediment accumulation rate of the Upper sand, measured at three sites in southern Eddy County, ranges from 0.080 to 0.110 mm per year, a similar level found in the other sheet sand deposits in the plain (Fig. 3.13). The much thicker occurrence of the Upper sand in northern Eddy County has a comparatively higher sediment accumulation rate of 0.896 mm per year; the greater thickness of the Upper sand unit in the north may be a consequence of the more rapid rate of sand accumulation and a source of abundant sand.

Episode IV

Episodes IV and V present a minor dilemma. In both episodes, eolian sand was deposited during the Holocene. The deposits have similar texture, the same absence of soil development, both are scattered across the south area of the plain (Fig. 3.14), and both were deposited up to 2 ka and are capped by the Eddy paleosol (Fig. 3.15). From a practical point of view, their appearance is similar and they could be regarded as one stratigraphic unit.

On the other hand, the single most important attribute of the eolian sand units is their geochronology. The sole significant difference between the Holocene and Late Holocene sets of deposits is their age (although their rates of sedimentation differ, 0.107 and 0.228 mm/yr, respectively). The sand of episode IV began to be deposited ca. 12 ka; the sand of episode V was first deposited much later, by ca. 6 ka. The difference in the timing of their initial deposition indicates to us that the geomorphic conditions of the availability of the supply of sand were not the same for the two sets of deposits. The episode IV sand began to accumulate at the Pleistocene-Holocene transition when the climate began to shift from cool-wet to warm-dry conditions. The episode V sand instead began to accumulate during the arid climate of the middle Holocene. The climatic conditions of the early formation of the two sand sheets were clearly dissimilar and must have played a pivotal role in their sand supply and initial development.

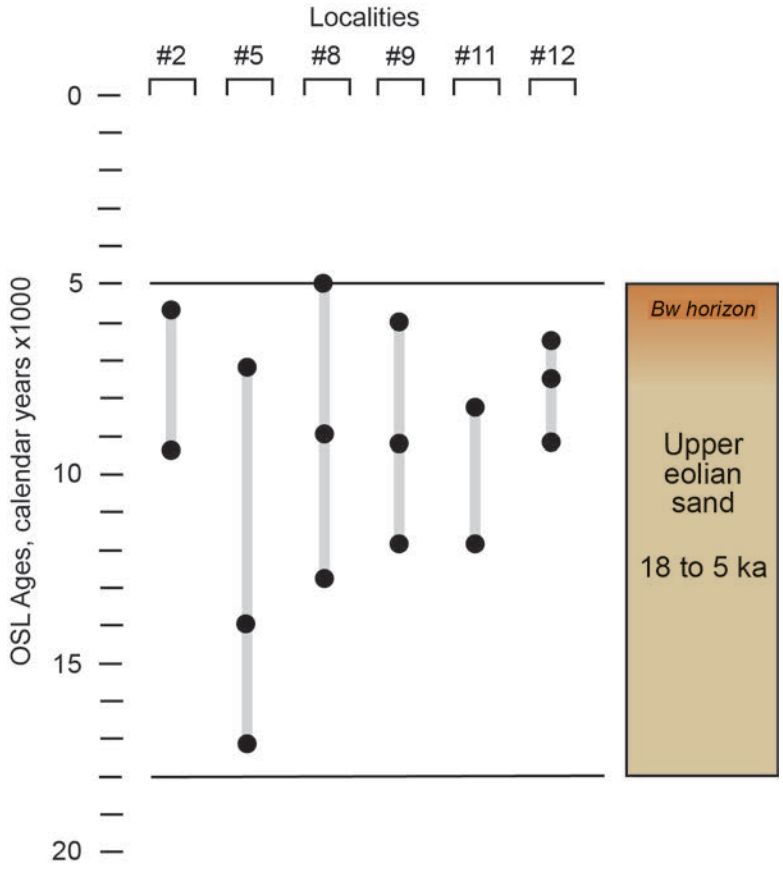

Figure 3.12. Episode III correlation chart. Sixteen OSL ages have been obtained from the Upper eolian sand at six localities across the Mescalero Plain.

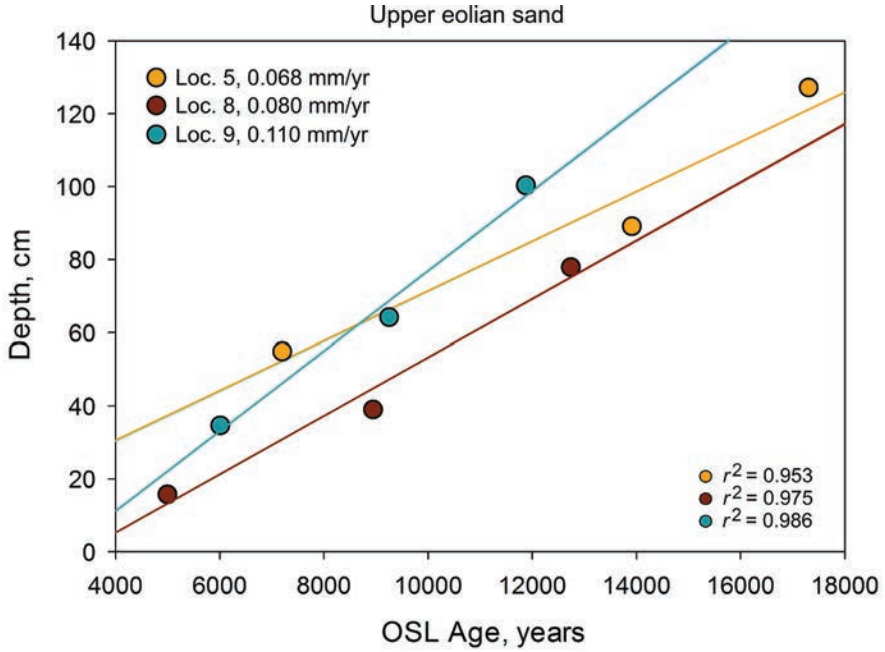

Figure 3.13. Upper eolian sand unit sedimentation rates of 0.068, 0.080, and 0.110 mm/yr at Locs. 5, 8, and 9, respectively; data in Table 5.1.

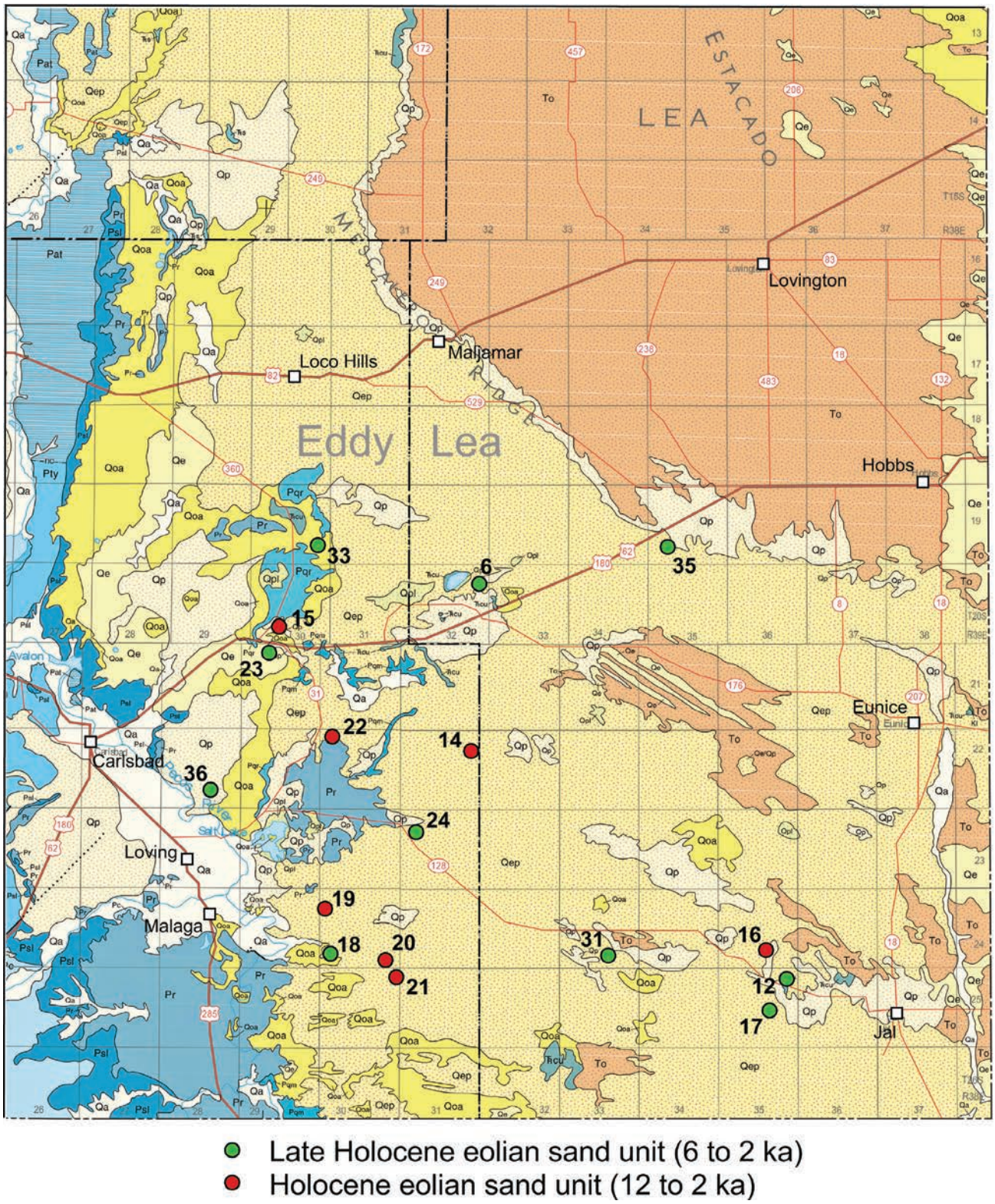

Figure 3.14. Map of Holocene (episode IV) and Late Holocene (episode V) eolian sand units; scale bar and description of geologic units in the legend of Figure 1.1.

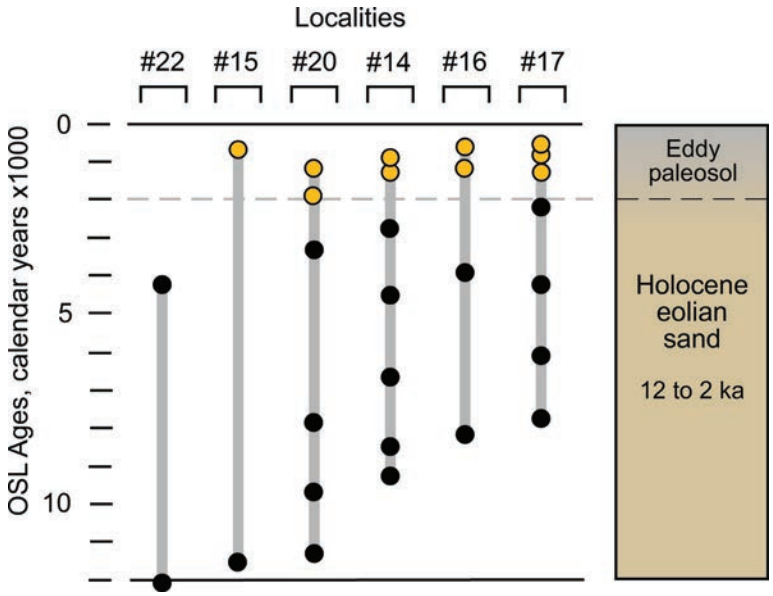

Figure 3.15. Episode IV correlation chart; OSL-dated sections of the Holocene eolian sand unit. All localities are capped by the Eddy paleosol (shown in yellow); the Eddy paleosol occurs at Loc. 22, but was not dated.

Another aspect of the situation concerns the geologic conditions under which the sand sheet was scoured down to weathered caliche (or sustained a long period of non-deposition) until the middle Holocene when the Late Holocene eolian sand began to accumulate. Our extensive research in the area has not provided a clear explanation of this phenomenon.

We are of the opinion that keeping apart these two individual packages of eolian sand is prudent; future studies may reveal information about the two sand bodies that further clarify their differences. At this stage, they appear to be products of different sources of sand that are related to different climatic conditions that in turn resulted in different timing of sheet sand accumulation events. In the meantime, we treat the episode IV and V sands as separate entities.

Holocene Eolian Sand Unit (12 to 2 ka)—At least six localities document the initiation of eolian sand deposition during the transition from Pleistocene to Holocene environments 12 to 8 ka. The same six records suggest continuous sand accumulation into the late Holocene with all of the deposits ending with the development of the Eddy paleosol A horizon (Figs. 3.15–3.18). Unlike Episode III where sand deposition ended about 5,000 years ago, the sand accumulation within Episode IV encompasses most of the Holocene to about 2 ka. Buried archaeology has the potential to occur anywhere within these eolian sand deposits.

The Holocene eolian sand rests directly on caliche of the Mescalero paleosol at three of the six study localities. At the other three sites, the unit overlies the Middle eolian sand unit. The massive Holocene eolian sand deposits range from about 0.7 to 1.1 m thick. The sand is commonly yellowish red (5YR 4/6) but can be redder, depending on the source sand. The sand is fine to medium textured. Grains are round to subround with some polish. Silt and clay are each about 2 to 5 percent. Carbonate is generally absent or occurs in very low amounts; calcic Bk horizons have not formed in the Holocene sand. An exception at Loc. 14 has up to 10 percent carbonate and 10 percent clay at depth, suggesting the presence of a Bk horizon (Fig. 3.16); however, the elevated percentages of carbonate may be related to the percentages of clay in the sediment and not to pedogenesis.

Age of the Holocene Sand—Eighteen OSL ages from the Holocene unit range from 12,400 ± 600 ka to 2,090 ± 70 ka. In some places, deposition of the sand did not begin until about 9 ka. The accumulation of the Holocene unit ends with the development of the Eddy paleosol A horizon beginning 2,000 years ago (Fig. 3.15).

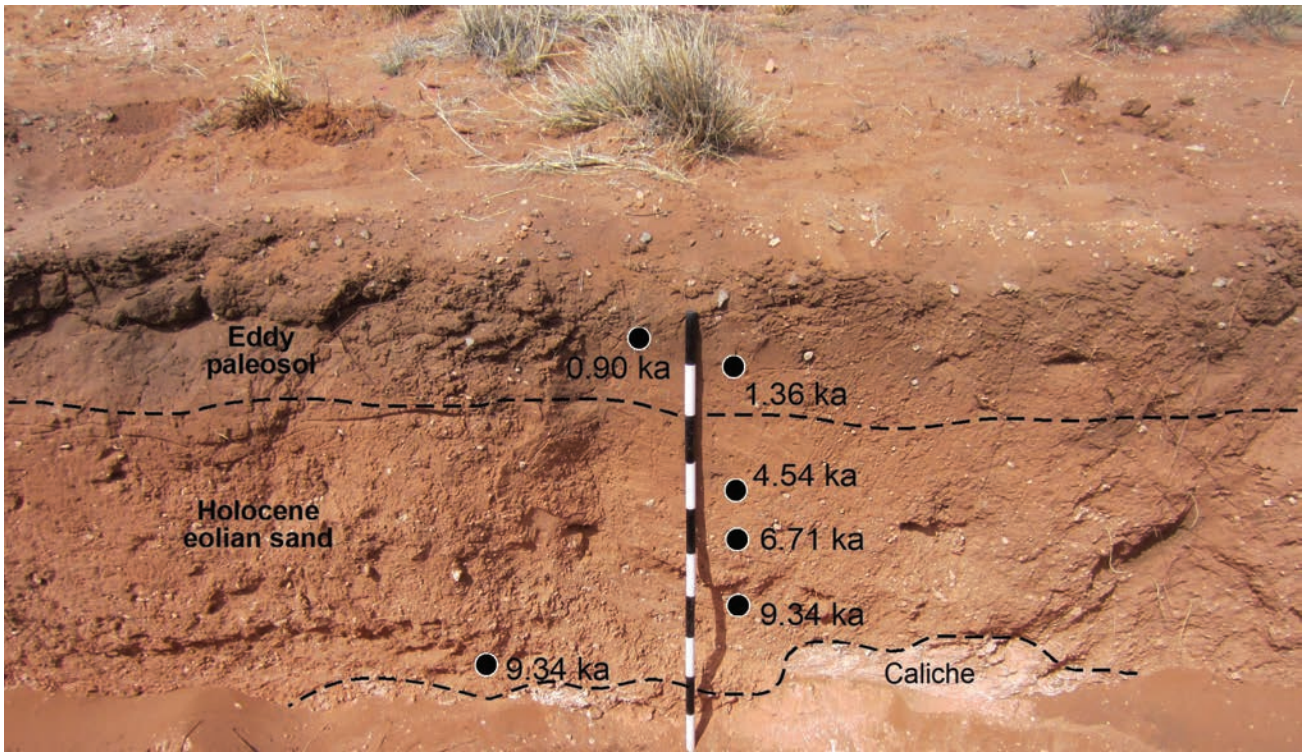

Figure 3.16. Holocene eolian sand capped by the Eddy paleosol at Loc. 14; two near-basal OSL ages from the Holocene sand above the caliche are the same; the sand contains many small caliche pebbles, probably due to bioturbation. Holocene eolian sand from an adjacent trench is OSL-dated 8.51 and 2.76 ka; 1-m scale.

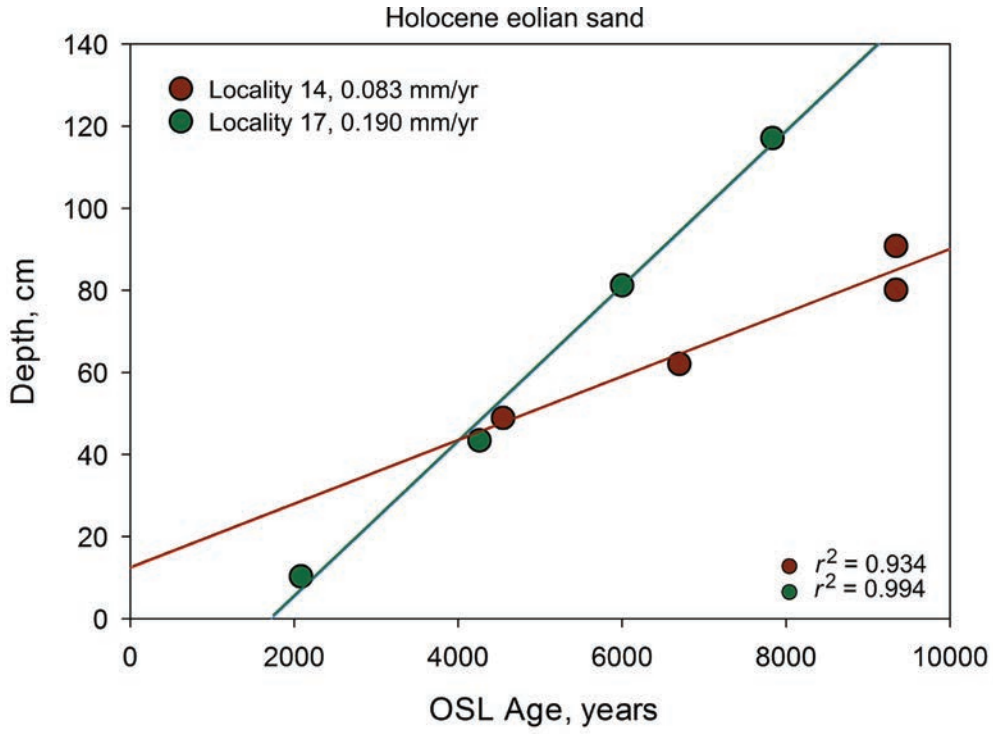

Figure 3.17. Sedimentation rates of OSL-dated Holocene eolian sand unit, Locs. 14 and 17; the accumulation rates are 0.083 and 0.190 mm/yr (data Table 5.1)

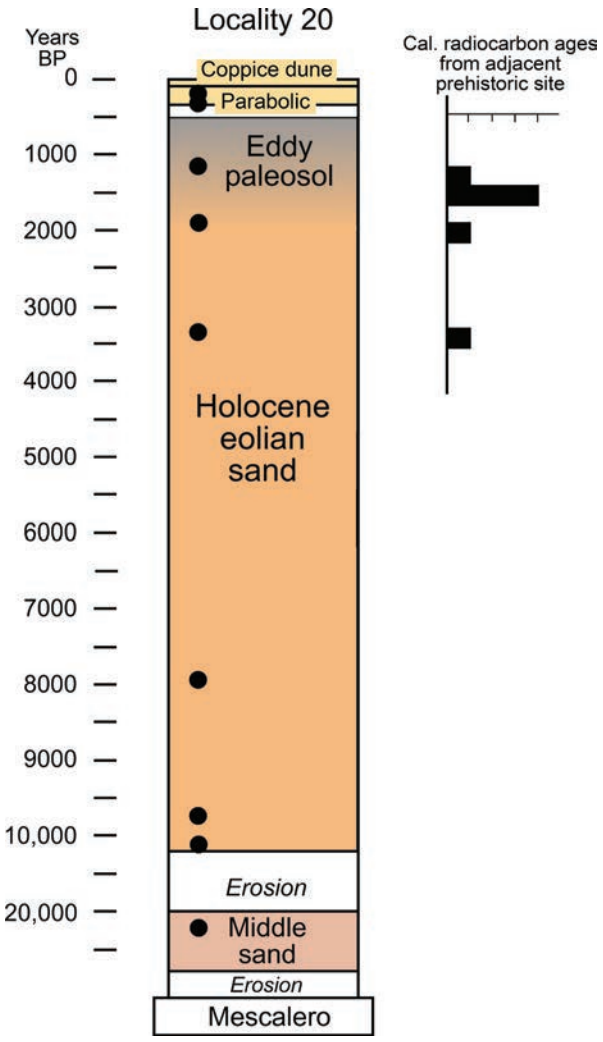

Figure 3.18. Episode IV Holocene eolian sand and underlying episode III Middle eolian sand at Loc. 20, southern Eddy County. Middle sand dated 21.7 ka; Holocene dated 11.3 to 3.39 ka; Eddy paleosol dated 1.86 and 1.06 ka; parabolic dune dated 280 and 220 years; coppice dunes have formed on top of parabolic dune sand at this site. Late Archaic and Early Formative archaeology is buried in the Holocene sand although partly exhumed in blowouts of parabolic dunes; a Middle Archaic feature was exposed in a trench; scale change at 10 ka.

Episode V

It is ironic that episode V eolian activity begins by ca. 5,000 years ago at the same time that episode III ends. The change in eolian deposition most likely represents a change in the sources of sand; the supply of sand available for eolian transport shifted from one source to another. Although the specific sources and changing conditions have not been identified, we speculate that the potential source sands are derived from (a) sandy channels of ephemeral streams and gullies or (b) deflation of older, pre-existing eolian sand deposits on the sand sheet. The availability of sand from these sources is likely determined by the interaction of climate and climate change with vegetation and fluvial geomorphology.

Late Holocene Eolian Sand Unit (6 to 2 ka)—The Late Holocene eolian sand rests either on caliche of the Mescalero paleosol or on Pleistocene deposits. This unit has not been found overlying the Upper eolian sand unit even though it post-dates the Upper unit. It is commonly about 0.8 to 1.5 m thick. Because of its young age, the sand is soft and lacks induration. The unit is generally capped by the Eddy or Loco Hills paleosol (Figs. 3.19, 3.20).

The sand is commonly yellowish red (5YR 4/6) or can have a slightly darker color where influenced by the overlying Eddy paleosol. The texture is fine- to medium-grained or fine- to very-fine-grained quartz sand. Silt and clay percentages are generally less than 5 percent each. Grains are round to subround; many grains lack coats; some grains have polish. Most Late Holocene sands are non-calcareous with laboratory measurements of less than 1 percent carbonate. In one case, carbonate increases from 1.0 to 2.3 percent with greater depth.

Age of the Late Holocene Eolian Sand Unit—The late Holocene sand is OSL dated at five localities, the ages ranging from 5,370 ± 280 years to 2,180 ± 100 years (Fig. 3.21). Overall, we summarize the age of the unit as 6 to 2 ka. After 2 ka, the Eddy paleosol A horizon formed at most localities. However, beginning 300 years ago, the Eddy paleosol and underlying Late Holocene sands were deflated, and parabolic dunes formed, especially at places where the underlying sand is thick, such as at Loc. 24.

Figure 3.19. Late Holocene eolian sand capped by the Loco Hills paleosol and mantled by the Cover sand unit at Loc. 23 along Quahada Ridge. Note that the Cover sand that buries the Loco Hills paleosol thickens upslope, away from the camera. The Cover sand at this locality is OSL dated 90 ± 20 years (A.D. 1918); its presence hides prehistoric sites unless the sand is disturbed, exposing underlying artifacts and features; 1-m scale.

Episode VI

Dunes and Cover Sand—Beginning about 2,000 years ago, the Mescalero sand sheet stabilized with the development of the Eddy paleosol. For the next 1,700 years, the plain was stable and the cumulic topsoil of the Eddy paleosol built up slowly across the region. Beginning about 300 years ago, the sand sheet became active; deflation carved into the soil, and winds transported sand across the plain. Sand from thick late Holocene-age sediments was redeposited as parabolic dunes (Fig. 3.22). Some of the sand escaped the dunes and was carried away and accumulated as a thin layer of cover sand on the ground surface. Where mesquite shrubs and small mesquite trees were present, sand accumulated around them, forming coppice dunes. Eventually, perhaps in response to heavy grazing by livestock in the nineteenth century, mesquite shrubs increased in abundance and expanded their range at the expense of grasses. The mesquite eventually overwhelmed the semi-arid vegetation. Where mesquite expanded and thrived, coppice dunes followed, and today coppice dunes dominate much of the sandy plain.

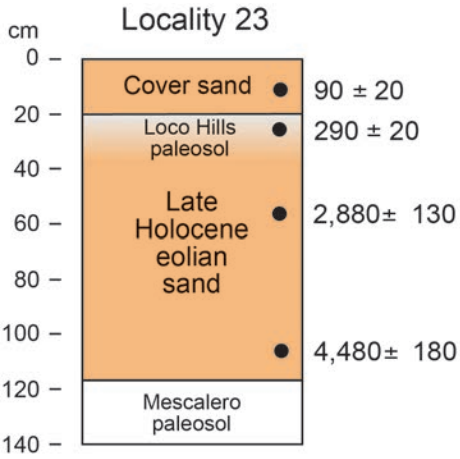

Figure 3.20. OSL-dated stratigraphy with Late Holocene eolian sand, Loco Hills paleosol, and Cover sand on Quahada Ridge, Loc. 23; prehistoric site occurs on the Late Holocene sand and is dated 670 and 1,420 cal yr BP; subsequently, the Loco Hills paleosol formed across the locality and the site.

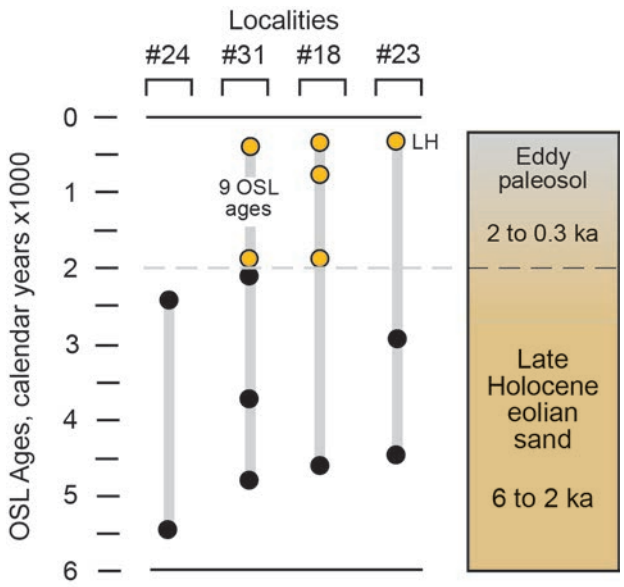

Figure 3.21. Episode V correlation chart. Summary of OSL-dated Late Holocene eolian sand localities; the Late Holocene sand rests directly on caliche of the Mescalero paleosol in three of these cases (Locs. 18, 23, 31). At Loc. 24, the Late Holocene sand rests on Pleistocene deposits. The Eddy paleosol (or Loco Hills paleosol, LH) caps the sequences. OSL ages from the Eddy A horizon are shown in yellow.

Parabolic Dunes—Parabolic dunes are common in areas of the sand sheet where Holocene sand is greater than about one meter in thickness. Dunes are rarely present where the eolian sand is less than one meter in thickness, and the dunes are absent where the substrate is Permian-Triassic bedrock, Pleistocene Lower sand, or the Mescalero paleosol. Many of the dunes are small and circular in outline around a blowout, extending 10 to 20 meters across and slightly elliptical in the long direction of prevailing winds (Figs. 3.23, 3.24). The relief of the dunes, from the lowest point in the blowout to the highest point at the downwind crest, can vary from 0.9 to 2.5 meters. Melton (1940) referred to these as blowout dunes. As blowouts become larger, they spread outward forming a U-shaped geometry. With the passage of time, blowouts merge, forming larger, higher dunes with elongated blowouts (Fig. 3.25). The relief of larger dunes can extend 3 to 4 meters above the floor of their blowouts.

The comparatively thick sand cover where parabolic dunes abound is characterized everywhere by shinnery oak (*Quercus havardii*) (Peterson and Boyd, 1998). Indeed, an abundance of shinnery oak is always an indication that at least one to two meters of Holocene sand is present in the subsurface.

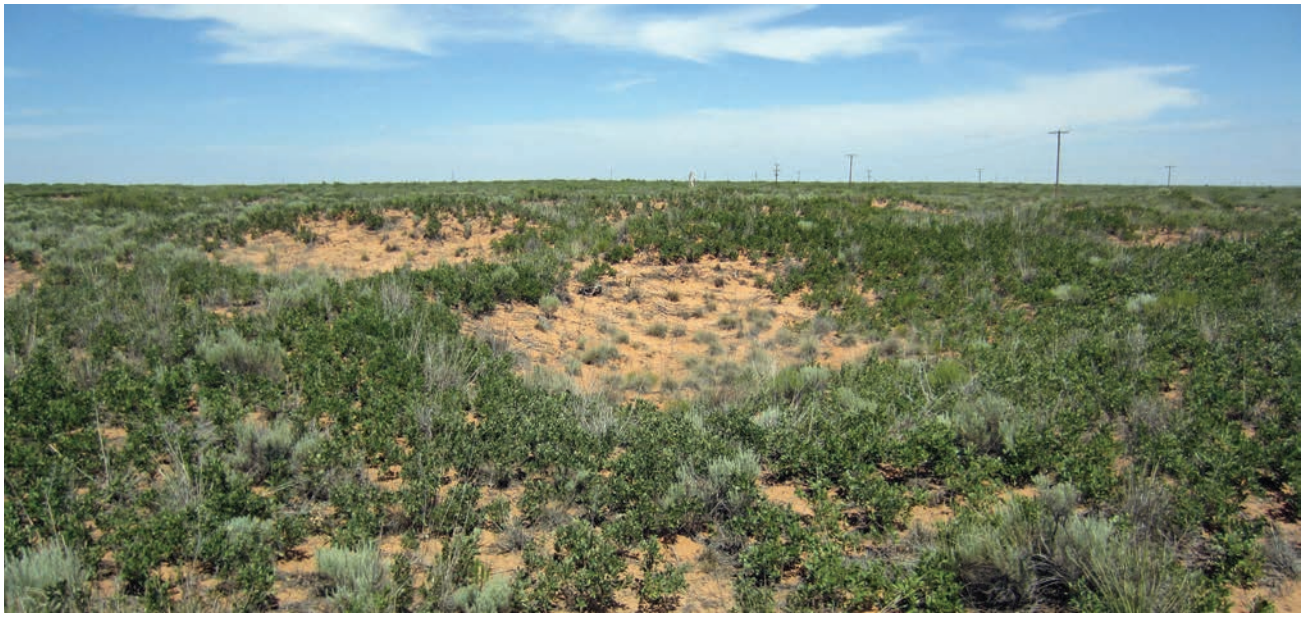

Figure 3.22. Small parabolic dunes, 10 to 20 m across, southern Lea County; these dunes and adjacent sand deposits are partly stabilized by shinnery oak (*Quercus havardii*); view facing east, dune-forming wind from behind.

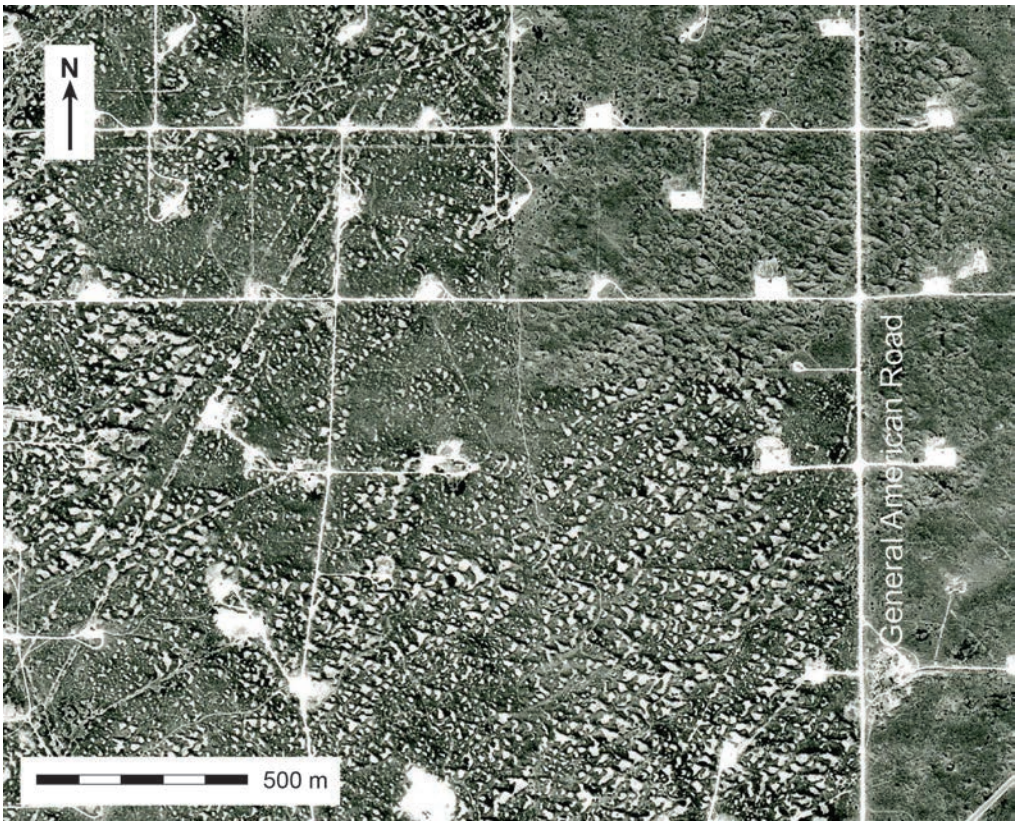

Figure 3.23. Parabolic dune field 2.8 miles southwest of Loco Hills, northern Eddy County, along General American Road; black and white aerial photo taken November 1, 1997. Most of the active parabolic dunes in this image appear to have a due west-to-east element in their orientation. Stabilized parabolic dunes occur in the northeast area of this image; this area appears to have become active by 2005 based on later aerial photos. The direction of orientation of the stabilized dunes is approximately 36° east of north, the winds are from the southwest (National Aerial Photography Program [NAPP], U.S. Geol. Survey, 9615-81).

Figure 3.24. Parabolic dune with U-shaped blowout, southern Lea County; view facing south, wind direction from right to left. The vegetation is shinnery oak with a few mesquite shrubs on the far edge of the dune; photograph August 27, 2011.

All blowouts of large and small dunes alike are eroded down into the Holocene sand in which the dunes have formed. If archaeology is present in the Holocene sand, artifacts will be exposed and concentrated on the floor of the blowout. In the largest parabolic dunes, the blowouts will extend deep unless a resistant layer in the substrate is encountered, such as caliche or lacustrine clay.

***Parabolic Dune Ages*—**The earliest OSL age of a parabolic dune in the Mescalero Plain is 310 ± 40 years or A.D. 1706. Elsewhere in the area, basal ages of parabolic dunes are 280 ± 20 years (A.D. 1734), 230 ± 70 years (A.D. 1785) and 170 ± 40 years (A.D. 1845). These are the first direct dates on eolian sand from parabolic dunes in the region. At present, we do not have enough information to detect geographic patterns on the timing of dune formation. The similarity of ages, however, suggests that parabolic dunes that we see across the sand sheet today are all a product of eolian activity that began about 300 years ago and that has continued into the twentieth century. Aerial photography indicates that different areas of parabolic dunes may be undergoing active formation in the late twentieth century.

The youngest OSL age from a parabolic dune is 100 ± 14 years (A.D. 1915), verifying early twentieth century eolian activity. In the field, some dunes have scoured blowouts and appear to be active today. In other areas, however, blowouts have a modest cover of grasses, weedy plants, and shinnery oak seedlings, suggesting that these areas of parabolic dunes have more or less stabilized, perhaps temporarily. Coppice dunes sometimes form around isolated honey mesquite shrubs on the flanks of parabolic dunes. In these cases, the mesquite coppice dunes post-date the age of the parabolic dunes.

***Coppice Dunes*—**Hundreds of thousands of coppice dunes occur in southern New Mexico. Nearly all of the dunes in the Mescalero Sands have formed around Torrey mesquite (*Prosopis glandulosa torreyana*). It has a low-growth profile around which most of the coppice dunes have formed. In some areas, honey mesquite (*P. glandulosa glandulosa*) is found; it is more tree-like, although coppice dunes form around it as well where sand is abundant. Small accumulations of sand may also occur locally with other shrubs such as javelina bush (*Condalia ericoides*) and soapweed yucca (*Yucca glauca*).

Figure 3.25. A complex of medium-sized parabolic dunes east of Loc. 21 about 0.6 km (1 mile) from where early dunes are dated 280 ± 20 years (A.D. 1734); the local vegetation is shinnery oak; photograph March 14, 2015.

Coppice dunes form where mesquite shrubs are present to capture wind-transported sand. Thus, the age of the dunes reflects the timing of the increased abundance and range of mesquite; dunes follow the mesquite. Prior to the increase in mesquite, wind-blown sand from late nineteenth century rangeland disturbance accumulated as thin layers of Cover sand across the ground surface. When mesquite showed up, most of the sand then accumulated around the shrubs, forming coppice dunes.

Most of the coppice dunes in southeastern New Mexico are fairly small, about 0.5 to 1 meter high and 3 to 9 meters in diameter (Figs. 3.26, 3.27). Dunes may be much larger where small dunes merge with closely growing mesquite, forming one large sand mass. Where dunes are prominent, dune density is about 90 to 105 per hectare. The sand that makes up the dunes is derived from deflation of Pleistocene or Holocene eolian sands that occur at the present-day surface. The texture of the sand in the dunes is generally the same or similar to that of the underlying sand, indicating that the dunes are formed from local sand in the immediate area of the dunes.

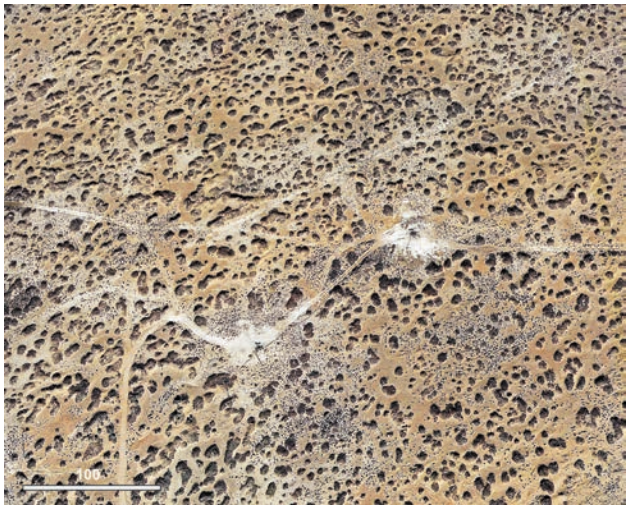

Figure 3.26. Mesquite coppice dune field 5.8 miles southwest of Loco Hills developed on the late Pleistocene Lower eolian sand; the Loco Hills paleosol is commonly present beneath the dunes in this area; the mesquite shrubs (dark green color) are Torrey mesquite (*Prosopis glandulosa torreyana*); natural color aerial photo, October 2017. The two disturbed white areas are old well pads with oil well pump jacks; north is up.

***Coppice Dune Ages*—**The ages for mesquite coppice dunes have been determined at five sites by OSL dating, along with trace radioisotopes at one locality (Fig. 3.28). The earliest OSL-dated dune in the region, 270 ± 30 years (A.D. 1745), occurs in the southwest corner of the Mescalero sand sheet (Loc. 27). It is developed on the eroded surface of the Eddy paleosol, which in turn was formed on Holocene eolian sand. The youngest coppice dune OSL age is 71 ± 6 years (A.D. 1943) at Loc. 31-B.

***Coppice Dune Sedimentation Rate*—**OSL ages from two coppice dunes at localities 4 and 31-B provide rates of eolian sand deposition: 16.2–24.0 and 14.6 mm/yr, respectively (Fig. 3.29). The accumulation of sand in coppice dunes represents the most rapid rate of sedimentation to be found in the Mescalero Sands.

***Cesium Age of Coppice Dune*—**Cesium-137 (^{137}Cs) is a fission product of atmospheric testing of nuclear weapons, first showing up in worldwide sediments in 1954 and peaking in 1963 (Jeter, 2000). Along Square Lake Road northeast of Loco Hills, a 96-cm-high mesquite coppice dune was selected for OSL and cesium-137 dating (Loc. 4) (Fig. 3.30). Cesium was found in the sand above 22 cm depth, indicating that that the sand above that level was deposited since about 1954. However, two high resolution

Figure 3.27. Mesquite coppice dunes, near Loc. 31, southern Lea County; the mesquite leaves are dropped in winter, leaving bare stems exposed; photograph February 7, 2014.

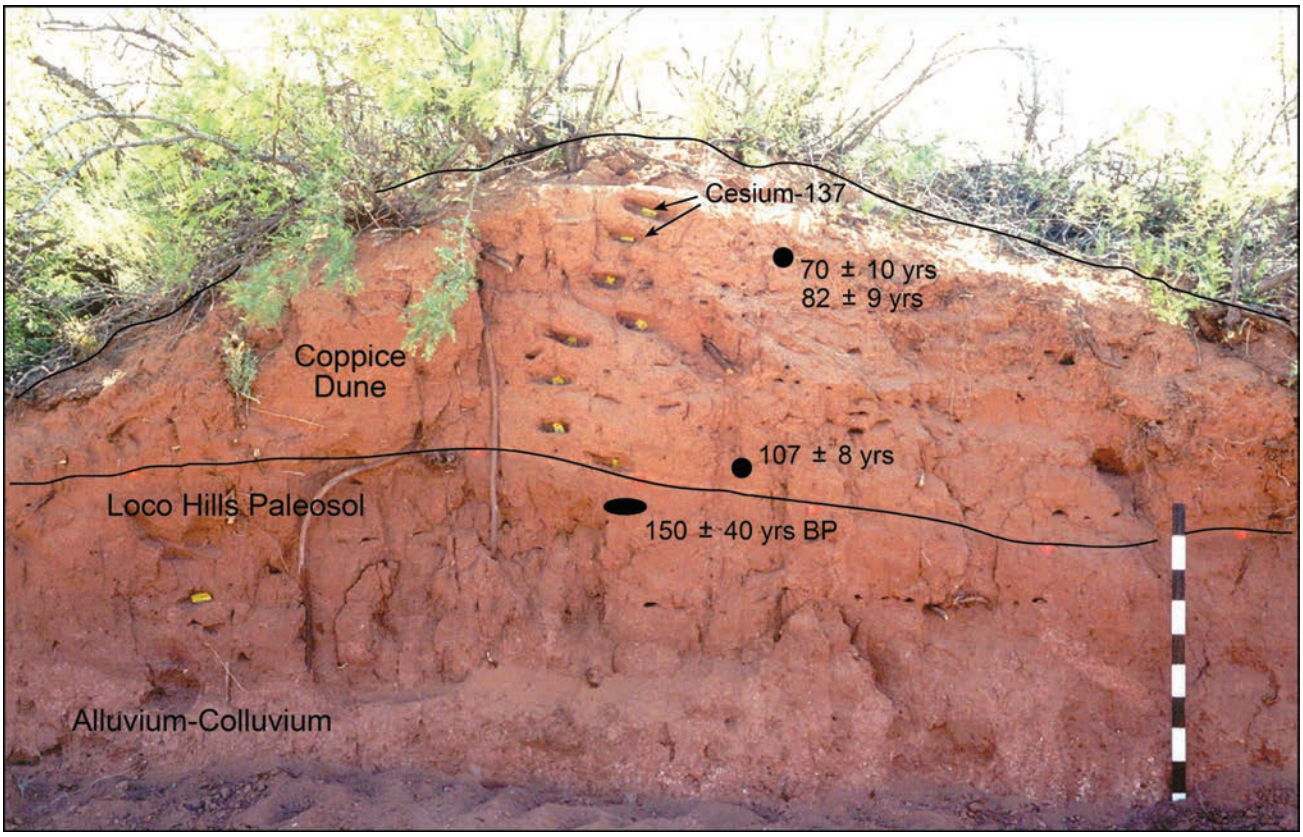

Figure 3.28. Coppice dune at Loc. 4 along Square Lake Road, just north of junction with Mallet Road; the OSL age of the dune is from A.D. 1894 to 1931; the dune overlies the Loco Hills paleosol, AMS dated 150 ± 40 yr BP (A.D. 1800); the cesium-137 content of the eolian sand was determined at this locality; the exposure has recently slumped and is largely gone today; 1-m scale; photograph June 1, 2001.

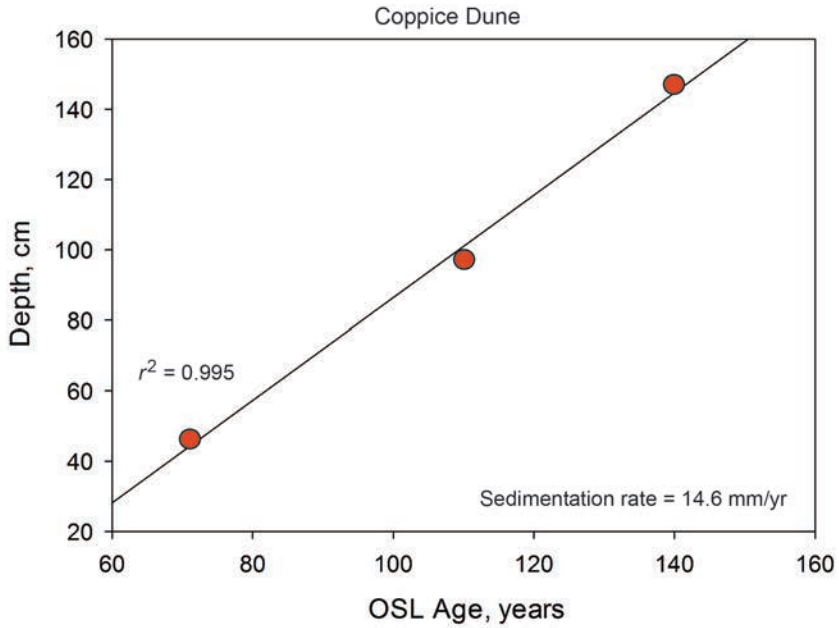

Figure 3.29. Sedimentation rate, 14.6 mm/yr, of an unusually large coppice dune, Loc. 31-B, Lea County based on 3 OSL ages (Appendix A, Table A-30).

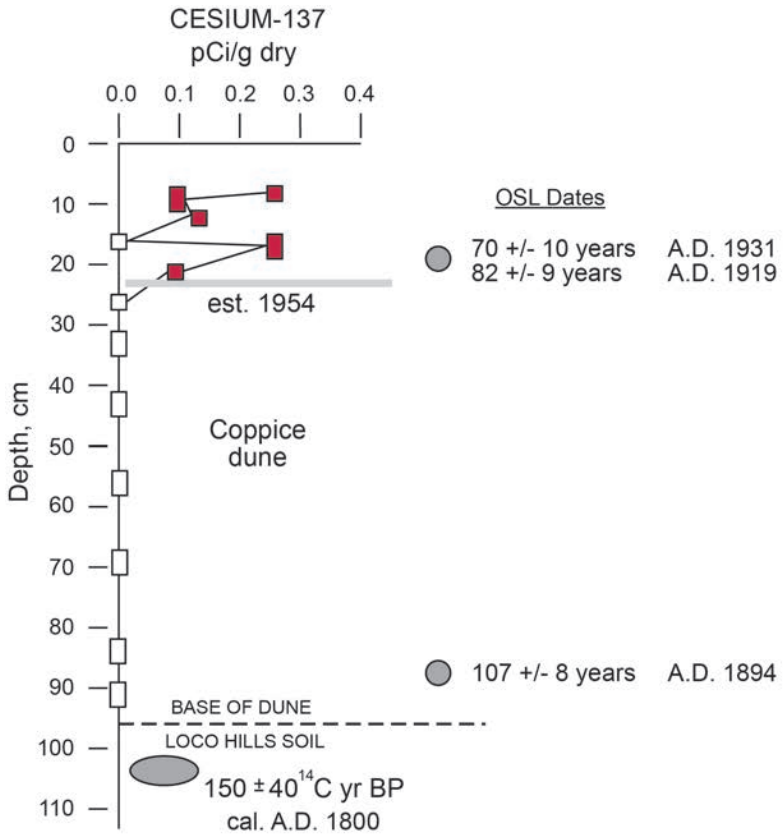

Figure 3.30. Sketch of analytical samples from a mesquite coppice dune along Square Lake Road at Loc. 4 where the presence of cesium-137 indicates an age of 1954; accompanying OSL ages indicate the age of the cesium-bearing sand as 1919 and 1931 and the base of the dune having begun to accumulate by 1894. The dune overlies the Loco Hills paleosol (Fig. 3.28) (Hall and Goble, 2016g) (data in Appendix C, Tables A-3, B-2, C-2).

OSL ages from 20 cm depth are 82 ± 9 and 70 ± 8 years (A.D. 1919, 1931), considerably earlier than the age indicated by cesium (Appendix A, Table A-3). The basal OSL age of the dune is 107 ± 8 years (A.D. 1894) (Hall, 2002a; Hall and Goble, 2016g). Lead-210 was also analyzed, but the amount of ^{210}Pb was too low for application to dune sand chronology (Appendix C, Table C-2).

We are uncertain why the cesium and OSL ages are incongruous. Considering the consistency of the high resolution OSL ages, however, we suspect that the cesium particles may have washed from the upper surface of the dune down into underlying levels in the dune sand, producing a false young age for the sand above 22 cm depth.

Transverse Dunes—Transverse dunes are uncommon in the Mescalero Sands. They are defined as asymmetrical sand ridges elongated perpendicular to the direction of the prevailing winds and are characterized by sparse vegetation (Neuendorf et al., 2005, p. 682). About twelve small patches of transverse dunes, less than a mile across, occur northeast of Loco Hills in areas underlain by thick deposits of Upper eolian sand (Fig. 3.31).

Inspection of a series of aerial photos from 1996 to 2017 shows the same configuration and size of the transverse dune fields in the past 21 years. Aerial photographs also show small patches of "ghost" transverse dunes that are inactive and covered by shinnery oak vegetation; their orientations are similar to those of the 1996 dunes. All of the dunes north of Loco Hills indicate dune-forming winds are from the southwest. Although we did not specifically investigate transverse dunes, we found that red sand of the Lower eolian sand unit and the underlying caliche of the Mescalero paleosol are exposed on the deflated floor of blowouts between dune ridges.

Figure 3.31. Transverse dunes located 7.9 mi. NE of Loco Hills at Lat. 32° 54′ 31.02″ N., Long. 103° 53′ 47.28″ W., at 3945 ft. elev.; the elongated dune field is 1.24 km (0.77 mi.) in length, and 0.43 km (0.27 mi.) in width; the area of the elongated dune field is 44.0 hectares. The direction of movement of the dunes is 42° E of N; dune-forming winds are apparently from the southwest. The dunes have formed in thick sand of the Upper eolian sand unit. The circular features in the image are small parabolic dunes. This black and white aerial photo was taken Oct. 22, 1996 (National Aerial Photography Program [NAPP], U.S. Geol. Survey, 9611-34); north is toward the top of the photo.

***Cover Sand*—**The Cover sand is defined as the loose wind-deposited sand that mantles the landscape (not to be confused with the earlier use of the term "Cover sand" on the Southern High Plains by Frye and Leonard, 1957, p. 28, 29, now called the Blackwater Draw Formation by Reeves, 1976). From the available evidence, we interpret the cover sand as derived from the erosion of the sand sheet beginning about 300 years ago (episode VI). Deflated sand that was not redeposited as parabolic dunes was transported across the plain and deposited as a thin sheet of massive cover sand. In a few places, the cover-sand deposits were buried and preserved by later-forming coppice dunes and in one study was found stratigraphically beneath parabolic dune sand. Where not protected, the cover sand has been blown away, probably feeding downwind coppice dunes. Today, the eroded surface of the sand sheet is mantled by several millimeters of fresh sand that masks the nature of the substrate. This fresh sand may be a modern component of the process of deflation and redeposition that began about 300 years ago and is continuing today.

***Cover Sand Ages*—**The cover sand has been OSL dated at four localities. The ages are 230 ± 80 years (A.D. 1784), 220 ± 20 (A.D. 1794), 140 ± 20 years (A.D. 1872), and 90 ± 20 years (A.D. 1918) at Locs. 6, 31, 25, and 23, respectively (Fig. 3.32).

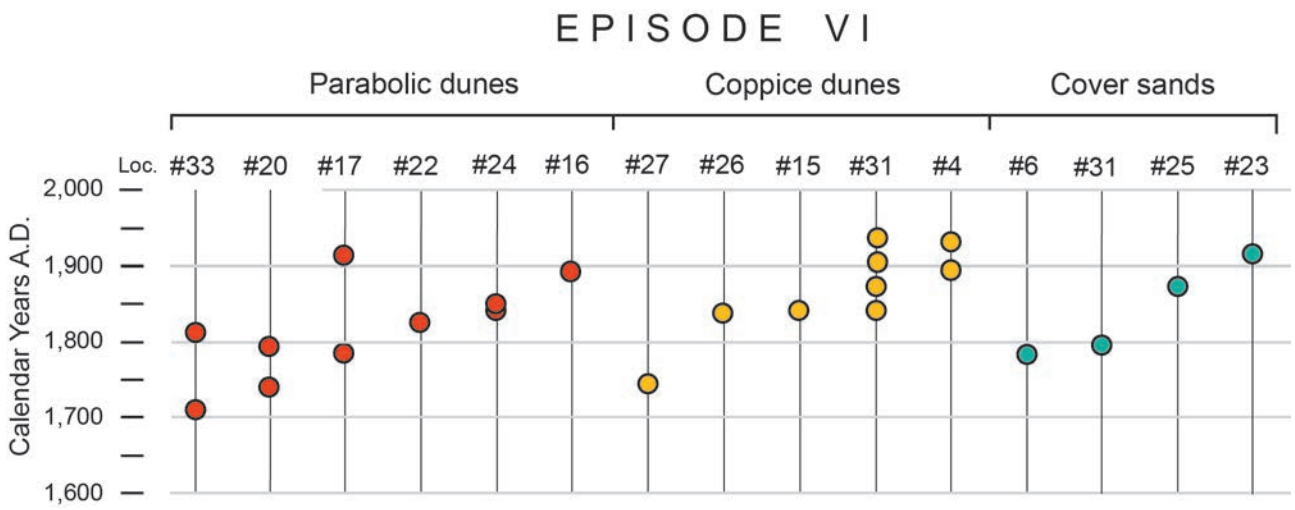

Figure 3.32. OSL ages of dunes and cover sand representing Episode VI eolian activity across the Mescalero sand sheet. The earliest dated episode VI sand is a parabolic dune at 310 ± 40 years (A.D. 1706) from Loc. 33. The early coppice dune is dated 270 ± 30 years (A.D. 1745) from Loc. 27. The episode VI eolian activity may be ongoing today; the latest dated eolian sand is from near the top of a large mesquite coppice dune at Loc. 31 and is 71 ± 6 years (A.D. 1943).

Episodes of Eolian Activity and Climate

The Mescalero sand sheet began forming 90,000 years ago and is still developing today. A period of stability occurred during the Pleistocene, but eolian sands were actively accumulating in one area or another throughout the Holocene. Given the broad paleoclimatic history of the southwestern region, we discuss the six episodes of eolian activity and how they relate to past climatic conditions. All of the eolian deposits are sheet sands except for the last episode that produced dunes. For the Pleistocene, we follow the North America time divisions in Šibrava et al. (1986).

Episode I, 90 to 50 ka—Episode I sand deposition (Lower sand) occurred after the end of the Sangamon and continued through the Early into the Middle Wisconsin. The 40,000-year period encompasses changes in long-term climatic conditions that may or may not be reflected in eolian sand accumulation at different localities. Even with uncertainties about the details, episode I sands were deposited during both comparatively dry and moist climates, although sand deposition did not take place until after the extreme aridity of the Sangamonian. The development of the non-calcic argillic Berino paleosol on the episode I sands is a product of time and a wet climate.

Episode II, 33 to 20 ka—Episode II sand accumulation (Middle sand) occurred during the Late Wisconsin period of continental and alpine glaciation and a time of cool and wet climate in the Southwest. The low latitude position of the jet stream during the Late Wisconsin resulted in strong west winds that in turn produced eolian activity in the region. The wetter climate, increased spring flow, and greater fluvial activity on the Mescalero Plain produced new and rejuvenated sand sources along streams. As a consequence of the combination of wetter climate, new sand sources along streams, and strong west winds, episode II sands were deposited across the plain. A non-calcic argillic Bt paleosol developed on the episode II sand and is a result of the wet Late Wisconsin climate.

Episode III, 18 to 5 ka—Episode III sheet sand (Upper sand) was deposited during the Late Pleistocene-Early Holocene transition. Although sand at one place began to accumulate about 18 ka, other records of sand deposition did not begin until 12 ka, towards the end of the Pleistocene. Eolian sand deposition continued through the Early Holocene into the Middle Holocene and ended by about 5 ka. The termination of episode III may be related to a reduction in fluvial activity on the Mescalero Plain as a consequence of the arid Altithermal climate. The rate of accumulation of sheet sands across the plain was low, reflecting the already sparse availability of sand. The drying of streams in the Middle Holocene led to the end of fresh supplies of sand that fed the episode III sheet sand.

The stabilization of the sand sheet in some areas resulted in the formation of a cambic Bw horizon and an underlying weak Bk horizon. Soil development began about 5 ka, when the episode III sands stabilized, and continued into the Late Holocene period of wetter climate.

***Episode IV, 12 to 2 ka*—**Episode IV sheet sand (Holocene sand) was deposited from the Pleistocene-Holocene transition to the Late Holocene about 2 ka, representing most of the Holocene. The sheet sand was deposited slowly, similar to the other sands. Although the deposition of episode III sands ended about 5 ka, episode IV sands continued to be deposited throughout the arid Middle Holocene and into the wet Late Holocene.

***Episode V, 6 to 2 ka*—**Episode V sheet sand (Late Holocene sand) formed directly on Pleistocene deposits or caliche of the Mescalero paleosol; Early Holocene sands are not present. The accumulation of eolian sands begins in the arid Middle Holocene and continued to 2 ka. The deposition of episode V sands ended with the formation of the Eddy paleosol, similar to the end of deposition of episode IV. The initiation of sand deposition may be related to the transition from Middle Holocene aridity to the wetter Late Holocene climate when stream activity on the plain became more active, thus rejuvenating local sand sources.

***Eddy Paleosol, 2 to 0.3 ka*—**The development of the Eddy paleosol A horizon was initiated about 2 ka in many places across the Mescalero Plain on eolian sand, alluvium, and colluvium alike. The deposition of the episode IV and V sheet sand ended at that time with the formation of the paleosol. The Eddy paleosol is a cumulic Mollisol that formed with grass-dominated vegetation in response to a wetter Late Holocene climate that characterized the Southwest and Southern Great Plains at that time. The soil continued to form until about 0.3 ka (A.D. 1700), a period of 1,700 years.

***Episode VI, 0.3 ka (A.D. 1700) to Present*—**Episode VI eolian activity produced parabolic and coppice dunes, unlike the other episodes that formed sheet sands. The difference between dune versus sheet sand is related to sand sources. Sheet sands are derived by slow accumulation from sand sources found along the narrow stream beds and floodplains of small drainages across the Mescalero Plain. Dunes, on the other hand, are derived directly from deflation of local, pre-existing Holocene and Pleistocene sheet sands. Thus, the dunes are predominantly a product of abundant and close-by sand sources. As deflation of local sand continues, the grains may be carried greater distances, enhancing the development of a dune field.

***Possible Cause of Erosion.*—**After many centuries of formation of the Eddy paleosol topsoil across the plain, geomorphic conditions changed drastically about A.D. 1700. The paleosol and sand sheet became severely deflated in most places. Dunes began to form. Many prehistoric sites that were buried in the paleosol were eroded and exposed at the deflated surface. The only widespread event at that time that may have been responsible for the erosion is the Little Ice Age, extending worldwide from about A.D. 1350 to A.D. 1850. Maximum cooling within the Little Ice Age, however, coincided with a period of low to zero sunspot activity, the Maunder Minimum, occurring A.D. 1645 to A.D. 1715. The amount of solar radiation reaching the Earth was greatly reduced during that interval, intensifying cool conditions (Eddy, 1976; Luterbacher, 2001).

If the above applies to southeastern New Mexico, it is possible that, after 70 years of maximum cool-wet conditions of the Little Ice Age, a change from those circumstances after A.D. 1715 might explain the beginning of deflation and dune development across the Mescalero Plain. Although speculative, it is possible that a shift from the cool-wet to a warmer-drier climate could lead to a shift in grass species dominance and a reduction in ground cover (such as the case of seven years of continuous drought, 1933 to 1939, inclusive, in western Kansas documented by Albertson and Weaver, 1942; Weaver and Albertson, 1956, p. 75–100). A reduction in plant cover, especially grasses, could lead to soil drying and deflation of the sheet sands and the formation of dunes. The change in climate and loss of ground cover would be widespread and it would occur quickly across the plain. Drier conditions could also increase the frequency of range fires, leading to further loss of ground cover. The historic introduction of livestock, with the expansion of mesquite shrubs and loss of grasses, has reinforced and exacerbated the natural geological processes of deflation and dune formation that began 300 years ago.

IV. OTHER RECORDS OF EOLIAN SAND DEPOSITION

The six episodes of eolian activity outlined in chapter 3 are repeated at study sites across the Mescalero Plain. However, two other records of eolian sand are also present, each a special case of deposition that diverges from the six episodes.

50,000 to 5,000 Year Sands

Most of the Mescalero sand sheet was inactive and stable during the period 50 to 33 ka and for various millennia in the latest Pleistocene and early Holocene. However, three localities experienced continuous sand deposition between about 50 to 5ka and 35 to 5ka. Interestingly, sand accumulation at all three sites appears to end about the same time at 5 ka, similar to the timing of the close of deposition of the Upper eolian sand unit of episode III (Fig. 4.1).

Locality 25 occurs on the east slope of the Maroon Cliffs, a topographically unique site. A single stratigraphic unit 1.2 m thick is without soil development except for a Bk horizon in the lower few decimeters that may be related to local concentration of groundwater; the eolian sand rests directly on Permian red beds. The unit is fine- to very fine-grained sand, coarsening upwards to a fine to medium texture. The 26,000 years of continuous eolian sand accumulation is probably related to the location of the site. It is on a west-facing topographic slope that receives wind-transported sand from the Red Lake basin. The eolian sands are then washed by gullies back down into the basin where the sands are available again for re-transport back up to the eastern slope. The process evidently continued without significant interruption from the late Pleistocene to the middle Holocene, although it ended by 5 ka.

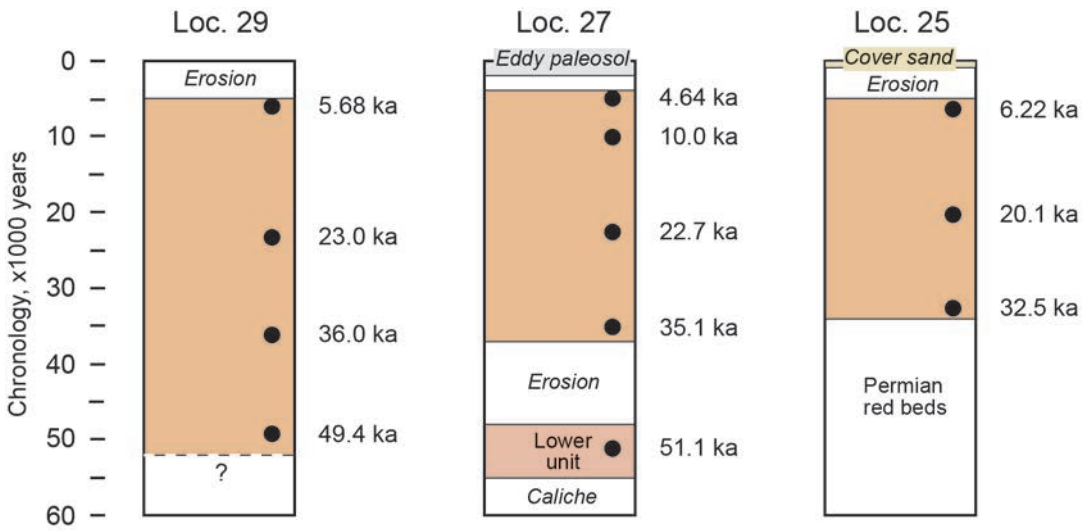

Figure 4.1. Three stratigraphic sections with eolian sand that appear to have accumulated continuously for 25,000 to 45,000 years; Loc. 27 is also shown in Fig. 5.1.

Locality 27 occurs on the far southwestern edge of the Mescalero sand sheet where eolian sand mantles Pleistocene terrace gravel of the Pecos River. A single stratigraphic unit about 0.8 m thick has A/Bw and weak Bk horizons and apparently accumulated for 30,000 years without a discernible break. The 30 ka sand rests directly on a 30-cm-thick Lower eolian sand unit which in turn rests on caliche at the top of the cemented terrace gravel. This is the only study site from this area of the sand sheet; future studies of additional sites in this area may reveal more examples of this sequence.

Locality 29 is solution-pipe fill in gypsum of the Rustler Formation (Permian); 1.4 m of eolian sand was exposed in a trench without encountering bedrock. The sediment is fine to very fine sand that appears to have accumulated without a break; however, a Bw horizon occurs in the upper 30 cm, a weak Bt horizon occurred in a 30 to 80 cm interval, and a weak Bk horizon was observed below 70 cm. The solution pipe occurs on the east, downwind side of a small playa, and the 45,000 years of fine-sand deposition may be related to deflation from the playa basin.

Los Medaños Sands

Two separate studies at localities 7 and 13 show an unusual sequence and chronology of eolian sand (Figs. 4.2, 4.3). The sites are close to each other and occur in an area of large parabolic dunes called Los Medaños. Both sequences incorporate a sand body that accumulated at about 2 ka and is referred to as Los Medaños eolian sand bed. At locality 7 the quartz sand is about 1.0 m thick and has a fine to very fine texture that coarsens upwards to fine to medium. The two OSL ages are identical even though separated vertically by 36 cm. At both localities, Los Medaños sand overlies a thin sand bed that is dated 4.5 to 4.0 ka; it is very fine to fine textured, considerably finer than Los Medaños sand bed.

The Los Medaños sequence has not been observed elsewhere on the sand sheet (Figs. 4.4, 4.5). Nearby, at locality 24, an investigation in the same area of parabolic dunes showed the presence of Late Holocene eolian sand (episode V), but not the two sand beds that are reported from localities 7 and 13. The Los Medaños sequence may represent a unique episode of eolian activity that is confined to this particular core area of the sand sheet.

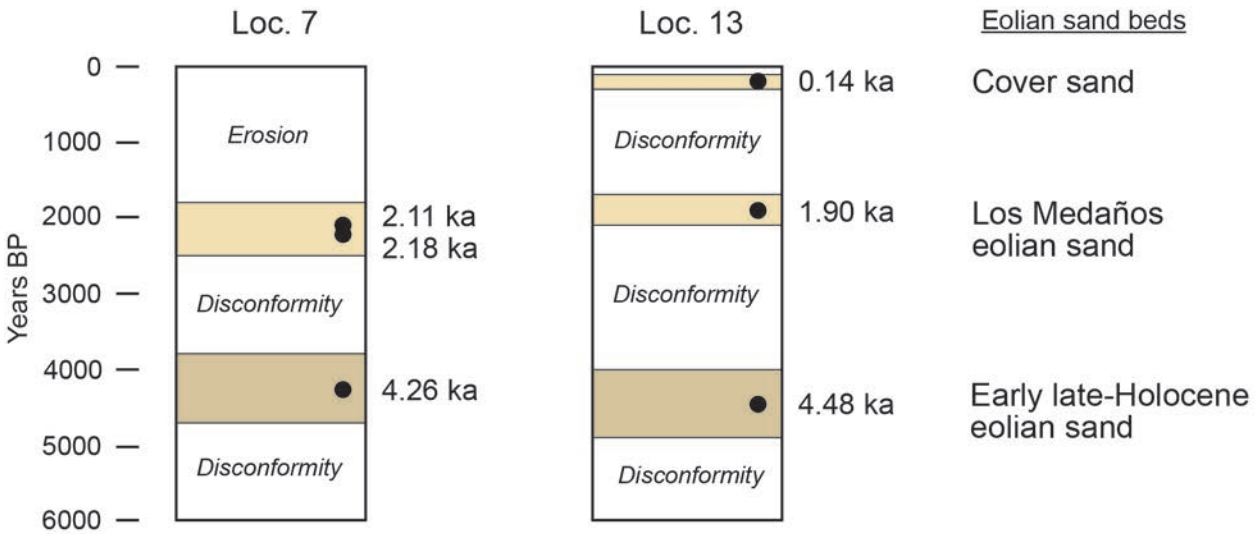

Figure 4.2. Los Medaños eolian sand, a 2000-year-old sand body that occurs in eastern Eddy County.

Figure 4.3. Los Medaños parabolic dunes with shinnery oak cover, Eddy County; photograph Sept. 9, 2008.

Figure 4.4. Area of active eolian sand along Square Lake Road (Eddy County 220) approximately 5.7 miles north of US Hwy. 82. Although the small mounds have the appearance of coppice dunes, they are instead erosional in origin. Stands of shinnery oak have protected various places of underlying Upper eolian sand unit (Episode III) from deflation, resulting in mound-like features that are erosional remnants. Clay bands occur here in the Upper unit. Photograph taken March 9, 2002.

Figure 4.5. Area of erosional remnants that have formed by deflation of Upper eolian sand (Episode III); stands of shinnery oak have protected the eolian sand from deflation, resulting in mound-like features. This area is about one mile southwest of the location of Fig. 4.4 in northeastern Eddy County. Photograph taken July 3, 2001.

V. SEDIMENTATION RATES

All geologists understand that the rates of accumulation of sedimentary strata are actually *net* rates. Nearly all deposits incorporate short-term episodes of non-deposition as well as scouring. This is especially the case with eolian environments on the Mescalero Plain. Nevertheless, net sedimentation rates provide useful information on the development of the sand sheet and accompanying dunes. Given the importance of the Eddy paleosol to prehistoric archaeology, the low rate of accumulation of the paleosol also bears directly on the preservation of sites (discussed in chapter 12).

Sedimentation rates were determined by OSL and or AMS dating of two to six horizons from one profile through single depositional units. Sedimentation rates with more than two dated horizons were determined by linear regression analysis; in all cases the correlation coefficient (r^2) was significant, exceeding 0.80 (Table 5.1), indicating continuous sediment accumulation with the passage of time. The high resolution of rates of sedimentation of the eolian sand bodies that make up the Mescalero Sands is made possible by optical dates from multiple horizons. Comparative information from eolian sand sheets elsewhere in the Southwest and the world are generally lacking.

Sheet Sands

The Pleistocene and Holocene sheet sands have low sedimentation rates ranging from 0.023 to 0.300 mm per year with fourteen measurements averaging 0.105 mm per year. Specifically, the Lower, Middle, Upper, Holocene, and Late Holocene sheet sands have average accumulation rates of 0.063, 0.053, 0.086, 0.107, and 0.228 mm per year, respectively. Consistently low rates of accumulation have been found throughout the Mescalero sand sheet from eolian sand deposits dated 90 to 2 ka, a period of 88,000 years.

The low sedimentation rates could suggest that the deposits may incorporate short-term episodes of non-deposition and scouring. However, close inspection of field exposures and laboratory texture and chemical data reveals no indication of disconformities or breaks of any kind within the depositional units.

We interpret the low sedimentation rates as indicating that the various sand sources across the plain contained only small amounts of sand that were available for entrainment and transport. The sand sources may also be far away, requiring grains to be transported great distances and for great periods of time before reaching a final place of deposition. Periods of stability with no sand deposition may indicate that the sources had shut down completely.

Dune Sands

Dune sands accumulated more rapidly than sheet sands, although only five examples from dunes are available. Parabolic dune sands are documented at three localities and have sedimentation rates of 5.15 to 8.50 mm per year, averaging 6.85 mm per year. Coppice dune sand is measured at two sites; high resolution OSL ages at one site indicate a sedimentation rate of 16.2 to 24.0 mm per year. The other locality yielded a rate of 14.6 mm per year. Dune sands have accumulated at rates that are an order of magnitude greater than found in associated sheet sands.

The high rate of dune sand accumulation is related to the ready availability of abundant sand at its source. Parabolic dunes and their blowouts form on top of thick, unconsolidated late Holocene-age eolian sand deposits that serve as a sand source for the dunes. The sand that makes up coppice dunes is also derived from pre-existing eolian deposits in the immediate vicinity of developing dunes. This contrasts with sheet sands, where the sources appear to have only small amounts of available sand and are located at some distance from the sand deposits.

Table 5.1. Sedimentation rates of dated eolian sands, the Eddy paleosol, and alluvium, southeastern New Mexico

Locality No.	Sedimentation Rate (mm/year)	Dating Method	Number of Ages	**Correlation Coefficient** (r^2)
SHEET SAND				
Lower eolian sand unit, 90 ka to 50 ka				
1	0.126	OSL	2	-
5	0.023	OSL	2	-
7	0.045	OSL	2	-
17	0.058	OSL	2	-
Middle eolian sand unit, 33 ka to 20 ka				
16	0.053	OSL	2	-
Upper eolian sand unit, 18 ka to 5 ka				
2 (thick sand facies)	0.896	OSL	2	-
5	0.068	OSL	3	0.953
8	0.080	OSL	3	0.975
9	0.110	OSL	3	0.986
Holocene eolian sand unit, 12 ka to 2 ka				
14	0.083	OSL	4	0.934
16	0.113	OSL	2	-
17	0.190	OSL	4	0.994
20	0.103	OSL	2	-
20	0.082	OSL	2	-
22	0.071	OSL	2	-
Late Holocene eolian sand unit, 6 ka to 2 ka				
23	0.300	OSL	2	-
31, Area C	0.155	OSL	2	-
DUNE SAND				
Parabolic dune sand, <300 years				
17	5.15	OSL	2	-
20	8.50	OSL	2	-
33	6.91	OSL	2	-
Coppice dune sand, <300 years				
4	16.2, 24.0	OSL	2	-
31, Area B	14.6	OSL	3	0.995
EDDY PALEOSOL				
12	0.571	OSL	2	-
12	0.693	AMS	2	-
14	0.130	OSL	2	-
16	0.400	OSL	2	-
18	CAM[1], 0.266; MAM[2], 0.333	OSL	3 CAM, 2 MAM	1.000 (CAM)
20	0.612	OSL	2	-
21	0.750	AMS	2	-
21	0.571	AMS	2	-
21	0.342	AMS	2	-
31, Area C	0.541	OSL	4	0.957
31, Area B	0.418	OSL	3	0.825
31, Area B	0.824	AMS	3	0.972
31, Area C	0.986	AMS	4	0.935

Table 5.1. Continued

Locality No.	Sedimentation Rate (mm/year)	Dating Method	Number of Ages	Correlation Coefficient (r^2)
ALLUVIUM				
Late Holocene alluvium				
10	0.370	AMS	3	0.986
26 (Pecos River)	0.268	OSL	2	-
32 (Red Bluff Draw)	0.182	AMS	6	0.988
MISCELLANEOUS DEPOSITS				
Depression-fill facies of the Eddy paleosol, ca. 1300 to 200 years BP				
17	1.46	OSL	4	0.845
17	1.91	AMS	4	0.797
35 ka to 5 ka eolian sand deposit				
25	0.0294	OSL	3	0.993
27	0.0192	OSL	4	0.994
50 ka to 5 ka eolian sand deposit, solution pipe				
29	0.027	OSL	4	0.992

[1] Central Age Model; [2] Minimum Age Model

Eddy Paleosol

The sedimentation rate of the Eddy topsoil has been determined from eighteen OSL ages from stratigraphic sections at seven localities across the plain; the sedimentation rates range from 0.130 to 0.612 mm per year and average 0.41 mm per year. The rate based on fifteen AMS ages (four localities) ranges from 0.342 to 0.986 mm per year with a mean of 0.694 mm per year, a notably higher rate than obtained from OSL dating (Table 5.1). The accumulation rate from OSL and AMS dating combined is 0.540 mm per year. Discussed below, we conclude that optical dating provides more reliable ages of the Eddy paleosol than do ages of soil humates, due to the movement of soluble humates through the sand that makes up the top soil. Thus, the best average sedimentation rate of the Eddy topsoil, in our view, is from OSL dating and is 0.41 mm per year.

It should be noted that the sedimentation rates of the various occurrences of the Eddy paleosol exhibit linear trends (Table 5.1). The significance of this fact is twofold: first, the Eddy topsoil is indeed a cumulic soil, formed by the gradual accumulation of fine-grained sand during a period of seventeen centuries; second, the linear trend of its sedimentation rates indicates that the cumulic soil developed without significant vertical bioturbation.

One of the findings in these investigations is that, with paired OSL and AMS dates, AMS ages are nearly always younger (Table 5.2). Furthermore, sedimentation rates from AMS ages are greater than those from OSL ages (Table 5.3). This is a consequence of the AMS ages being based on soluble humates that have migrated down profile into older sands. In a few instances, humates have also migrated laterally into younger sands. Because of the migration of humates in sand deposits, we conclude that OSL dating provides the more reliable age for the cumulic Eddy topsoil.

OSL and AMS Dates From Eddy Subsoil Sand

In Eddy subsoil sand, the dichotomy between OSL and AMS ages is even greater. In an extreme case of paired dates, the AMS age of humates is A.D. 750 and the OSL age of sand grains is 10,000 years, a difference of 8,735 calendar years (Table 5.2, Loc. 27) (Figs. 5.1, 5.2). In this situation, AMS dates on mobile humates clearly do not provide a valid chronology for the subsurface sand. At the same time, however, the humate ages (even though too young for the sand from which they are obtained) are indicative of the presence at that time of the active topsoil development at the ground surface.

Unequivocally, OSL is the dating method of choice in our investigations. It provides an age of the quartz sand particles that make up the eolian, alluvial, and colluvial deposits. We found that AMS radiocarbon dating of soluble organic humates that coat sand grains are nearly always younger than the optical age of the sand grains by hundreds and thousands of years. The soluble humates move through pre-existing sediments with water fronts accompanying precipitation events. In one case the AMS ages were older due to slight topographic differences where movement of humates was both lateral as well as vertical. The geomorphic process is known to soil scientists as *eluviation*; it is defined as "the removal of soil material in suspension (or in solution) from a layer or layers of a soil. Usually the loss of material in solution is described by the term 'leaching'". A related term, *illuviation*, is defined as "the process of deposition of soil material removed from one horizon to another in the soil; usually from an upper to a lower horizon in the soil profile" (Soil Science of America, 1997, p. 32, 50).

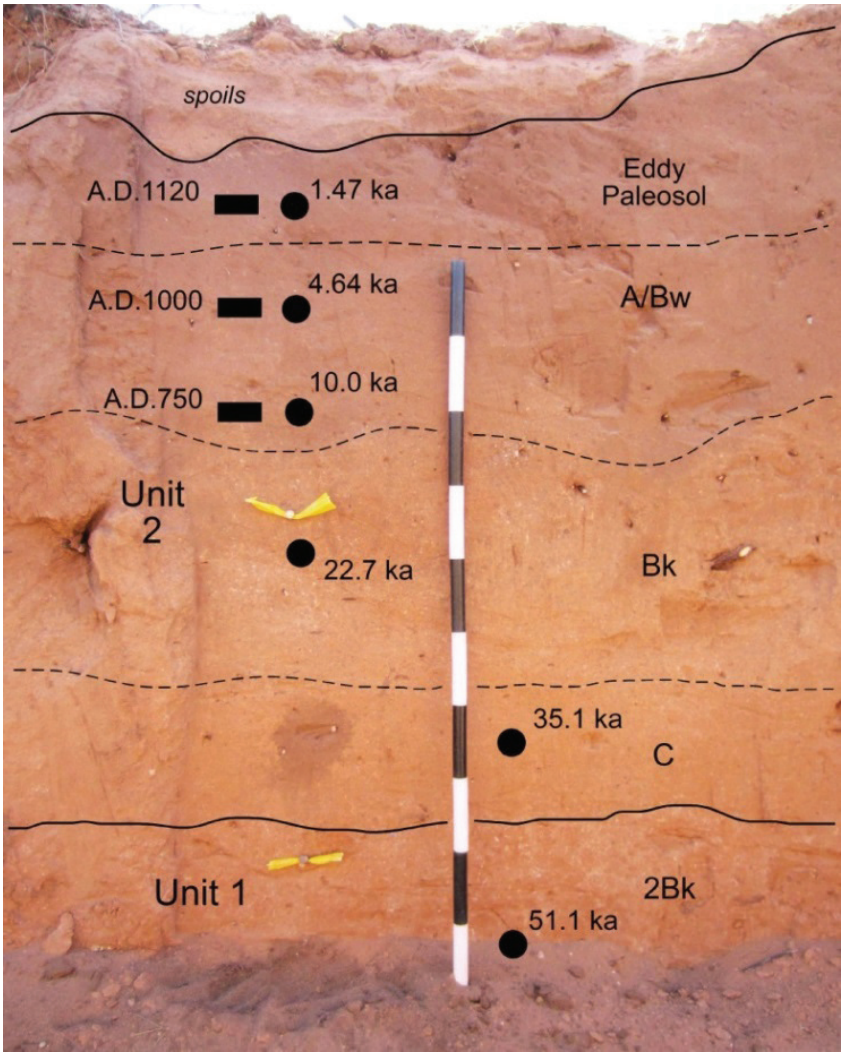

Figure 5.1. Eolian sand with paired OSL-AMS dates showing strong divergence in age of sand and humates at Loc. 27 (see Fig. 5.2). Black circles are OSL dates, black rectangles are AMS dates. Unit 1 is the Lower eolian sand unit, although the Berino paleosol is absent here; Unit 2 is an atypical sand body discussed in chapter 4; 1-m scale.

Table 5.2. Paired OSL and AMS Dates from the Mescalero Plain, southeastern New Mexico (OSL and AMS ages are listed in Appendix A and B)

Locality	OSL Age	OSL Age (A.D./B.C.)	Corrected Radiocarbon Age (BP)	Calibrated Radiocarbon Age (A.D.)	Difference in Calendar Years, **AMS older
11*	1830 ± 90	A.D. 178	1280 ± 40	A.D. 726	548
12*	1200 ± 80	A.D. 808	1080 ± 40	A.D. 955	147
12*	1970 ± 130	A.D. 38	1720 ± 40	A.D. 320	282
17†	620 ± 70	A.D. 1395	100 ± 30	A.D. 1820	425
17†	790 ± 40	A.D. 1225	470 ± 30	A.D. 1430	205
17†	1250 ± 100	A.D. 765	590 ± 30	A.D. 1350	585
17†	1240 ± 130	A.D. 775	790 ± 30	A.D. 1240	465
27*	1470 ± 70	A.D. 545	900 ± 30	A.D. 1122	577
27‡	4640 ± 240	2625 B.C.	1030 ± 30	A.D. 1000	3,625
27‡	10,000 ± 500	7985 B.C.	1250 ± 30	A.D. 750	8,735
31, Area C*	1420 ± 60	A.D. 590	1270 ± 30	A.D. 720	130
31, Area C*	970 ± 60	A.D. 1040	1020 ± 30	A.D. 1010	30**
31, Area C*	510 ± 90	A.D. 1500	880 ± 30	A.D. 1140	360**
31, Area C*	380 ± 30	A.D. 1630	610 ± 30	A.D. 1300	330**
31, Area B*	1950 ± 140	A.D. 60	1250 ± 30	A.D. 750	690
31, Area B*	1840 ± 100	A.D. 170	1010 ± 30	A.D. 1020	850
31, Area B*	620 ± 140	A.D. 1390	340 ±30	A.D. 1550	160
31, Area B§	220 ± 20	A.D. 1790	670 ± 30	A.D. 1330	460**

Localities: *Eddy topsoil; †Depression-fill facies of the Eddy paleosol; ‡Eddy subsoil; §Cover sands overlying Eddy paleosol.

Table 5.3. Sedimentation rates from paired OSL-AMS dates, Eddy topsoil (from Table 5.1)

Locality	Number of Dated Horizons	OSL Ages, Sedimentation Rates (mm/yr)	Correlation **Coefficient** (r^2)	AMS Ages, Sedimentation Rates (mm/yr)	Correlation **Coefficient** (r^2)
12	2	0.571	-	0.693	-
31, Area B	3	0.418	0.825	0.824	0.972
31, Area C	4	0.541	0.957	0.986	0.935

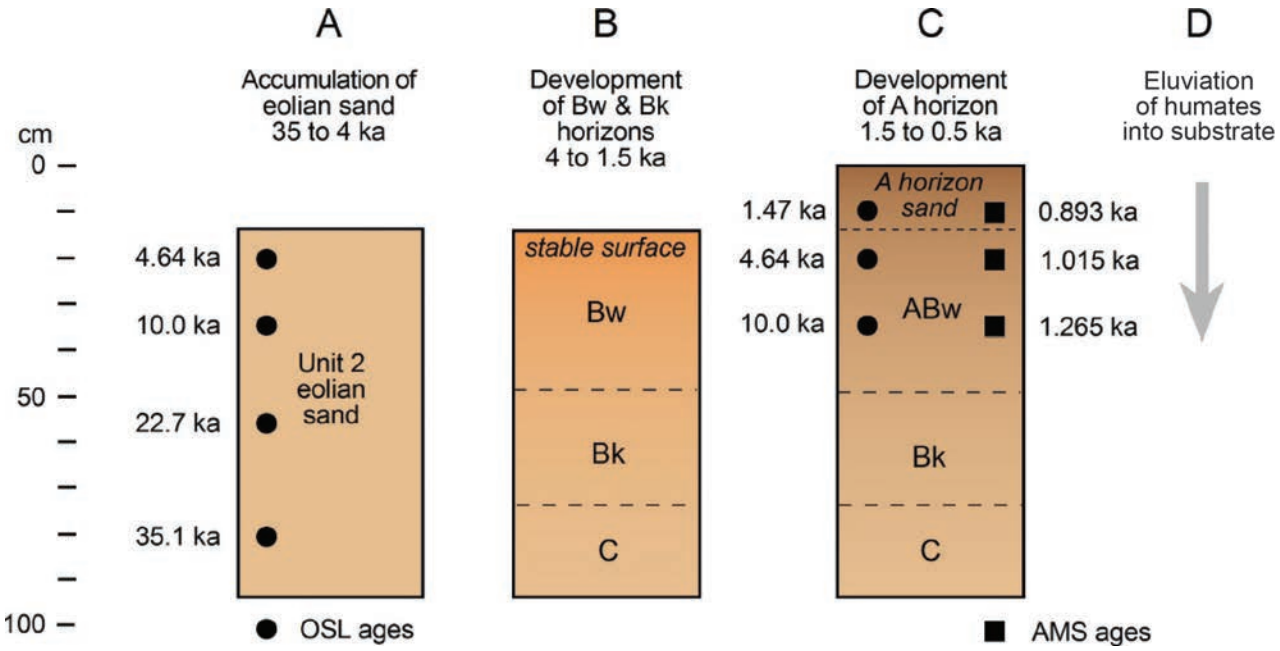

Figure 5.2. Progressive development (A to C) of the Eddy paleosol at Loc. 27, southern Eddy County (modified from Hall and Goble, 2016c); unit 2 is an atypical sand body discussed in chapter 4. The AMS radiocarbon dates are converted to calendar years before 2015 for comparison with the OSL ages. Paired AMS and OSL dates show as much as 8,735 years difference in ages of humates and sand grains (Fig. 5.1, Table 5.2).

VI. SEDIMENTOLOGY

As stated previously, the focus of our studies from site to site across the plain has been stratigraphy, sedimentology, and geochronology. Sedimentology is defined as "the scientific study of sedimentary rocks and of the processes by which they were formed; the description, classification, origin, and interpretation of sediments" (Neuendorf et al., 2005, p. 585). We routinely take a close look at sedimentary structures and other sediment properties in the field, followed by particle size and chemical analysis of the sediments by a dedicated geotechnical laboratory, which is a must. Additional discussion of sedimentology and other aspects that we have applied to our research is presented as Appendix D, Standards and Guidelines for Geologic Field and Laboratory Studies (Hall and Goble, 2016g, p. 151–170).

The physical and chemical properties of sediments that make up stratigraphic units are a product of the various processes leading to the deposition (primary features) and post-depositional alteration (secondary features) of the sediments (soils are secondary features). We have paid close attention to primary versus secondary properties in the field. An excellent guide in these matters is the classic *Principles of Sedimentology by Friedman and Sanders* (1978).

Laboratory Methods

In addition to field observations, we have submitted sediment samples to dedicated geotechnical laboratories, especially the Milwaukee Soil Laboratory, Milwaukee, Wisconsin; Energy Laboratories, Inc., Billings, Montana; and A&L Great Lakes Laboratories, Fort Wayne, Indiana. Since the beginning of our research on the Mescalero Plain, we have had 642 samples from 38 localities analyzed for particle size (discussed below), calcium carbonate content, organic carbon, and in a few cases, iron, phosphorus, cesium-137, and lead-210 content (this is in addition to 585 separate radioisotope analyses accompanying the OSL dates). All of these data are presented in Appendix C (the OSL-related radioisotope measurements are in Appendix A).

Particle-Size Analysis

The general texture of sediment can be estimated in the field, such as gravelly, coarse sand, fine sand, silty, or clayey. However, laboratory analysis is absolutely vital to produce quantitative particle-size data than can be applied to (a) define a stratigraphic unit, (b) assess the origin of the sediment that makes up a unit, (c) compare and distinguish different units locally and throughout the region, and (d) assess the degree of post-depositional soil development. We have often consulted the guide to sediment particle science written by the late Robert L. Folk (1968).

The Wentworth (1922) grade scale has been used by geologists, sedimentologists, and geomorphologists for a century. Virtually all of the vast number of U.S. publications dealing with the entrainment, transportation, and deposition of sediment are based on the Wentworth particle-size categories (Europeans use other scales). The Wentworth grade scale has been used in all of our geologic and geomorphic investigations in southeastern New Mexico. It is recommended that the Wentworth grade scale continue to be used in all future earth science studies in southeastern New Mexico.

In a dedicated sediment laboratory, gravel-size particles (>2.0 mm) are mechanically separated from a sediment sample and set aside for further study (we usually did this ourselves). The remaining sediment in our studies has been analyzed by two separate procedures, using the Wentworth grade scale. (a) The relative percentages by weight of silt (62.5–3.9 μm) and clay (<3.9 μm) are determined by the hydrometer method (although the pipette method is more accurate). (b) Secondly, the sand fraction is mechanically sieved with brass sieves, separately

from gravel, silt, and clay, resulting in percentages by weight of very coarse sand (2.0–1.0 mm), coarse sand (1.0–0.50 mm), medium sand (0.50–0.25 mm), fine sand (0.25–0.125 mm), and very fine sand (0.125–0.0625 mm). With these data, one can compare the independent percentages of sand size classes. The sand-size distributions have been useful to us in distinguishing deposits of eolian origin as well as changes in sand sources. Percentages of silt are a general index to the presence of atmospheric dust in eolian sediments. Clay is a component of atmospheric dust, although high percentages of clay in a deposit may be a product of pedogenesis.

Sieving and Hydrometer Versus Laser Diffraction

The use of laser diffraction for particle-size analysis came to our attention during the study of the surficial geology at Spaceport America in Sierra County, New Mexico (Hall and Goble, 2014). The reader should be aware that the newly-developed laser diffraction methodology produces particle size percentages based on volume. Sieving, in contrast, produces particle size percentages based on weight.

In our work at Spaceport America, we found striking inconsistencies in sand, silt, and clay percentages provided by the laser method. Compared with sieving and hydrometer of splits of the same five samples, laser diffraction consistently measured lower percentage values of sand, higher percentages of silt, and lower percentages of clay. The lower values of clay percentages with laser diffraction have been found universally; in study after study, the percentages of clay determined by laser diffraction are consistently low.

A summary of the problems noted by many technicians around the world concerning laser diffraction methods and results was presented in our report on the Spaceport America project (Hall and Goble, 2014, p. 574):

> A number of studies have documented a variety of problems with the results of laser diffraction methods in particle-size analysis: (*a*) different brands and models of commercial instruments yield dissimilar particle-size results; (*b*) all laser studies systematically underestimate the amount of clay; (*c*) clay mineralogy affects volume estimates; (*d*) volume overestimates may be caused by overestimated particle size or by overestimated number of particles; (*e*) variability of particle size and shape affects volume estimates; (*f*) non-uniform particle mineralogy and density affects volume estimates; (*g*) non-sphericity of particles produces overestimated volume; (*h*) different sediment types, such as from fluvial, eolian, lacustrine, and marine deposits, yield different levels of numerical bias between laser and pipette particle size information (Di Stefano et al., 2010; Loizeau et al., 1994; Eshel et al., 2004; Campbell, 2003; Buurman et al., 2000; Beuselinck et al., 1998; Konert and Vandenberghe, 1997).

Laser diffraction has several advantages over sieving and hydrometer measurements: "short time of analysis (5-10 minutes per sample), high repeatability, small size of sample needed (≤1 g), and wide range of size fractions into which the entire range of particles can be divided" (Eshel et al., 2004, p. 737). However, the above advantages are moot. The particle size data produced by laser diffraction do not hold up to comparison with particle size analysis by sieves and a hydrometer. Given the above insurmountable problems at this time, it is recommended that laser diffractometry not be used in particle size analysis.

Particle Size of the Mescalero Sands

Particle size analysis has provided useful information about the wind-deposited sand bodies that make up the Mescalero Sands. Although we have information on 642 sediment samples, we selected the sand particle size data of 94 samples from the six episodes of eolian activity, each sample from a stratigraphic horizon that has been OSL dated (Table 6.1).

The eolian deposits of the Mescalero Sands are predominantly fine-grained quartz sand (0.25 to 0.125 mm; Wentworth scale). Four suites of episode samples are fine- to medium-grained sand, and two are fine- to very fine-grained sand. A plot of all 94 particle size samples shows some variability although, as a whole, the data appear to cluster (Figs. 6.1, 6.2).

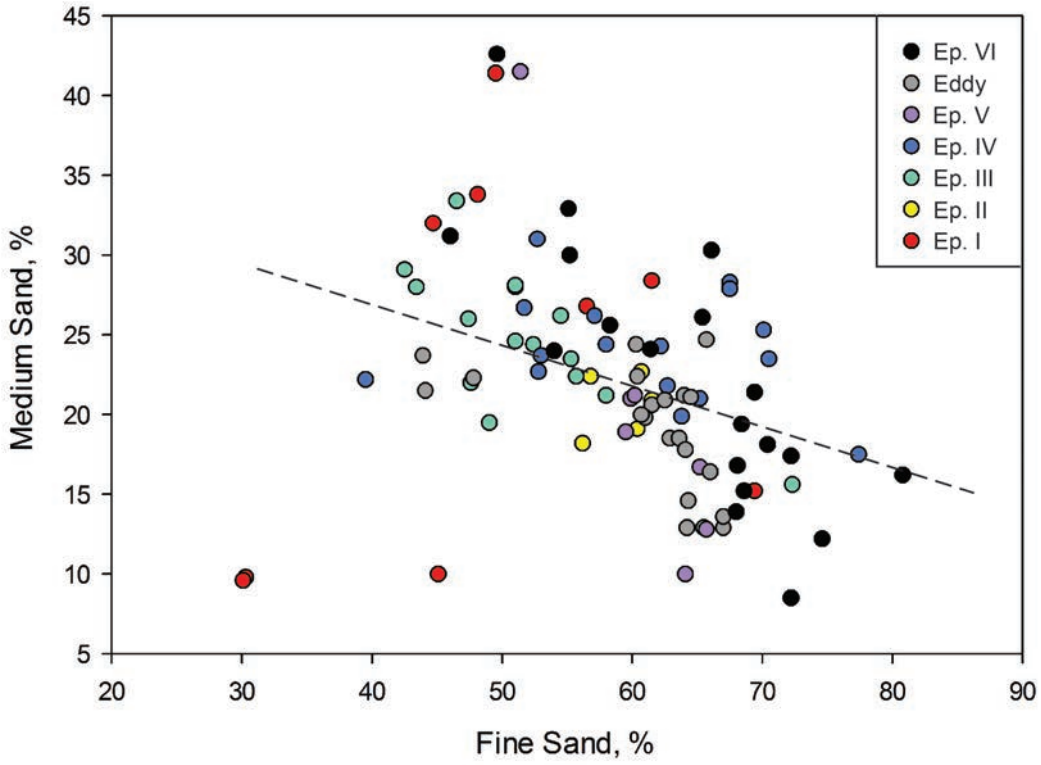

Figure 6.1. Fine versus medium sand percentages, episodes I through VI and Eddy paleosol, Mescalero Sands, SE New Mexico; same data (94 samples) as in Table 6.1; linear regression, $r^2 = 0.126$ (SigmaPlot 12).

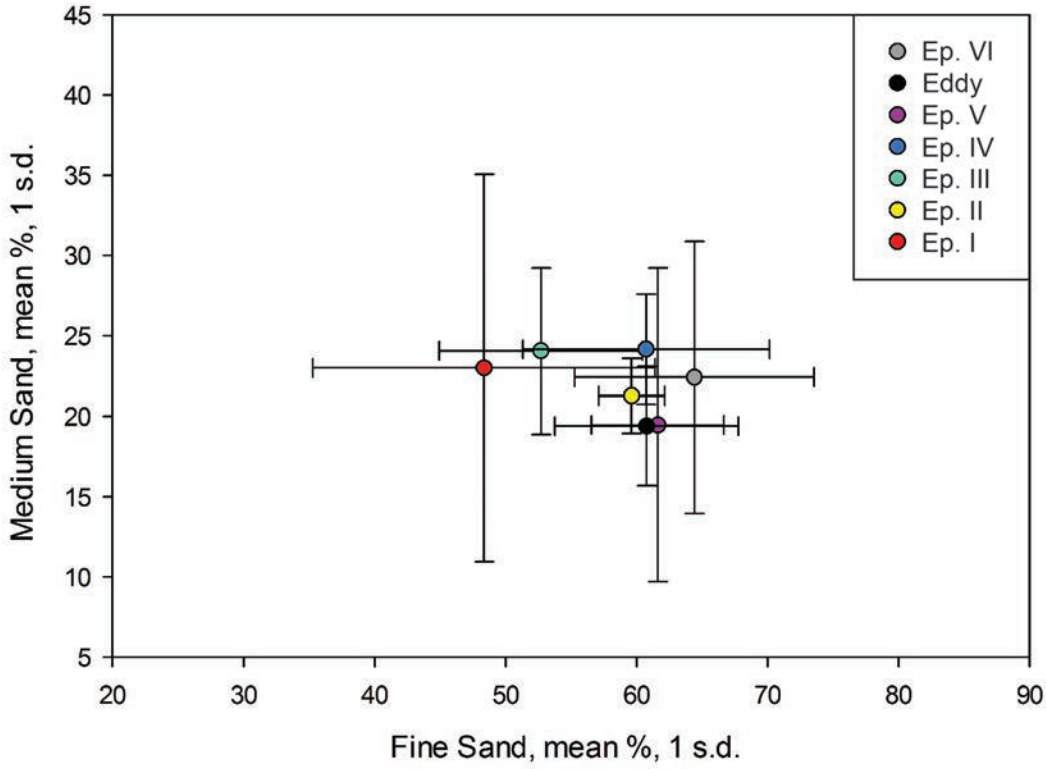

Figure 6.2. Fine versus medium sand, mean percentages, 1 standard deviation bars, of the six episodes of sand deposition and the Eddy paleosol; same data from Table 6.1 and in Fig. 6.1.

The finest-textured suite of samples is from episode I, the Lower eolian sand, the first eolian sand body deposited in the Mescalero Sands with the highest amounts of very fine sand; it also has the greatest variability (Table 6.1). The coarsest-textured suite of samples is from parabolic dunes with the highest percentage of medium sand and the lowest percentage of very fine sand.

All of the sand particle-size data taken together appear to exhibit a slight inverse relationship between fine and medium size classes, with higher percentages of medium sand corresponding to lower percentages of fine sand, although statistically there is no correlation (Fig. 6.2). However, there is a somewhat significant correlation between fine and medium size classes in the episode VI dune and cover sands (Fig. 6.3).

Sedimentology: Case Studies

From a practical view, particle size and other routine sediment measurements from a stratigraphic section can be a guide to the style of deposition. Slight changes in particle size may also indicate a shift in the sand source. A large change may mark the presence of more than one stratigraphic unit and/or a major shift in sand source.

Locality 5

This locality exhibits deposits of possibly three different sand sources (or changes in sand texture at one source) (Fig. 6.4). The Lower sand, dated here 87.0 and 61.1 ka, shows a small change in texture to less medium sand and more very fine sand at the horizon (sample no. 20) of the 61.1 ka date. There is no indication from our other studies that suggests a change in sand source in the area at that time.

A second change in texture that is more abrupt occurs between the time of the deposition of the Lower sand and the accumulation of the Upper sand, sometime between 61.1 ka and 17.3 ka (the OSL-dated stratigraphy of locality 5 was presented previously in chapter 3). During that interval, a regional regeneration of fluvial sand sources occurred throughout the Mescalero Sands, resulting in a shift in the radioisotope content of the sheet sand (discussed later in chapter 8). The change at locality 5 resulted in a fining of the texture: a decrease in the amount of medium-grained sand and an increase in the amount of fine-grained sand. Fine-grained sand perhaps dominated overbank deposition along narrow floodplains across the plain, the fine particles subsequently becoming available for eolian activity. The young post-Upper sand at the top of the sequence was probably derived from the local underlying Upper sand.

Table 6.1. Particle size of eolian sand units from the Mescalero Sands; 94 samples; Wentworth scale; each sediment sample is from an OSL-dated horizon; the percentages are mean values with 1 standard deviation (SigmaPlot 12)

Episode	Stratigraphic Unit	Very Coarse Sand (%)	Coarse Sand (%)	Medium Sand (%)	Fine Sand (%)	Very Fine Sand (%)	No. of Samples	Localities
VI	Coppice dunes	0.0	0.8 ± 1.50	17.7 ± 7.76	66.6 ± 10.39	14.9 ± 3.43	6	15,27,31
	Parabolic dunes	0.0	1.5 ± 1.37	26.7 ± 7.80	63.35 ± 9.33	8.6 ± 3.96	10	16,17,20,22, 24,33
	Cover sand	0.0	0.03 ± 0.06	17.7 ± 5.49	63.5 ± 8.26	18.4 ± 2.47	3	23,25,31
	All VI units combined	0.0	1.04 ± 1.36	22.4 ± 8.47	64.4 ± 9.14	12.1 ± 5.28	19	15,16,17,20,22, 23,24,25,27,31,33
-	Eddy paleosol	0.06 ± 0.12	2.05 ± 2.09	19.4 ± 3.69	60.8 ± 7.02	18.5 ± 4.86	20	11,12,14,15,16, 18,31,33
V	Late Holocene sand	0.625 ± 0.18	0.56 ± 0.90	19.5 ± 9.76	61.6 ± 5.05	18.25 ± 5.74	8	18,23,24,31
IV	Holocene sand	0.0	1.8 ± 0.86	24.15 ± 3.41	60.7 ± 9.41	13.3 ± 9.20	16	14,15,16,17, 20,22
III	Upper sand	0.075 ± 0.11	2.7 ± 2.58	24.1 ± 5.17	52.7 ± 7.75	20.4 ± 3.91	16	2,5,8,9,11,12
II	Middle sand	0.0	2.4 ± 0.90	21.3 ± 2.31	59.6 ± 2.51	16.6 ± 4.92	6	15,16,19,20, 22,33
I	Lower sand	0.02 ± 0.067	1.7 ± 1.58	23.0 ± 12.06	48.4 ± 13.07	26.8 ± 21.66	9	1,5,6,7,16,27

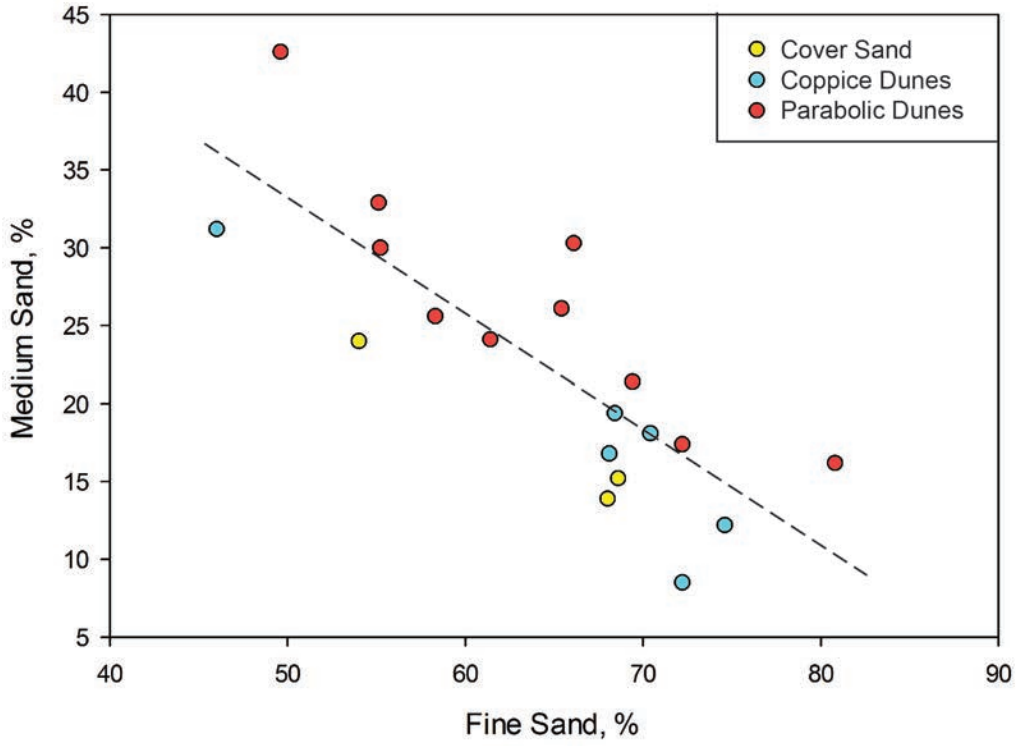

Figure 6.3. Fine versus medium sand percentages of parabolic dunes, coppice dunes, and cover sand (episode VI); 19 samples; linear regression, $r^2 = 0.659$.

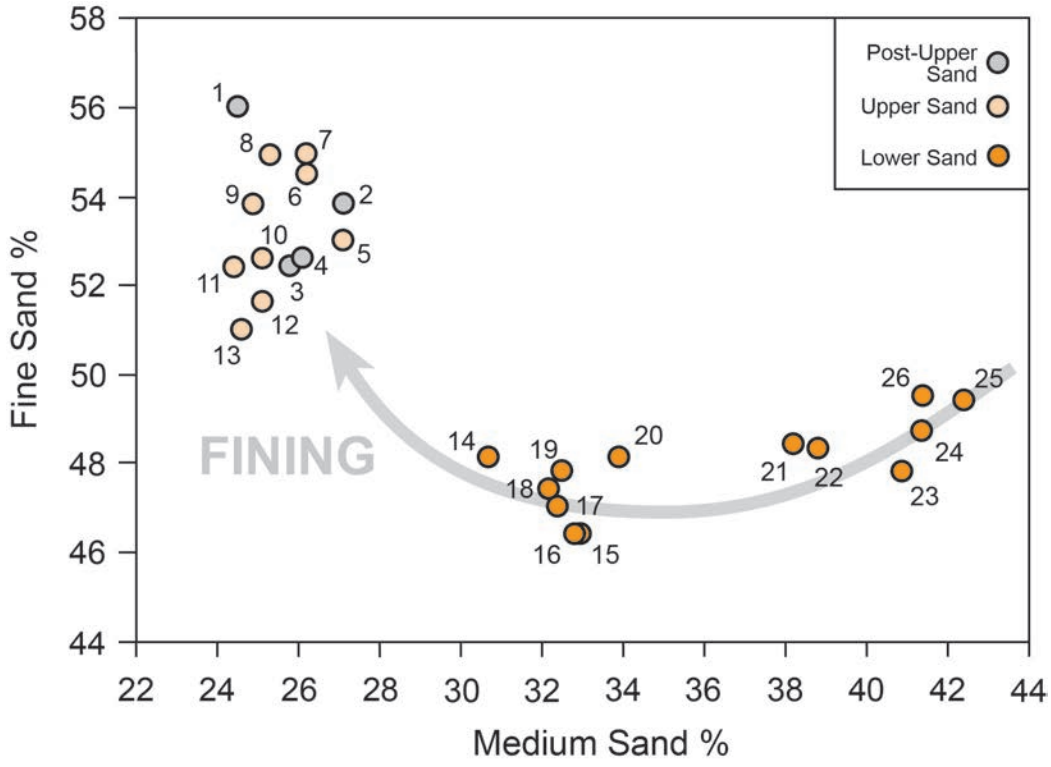

Figure 6.4. Three groups of particle size of eolian sands at Loc. 5. The overall trend is first a slight coarsening, then fining between the Lower sand the younger sand deposits. The numbered samples are in stratigraphic order, 1 through 26, youngest to oldest. The Loc. 5 stratigraphic section was previously shown in Fig. 3.1.

Locality 7

A major change in sand texture at Loc. 7 in the Los Medaños parabolic dune field marks different stratigraphic units (Fig. 6.5). The lower 20 cm of the Holocene sand was much finer textured than the overlying 120 cm, indicating the presence of two different sand units; the OSL ages suggested that as well. Also, the 20-cm sand and the underlying Lower sand unit have similar texture, suggesting that the fine-textured Holocene sand may be derived from the fine-textured Lower unit. The coarse-textured upper 120 cm Los Medaños sand was likely derived from a more distant source, the finer particles carried away. Another aspect of the sediment data is the high clay content of the Lower sand. The clay is secondary and a consequence of the development of the argillic Berino paleosol. The carbonate content is a result of the clay; clay minerals absorb water and, upon drying, the carbonate is precipitated.

Locality 9

A number of localities exhibit a steady, constant accumulation of sand that varies little with the passage of time. Locality 9 is such a place (Fig. 6.6). The nearly unvarying accumulation of sand, silt, and clay suggests the same sand source through time. The increase in carbonate with depth from 1.1% to 7.2% represents stage I calcic soil development.

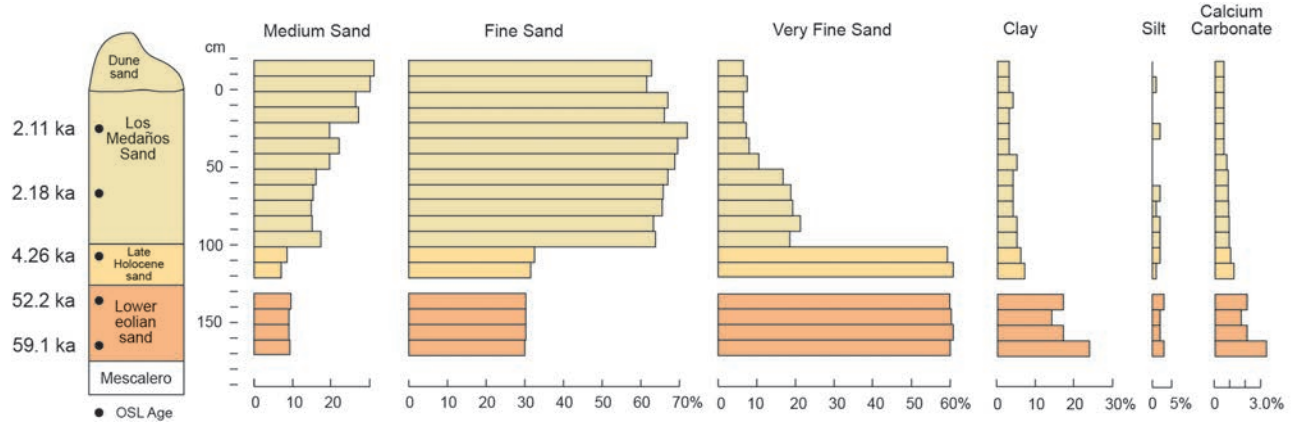

Figure 6.5. Sediment diagram from Loc. 7, eastern Eddy County, showing the dichotomy of particle size distribution of Los Medaños and older sand units (data in Appendix C, Table C-5).

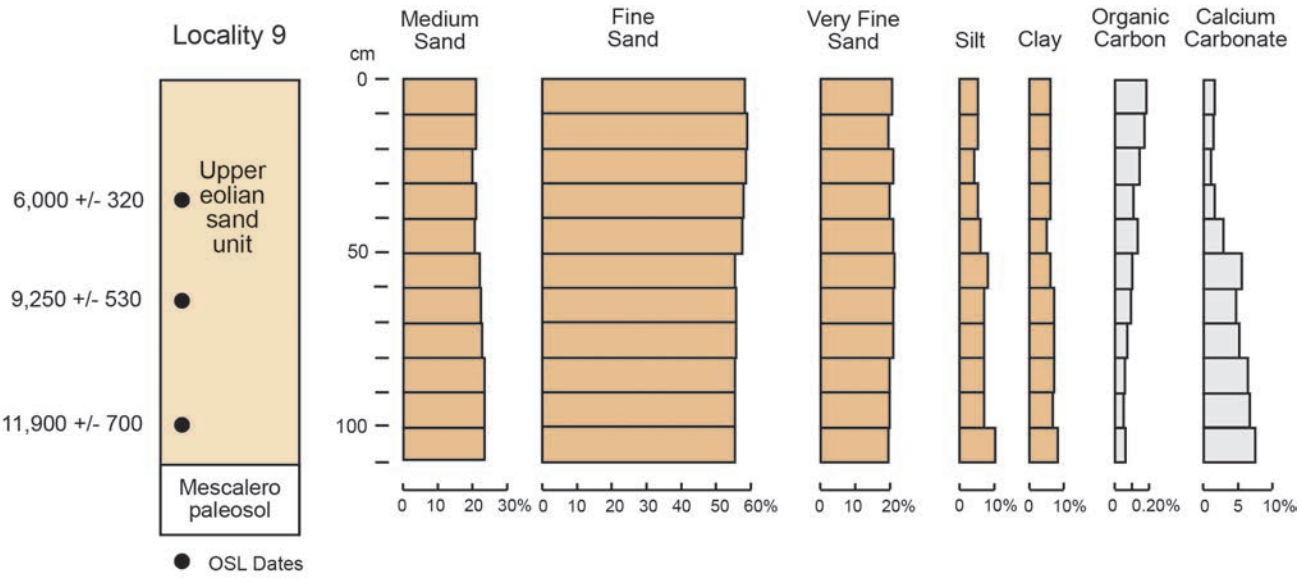

Figure 6.6. Sediment diagram from Upper eolian sand unit, Loc. 9, Eddy County.

Locality 20

The particle size trend at Loc. 20 shows an interesting picture of fine-grained sand being deposited in the late Pleistocene (Middle sand unit) that became increasingly coarse into the late Holocene (Fig. 6.7) as fine-grained sand was continuously carried away. About 300 years ago, the thick Holocene sand was deflated and a parabolic dune field began to form. At first, the dune sand was coarse, mimicking the underlying sand source. Very soon thereafter, however, the expansion of the dune field brought finer textured sand to the site and the upper part of the dune was dominated by fine-grained sand.

Locality 25

The east, down-wind side of the Red Lake area is marked by the Maroon Cliffs. Eolian sand is carried from the basin floor eastward upslope to the cliff area, where it is dropped, then carried downslope by fluvial-colluvial processes back into the basin. This process appears to have continued without discernible interruption for about 35 ka, resulting in a similar texture of sand and silt throughout that time (Fig. 6.8). The depositional period ended about 5 ka, similar to the timing of the termination of the Upper sand unit elsewhere on the Mescalero Plain. The one coppice dune sample is coarser than the other units, indicating that it formed from local pre-dune sands at this site with the finer particles carried away.

Locality 31

The locality consists of three small sub-areas, A, B, and C, in southwestern Lea County; sub-area A does not have sedimentologic data. Overall, the particle-size distributions of the Late Holocene eolian sand, Eddy paleosol topsoil, cover sand, and coppice dunes exhibit a surprising degree of variability (Fig. 6.9). At area C, the Eddy paleosol sand rests directly on the Late Holocene eolian sand, and their particle size distributions are similar. However, in area B, about 730 meters northwest of area C, the Eddy paleosol directly overlies caliche of the Mescalero paleosol and its texture is significantly finer than found in the Eddy paleosol in area C; even within area B where the two trenches are only 80 meters apart, the Eddy sands are divergent.

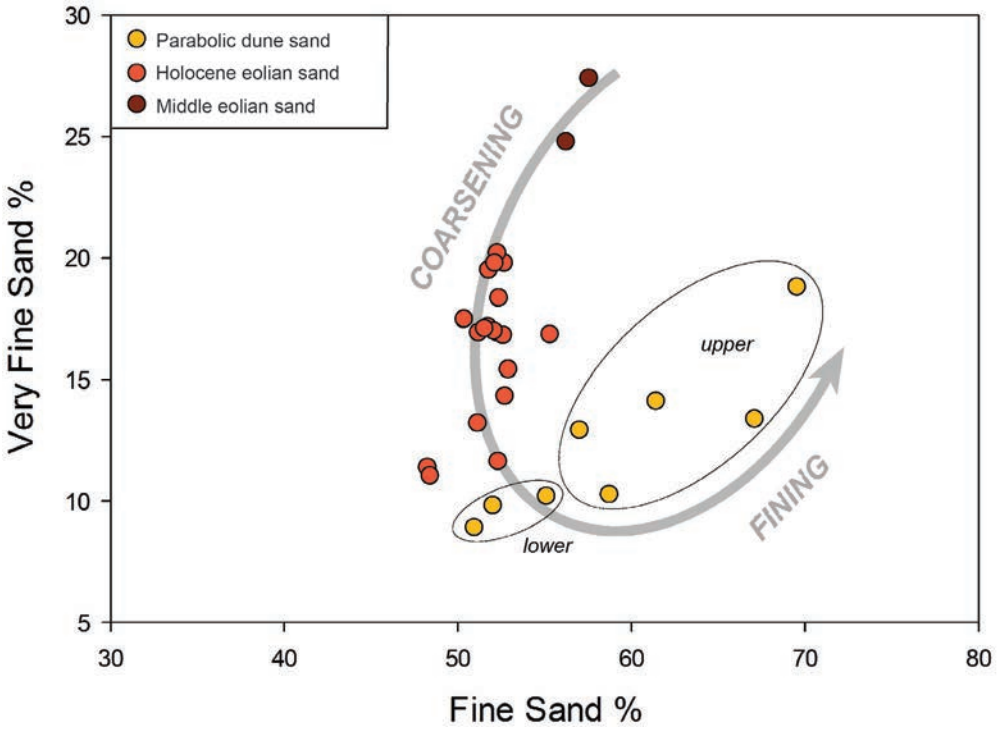

Figure 6.7. Particle size of eolian sands from southern Eddy County at Loc. 20 illustrating the coarsening of texture with the passage of time. Parabolic dune development started out with coarse particles as finer particles were carried away; eventually, fine particles were deposited at the site as the parabolic dune field continued to grow across the area and fine particles were transported widely across Loc. 20.

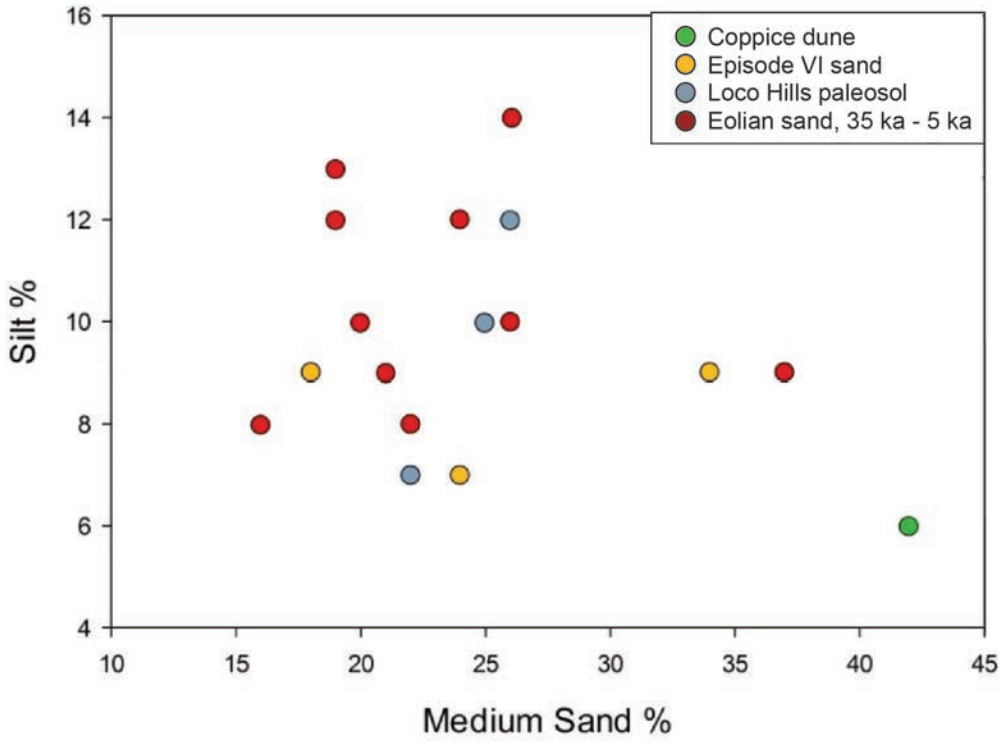

Figure 6.8. Particle size of eolian sands from the Maroon Cliffs at Loc. 25; the similar texture of the sands suggests that the same source and the same eolian processes have dominated sediment accumulation at this locality for 30 ka; the coarser coppice dune sand may be derived from deflation of local pre-dune sand, the fine sand and silt being carried away.

The cover sand overlies the Eddy paleosol in area B and its texture is very close to the underlying paleosol. Coppice dune texture, however, is uniformly coarser-textured with less very-fine-grained sand than found in the pre-dune sands. The dunes systematically have slightly higher percentages of medium-grained sand than the immediate underlying Eddy paleosol sand; the finer particles have been carried off by winds during the development of the dunes.

Eolian Sedimentology and Sand Sources on the Mescalero Sands

A number of assumptions and interpretations have been made in this chapter regarding the processes of eolian geology on the Mescalero Sands.

1. Wind transports fine-textured particles farther than coarse-textured particles. Thus, fining-upwards in a deposit suggests that a wider geographic range of sources are in play, bringing fine particles to a site of accumulation.
2. An eolian sand deposit, such as a dune that is derived from the immediately underlying eolian sand body, such as late Holocene sand or the cumulic Eddy paleosol, will have a similar particle-size distribution. Alternatively, the derived sand may be slightly coarser because the finer particles have been carried away from that place.
3. An eolian sand deposit that has the same particle-size distribution, bottom to top, without significant variability, suggests that the sand source has been the same throughout the period of sand accumulation.
4. The generally slow sediment accumulation rate of an eolian sand deposit suggests that the supply of sand was distant or not overly abundant. Rapid sediment accumulation suggests that the sand supply was abundant and readily available.

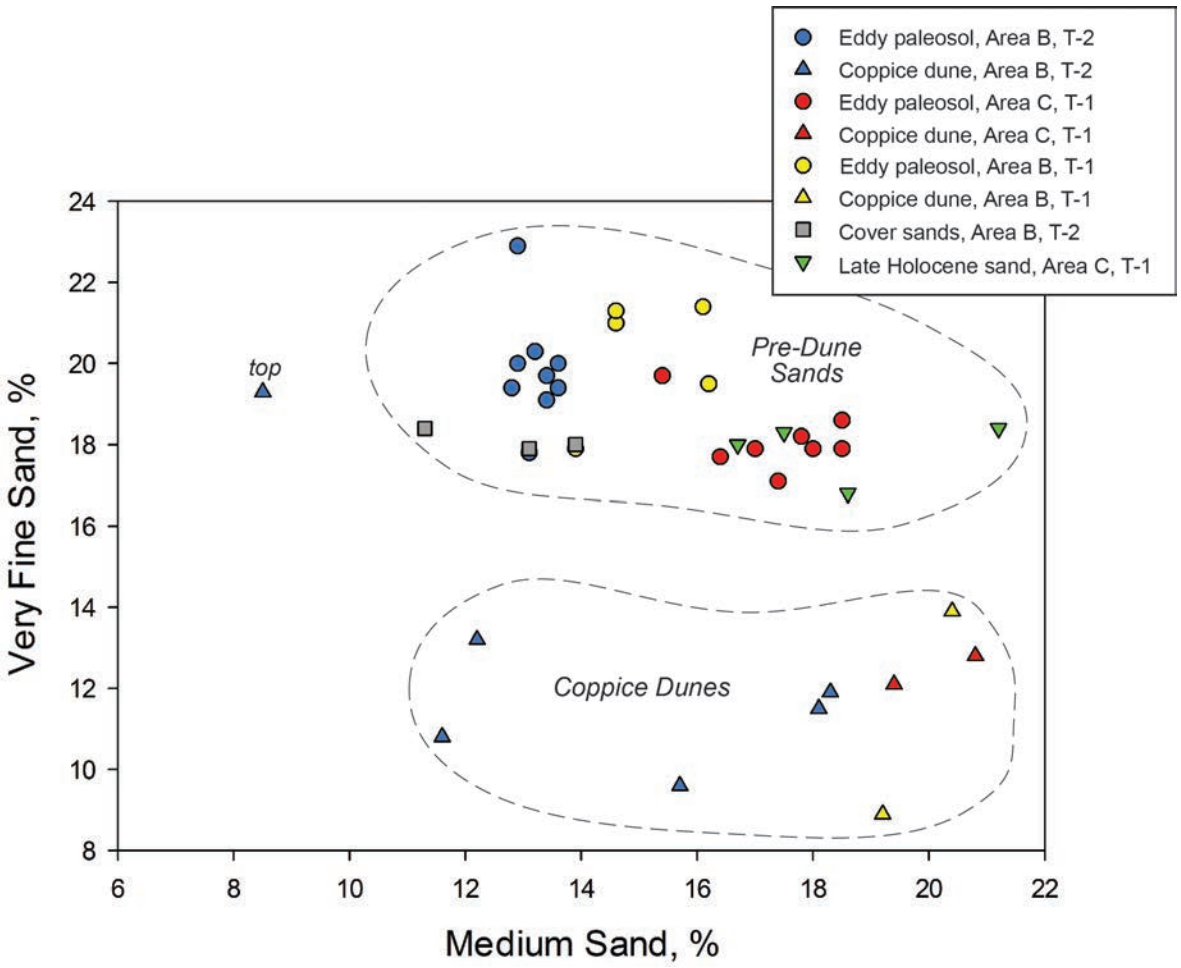

Figure 6.9. Divergent medium-sand and very-fine-sand distributions in the Late Holocene sand, Eddy paleosol, cover sand, and coppice dunes at Loc. 31 (sub-areas B and C), southern Lea County; in the legend, T = trench.

5. The beginning of a period of eolian sand deposition at a locality suggests that a new supply of sand has become available. The end of a period of deposition suggests that the sand supply has been depleted or cut off.
6. Sheet sand deposition is enhanced by grassland vegetation; vegetation dominated by shrubs will not hold wind-transported particles.
7. On the other hand, coppice dunes form by the capture of wind-transported particles by mesquite shrubs, especially Torrey mesquite, which has a low-growth, radiating-branch geometry. With time, the margins of a coppice dune and the underlying deposit that is not protected by the dune can be eroded, leaving the dune at the top of a pedestal of older sand.
8. Once the supply of new sand to a sand sheet has ended, sand-starved winds can deflate the previously deposited sheet sand, resulting in new deposits of cannibalized sand that are derived from the older deposits.
9. The shoreline and beach deposits of playa basins, even during standing water wet periods, are sand sources. Upon drying out, the playa floors may become particle sources as well, although they may be finer-textured than particles found in shoreline deposits.
10. Wind-deposited particles can be transported downslope by colluvial processes in areas with some topographic relief, such as the margins of basins.

11. Sand sources in small streams can be channels or floodplains. Channel particles tend to be coarse, reflecting the composition of the bed load. During wet periods and overbank deposition on narrow floodplains, floodplain particles tend to be finer-textured than particles in the channel.
12. During middle Holocene aridity, the Altithermal, some streams dried out completely and, upon depletion of channel sands, were no longer sources of particles to the sand sheet, and down-wind sheet sand growth ended (Episode III). With the late Holocene change in climate to wetter conditions, stream flow returned and particles became available, resulting in renewed eolian transport and deposition (Episode V).
13. Increased stream flow during full-glacial time resulted in rejuvenation of sediment transport in local streams that were serving as sand sources; the "new" sand had different radioisotope chemistry than the "old" sand, resulting in a change in isotope signatures in the down-wind eolian deposits, beginning with Episode II.

Note on Sand Sources and Winds

We should note that a specific sand source locality or group of localities have not been identified or equated with a specific eolian sand deposit (except for playa basins). Also, we have not taken into account the possibility of variable wind strengths over time or the possibility of changing wind directions, although the geometry of parabolic dunes suggests that the effective net wind direction in southeastern New Mexico has been persistently from the west and southwest, at least in the past 300 years.

Bioturbation

Turbation refers to processes that disturb and disrupt the natural bedding of a deposit. Bioturbation is caused by plants and animals. The most commonly observed bioturbation is rodent burrow fills. They are obvious in the field because the burrow fill material always has a different color, texture, and compaction than the surrounding sediment.

Carnivores such as coyotes and especially badgers can severely disrupt the natural stratigraphy as they dig after rodents. While coyotes dig away at the entrance to rodent dens, badgers plow through the sediment into the heart of underground dens. Badgers also dig home burrows as deep as three meters with ten meter long tunnels that are 30 cm in diameter. They have obliterated areas of alluvial fan stratigraphy at Ft. Bliss (Johnson, 1997) and have caused notable disturbance of fan deposits at the Spaceport America (Hall and Goble, 2014). Fortunately, rodent bioturbation is minimal on the Mescalero Plains, and evidence for subsurface burrowing activity by coyotes and badgers is rare.

Cicada Insects

Cicada nymphs live and burrow underground, feeding on juices from rootlets for periods of 13 or 17 years, after which they emerge for four to six weeks as adults. Their burrows are cylindrical and about 10 to 20 mm in diameter. As they dig forward, they push the sediment back into the passage through which they have moved, resulting in crescent-ridged burrow fills. Since the sediment left behind in their burrows is the same sediment through which they are digging, the burrow fills are virtually invisible in outcrops (Fig. 6.10) (Hall and Goble, 2006).

We suspect that eolian sands of all ages on the Mescalero Plain have been infested with cicada nymphs at one time or another. We occasionally see cicada burrow fills with a slightly different color from the surrounding sediment, especially at unit boundaries. Also, we have observed cicada burrows in the upper layers of caliche of the Mescalero paleosol at the contact with eolian sand where cicada nymphs have actually penetrated the carbonate, forming small cylindrical cavities. In some cases in sand, the burrow fills are preferentially cemented with carbonate and are prominent upon weathering, such as seen in Figure 6.10.

We also consider the possibility that cicada burrowing may disrupt subtle disconformities in eolian sands. The very slow sedimentation rates of the sand sheet, generally less than 0.2 mm per year, set the stage for erosion or scouring of the sand sheet surface at any time in the past. The fact that we do not see

any evidence for breaks in the sediments whatsoever suggests to us that delicate disconformities might have been obliterated by cicada burrowing activity. On the other hand, it is reasonable to expect that if disconformities are at all present, they would have been found by now in the dozens of study trenches that have been closely inspected and from which the sand has been analyzed for particle size and carbonate content as well as OSL dating.

Buried archaeological sites are especially susceptible to burrowing cicada; the soft sediment at site footprints seems to attract cicada nymphs. When cicadas encounter stones of a buried feature, they simply move around each stone, leaving it in place and intact but disturbing the sediment surrounding the stones. Cicada burrowing can move small flakes and other small materials a short distance in the sediment (Hall and Goble, 2006; 2008, p. 287).

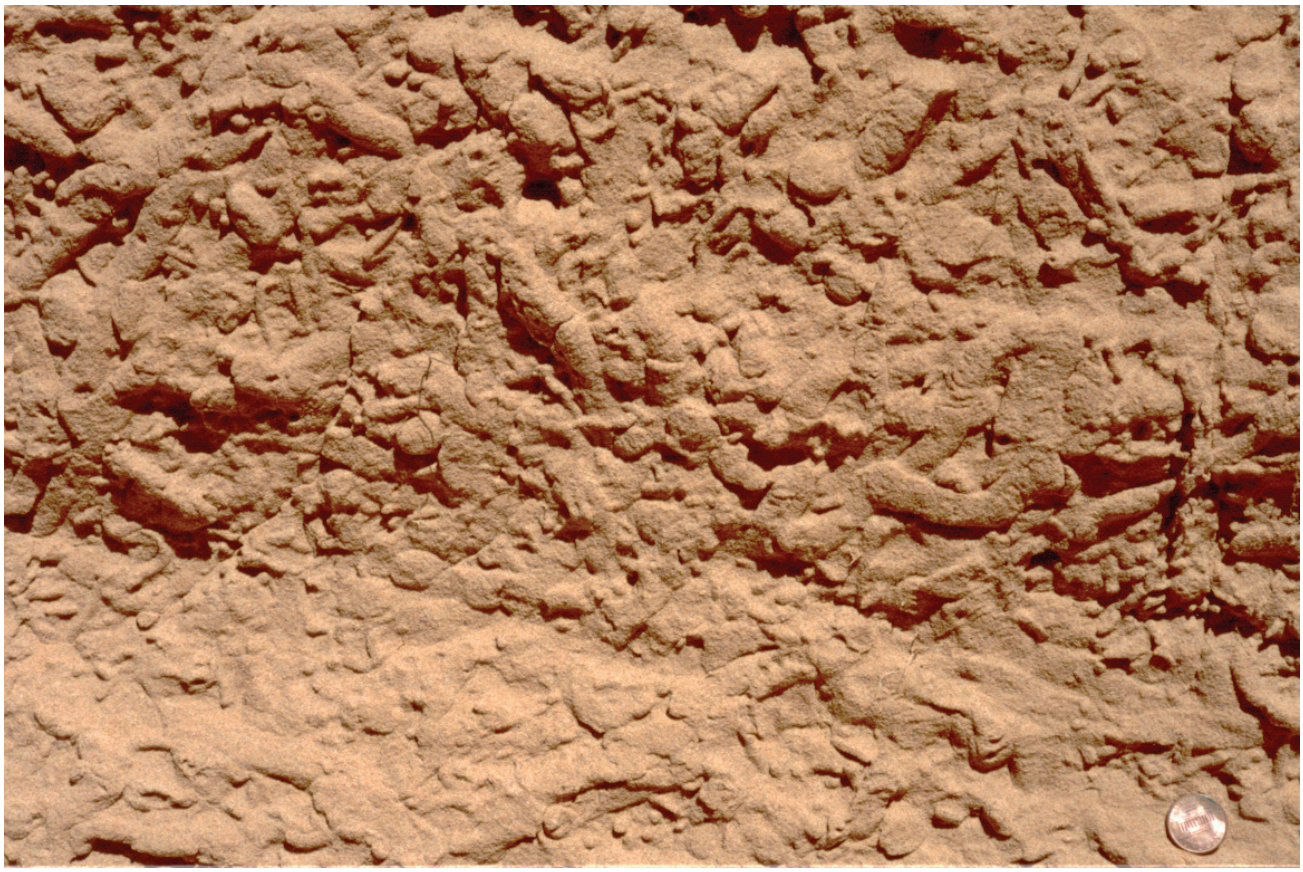

Figure 6.10. Cicada insect burrow fills at about 4.0 m depth in Upper eolian sand at Loc. 2, northern Eddy County; the age of the sand at this horizon is ca. 8,700 years BP; this remarkable photo has appeared in earlier publications (Hall, 2002a; Hall and Goble, 2006, 2008; Hall and Boggess, 2013); U.S. cent for scale, lower right.

VII. MESCALERO, BOLSON, AND STRAUSS SAND SHEETS: A BRIEF COMPARISON

The Mescalero, Bolson, and Strauss are the principal sand sheets in the northern Chihuahuan Desert and southern New Mexico (Fig. 7.1). The region has experienced the same broad paleoclimatic history during the late Quaternary. The chronology of periods of deposition, stability, and erosion of the three sand sheets, however, appears to exhibit some major differences as well as some commonality (Fig. 7.2).

Given perennial winds, the development of these sand sheets is a consequence of sand availability from their sources. The primary difference among these sand sheets is a direct result of their unique sources of sand and their history of sand availability.

Mescalero Sand Sheet

The Mescalero sand sheet occurs over a broad area of the Mescalero Plain with diverse topography and bedrock geology. The sand sources appear to be a number of small streams that cross the plain. Thus, the sand sources are many, and the availability of sand is dependent upon local fluvial conditions and geomorphology.

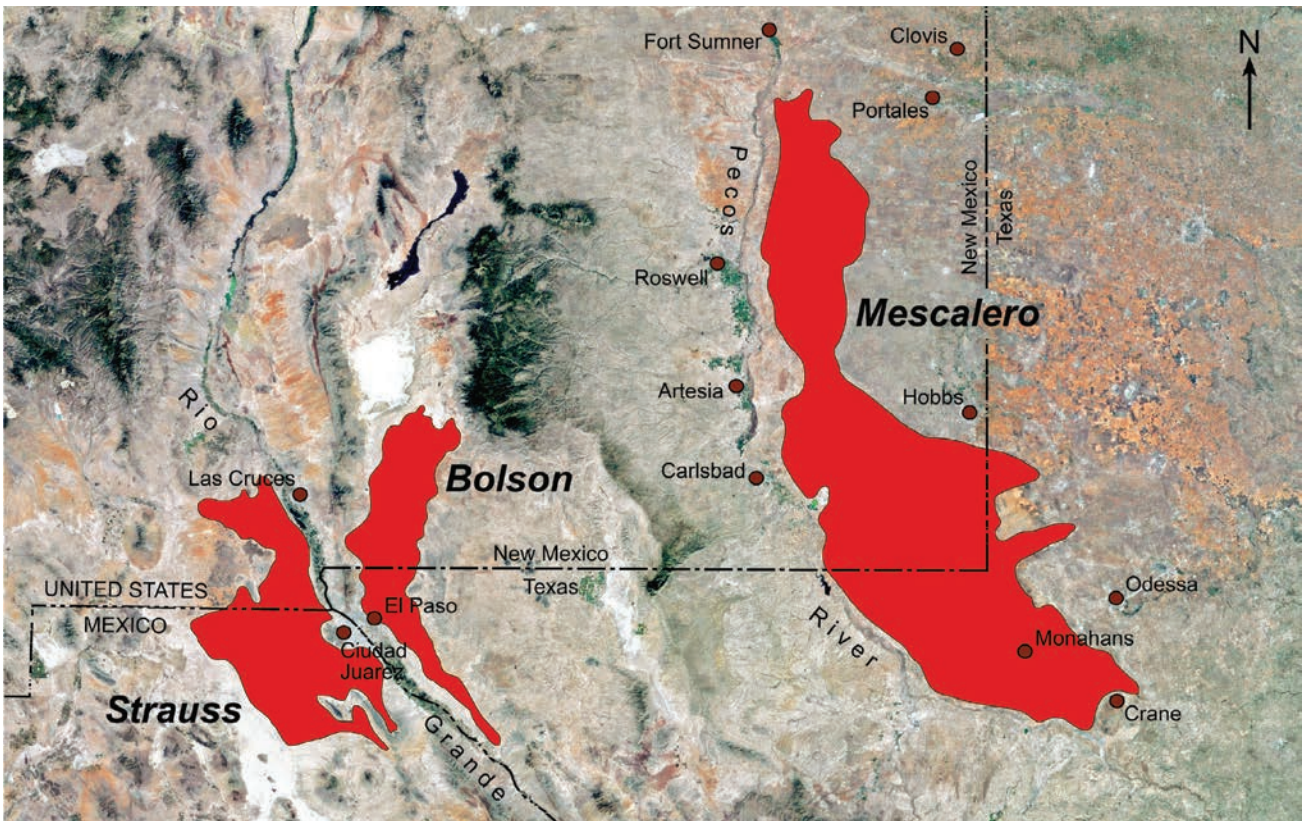

Figure 7.1. The three sand sheets of the northern Chihuahuan Desert; Mescalero (this bulletin), Bolson (Hall et al., 2010), and Strauss (Hall and Goble, 2015d); the white-colored terrane north of the Bolson sand sheet is the White Sands dune field, which has a very different history from that of the Bolson.

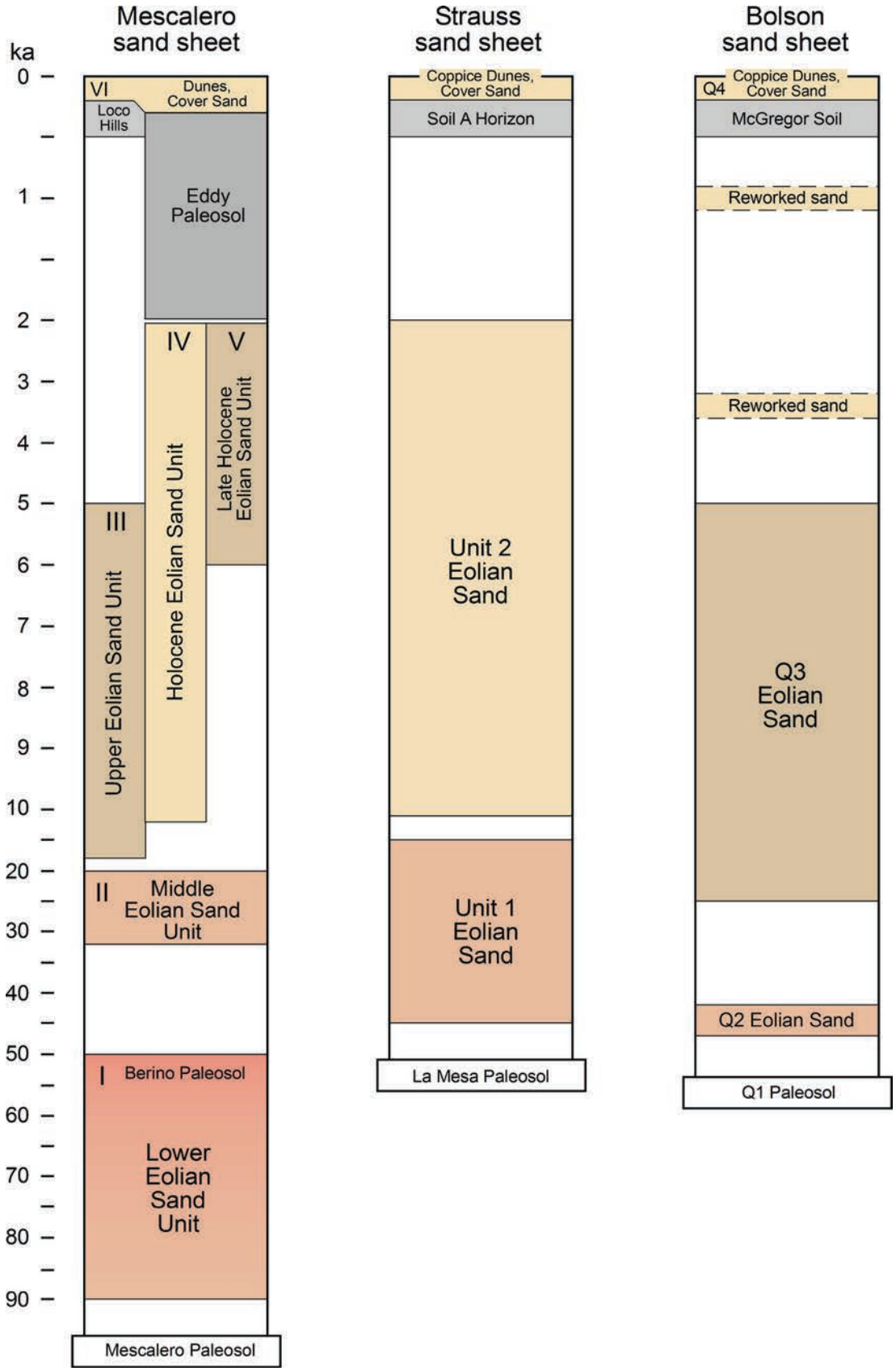

Figure 7.2. Summary chart of the three major sand sheets in southern New Mexico (Hall and Goble, 2015d; Hall et al., 2010; this bulletin); the chronologies are based on OSL dating; scale change at 2 ka and 10 ka.

Bolson Sand Sheet

The Bolson sand sheet occurs in the Hueco Bolson and Tularosa Basin in southern New Mexico and adjacent Texas, and its geology is comparatively simple. The Rio Grande appears to have been the sole source of sand to the sand sheet. The sandy floodplain in the Rio Grande downstream of El Paso was the sand source during the late Pleistocene and early to middle Holocene. Sand was entrained by westerly winds and funneled northward by local topography into the Hueco Bolson–Tularosa Basin. After the arid middle Holocene, the Rio Grande shifted to an overbank flooding condition in response to wetter climate. As a consequence, the sandy floodplain was buried by fluvial muds, and the sand supply to the Bolson was terminated, ending the accumulation of the sand sheet by 5 ka (Hall et al., 2010; Hall and Peterson, 2013).

Subsequently, in the late Holocene, sand was removed from some areas of the Bolson sand sheet by sand-starved winds and redeposited as thin patches of eolian sand across the basin floor, especially along basin margins. The slow sedimentation rate of the sand sheet, less than 0.10 mm per year, suggests that the Rio Grande was not an overly abundant source of sand to the Bolson during the late Pleistocene and early Holocene.

Strauss Sand Sheet

The Strauss sand sheet occurs in south-central New Mexico and extends southward into northern Chihuahua, Mexico. The sands were derived ultimately from the pluvial Lake Palomas in northern Chihuahua. The sand sheet formed during three phases of eolian deposition. During the Late Wisconsin, strong west winds associated with southward displacement of the jet stream resulted in the entrainment of sand from beach-related deposits of the Palomas basin. Sand was transported northward into New Mexico and deposited as sheet sand ca. 45 to 15 ka. After an interval of stability, the late Pleistocene sand was eroded and redeposited during the Holocene about 11 ka to 1.9 ka as a second layer of sheet sand. After another period of stability, the sand sheet was again reactivated by about 0.5 ka, forming a weak cumulic A horizon soil (unnamed), cover sands, and coppice dunes. This third phase of eolian activity beginning 500 years ago is ongoing today (Hall and Goble, 2015d).

Holocene Similarities of the Sand Sheets

Overall, the controlling factor for the development of the sand sheets appears to be the conditions surrounding sources of sand. Climate and climate change play a role, but indirectly through their influence on sand sources, especially whether or not a supply of sand is readily available for wind-transport.

5,000 Years Ago

The Bolson and part of the Mescalero sand sheets experienced an end in primary sand accumulation at 5 ka. In the Bolson region, unit Q3 was forming by 24 ka but was terminated at 5 ka; archaeological sites that post-date 5 ka, Archaic to Formative sites, occur on the surface of the sand sheet (Miller, 2007; Hall et al., 2010). In the Mescalero region, the Upper sand (episode III) began accumulating about 18 ka and ended at 5 ka.

The end of sand accumulation at each place was due to the shutting off of the sand supply. The sand source of the Bolson is the adjacent Rio Grande downstream from El Paso, Texas, and Ciudad Juarez, Mexico (Hall and Peterson, 2013). During the early Holocene, alluvium in the local Rio Grande valley was characterized by massive to small cross-bed quartz sand, very fine- to medium-grained; the sediment was deposited across the valley by lateral migration of the channel. During the arid middle Holocene, the river may have dried; sand dunes formed on the stable floodplain. After 5 ka, a shift to wetter climate resulted in greater discharge and the beginning of overbank deposition of very fine sand, silt, and clay on the Rio Grande floodplain, a process that continued throughout the late Holocene. As a consequence, the accumulation of overbank mud on top of the channel sand sealed off the broad floodplain as a source of sand to the Bolson sand sheet. Subsequently, with the source of fresh sand from the Rio Grande eliminated, winds across the sand sheet cannibalized the pre-5 ka Bolson unit Q3, resulting in scattered thin deposits of reworked eolian sand across the sand sheet.

Accumulation of the Upper sand of the Mescalero sand sheet also ended in places at 5 ka. In northern Eddy County, clay laminae developed in the thick sand, and in southern Eddy County a soil Bw horizon with a lower Bk horizon formed in the Upper sand. The specific sand source that was eliminated at 5 ka has not been identified. Elsewhere on the sand sheet, however, two other sheet sands were accumulating at that same time (episodes IV and V) across the Mescalero Plain, supplied by small stream channels.

2,000 Years Ago

The principal sheet sand (Unit 2, Figure 7.2) of the Strauss formed largely during the Holocene from 11 ka to 1.9 ka (Hall and Goble, 2015d). The source of the sand was through cannibalization of the late Pleistocene eolian sand (Unit 1, Figure 7.2) that had been deposited 45 ka to 15 ka. After the end of deposition of unit 2, a weak Bw and Bk soil horizons formed in the unit sand. The end of accumulation of unit 2 is probably related to the comparatively wetter climate during the late Holocene, resulting in dense grassland vegetation across the region and shutting down the erosion and cannibalization of unit 1.

At the same time, at 2.0 ka, the cumulic Eddy paleosol A horizon topsoil began forming on the Mescalero sand sheet, also a consequence of a wetter climate and prairie vegetation. Paleosol development across the plain resulted in the end of deposition of the Holocene and Late Holocene sheet sands. Although a soil A horizon did not form on the Strauss sand sheet, its accumulation ended and a weak Bw and Bk horizons developed in the sand during the period of the Eddy paleosol on the Mescalero sand sheet.

500 Years Ago

During the past 500 years we see a parallel in all three sand sheets; in all cases, a weak soil A horizon formed on the sheet sands. On the Mescalero it is called the Loco Hills, and on the Bolson it is called the McGregor; it is unnamed on the Strauss. The A horizon may have formed on a grassland during the slightly cooler and wetter Little Ice Age. By 300 years ago the Little Ice Age had peaked, and the sand sheets began to deflate, forming parabolic and coppice dunes on the Mescalero and coppice dunes on the Bolson and Strauss; cover sands were deposited across all three. Sand deflation and dune formation is continuing today on the Strauss sand sheet and perhaps the others as well.

VIII. CHEMICAL SIGNATURES OF SAND DEPOSITS

As already noted, the OSL dating method produces information on the amount of potassium oxide (K_2O), uranium (U), and thorium (Th) in the dated sediment. In our research, we have measurements of the three isotopes from 195 sediment samples. These data provide a chemical signature of the sediment. Different packages of sediment chemistry are commonly found in unrelated eolian sands at geographically separated localities. Looking at deposits at one locality, however, changes in the chemistry of sand of different ages may indicate either a shift in the chemistry of the sand at its source, such as an influx of fresh or old sand that is newly made available, or a change in sand source from one locality to another.

Sand Chemistry, Dose Rates, and OSL Dating

The ^{40}K found in quartz-dominated sand deposits is mostly in the form of K-feldspars, such as orthoclase ($KAlSi_3O_8$). Feldspars and heavy minerals, such as zircon, contain U and Th. The total amount of these radioelements in a sand deposit are used to calculate the dose, which is defined as "the energy absorbed per kilogram and the unit of measurement is the *gray* (Gy)" (Aitken, 1998, p. 39). The dose rate is expressed as gray per thousand years (Gy/ka). The dose rate is the primary variable in the calculation of the burial age of sand grains.

In the Mescalero sand sheet, the K_2O content of eolian sand deposits ranges from 0.29 to 1.69 percent, U content ranges from 0.4 to 2.12 parts per million (ppm), and Th content ranges from 1.0 to 4.48 ppm (Table 8.1, Appendix A). The amounts of K_2O, U, and Th in deposits at a single study site may be unique to that locality, thus providing a chemical signature for that sand and its source.

Radioelement Depletion with Sand Grain Recycling

Nearly all of our OSL studies at specific sites show a decline in the amount of radioelements and dose rates with the passage of time (Figs. 8.1, 8.2). In situ weathering of the sediment does not appear to be

Table 8.1. Summary OSL laboratory data, Mescalero Sand Sheet, southeastern New Mexico; mean values and 1 standard deviation (Figs. 8.3, 8.4) (Appendix A)

Stratigraphic units	K_2O (%)	U (ppm)	Th (ppm)	U/Th (ppm)	No. of samples	Localities
Mescalero Sands, all eolian units	0.79 ± .25	0.88 ± 0.33	2.72 ± 0.80	0.33 ± 0.098	171	28 locs.
Dune and cover sands	0.61 ± 0.24	0.68 ± 0.24	2.05 ± 0.58	0.33 ± 0.087	19	15,16,17,20, 22,23,24,25, 27,31,33
Eddy paleosol	0.71 ± 0.15	0.85 ± 0.38	2.45 ± 0.44	0.34 ± 0.12	20	11,12,14,15, 16,18,31,33
Late Holocene	0.73 ± 0.16	1.06 ± 0.56	2.58 ± 0.50	0.40 ± 0.16	8	18,23,24,31
Holocene	0.70 ± 0.21	0.81 ± 0.21	2.61 ± 0.74	0.31 ± 0.038	18	14,15,16,17, 20,22
Upper	0.84 ± 0.14	0.82 ± 0.27	2.86 ± 0.96	0.30 ± 0.10	11	2,5,8,9
Middle	0.94 ± 0.25	1.04 ± 0.23	3.86 ± 1.11	0.28 ± 0.039	8	15,16,19,20, 22,33
Lower	0.84 ± 0.18	0.91 ± 0.34	3.17 ± 0.80	0.30 ± 0.12	9	1,5,6,7,16, 27

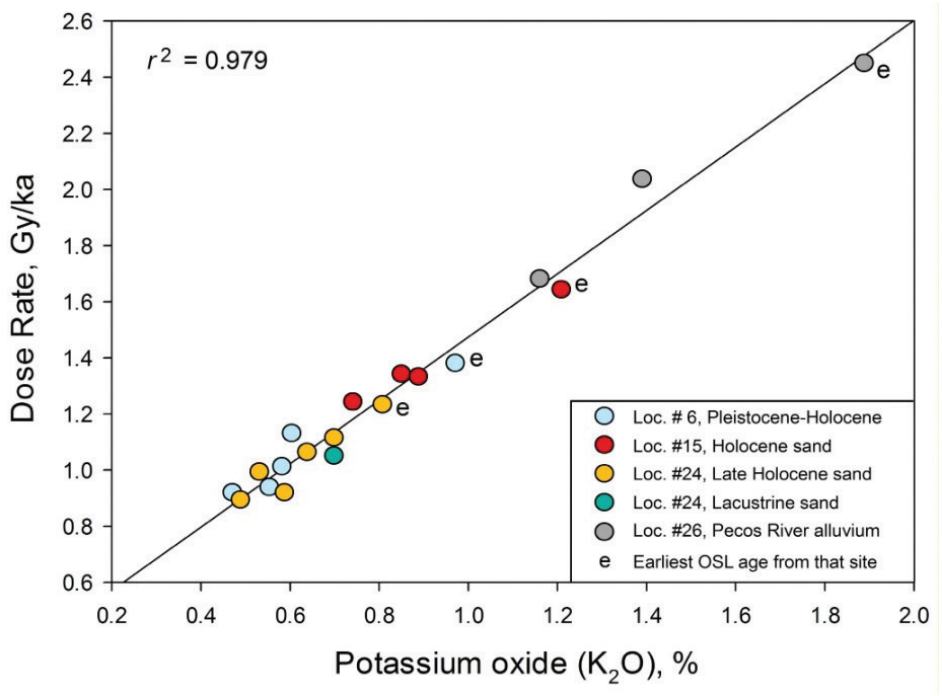

Figure 8.1. Strong correlation of K_2O content and dose rate (modified from Hall and Goble, 2015a). Pecos River alluvium has a greater amount of K_2O than eolian sand in the Mescalero sand sheet. Also, the sample with the highest amount of K_2O is the oldest sample in these four suites of ages.

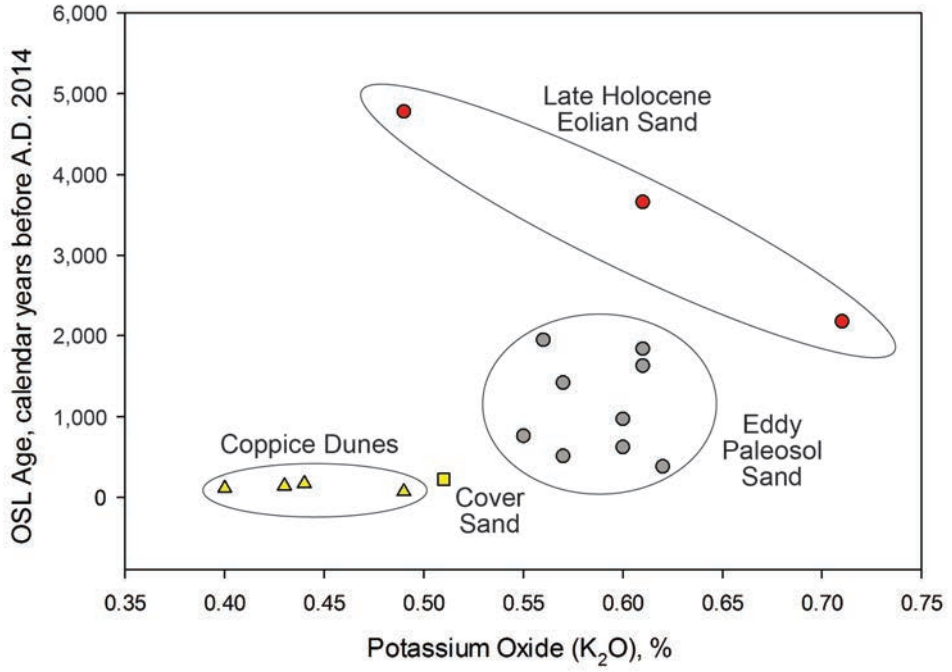

Figure 8.2. The decrease in K_2O% from the Eddy paleosol sand to the cover sand to the coppice dune sand at Loc. 31-A,B,C illustrates the loss of potassium feldspar with the entrainment–transportation–deposition etc. of particles with the passage of time, in this case less than 2000 years. The increase in K_2O% in the Late Holocene sand may reflect new, fresh sand becoming available at the sand source as a consequence of rejuvenated fluvial activity in response to wetter post-Altithermal climate.

the cause of the decline in radioelements. Weathering would result in loss of K-feldspars, thereby producing different ages. Instead, old and young sands alike with well-documented stratigraphy have retained their antiquity with internal consistency.

We propose that the losses of K, U, and Th are a direct consequence of continued reworking of sand grains across the sand sheet. The process of reworking involves entrainment–transportation–abrasion–fracturing–redeposition of mineral grains in a continuous cycle, extending over millennia. Eventually, the grains are deposited at some place, perhaps miles from their source, where they are buried and removed from the rework cycle. Sand grains that were buried thousands of years ago and were taken out of the recycle loop at that time will have high amounts of radioelements and high dose rates. In contrast, sand grains that were buried only hundreds of years ago and have been reworked for a longer period of time will have reduced amounts of radioelements and lower dose rates. Thus, in an eolian system, younger and younger sand deposits will exhibit increasingly greater losses of radioelements and lower dose rates (Fig. 8.1). This relationship is expected with constant reworking of grains. It is reassuring that the oldest samples have the higher concentrations, since that rules out weathering as a significant variable.

Coarse-Scale Patterns of Chemical Signatures

The chemical signatures of the three sand sheets of the northern Chihuahuan Desert in New Mexico are dissimilar, indicating their divergent geology and the unique chemistry of their sand sources (Figs. 8.3, 8.4). At the same time, it is clear from the diagrams that the chemistry of the Bolson and Strauss sand sheets each has a fairly narrow range of variability, indicating that the development of each is a consequence of their specific confined sand source (discussed in chapter 7). On the other hand, the chemistry of the Mescalero sand sheet is much more variable, reflecting the diverse geology and multiple sand sources across the comparatively broad Mescalero Plain. The six episodes of eolian activity on the Mescalero are plotted separately. They show no clear trends, indicating that, taken together, the six episodes are a product of variable conditions throughout time across the plain (Figs. 8.3, 8.4).

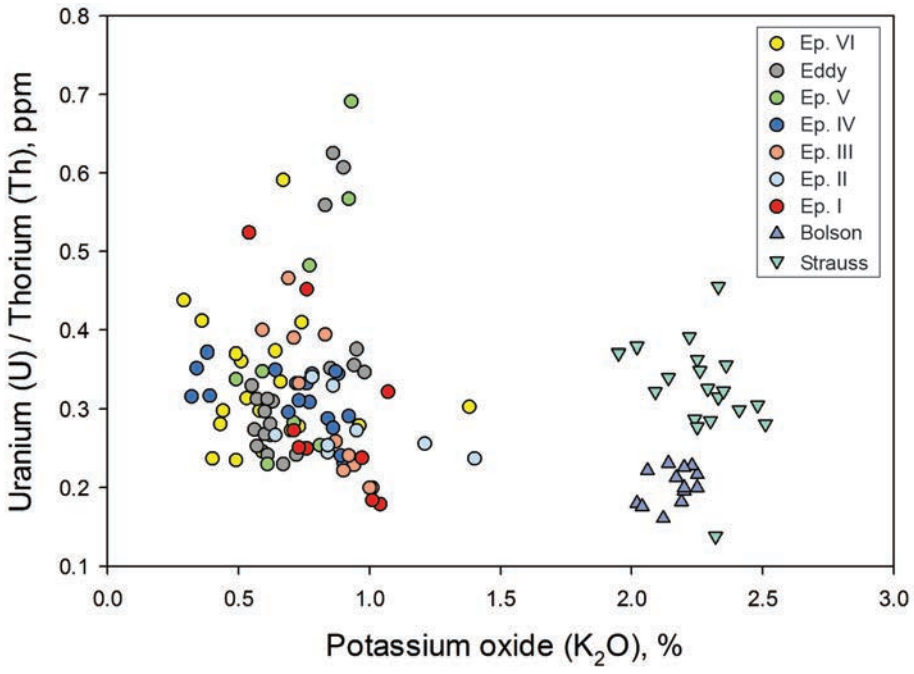

Figure 8.3. Chemical signatures of the six different episodes of eolian activity and the Eddy paleosol of the Mescalero sand sheet (94 samples) and the Bolson and Strauss sand sheets (Hall et al., 2010; Hall and Goble, 2015d). Note the greater variability in the Mescalero chemistry compared with the Bolson and Strauss. The isotopes are from the OSL dated samples from the sedimentology chapter (Table 6.1).

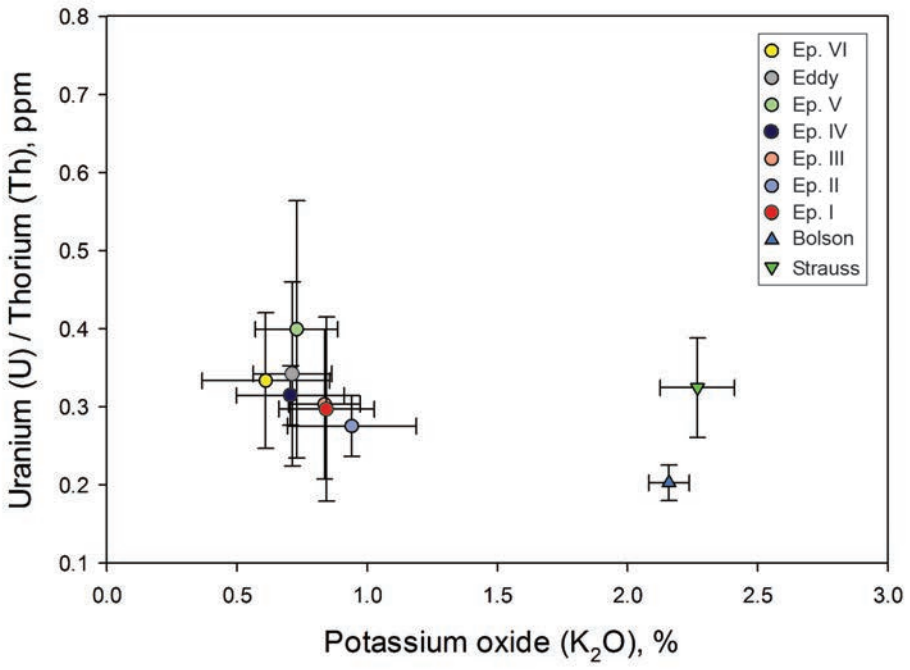

Figure 8.4. Mean values of potassium oxide (%) and uranium/thorium (ppm), 1 standard deviation bars, episodes I through VI, Eddy paleosol, and the Bolson and Strauss sand sheets (same data as in Fig. 8.3).

Fine-Scale Patterns of Chemical Signatures

Some patterns emerge when chemical data from specific study sites are plotted individually (Figs. 8.5, 8.6). The site patterns indicate that each locality across the plain reflects a specific set of sand sources and depositional conditions, resulting in differences in chemical signatures from place to place. Four localities (17, 18, 23, and 25) are especially divergent from the mean and from each other (Fig. 8.6).

Radioisotope signatures from Monahans Sandhills, Texas, from the Mescalero Sands North Dune Off-Highway Vehicle Area (Mescalero North), and from the Jal-Andrews dune area (Rich and Stokes, 2011) are compared with the geographically nearest samples from far southeastern New Mexico in this study (Locs. 11, 12, 16, and 17) (Fig. 8.7). While some data points overlap, a noticeable incongruence is present. The north and south samples generally have lower amounts of K_2O than found in the samples from this study (except Loc. 17). The low values of K_2O may indicate that these localities represent a terminal end-location for sand recycling and deposition, with the sand grains originating perhaps from a distant source.

Late Wisconsin Shift in Chemistry of Sand Source

At least five stratigraphic records show a significant change in the sand chemistry during the late Pleistocene that is not related to the gradual loss of radioelements by reworking: localities 5, 7, 16, 27, and 29 (Figs. 8.8, 8.9). The most definitive shift is observed at locality 16, where a shift in chemistry occurs between 31.4 ka and 20.7 ka during the Late Wisconsin (Fig. 8.8) (the last glacial maximum was 26.5 ka to 20-19 ka; Clark et al., 2009). The change in chemistry is an increase in K_2O content from 0.64 percent to 0.86 percent. After the shift, a new trend in K_2O depletion kicks in as a consequence of the sand grain recycling process described earlier. The chemistry change evidently occurred at the sand source as new assemblages of sand grains with higher amounts of potassium feldspar were introduced to and became freshly available at the source.

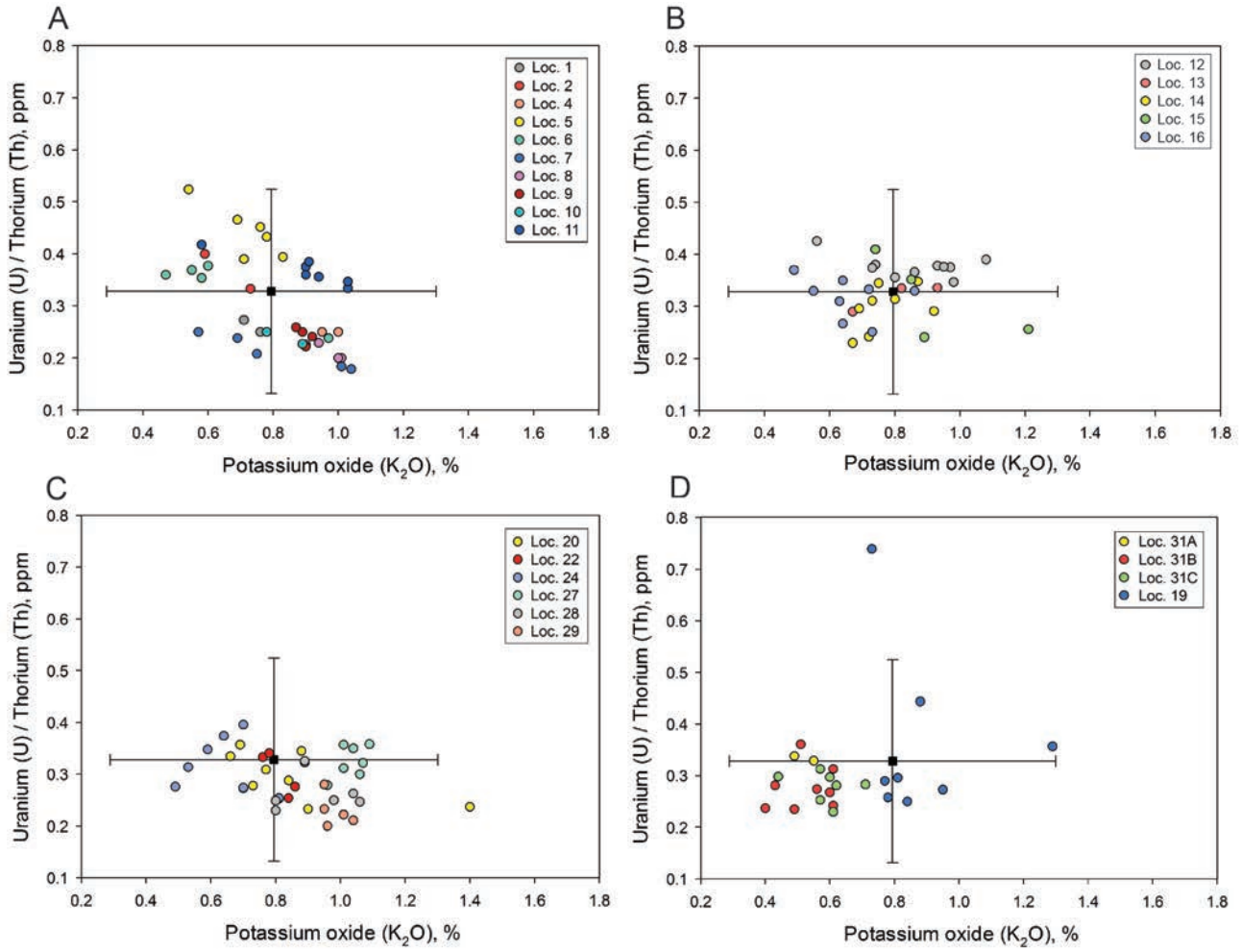

Figure 8.5. Potassium oxide (K_2O) ppm versus Uranium (U)/Thorium (Th) ppm for study localities on the Mescalero Plain; A, Locs. 1, 2, 4, 5, 6, 7, 8, 9, 10, 11; B, Locs. 12, 13, 14, 15, 16; C, 20, 22, 24, 27, 28, 29; D, 19, 31A-C; for comparison, the mean value of 171 OSL dates from the Mescalero Plain is shown with 2 standard deviation bars (data in Appendix A).

One might suppose that the processes that introduced new sand at the source would trigger a change in the sedimentology or stratigraphy. Not so, in the case of Locality 16. The introduction of new sand (and the shift in K_2O content) at the source occurred within the period of deposition of the Middle eolian sand unit (age 33 to 20 ka) (Fig. 8.8). The dominant local eolian processes evidently continued without modification even though new sand was introduced at the source (and the chemistry of the sand had changed).

The record from Loc. 27 provides additional information on the chronology of the change in sand source chemistry. An OSL sample dated at 22.7 ka has a K_2O content that is intermediate between the older and younger trends in chemistry (Fig. 8.9C). Thus, the change in sand source chemistry was well-underway at the time of the last glacial maximum (Clark et al., 2009).

The shift in radioisotopes at Loc. 5 was accompanied by a change in texture (although a change in texture was not found at Loc. 16). Before the shift, the sand was comparatively coarse-grained. After the shift, the texture was consistently fine-grained (Fig. 6.5). The Late Wisconsin change at Loc. 5 resulted in a decrease in medium-grained sand and an increase in fine-grained sand. The reshuffling of the fluvial sand source during full-glacial stream activity resulted in the availability of finer-textured sand, the fine sand perhaps dominating overbank deposition along narrow floodplains and becoming available as the renewed sand source (from chapter 6).

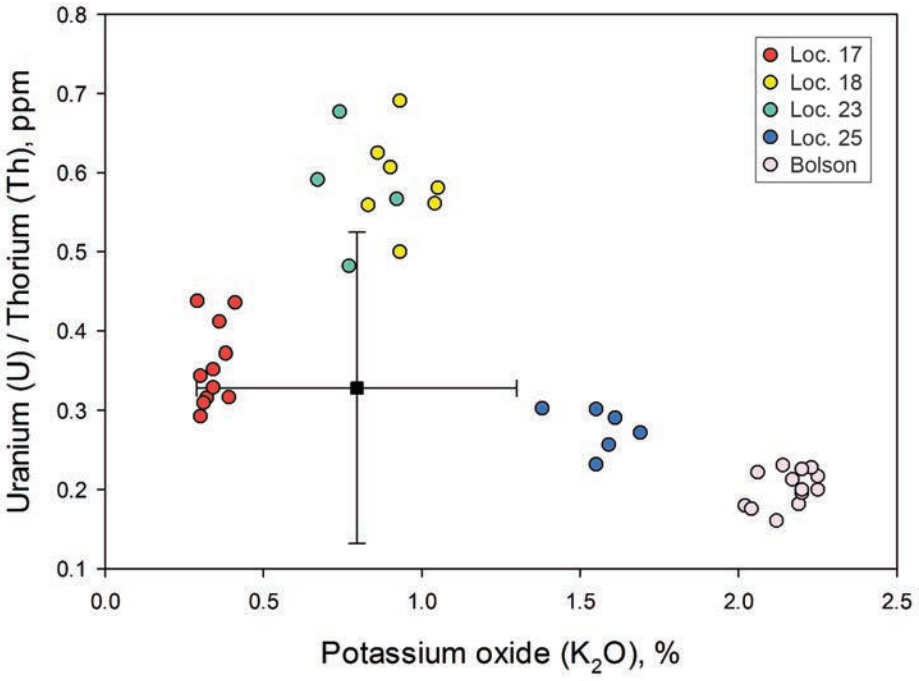

Figure 8.6. Potassium oxide (K_2O) versus Uranium (U)/Thorium (Th) of atypical chemical signatures of Locs. 17, 18, 23, 25; mean value of 171 OSL dates with 2 standard deviation (SigmaPlot 12); the Bolson sand sheet is shown for comparison (Hall et al., 2010).

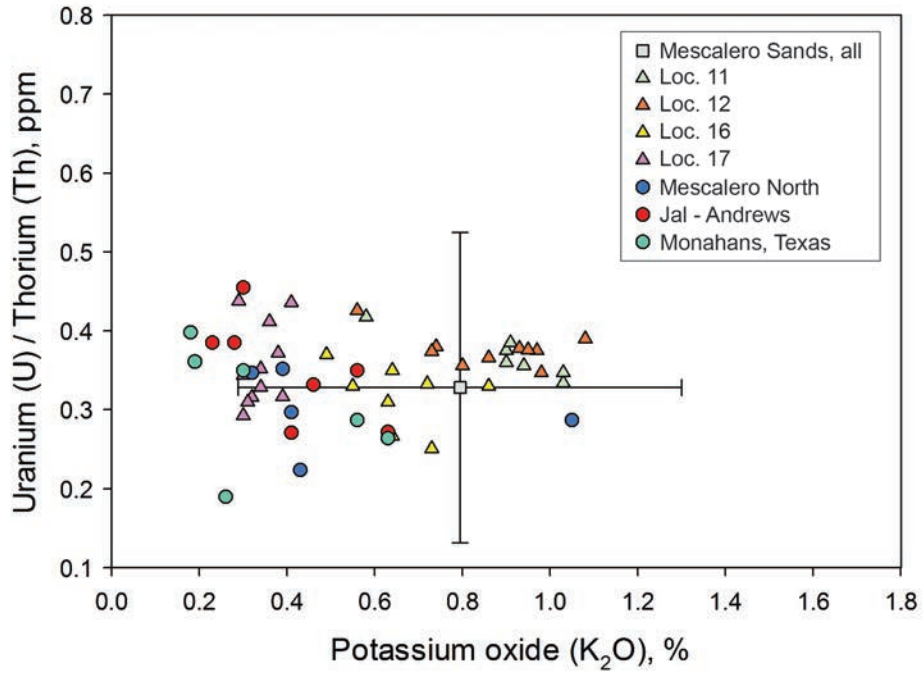

Figure 8.7. Radioisotope signatures from the southeastern corner of New Mexico (Locs. 11, 12, 16, 17; this bulletin) compared with Mescalero North, Jal-Andrews, and the Monahans Sandhills, Texas (from Rich and Stokes, 2011; 2 samples from the Jal area have U/Th values in the 1.4 ppm range and are excluded from the diagram); all of the data, 171 samples, from the Mescalero Sands (this bulletin), mean with 2 standard deviations (such as shown in Figs. 8.5, 8.6). Some of these data are also shown in Fig. 8.11.

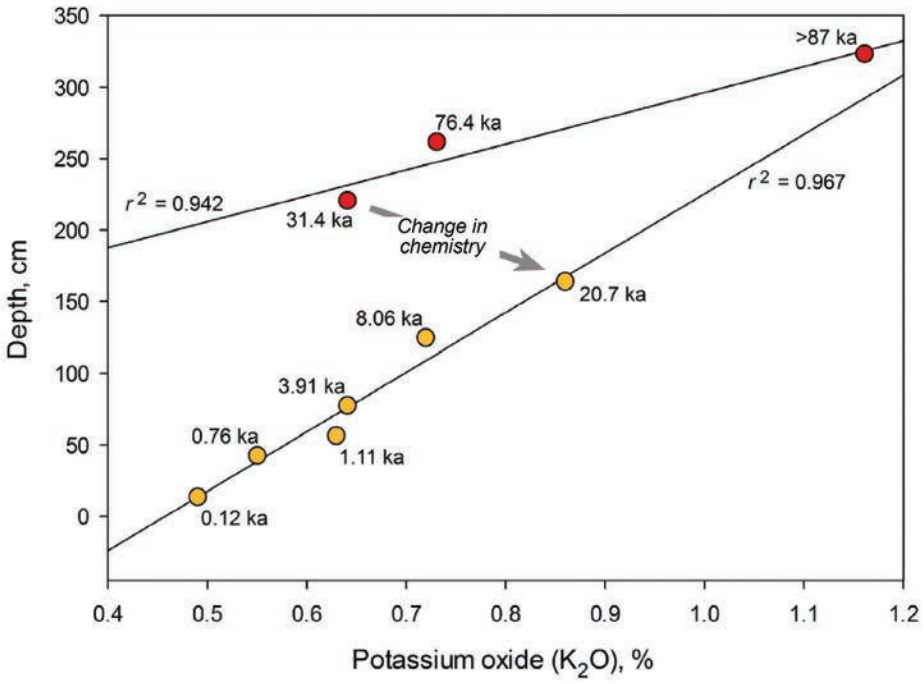

Figure 8.8. Potassium oxide versus depth, Loc. 16, southern Lea County. Nine OSL ages from a single trench, the ages ranging from >87 ka to 0.12 ka, show a shift in K_2O content between 31.4 ka and 20.7 ka, suggesting a significant change in the chemistry at the sand source, probably Antelope Draw, during the Late Wisconsin.

Origin of the Sand that Makes Up the Mescalero Sands

Various aspects of the origin of the sand that formed the Mescalero Sands have been alluded to throughout this bulletin. Overall, there appear to be only four potential identifiable sand sources for the Mescalero Sands in southeastern New Mexico: (a) underlying Permian-Triassic-Gatuña Formation, (b) Pecos River alluvium, (c) playa basins, and (d) alluvium from small streams across the plain, sourced by sand derived from the Ogallala Formation. These potential sand sources are discussed below.

Bedrock Sand Source

The Mescalero Plain is underlain by Permian and Triassic evaporites and red beds (Kelley, 1971; Lucas and Anderson, 1993). The late Cenozoic Gatuña Formation with variable lithology also occurs in southeastern Eddy County (Powers and Holt, 1993). However, it is unlikely that Permian, Triassic, and Gatuña sedimentary rocks could be sources of eolian sand to the Mescalero Sands. In nearly all cases, caliche of the Mescalero paleosol has formed directly on the late Pleistocene erosional surface on these strata, sealing them off in most areas and eliminating them from being sand sources.

Pecos River Alluvium

The distribution of the Mescalero Sands in New Mexico and Texas (the Monahans Sandhills) is located on the east, down-wind side of the Pecos River (Fig. 1.1). A conventional view is that its geographic location suggests that the Pecos River is the sand source due to its down-wind location, similar to the situation with other dune fields next to river valleys.

The geochemical properties of the Pecos alluvium and Mescalero sand, however, appear to be quite different. The alluvium is characterized by higher amounts of titanium (Ti), strontium (Sr), zirconium (Zr), barium (Ba), and rubidium (Rb) than found in the eolian sand; from these data, Muhs and Holliday (2001) concluded that the Mescalero sands are *not* derived from Pecos River alluvium. Their Zr and Sr data also indicate dissimilarity of the Mescalero Sands of New Mexico, the Monahans Sandhills of Texas, and the Blackwater Draw Formation of the Texas Southern High Plains, compared to each other (Fig. 8.10).

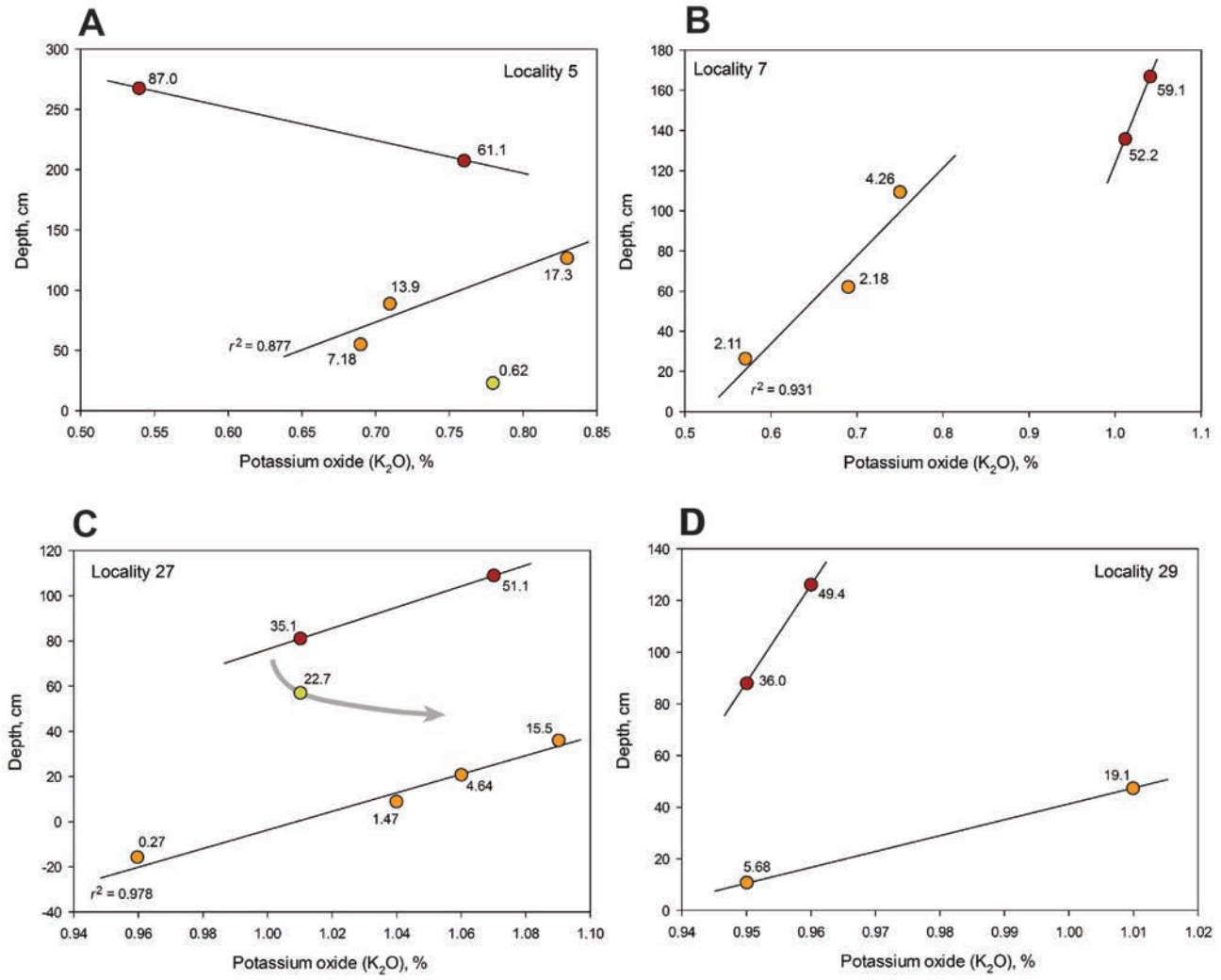

Figure 8.9. Four additional examples of changing chemistry during the late Wisconsin on the Mescalero sand sheet, all indicating a shift in the chemistry of the sand source; the numbers associated with each data point are OSL-derived years (ka); A, Loc. 5 showing a possible second change in source chemistry by 620 years ago, perhaps related to regional downcutting event in alluvial valleys about 1000 years BP (Hall and Peterson, 2013); B, Loc. 7, from the area of Los Medaños dunes; in this atypical case, the trend was to less K_2O, not more; C, Loc. 27 with a transitional sample from the changing-chemistry event dated 22.7 ka, right at the peak of the last glacial maximum; the youngest dated sample is 270 years from 16 cm above base of coppice dune sand; D, Loc. 29, from a solution-pipe fill in gypsum of the Rustler Formation (Permian).

Radioisotopes also show similar divergent patterns (Fig. 8.11). The Mescalero Sands (southeastern New Mexico), Pecos River late Holocene alluvium, and the Blackwater Draw Formation (from near the type locality, Texas Southern High Plains) are chemically dissimilar. Interestingly, the Gatuña Formation (capped by the Mescalero paleosol) has a signature that falls within the measurements from the Mescalero Sands.

In summary, at this stage, sediment chemistry (Zr-Sr and radioisotopes) eliminates the Pecos River alluvium as a sand source of the Mescalero Sands. The same data also show a general disparity between the sediment chemistry of the Mescalero Sands and the Blackwater Draw Formation, indicating they were likely derived from different sources..

Playa Basins

Seven large playa basins occur on the Mescalero Plain in southeastern New Mexico, each covering approximately 1 to 6 km^2 in area; the playas may have formed by surface collapse due to dissolution of underlying Permian evaporites. Other smaller playa basins are also present, and numerous small depressions only 100 to 200 m in diameter occur in some areas. The geologic histories of these basins and their deposits have not been systematically investigated.

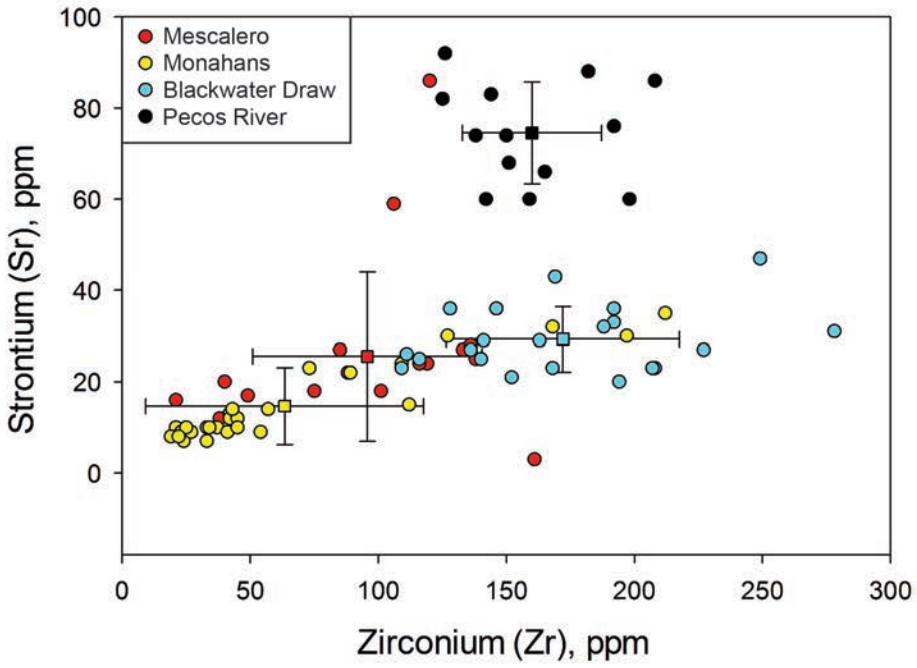

Figure 8.10. Zirconium (Zr) versus strontium (Sr) from the Mescalero Sands (SE New Mexico), Monahans Sandhills (Texas), Blackwater Draw Formation, and alluvium from the Pecos River; from Muhs and Holliday, (2001), Supplemental Data; squares are mean values with one standard deviation bars, SigmaPlot 12.

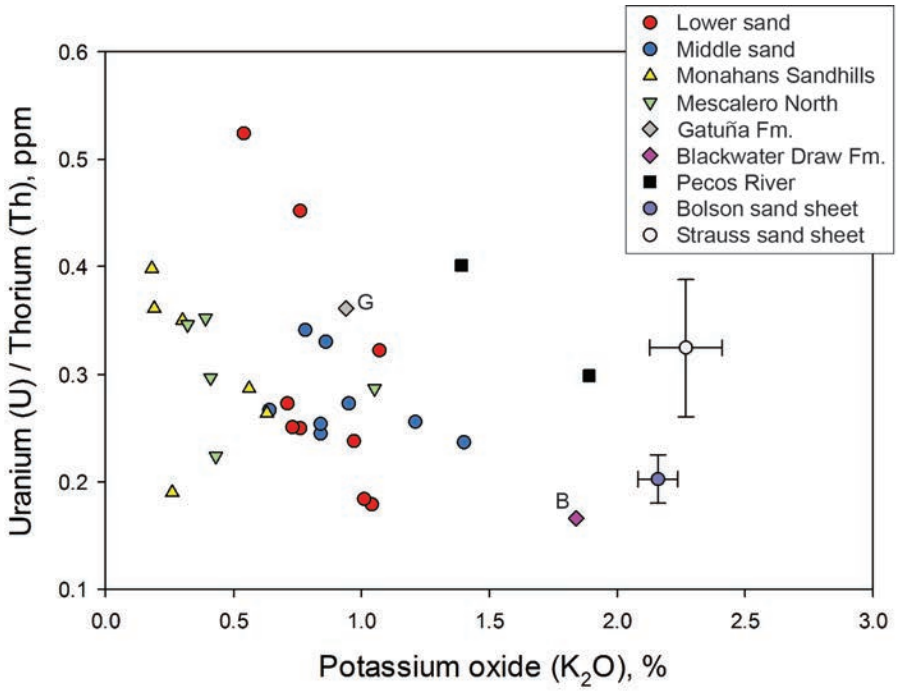

Figure 8.11. Radioisotopes from the two Pleistocene sheet sands of the Mescalero Sands (Lower and Middle units; this bulletin); the Monahans Sandhills State Park, Texas, and the Mescalero Sands North Dune Off-Highway Vehicle Area (Mescalero North; Rich and Stokes, 2011); the Gatuña Formation, "G" (Loc. 30, this bulletin); the Blackwater Draw Formation, "B" (Hall and Goble, 2020); Pecos River alluvium (Loc. 26, this bulletin); Bolson sand sheet (Hall et al., 2010); Strauss sand sheet (Hall and Goble, 2015d). The report by Rich and Stokes (2011) lists the potassium content as K instead of potassium oxide (K_2O); the potassium measurements from Monahans Sandhills and the Mescalero North sands tend to be lower values than from the other localities. Signatures of the Bolson and Strauss sand sheets are mean values with 1 standard deviation (SigmaPlot 12). Some of these data are shown in Fig. 8.7.

Laguna Plata

Three of the large playas, Laguna Plata, Laguna Gatuna, and Laguna Tonto, occur in the same area of the plain and are characterized by lunette dunes along their eastern flank, indicating a prominent role in local eolian geology (as well as westerly winds). Although the dunes were not studied, we investigated eolian deposits located 2.9 km (1.8 mi.) east (downwind) from Laguna Plata (Loc. 6). We found a 115 cm thick deposit of light brown "whitish" eolian fine-grained sand buried by about 1.1 m of Holocene eolian sand (see chapter 12). The whitish sand is OSL dated 22 ka to 11 ka and is interpreted as derived by deflation of sandy shoreline features at Laguna Plata. During the Holocene, some of the whitish sand was deflated and redeposited, forming a mantle of younger eolian sand extending over a distance of about 12 km and about 2 km wide downwind of Laguna Plata. Thus, the large playa was the primary source of local eolian sand from the last glacial maximum to the end of the Younger Dryas at the end of the Pleistocene as well as secondary younger eolian sands reworked from the playa-derived sand.

On the Southern High Plains of Texas, OSL dating of lunette dunes associated with large playas showed dune development during the period 16 ka to 11 ka, similar to the Laguna Plata-related record. Lunette dunes were also forming during the arid middle Holocene (Rich, 2013).

Red Lake and Cedar Lake

We examined the surficial geology at two other playa basins, Red Lake (Loc. 25) and Cedar Lake (Loc. 28), studying the stratigraphy of the deposits on the east (downwind) side of each basin. In both of these cases, sand was deflated from the basin floor, transported upslope, and deposited on the east side of the basin, not as dunes but rather as slowly accumulating eolian sand in the case of Red Lake and as colluvium at Cedar Lake.

Red Lake basin is located west of the Maroon Cliffs and red-colored sand was deposited very slowly (0.029 mm/yr) on the upper margin of the basin during the period ca. 35 ka to 5 ka; the red color is derived from Permian red beds that make up the cliffs (Loc. 25). After a late Holocene hiatus, eolian sand began to be deposited again by about 400 yr ago. The texture of the sand is the same throughout the sequence, late Pleistocene to middle Holocene, indicating little or no discernible change in particle sorting in a somewhat closed system (see chapter 6).

At Cedar Lake, eolian sand was deposited on the basin margin and partly trapped as colluvium during the period ca. 5 ka to 1.8 ka. Somewhat similar to the Red Lake record, a late Holocene hiatus in sedimentation occurred from 1.89 ka to 300 yr ago. The renewal of sand deposition at that time at both basins may be part of the widespread erosion across the plain that marked the beginning of episode VI eolian activity.

Neither study found evidence that these basins were significant sources of sand to the Mescalero Sands. At the same time, the sedimentary record provided information about local geomorphic history. The hiatus in deposition, for example, may be related to the late Holocene wet period when local moister conditions may have led to a significant reduction in the amount of sand deflated from the basin floors. However, in the looking at the Mescalero Sands in general, the influence of playa basins as sand sources appears to have been minimal.

Ogallala Sand Source

Long ago, George Bachman studied the Cenozoic geology of southeastern New Mexico in preparation for the disposal of nuclear waste (eventually the Waste Isolation Pilot Plant). He also reported his observations concerning the dune fields. "I believe that most of the windblown sand in areas such as Los Medaños was derived from the Ogallala Formation. During wet intervals in the Pleistocene the sand was eroded from the Ogallala, and during arid intervals it was blown across the Mescalero plain" (Bachman, 1976, p. 145). We concur with his conclusion, discussed herein, although we now know that eolian sand was also accumulating during the cool-wet Wisconsinan. We also wonder, however, about the origin of the Monahans eolian sand farther south in Texas where the Ogallala is not exposed and thus is not immediately available as a sand source.

The geomorphology of the Mescalero Plain suggests that sandy channels of streams and gullies are a dominant source of sand for the much of the eolian sand sheet. Even though the stream drainages

are today ephemeral (and some are likely buried by eolian sand), they would be more active during periods of wetter climate.

The Late Wisconsin change in sand chemistry, discussed above, provides strong support for Bachman's conclusion that the Ogallala Formation is the ultimate sand source for the sand sheet. During the cool-wet climate of the Late Wisconsin, numerous springs emanating from the Ogallala aquifer produced active streams flowing across the Mescalero Plain. We propose that these glacial-age streams carried a bed load of new sand, derived by erosion from the Ogallala escarpment (the Ogallala Formation below the Caprock is eolian in origin and predominantly fine- to very fine-grained sand; Gustavson, 1996; Hall, 2002a, p. 35; Appendix C, Table C-34). Increased fluvial activity would also scour stream beds and banks, eroding older deposits and picking up sand grains that had not yet been worn down by the eolian recycling process described previously. Thus, the fresh sand associated with the glacial-age streams across the plain would serve as a rejuvenated source of radioelements, resulting in an increase in potassium oxide in late glacial-age and younger eolian sand deposits (Figs. 8.8, 8.9).

The full-glacial renewal of sand in stream beds occurred during the deposition of the Middle eolian sand unit (dated 33 ka to 20 ka). The Middle sand occurs both on eroded deposits of the red Lower sand and on weathered caliche of the Mescalero paleosol. The radiochemistry of post-Middle sand shows a continuing pattern of K_2O depletion from the latest Pleistocene through the Holocene and into recent dunes (Figs. 8.8, 8.9). This tells us that, at least for those records, the sand source for each site has remained the same for that specific site for approximately the past 20.7 ka (Loc. 16), perhaps beginning with and certainly during the deposition of the Middle sand.

Origin of the Lower Sand Unit

The Lower sand is the first sheet sand to be deposited across the Mescalero Plain. It differs somewhat from the other eolian units. Its texture is fine- to very fine-grained sand, finer overall than the other sand units (Table 6.1); it also has greater variability in particle size (Figs. 6.1, 6.2). Its radiochemistry is also variable but falls within the range of the younger sand units (Figs. 8.3, 8.4; Table 8.1). And, similar to the other eolian units of the Mescalero Sands, its radiochemistry differs from the Pecos River alluvium and the Blackwater Draw Formation. With the information in hand, we conclude that the sand that makes up the Lower eolian sand unit was derived from stream beds containing sand washed from erosion of the Ogallala Formation, similar to the circumstances surrounding the origin of the Middle and younger sands.

Summary of the Origin of the Mescalero Sands

In our studies of the Bolson and Strauss sand sheets, we found that, once the primary sand source was cut off and eliminated from supplying fresh sand to the sand sheets, the primary sand deposits themselves were deflated and cannibalized, becoming the new source of sand to the younger phases of the sand sheets (Hall et al., 2010; Hall and Goble, 2015d).

The Mescalero sand sheet differs from the above scenario. A number of small streams across the Mescalero Plain have apparently provided a continuous supply of fresh sand to the Mescalero sand sheet (it should be pointed out that the late Pleistocene fluvial geology of the plain is completely unknown).

The deposition of the Lower sand from about 90 ka to 50 ka was followed by 17,000+ years of landscape stability, soil development (Berino paleosol), and erosion. The eroded sand, however, apparently did not end up in the younger Middle sand unit; the radioisotope content of the Lower and Middle sand is similar (the K_2O content of the Middle sand should be less than that found in the Lower sand if the Middle sand was derived from the Lower unit).

The sand source for the Middle sand unit across the plain was stream beds. During the deposition of the Middle sand, fluvial conditions were rejuvenated during the wetter climate of the last glacial maximum (26.5 ka to 20–19 ka), discussed above. Even though the Middle sand was subsequently eroded and completely removed in some areas, its sand does not appear to have become incorporated into younger eolian units. The primary source for Middle and post-Middle sand deposits continued to be stream beds.

The deposition of Holocene eolian sand sheets shifted direction about 2.0 ka with the development of the Eddy paleosol. The Eddy top soil continued to expand until about 300 years ago when sand accumulation across the plain ended and deflation began. At that time, thick deposits of the Holocene and Late Holocene sand units were deflated. The eroded sand accumulated close by, forming parabolic and coppice dunes and cover sand. Parabolic dunes are made up of comparatively coarse-textured sand, with the finer particles carried away. The dunes and cover sand appear to be locally derived by deflation of underlying Holocene sands and unrelated to stream beds that had been sand sources in the past.

IX. PALEOSOLS

A paleosol is defined as "A soil that formed on a landscape in the past with distinctive morphological features resulting from a soil-forming environment that no longer exists at the site" (Neuendorf et al., 2005, p. 466). After a fashion, due to ever-shifting climate and vegetation, all soils that are at least a few centuries old are paleosols. In the context of our work in southeastern New Mexico, however, another element is added: the soils we have encountered and described are not forming today. Thus, it is justified and technically correct to call all of them paleosols. The presence of soils or paleosols in stratigraphic sequences provides important information on landscape development and history. We recommend *Soils and Geomorphology* by Birkeland (1999) for an excellent discussion of soils related to Quaternary geology.

Soil A Horizons

Organic Matter and Organic Carbon

Soil A horizons are characterized by elevated percentages of organic matter. Aridisols, such as those that occur in southeastern New Mexico, commonly have < 0.5 percent organic matter (Birkeland, 1999, p. 279). Organic matter in a soil A horizon comes in many forms of plant and animal origin and is categorized as humus and humates. Humus is "the generally dark, more or less stable part of the organic matter of the soil, so well decomposed that the original sources cannot be identified" (Neuendorf et al., 2005, p. 309); humus is solid, non-soluble organic matter. On the other hand, humates are soluble and are salts or esters of humic acids; they can be removed by dilute alkali reagents. Humates are mobile and infiltrate all deposits through which water can move. We have found that, in some cases, humates have indeed been transported through eolian sands: matched OSL and AMS dating shows that the ages of humates are nearly always younger than the age of quartz sand grains that they coat.

In a soil A horizon, "humus commonly makes up the bulk of the soil organic matter. Organic carbon makes up over one-half of the organic matter, and organic carbon content is commonly used to characterize the amount or organic matter in soils. Generally, the percentage of organic matter in a soil is considered to be approximately 1.724 times the percentage of organic carbon" (Birkeland, 1999, p. 11). The Walkley-Black method is used by most labs to measure the amount of organic carbon in a soil. In our studies, paleosol A horizons are routinely analyzed for organic carbon. Elevated percentages of organic carbon provide a general index to A horizon development.

Soil B Horizons

Calcium Carbonate

Soil formation is the predominant process by which carbonate accumulates in sedimentary deposits in semi-arid southeastern New Mexico. Informative discussions of carbonate content of soils can be found in Gile et al. (1981, p. 66–71) and Birkeland (1999, p. 202–216).

In this bulletin, we use the term caliche to refer to the calcic Bk horizon of the Mescalero paleosol; the term is used throughout the Southwest for pedogeneic carbonate, especially calcic or petrocalcic horizons or calcrete. The only prominent calcic paleosol in the Mescalero Plain is the Mescalero paleosol. The calcic Bk horizon is generally 0.8 m to 1.5 m thick and has 51% to 69% carbonate with a stage III to IV carbonate morphology (Birkeland, 1999, p. 357). Additional information about the paleosol is presented later in this chapter.

A weak Bk horizon occurs at depth beneath the Bw horizon in Upper eolian sand unit (18 ka to 5 ka) with carbonate content up to 8–10 percent. The carbonate most commonly occurs as coats on sand

grains, giving the sediment a "whitening" effect. Less common are accumulations along rootlets and root traces, forming carbonate filaments.

Carbonate also accumulates preferentially in sedimentary beds that have a high clay content. The clay minerals absorb moisture that contains carbonate in solution. Upon drying, the carbonate is precipitated in the clay bed. A zone of elevated percentages of carbonate where significant amounts of clay are present can be misinterpreted as a soil Bk horizon. For example, slight amounts of carbonate, 1.3 to 3.5%, occur in the clayey Bt horizon of the Berino paleosol at its type locality; measurements of percentages of clay and carbonate from 43 samples correlate strongly with each other ($r^2 = 0.912$); greater amounts of carbonate correspond to higher percentages of clay, (Hall and Goble, 2012, p. 342; Appendix C, Table C-1 of this bulletin).

Clay

Pedogenic clay is found in argillic soils and paleosols. The most prominent argillic paleosol on the plain is the Berino. At its type locality (Loc. 1) it is a red 2.5YR hue Bt horizon, 120 cm thick, with 25% clay and 0.36% Fe (Hall and Goble, 2012). This horizon is described later in this chapter.

The almost-never-seen red 2.5YR Bt horizon of the Mescalero paleosol has a maximum of 42% clay and 0.55% Fe content at Loc. 1 (Appendix C, Table C-1), a much stronger argillic development than found in the Berino paleosol at the same locality.

Iron

Iron minerals commonly found in soils throughout the world include hematite, goethite, lepidocrocite, maghemite, and ferrihydrite. Although paleosols in the Mescalero Plain have not been specifically studied for iron mineral composition, goethite (FeOOH) is the most likely constituent (Holliday, 2004, p. 195). Goethite is a weathering product of iron-bearing minerals. As a coat on sand grains, it can give the sand a red hue of 7.5YR to 2.5YR (Birkeland, 1999, p. 91).

The iron content of argillic paleosol Bt horizons has been determined in a few of our studies. The total iron (Fe) content was determined for us by Energy Laboratories, Inc., a geotechnical laboratory in Billings, Montana. They use a method called inductively coupled plasma-atomic emission spectrometry (ICP-AES), also known as the SW6010B method.

The red (2.5YR) Bt horizons of the Berino paleosol and the overlying paleosol of the Middle sand (Loc. 16) were found to contain 8,650 mg/kg and 4,740 mg/kg of iron, or 0.865 percent and 0.474 percent, respectively. In this particular case, the nearly twice amount of iron in the Berino reflects the fact that it formed during a period of about 17,000 years, while the Middle Bt formed during a shorter period of 8,000 to 12,000 years (variability due to burial) and, accordingly, resulting in the accumulation of less iron.

The reddish hue of the cambic (Bw) horizon that occurs at the top of the Upper sand is a product of the weathering of iron minerals and coating of sand grains by iron oxides. The Bw does not have an enhanced clay content beyond what is already present in the sediment.

Paleosols in the Mescalero Sands

Soil formation occurred during periods of landscape stability. At present, four paleosols are recognized in the region: the Mescalero, Berino, Eddy, and Loco Hills. A Bw horizon and a Bt horizon paleosol associated with eolian sand are briefly described but have not been named. A soil Bk horizon also occurs in the sands below the Bw horizon. The paleosols and soil horizons are discussed below and summarized in Table 9.1.

Mescalero Paleosol

The Mescalero paleosol is a caliche-calcrete that occurs throughout southeastern New Mexico (Fig. 9.1). It is developed on Permian and Triassic bedrock and in a few cases at the top of the Gatuña Formation (Middle-Late Pleistocene). It was first recognized by George Bachman (1976), who referred to it as the Mescalero caliche. Wind-deposited sand of the Mescalero sand sheet rests directly on caliche of the Mescalero paleosol. In all of our studies in the region, we have called it the Mescalero paleosol (Hall, 2002a; Hall and Goble, 2006; Hall and Goble, 2016g). The Mescalero paleosol encompasses both Bt and Bk horizons, although the Bt horizon is rarely preserved.

Table 9.1. Paleosols and soil horizons, Mescalero Sand Sheet, southeastern New Mexico

Paleosol, Soil Horizon	Age	Notes
Loco Hills paleosol	500 to 200 BP; formed on older sands; overlaps in time but separate from Eddy paleosol	Weak A horizon, 10 to 30 cm thick; commonly preserved under coppice dunes, especially in the Loco Hills area
Eddy paleosol	2000 to 300 BP; formed at top of Holocene and late Holocene sands	Strong to weak cumulic A horizon, 15 to 50 cm thick; organic carbon 0.13 to 0.23%, averaging 0.17%
Bw horizon	Formed at top of Upper eolian sand unit during past 5 to 3 ka	Prominent Bw horizon gives the Upper eolian sand a reddish color in the field
Bk horizon	Formed at depth in Upper eolian sand unit below the Bw horizon during past 5 to 3 ka	Weak stage I carbonate accumulation, 3 to 8% carbonate, carbonate coats on sand grains produce a whitening appearance in the field
Bt horizon	Formed after 20 ka and before deposition of Holocene sand	Found only capping Middle eolian sand unit
Berino paleosol	Formed between 50 and 33 ka, or 50 ka and before the deposition of Holocene sand	Occurs only at the top of the Lower eolian sand; argillic non-calcic Bt
Mescalero paleosol	Formed ca. 135 to 100 ka	Formed during the extremely arid Sangamon Interglaciation; carbonate stage III to IV

Figure 9.1. Caliche of the Mescalero paleosol at old NM 128 road cut at Loc. 10. The Btk horizon has been removed by erosion. The 1.4 m thick paleosol is developed directly on red shale of the Rustler Formation (Upper Permian). The narrow solution pipe is filled with Holocene sediment; photograph March 2007; 1-m scale.

In a few places in northern Eddy County, a Bt and Btk horizon above the Bk calcrete is present. It is not widely documented but has been reported in a soil pit (Loc. 10 in Hall, 2002a, p. 40). The B horizon is more than 1.7 m thick and is red (2.5YR 4/6) fine to very fine sand but with 50 percent clay. Soil peds are 10 cm across with clay and manganese coats on ped surfaces. Below 50 cm depth, soft and hard concretions 2 to 3 cm across and vertically aligned pockets and lenses of carbonate are present. A similar occurrence of a Bt and Btk horizon in the upper part of the Mescalero paleosol is found below the Lower eolian sand at Loc. 1, where the maximum clay is 42% and maximum iron (Fe) is 0.55% (Hall and Goble, 2016g; Appendix C, Table C-1 of this bulletin).

In most areas, however, the Bt horizon is missing entirely, and eolian sands rest directly on weathered, eroded caliche. Overall, it is a calcic paleosol with stage III to stage IV carbonate morphology (Birkeland, 1999, p. 357). The amount of carbonate in the caliche ranges from 51 to 69%. By comparison, the calcrete caprock of the Ogallala Formation has 81 to 90% carbonate (Hall, 2002a, p. 35; Appendix C, Table C-34 of this bulletin).

The caliche-calcrete of the Mescalero varies considerably across the plain. At some localities, the caliche is a weakly-cemented mass of carbonate that can be crushed by hand. At other places, the carbonate is a dense mass that is concrete-hard. The soft caliche is commonly about 0.8 to 1.5 m thick. The dense hard caliche or calcrete may be 3.0 m or more in thickness (exposed in caliche pits). We suspect that the friable caliche represents a single episode of carbonate development during the Sangamon Interglaciation ca. 132 ka to 122 ka (Šibrava et al., 1986). The thicker, denser carbonate may instead represent multiple periods of carbonate accumulation over several hundreds of thousands of years, welded together and forming a single calcrete.

By comparison, the caprock calcrete at the top of the Ogallala Formation has a stage IV to a thick stage VI carbonate morphology and likely formed from the late Miocene to the early Pleistocene, a period of about 6 million years. An excellent review of the Ogallala Formation and related Pleistocene geology of the High Plains is presented by Gustavson (1996).

Age of the Mescalero Paleosol

The caliche of the Mescalero paleosol has not been directly dated. However, several OSL ages above and one age below the paleosol indicate that it formed during the broad period from 143 ± 8.0 ka to 90.7 ± 6.70 ka (Fig. 9.2) (Hall and Goble, 2016g). Allowing for post-paleosol erosion, the Mescalero more likely formed between about 135 to 100 ka. Thus, caliche developed over a period of at least 35,000 years during the Sangamon Interglaciation, a time of hot, dry climate that was more extreme than the warm Holocene climate (Clark et al., 1993).

Uranium-trend Dating of the Mescalero and Berino Paleosols

***Mescalero Paleosol*—**During the geologic evaluation of the proposed Waste Isolation Pilot Project (WIPP) east of Carlsbad, George Bachman collected samples of the Mescalero and Berino paleosols for uranium-trend dating (a uranium-series disequilibrium technique). The dated samples were collected at a caliche quarry, NE¼ SW¼ sec. 12, T. 22 S., R. 31 E. about 9½ mi. east of Nash Draw, from the upper and lower levels of a 150-cm exposure of caliche of the Mescalero paleosol and from a 73-cm exposure of the Berino paleosol above the caliche. The upper part of the Mescalero caliche returned a date of 420 ± 60 ka and the lower sample was dated 570 ± 110 ka (Rosholt and McKinney, 1980, p. 15). Preliminary ages were cited in Bachman (1980, p. 42; 1984, p. 14). The uranium-trend ages are too old in comparison with the OSL dates that bracket the paleosol with an age of about 135 to 100 ka (discussed previously).

***Berino Paleosol*—**In the same study cited above, the Berino paleosol yielded a uranium-trend age of 330 ± 75 ka (Rosholt and McKinney, 1980, p. 15). A preliminary age is quoted by Bachman (1980, p. 44; 1984, p. 14). The Berino paleosol is developed in the upper part of the Lower eolian sand unit that is OSL dated 90 to 50 ka at localities throughout the Mescalero Plain. At the thick type section of the Berino (Loc. 1), the age of the sand that contains the Bt horizon is younger than about 80 ka (Fig. 3.1). Elsewhere the top of the Berino and Lower sand are commonly missing due to erosion. Regardless, the uranium-trend age is too early.

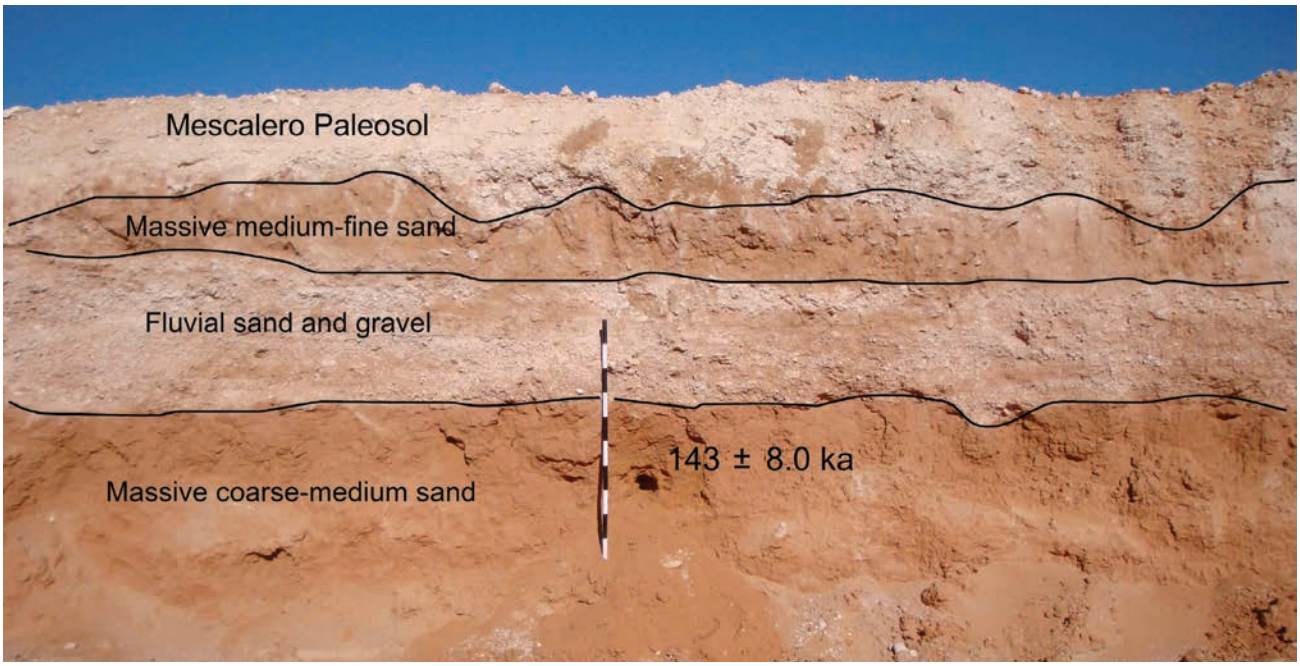

Figure 9.2. OSL age from below the Mescalero paleosol. Sand below the Mescalero is dated 143,000 ± 8,000 years; Loc. 30; Lat. 32° 12′ 3.0″ N., Long. 103° 55′ 35.3″ W; the paleosol is at the top of the Gatuña Formation; the pit with this exposure has been filled in and is no longer available for study; photograph November, 2008; 1-m scale.

Berino Paleosol

The Berino paleosol was first mentioned by Bachman (1980), who called it the Berino soil; he suggested that it might be a remnant B horizon of the underlying Mescalero caliche. In the course of our studies, we have encountered the Berino at several localities. It always occurs at the top of the Lower eolian sand unit (Fig. 3.1), which in turn forms a sharp unconformity with the underlying caliche of the Mescalero paleosol. The Berino paleosol also crops out at the surface of the sand sheet west of Loco Hills along Bear Grass Draw, forming a red-sand landscape (Fig. 9.3). Because of its stratigraphic significance and wide occurrence across the Mescalero Plain, the Berino paleosol has been formally named as a pedostratigraphic unit (Hall and Goble, 2012).

The Berino is a non-calcic argillic Bt horizon of an Aridisol. The overlying A horizon has been removed by erosion long ago and is nowhere preserved. The Berino is red (2.5YR 4/6) with a maximum clay content ranging from 17 to 25 percent and with the maximum Fe content of 0.86 percent (Hall and Goble, 2012). The horizon has a small amount of carbonate, 0.9 to 3.5 percent, although the carbonate is directly related to clay content; the carbonate was precipitated during the Holocene and is unrelated to the development of the Berino paleosol (Hall and Goble, 2012).

Age of the Berino Paleosol

The Berino occurs at the top of the Lower eolian sand unit that is dated ca. 90 to 50 ka. Thus, the Berino formed after 50 ka until the time it was buried by younger eolian sand. In one documented case, the paleosol was buried by 33 ka by the Middle eolian sand (Fig. 3.5). In this situation, the Berino formed during a period of 17,000 years and is less well developed. In most cases, however, the Berino was buried by the Upper eolian sand by about 18 ka, resulting in pedogenesis for 32,000 years throughout the Wisconsinan period. Thus, in most areas, the strongly argillic Bt horizon is a product of time and cool, wet climatic conditions.

The Berino pre-dates the archaeological record. However, prehistoric hearths intrude into the paleosol, and archaeological sites are commonly deflated with artifacts scattered across its eroded surface, especially in northern Eddy County.

Figure 9.3. Eroded Berino paleosol cropping out at the surface west of Loco Hills, near Loc. 1. The recent mesquite coppice dunes are formed by red sand derived from the Berino paleosol; the Berino and associated Lower eolian sand unit are OSL dated 90.7 and 81.2 ka at this locality. All prehistoric sites in this setting are deflated with artifacts scattered across the eroded surface; some prehistoric features may intrude into the Lower sand (see Fig. 3.2); photograph February, 2016.

Bt Horizon, Capping Middle Eolian Sand Unit

The noncalcic argillic paleosol that caps the Middle sand is an Aridisol. It has a red color (2.5YR 4/6-8) because of iron coats on sand grains; iron content ranges from 0.47 to 1.0 percent. The texture is fine to medium quartz sand; it has up to 21% clay as a result of pedogenesis. Where the Middle sand is thick (Loc. 16), an OSL age taken directly from the Bt horizon is 20,700 ± 900 years, the youngest age for the sand unit. In all cases, the Bt horizon is buried by Holocene eolian sand. Thus, looking at the ages of the Holocene sand, the period of time available for Bt pedogenesis before it is buried is about 8,000 to 12,000 years, spanning the late glacial and Younger Dryas. The Middle sand and its Bt paleosol have been observed at only six of our study localities across the plain. Its absence is because of non-deposition or erosion; we suspect the latter.

Bw Horizon, Capping Upper Eolian Sand Unit

The Upper eolian sand is the only stratigraphic unit on the Mescalero Plain with a soil Bw or cambic horizon. The Bw horizon is defined as "development of color or structure in a horizon but with little or no apparent illuvial accumulation of materials" (Soil Science Society of America, 1997, p. 134).

In our studies, the Bw horizon is about 25 to 40 cm thick and occurs at the top of the Upper sand. The Bw is characterized by a color that is slightly darker than the underlying sand. The Bw is red, reddish brown, and dark reddish brown (2.5YR 4/4-6, 5YR 3-4/4), whereas the underlying sand is yellowish red and reddish brown (5YR 4/4-6). In three cases, an overlying A horizon (Eddy paleosol) blends with the Bw, forming an AB horizon. In all cases, sand grains in the Bw have weak iron coats but no clay coats. Laboratory analysis shows no additional clay in the Bw. Overall, the texture of the Bw sand is identical to that of the underlying sand.

The chronology for the development of the Bw horizon is straightforward. Deposition of the Upper eolian sand ended by about 5.0 ka. The geographic areas of the plain with the Upper unit apparently stabilized at that time until 2.0 ka when the cumulic A horizon of the Eddy paleosol began to develop on top of the Bw. Thus, the Bw horizon formed during a minimum period of 3000 years.

Bk Horizon, within the Upper Eolian Sand

The Bk horizon is defined by the accumulation of pedogenic carbonates. In the Upper eolian sand, the Bk horizon begins to show up below 40 to 50 cm depth where carbonate increases in the sand from 3 to 7 percent. The sand grains have thin, discontinuous carbonate coats; filamentous carbonate is uncommon. The carbonate coats give the sediment a whitish appearance. This degree of secondary carbonate is categorized as stage I carbonate morphology (Birkeland, 1999, p. 357).

The Bk horizon carbonate probably started to accumulate at 5.0 ka, similar to the timing of the initiation of Bw horizon development in the Upper sand. However, the appearance of the Eddy paleosol A horizon may not have ended the Bk development, as it likely did for the Bw. Thus, the Bk may have continued to form to recent times beneath the AB horizon in some cases. In broad terms, the stage I carbonate may be a product of 3,000 to 5,000 years of development.

Eddy Paleosol

As discussed below, the Eddy is a cumulic Mollisol; the Loco Hills is a cumulic A horizon, as well. A cumulic soil differs from all other soils. In pedology, a soil A horizon is traditionally viewed as forming at the surface of the ground by a mixture of decaying organic matter and underlying parent material. The A horizon thickens as the organics are physically mixed deeper into the weathered substrate.

The cumulic A horizon, in contrast, is literally an aggrading soil horizon where sediment is continually added to the ground surface and, with the passage of time, the A horizon builds up to a greater thickness. Cumulic A horizons are well known in alluvial sequences where they have formed on slowly aggrading floodplains. Cumulic A horizons can also form at the toe of slopes where sediment from slope wash accumulates. Cumulic soils are important in archaeology; as the soil accumulates thickness, archaeological features become buried within it.

The Eddy paleosol is a comparatively thick A horizon that occurs in eolian sand, colluvium, and alluvium in Eddy and Lea counties (Figs. 9.4–9.6); it has been documented at sixteen study sites (Table 1.1). It is classified as a cumulic Mollisol but has not been recognized or mapped in the county soil survey reports (Chugg et al., 1971; Turner et al., 1974), probably because it is either buried by dunes or cover sand, or it has been removed from many places by deflation in the past 300 years.

Figure 9.4. Late Holocene eolian sand with the cumulic Eddy paleosol A horizon at Loc. 18 in the Pierce Canyon area; see Fig. 9.5; 1-m scale.

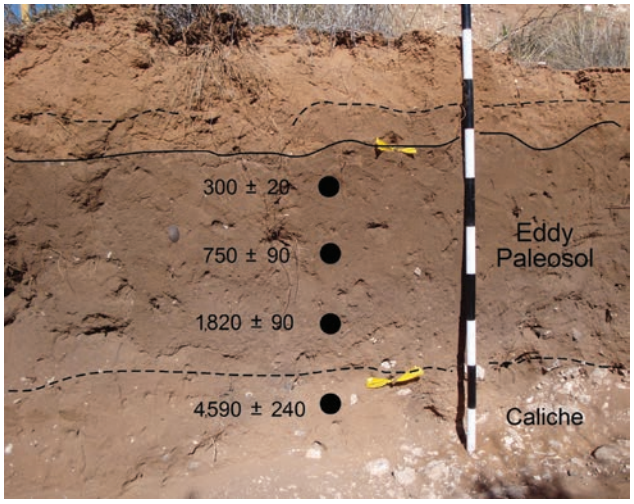

Figure 9.5. OSL-dated Eddy paleosol sand capping late Holocene eolian sand at Loc. 18 in the Pierce Canyon area; the 300 ± 20 year age is the youngest from the Eddy; the sedimentation rate of the Eddy here is 0.187 mm/yr; 1-m scale.

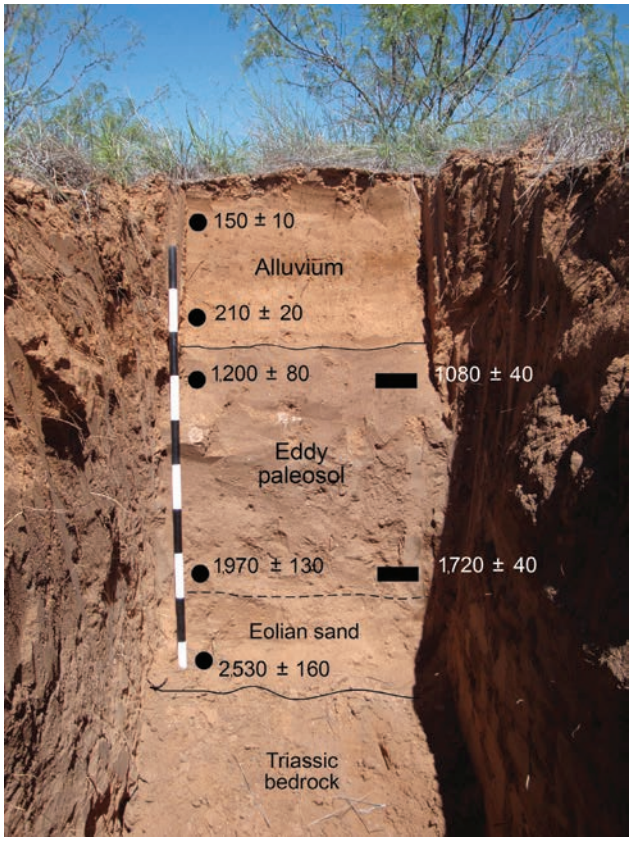

Figure 9.6. Early age for the Eddy paleosol near Custer Mountain along NM 128 (Loc. 12, Trench 6); paired OSL (black circles) and AMS (black rectangles) ages; the paleosol is developed at the top of local eolian sand and is buried by local alluvium; the entire sequence rests directly on Triassic bedrock; 1-m scale. The Eddy paleosol is well exposed in the road cut on the north side of NM 128 at Custer Mountain.

In our first geologic investigations at archaeological sites, we indicated that a soil A horizon, if present, may be an anthrosol. In all of those cases, we have changed our interpretation. We are now convinced that the A horizon at nearly all sites in the Mescalero Plain is a natural soil with only minimal, if any, cultural influence. The soil A horizon at these sites is the Eddy paleosol. The issue of natural versus cultural A horizons is discussed further in chapter 12.

The Eddy paleosol has a strong connection to the archaeological record. It formed during the Late Archaic and Formative periods. In a breakdown of the 841 radiocarbon dates from all of the sites on the Mescalero Plain, 652 or 78% of the dates fall into the time range of the Eddy paleosol (Railey, 2016). The Eddy has clear prehistoric cultural significance.

Before discussing the Eddy paleosol, it is important for the reader to be aware that the paleosol is composed of two separate parts, the topsoil and subsoil. The upper part, referred to as the topsoil in this bulletin, is formed by the accumulation of wind-deposited particles that are trapped by grasses that form the ground cover (more on this later). In this situation, the topsoil is a cumulic A horizon and is a geological deposit that can contain and bury archaeological sites. Sand grains in the topsoil become coated by humates from local decayed plants, giving the topsoil a dark color.

The sediment below the topsoil is referred to as the subsoil in this discussion. The sediment of the subsoil is generally Holocene in age. With the passage of time, sand grains in the subsoil are coated with soluble humates, giving the subsoil a dark color, similar to the color of the topsoil. The subsoil can extend 40 to 60 cm below the base of the top soil. However, the subsoil sediment can be hundreds to thousands of years older than the eolian sand in the topsoil. And, accordingly, the humates in the subsoil sediment can be hundreds and thousands of years younger than the subsoil sands.

Cultural activity at a site can severely disturb the natural topsoil and subsoil of the Eddy paleosol, producing a site footprint that is a mix of soil and sand and cultural materials. Where this disturbance has occurred, the original stratified physical and

chemical properties of the paleosol are no longer intact. The identity of the paleosol is lost even though the dark-colored sand in the site footprint represents the once-present in situ soil. Because of site-related disturbance, paleosol studies, such as dating and sediment analysis, are best conducted off-site. The site footprint is discussed further later in this bulletin.

***Description of the Eddy Paleosol*—**The paleosol is commonly 15 to 50 cm thick. It is darker in color than associated sands; its dark color distinguishes it in the field. It has been described as dark brown (7.5YR 3/2-3), dark reddish brown (5YR 3/2-3), and reddish brown (5YR 4/4) (Figs. 9.4, 9.5). The paleosol has an organic carbon content ranging from 0.13 to 0.48 percent and an organic matter content from 0.22 to 0.83 percent, significantly higher than that of associated non-soil sand. Inspection of the paleosol with a binocular microscope reveals that, in every case, the organic carbon consists of soluble humates that coat sand grains, giving the grains and the paleosol its dark color. Charred particles or humus in the paleosol are rare or entirely absent, even at archaeological sites; all AMS radiocarbon dates from the paleosol are on soluble humates.

The quartz sand grains in the paleosol commonly exhibit polish, are round to subround, and have a moderate level of sphericity. The particle sizes of the sand are almost always the same as the particle size of the underlying eolian sand. Also, the silt and clay content of the paleosol is generally the same as those of underlying deposits. The paleosol is always massive and does not display layering or bedding features.

The Eddy paleosol is associated with Holocene-age eolian sands, alluvium, and hillslope colluvium. It has not yet been observed on the late Pleistocene Lower or Middle sand although in a couple of cases it rests directly on weathered caliche of the Mescalero paleosol. In its occurrences with eolian sand, it is always found at the present-day surface of the sand sheet, although it may be obscured from view by thin cover sand or dunes. In many cases, however, it is entirely missing due to recent deflation. It is generally preserved beneath parabolic and, especially, coppice dunes. In blowouts and between coppice dunes, the A horizon has been partly or completely removed by deflation during the past 300 years. Where the Eddy occurs in alluvium or colluvium, it is commonly buried by younger sediment.

An exceptionally thick, mature expression of the cumulic Eddy paleosol occurs at Loc. 31 in southwestern Lea County. The well-developed paleosol varies from 42 to 103 cm thick and is developed on a thin deposit of Late Holocene eolian sand and, in two cases, the paleosol rests directly on weathered caliche of the Mescalero paleosol (Figs. 9.7, 9.8). In the field, the reddish to dark reddish brown (5YR 3-4/3-4) paleosol is almost completely obscured by several millimeters of lighter colored cover sand. In the field, kicking aside the thin cover sand reveals the dark color of the paleosol, conjuring thoughts of an anthrosol. Subsequent trenching at this locality revealed the thick paleosol.

***Age of the Eddy Paleosol*—**The Eddy paleosol has been dated at eighteen different localities by OSL and/or AMS radiocarbon methods; 23 OSL and 39 AMS dates are regarded as reliable ages for the paleosol (Fig. 9.9; Appendix A, B). The OSL ages of sand grains in the paleosol topsoil range from 1,970 ± 130 to 300 ± 20 years (A.D. 38 to 1708) at locs. 12 and 18. AMS ages of soil humates from the topsoil range from 1,720 ± 40 to 280 ± 30 ^{14}C years BP (A.D. 320 to 1600) at locs. 12 and 35. Rates of sediment accumulation can be calculated from the OSL and AMS dates at different levels within the topsoil. The linear trend of the sedimentation rates confirm the cumulic origin of the paleosol and indicate that vertical turbation of the soil has not been significant (more about sedimentation rates in chapter 5).

OSL dating indicates that the cumulic topsoil of the Eddy paleosol A horizon formed during a period of 1,700 years, from 2,000 to 300 years ago (A.D. 1 to A.D. 1700); AMS radiocarbon dates support this chronology. The eolian buildup of the topsoil may have slowed towards the end of that period, coinciding with a possible shift to increased shrub dominance in the vegetation across the Mescalero Plain (chapter 14). As discussed below, grasses capture wind-transported sand, forming sand sheets. Thus, a vegetation change to a greater abundance of shrubby vegetation may have significantly slowed the cumulic phase of the Eddy topsoil towards the end of its formation.

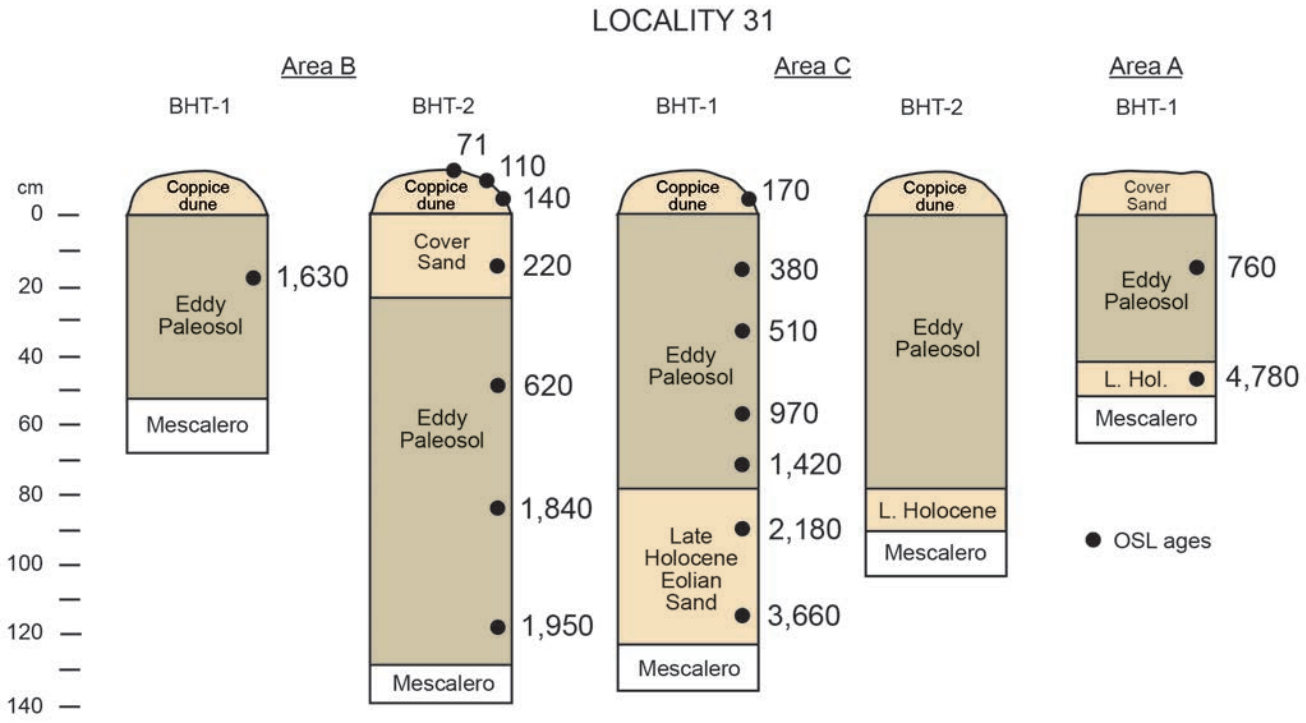

Figure 9.7. Thick expression of the Eddy paleosol, Loc. 31, southern Lea County; paleosol overlies the Late Holocene eolian sand and weathered caliche of the Mescalero paleosol (Hall and Kettler, 2019); ages in calendar years before A.D. 2014; L. Hol. = Late Holocene; Appendix A, Table A-30.

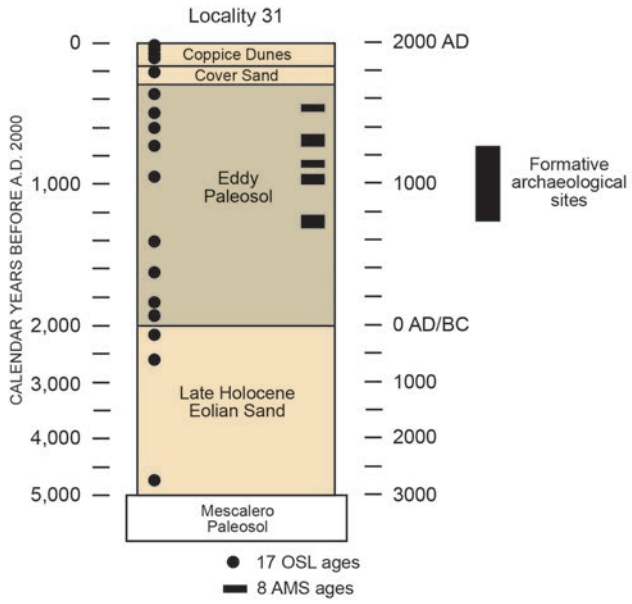

Figure 9.8. Summary time-stratigraphy chart of the Late Holocene sand, Eddy paleosol, cover sand, and coppice dune sand, Loc. 31, southern Lea County; some of the OSL and AMS dated samples from the Eddy paleosol are paired; associated archaeological features in the Eddy paleosol are AMS-radiocarbon dated A.D. 700 to 1250 representing the Formative period (shown to the right of the stratigraphic column). The time scale shifts at 2,000 years.

The Eddy was always a cumulic A horizon. The A horizon topsoil persisted as an active soil and continued to develop, however, until the widespread deflation of the sand sheet about A.D. 1700 when the paleosol was eroded and reduced in thickness or removed entirely from many areas of the plain. The upper levels of the Eddy topsoil were scoured first, perhaps resulting in fewer young ages from the paleosol in our studies. The entire time span of the Eddy is preserved at only a few localities; in most field conditions, only a portion of the Eddy is preserved, suggesting that local topography and geomorphic circumstances played a role in paleosol development as well as its preservation.

Correlation of the Eddy Paleosol—The late Holocene moist conditions that promoted the development of the Eddy top soil on the Mescalero Sands also greatly influenced streams in the southern Great Plains and Southwest. Throughout the region, steams were more permanent and channels were shallow. Overbank flow resulted in deposition of fine-textured sandy muds on floodplains. By about 2.4 ka, a cumulic soil A horizon began forming on slowly aggrading floodplains (Hall, 1990; Hall et al., 2012; Hall and Peterson, 2013). The soil A horizon has been reported

by a number of investigators and is known by various names; its primary name is Copan paleosol from early fieldwork in northeastern Oklahoma (Hall, 1977). The development of the Copan paleosol ended about 1.0 ka with the down-cutting of stream channels in response to a shift from wet to dry climate during that time, the Medieval Warm Period. However, the Eddy paleosol continued to form through the warm period and into the Little Ice Age until about 0.3 ka when an episode of erosion and deflation across the Mescalero Plain ended its development. The Eddy and Copan paleosols are both cumulic soil A horizons, Mollisols, forming under conditions that were comparatively moist, the Eddy beginning to form about 2.0 ka and the Copan about 2.4 ka. Soil development ended for each with an episode of erosion, the Eddy at about 0.3 ka and the Copan about 1.0 ka. The two paleosols are products of late Holocene climate and climate change in the region. Neither paleosol is forming today.

Loco Hills Paleosol

The Loco Hills paleosol has been recognized in the field throughout the Loco Hills area of the Mescalero Plain in northern Eddy County and takes its name from that community (Fig. 9.10) (Hall, 2002a, p. 7; Hall and Goble, 2006). This paleosol occurs on eolian sand, colluvium, and alluvium, and it is commonly found beneath coppice dunes. It has been found under a parabolic dune in northern Eddy County (Loc. 2). While the Loco Hills paleosol is a common occurrence beneath coppice dunes in the Loco Hills area, this paleosol is seldom seen in the dune fields of the southern areas of Eddy and Lea counties.

***Description of the Loco Hills Paleosol*—**The Loco Hills is a cumulic soil A horizon about 10 to 30 cm thick without B horizon development; the soil is noncalcareous. Its color is reddish brown to reddish yellow to yellowish red (5YR 4-6/4,6). The soil color is similar to that of the underlying sediment. The texture of the soil is silty very fine- to fine-grained quartz sand; grains are subround to round. The texture is similar to that of the Lower eolian sand that underlies the soil in the Loco Hills area (Hall, 2002a).

***Age of the Loco Hills Paleosol*—**Bulk sediment from three different localities of the Loco Hills A horizon has been directly dated by AMS radiocarbon as 370 ± 40 (Loc. 41; loc. 3 in Hall, 2002a), 330 ± 40 (Loc. 3), and 150 ± 40 ^{14}C years BP (Loc. 4); the ages calibrate to A.D. 1535, 1556, and 1800, respectively. Two OSL ages of the sand from the A horizon are 290 ± 20 (Loc. 23) and 300 ± 20 years (Loc. 25), or A.D. 1718 and 1712, respectively (Fig. 9.11).

Looking at both AMS and OSL ages, the Loco Hills paleosol appears to have formed during a broad period of 300 years, from 500 to 200 years ago (A.D. 1500 to A.D. 1800), overlapping the end of the Eddy paleosol by 200 years. At Loc. 25, eolian cover sand overlying the Loco Hills is OSL dated 140 ± 20 years (A.D. 1870), supporting the chronology that the formation of the Loco Hills ended by the early nineteenth century.

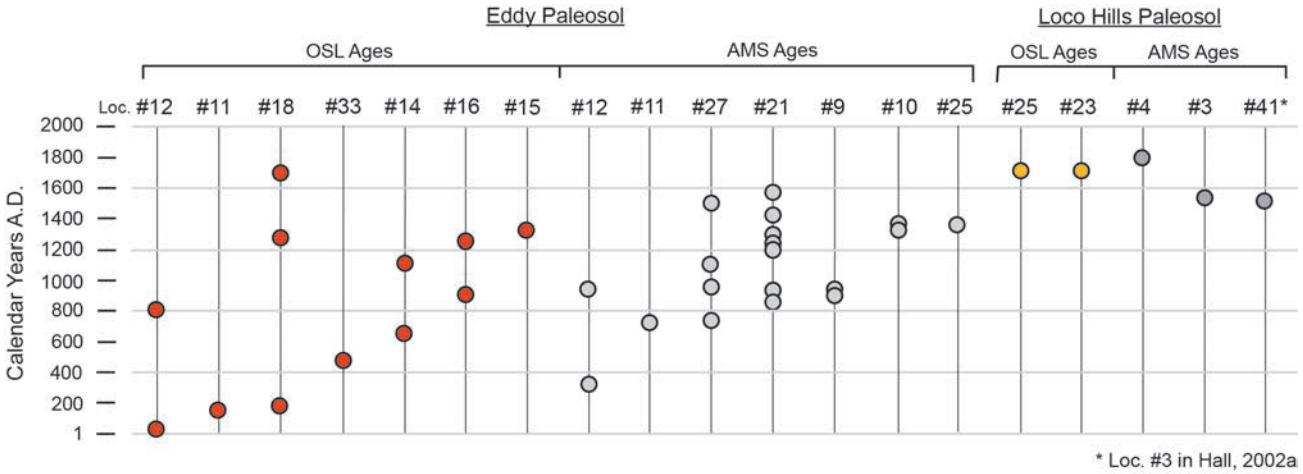

Figure 9.9. OSL and AMS ages of the Eddy paleosol and the Loco Hills paleosol; not shown are 9 OSL and 7 AMS ages from the Eddy paleosol at Loc. 31; the OSL ages at Loc. 31 range from 1,950 ± 140 years (A.D. 64) to 380 ± 30 years (A.D. 1634), and the AMS ages range from 1,270 ± 30 years (A.D. 720) to 340 ± 30 years (A.D. 1550) (Figs. 9.7, 9.8 and Appendix A and B).

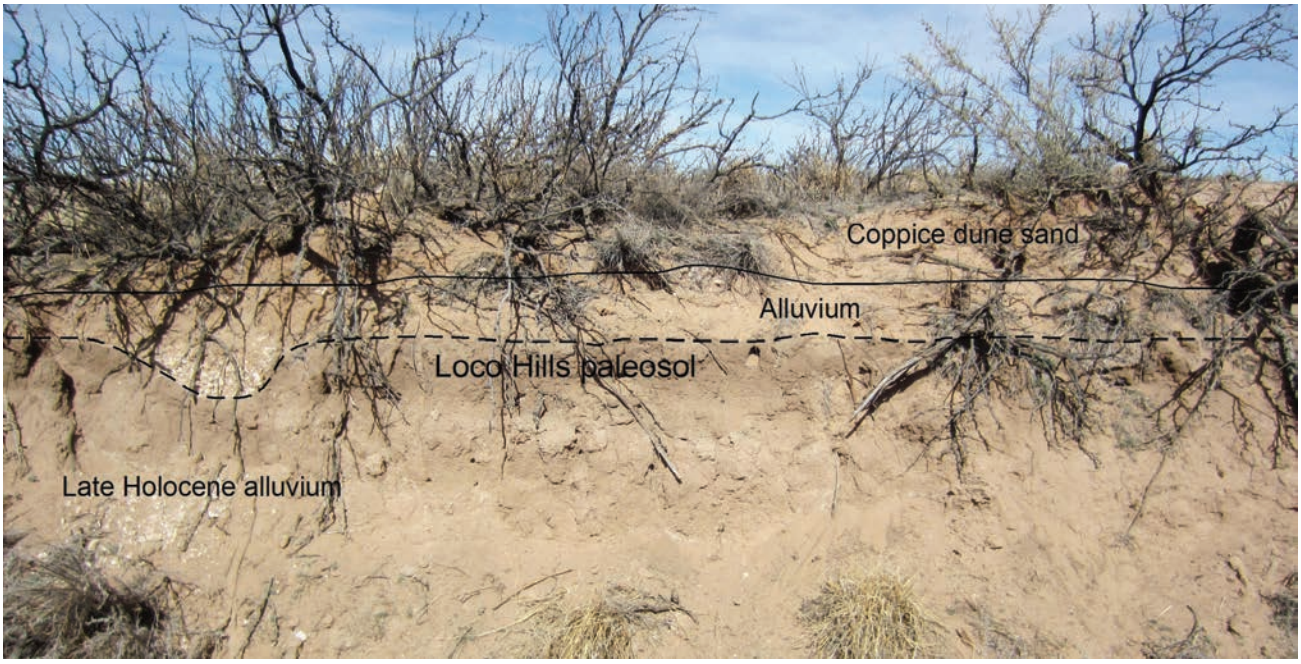

Figure 9.10. Loco Hills paleosol in late Holocene alluvium at Loc. 3, northern Eddy County; organics from the paleosol at this locality are radiocarbon dated 330 ± 40 ^{14}C years BP (A.D. 1556) (loc. 12 in Hall, 2002a; Hall and Goble, 2006); photograph February, 2016.

Neither the Loco Hills nor the Eddy paleosols are forming today. Both have been eroded and partly or entirely removed from the landscape by episode VI deflation in the past 300 years since A.D. 1700. The original thinness of the Loco Hills may result in it being more susceptible to complete removal by erosion. In some areas of the plain, the paleosols are covered and preserved by coppice dunes.

Development of Cumulic Soils

The Influence of Vegetation

The Eddy and the Loco Hills paleosol A horizons in southeastern New Mexico are the product of a semi-arid eolian environment (discussed previously). Eolian sand and atmospheric dust particles become trapped by the grass vegetation cover on the sand surface. With the passage of time, the buildup of particles in the topsoil forms a cumulic A horizon. This phenomenon has been described from extensive studies of eolian landscapes in North Africa (Bagnold, 1954, p. 183, 184):

> Physically, vegetation can be regarded as a special kind of surface roughness. The simplest case is that of a loose surface of dry sand on which sufficient rain falls at intervals, and is retained below, to cause the germination of wind-blown seeds and the growth of a uniform but thin distribution of light grass or other herbage. The grass blades, by projecting into the air stream, have the effect of raising the height *k* of the level about the surface at which the wind velocity is on an average zero, in just the same way as do the pebbles or stones… The sand surface is therefore converted by the growing grass into the equivalent of one containing scattered pebbles, and it will tend to store oncoming sand between the grass blades. But there is an important difference; the blades being light and yielding, the sand grains do not bounce off them as they do off pebbles…as long as the vegetation is alive, the surface on which it grows cannot ever become fully charged with sand, for the grass grows higher as the sand around it accumulates. The result is that under all wind conditions the grassy surface acts as a continuous deposition area, and we get great undulating tracts of accumulated sand…which are devoid of steep-sided dunes.

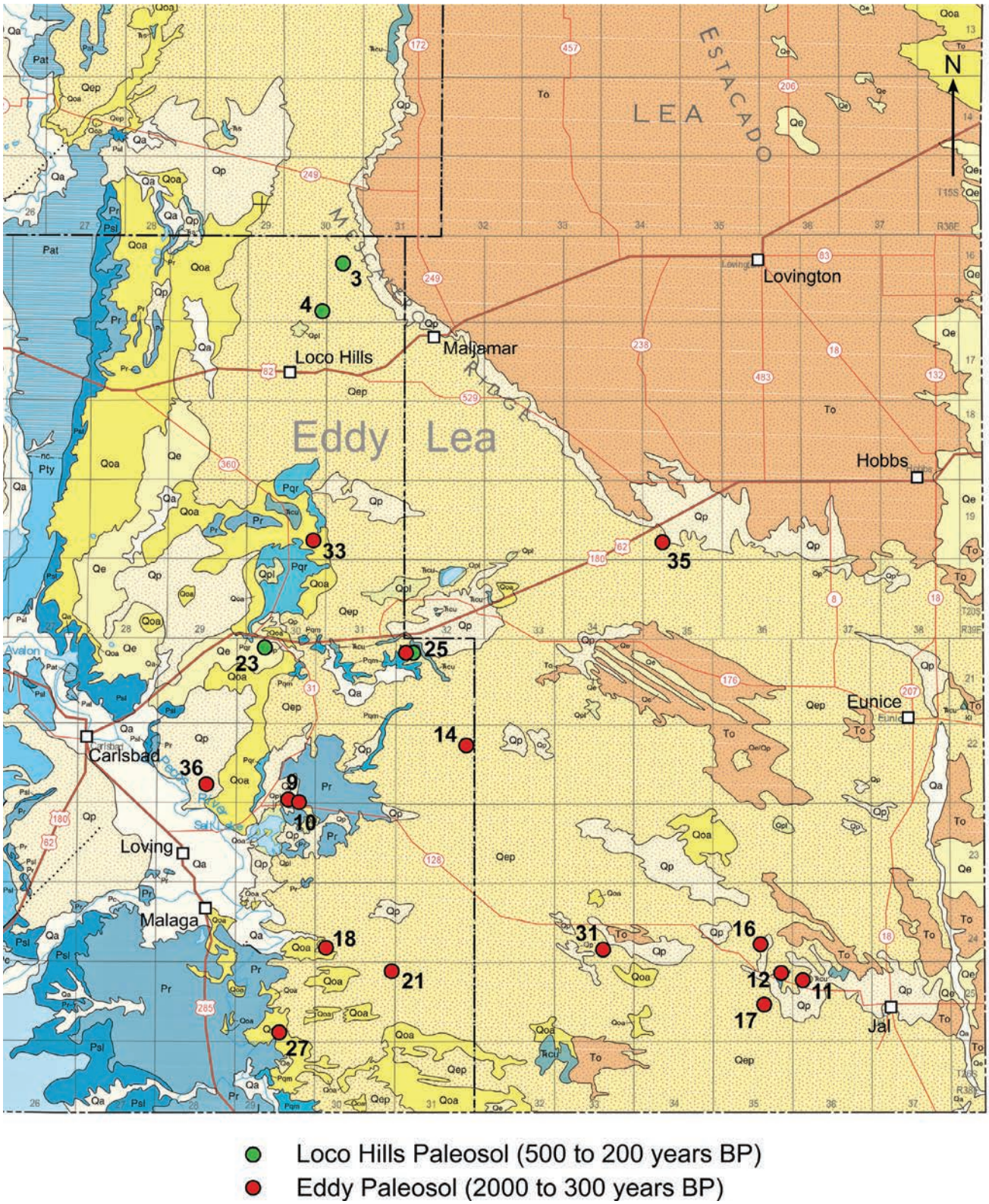

Figure 9.11. Distribution of study localities with the Eddy and Loco Hills paleosols; scale bar and description of geologic units in the legend of Figure 1.1.

The Influence of Past Climate

Bagnold's observations apply to the development of the Eddy and Loco Hills paleosol A horizons on the Mescalero sand sheet. The key to sand accumulation is vegetation, especially grasses (temporarily setting aside sand source conditions). A grass-dominated plant cover will capture sheet-forming sand, while shrub-dominated vegetation will not. It is not a coincidence that the Eddy paleosol began forming about 2,000 years ago in southeastern New Mexico during a time of exceptionally wet climate (compared with previous millennia). The wetter climate likely promoted grass-dominated vegetation over much of the Mescalero Plain, facilitating the formation of the Eddy paleosol A horizon.

Stratigraphic Nomenclature of Cumulic Soils

The North American Stratigraphic Code recognizes lithostratigraphic and pedostratigraphic units, among others (North American Commission on Stratigraphic Nomenclature, 2005, p. 1566-1570, p. 1576-1578). Pedostratigraphic units are defined as a "buried, traceable, three-dimensional body of rock that consists of one or more differentiated pedologic horizons" that is "a product of [in situ] surface alteration of one or more older material units by specific processes (pedogenesis)" (North American Commission on Stratigraphic Nomenclature, 2005, p. 1577, 1578). In contrast, a lithostratigraphic unit is defined as a "body of sedimentary [and other] strata that is distinguished and delimited on the basis of lithic characteristics and stratigraphic position" (North American Commission on Stratigraphic Nomenclature, 2005, p. 1566). Because a cumulic soil is a depositional body of sediment with lithic characteristics, it can be classified as a rock unit instead of a soil unit. Thus, the Eddy and Loco Hills paleosols, especially the longer-forming Eddy, are technically lithostratigraphic units.

As a footnote to soil stratigraphy, the formal name of a pedostratigraphic unit is a "geosol," according to the 2005 North American Code (North American Commission on Stratigraphic Nomenclature, 2005, p. 1578) (the term "geosol" was introduced in the 1983 Code in North American Commission on Stratigraphic Nomenclature, 1983, p. 850, 864, 865, following the proposal by Roger Morrison, 1967; previous codes from 1970 and 1961 used the term "soil" with the stipulation that formal soil-stratigraphic units should be chosen in accordance with the rules that govern naming of rock-stratigraphic units). Based on its definition in the 2005 Code, it is stipulated that a "geosol" must be buried by a defined rock unit. In our view, the term geosol is somewhat restrictive for the field condition. It does not recognize relict soils that formed on ancient landscapes but were not buried. It also does not recognize exhumed soils that were once buried but have been re-exposed at the land surface by erosion. An earlier term "paleosol" represents relict, exhumed, as well as cumulic soils, and many field workers in the United States and Europe continue to use the more inclusive term paleosol (Ruhe, 1965; Valentine and Dalrymple, 1976). We use the term paleosol in our investigations.

X. ALLUVIUM AND COLLUVIUM

Alluvium is defined as "a general term for clay, silt, sand, gravel or similar unconsolidated detrital material, deposited during comparatively recent geologic time by a stream or other body of running water, as a sorted or semisorted sediment in the bed of a stream or on its flood plain…" (Neuendorf et al., 2005, p. 17). Alluvium can provide geomorphic and paleoenvironmental information that is neither available nor forthcoming from eolian sands. Combined alluvial and eolian records should provide new insights to the landscape condition, especially for the late Holocene.

Several small drainages flow southwest and south across the Mescalero Plain. The small streams may have been more active in the past. Today, their shallow beds end in the sand sheet. One such stream is Bear Grass Draw. Many prehistoric sites occur in its vicinity. It may have served as a water resource in the past, especially during the late Holocene wet period. However, nothing is yet known about its fluvial history and how it could be related to past climate.

Pecos River: Late Holocene Alluvium

Late Holocene alluvium forms a terrace about 6 m above the Pecos River floodplain downstream from the community of Malaga (Loc. 26) (Fig. 10.1).

The alluvial sediment that makes up the terrace is light brown, fine-textured sandy silt and silty sand with discontinuous gravel beds in lower levels. The silty alluvium was deposited on the river floodplain by slow aggradation that accompanied overbank flooding. OSL ages from the alluvium are 6,640 ± 280 and 3,250 ± 150 years at 117 cm and 26 cm depth below the modern surface of the terrace (Hall and Goble, 2015a). Remarkably, this is the first study where Pecos River alluvium has been directly dated anywhere in the state of New Mexico.

The terrace at Loc. 26 was formed by down-cutting of the late Holocene floodplain, probably ca. 1,000 years ago when other river channels in the region were incised (Hall and Peterson, 2013). The Pecos River alluvium and terraces in the area of our investigation have not been mapped. The closest mapped stretch of the river is in the nearby Loving quadrangle (Pederson and Dehler, 2004a, 2004b). A possible correlation of the late Holocene terrace is the alluvium mapped as "Qasm1, alluvial sand mainstream (Pleistocene? to Holocene)" (Pederson and Dehler, 2004a). The Qasm1 map unit is described as light brown silt to fine sand that forms a T-1 terrace 5 meters above the modern Pecos River; the terrace surface commonly has coppice dunes (Pederson and Dehler, 2004b), similar to the terrace at Loc. 26.

Figure 10.1. Late Holocene terrace along Pecos River at Loc. 26; the upper 1.2 m of the alluvium is OSL dated 6.64 and 3.25 ka; the river channel and associated floodplain are to the right in this view. The terrace surface is about 6 m above the modern floodplain; photograph November, 2014.

Pecos River: Terrace Gravel

Pleistocene terrace gravels occur topographically 2 to 4 m above the late Holocene alluvial terrace at Loc. 26. The terrace gravels have been mapped for many miles up and down the Pecos River. The gravel contains pebbles and cobbles of fossiliferous limestone, light gray quartzite, purple quartzite, dark gray chert, banded gray chert, quartz, brown sandstone, reddish brown sandstone, red jasper, dark red rhyolite, chalcedony, and fossil wood (Fig. 10.2). Many of these rock types have been reported in lithic assemblages at archaeological sites across the Mescalero Plain (Kremkau et al., 2013).

The terrace gravels at Loc. 26 may correspond in part to the "Qagm2 alluvial gravel mainstream" of Pederson and Dehler (2004a, 2004b) in the Loving quadrangle. The lithology of the gravel of the Qagm2 terrace unit is similar to that at the Loc. 26 gravel terrace. The terraces at both localities are capped by a calcrete.

Boot Hill Alluvium

The alluvial geomorphology of an arroyo near the Boot Hill site was examined during archaeological investigations. Six possible stratigraphic units were identified in cut banks (Loc. 37). Four radiocarbon dates range from 8.8 to 1.25 ka, indicating that all of the exposed alluvium is Holocene. In different places, the sediments contained terrestrial and freshwater snails. A weathered proboscidean tusk was found at the base of a cut bank; the fossil had been reworked and washed in from another place. Two different occurrences of buried archaeology were found in the alluvium at 20 to 40 cm and 80 to 100 cm depth. The lower site was thought to be Late Archaic; the upper site contained ceramics and may be contemporaneous with the Boot Hill occupation (Brown, 2011).

Figure 10.2. Carbonate-cemented Pecos River gravels about 8 m above the modern floodplain near Loc. 26; rock types include fossiliferous limestone, light gray quartzite, purple quartzite, dark gray chert, banded gray chert, quartz, brown sandstone, reddish brown sandstone, red jasper, dark red rhyolite, and chalcedony; 1-m scale.

Highway 128 Alluvium

A 1-m thick deposit of late Holocene fine-textured alluvium capped by the Eddy paleosol was inadvertently discovered by backhoe trenching in a dry wash (Loc. 10). The alluvium yielded a pollen record and a fauna of four terrestrial snails, discussed in chapter 12. Three AMS dates range from 2.96 to 0.58 ka. The alluvium is a dark reddish brown (5YR 3/4) silty very fine sand. The Eddy paleosol is very fine textured with 60 percent silt and 0.95 to 1.05 percent organic carbon; it is AMS dated at A.D. 1360. The alluvium accumulated at a rate of 0.370 mm per year. It is buried by about 0.5 m of recent channel alluvium (Hall and Goble 2016a) (Fig. 10.3).

Alluvium West of the Pecos

Recent studies in the area between the Pecos River and the slopes of the Guadalupe Mountains have revealed a very different surficial geology than found in the area of the Mescalero sand sheet. The geology is characterized by commonly denuded Permian bedrock with thin deposits of colluvium on hill slopes, thickening down-slope where the topographic gradient decreases. Deposits in narrow shallow draws are dominated by massive sandy silt, in some cases capped by the Eddy paleosol A horizon (Loc. 34; Hall, 2017a). Larger drainages may contain thick deposits of Pleistocene sand and gravel that in some places are mantled by Holocene silty alluvium that can incorporate prehistoric archaeology (Loc. 32; Hall, 2016).

The modern cutbank of Red Bluff Draw exposes about 4.3 meters of Pleistocene alluvium. The Pleistocene deposits are visible for several miles along the draw. The lower 2.3 meters is coarse-textured gravel with large cross-beds (Fig. 10.4). Several well-preserved horse teeth (*Equus* sp.) were observed at different places in the coarse gravel (Fig. 10.5).

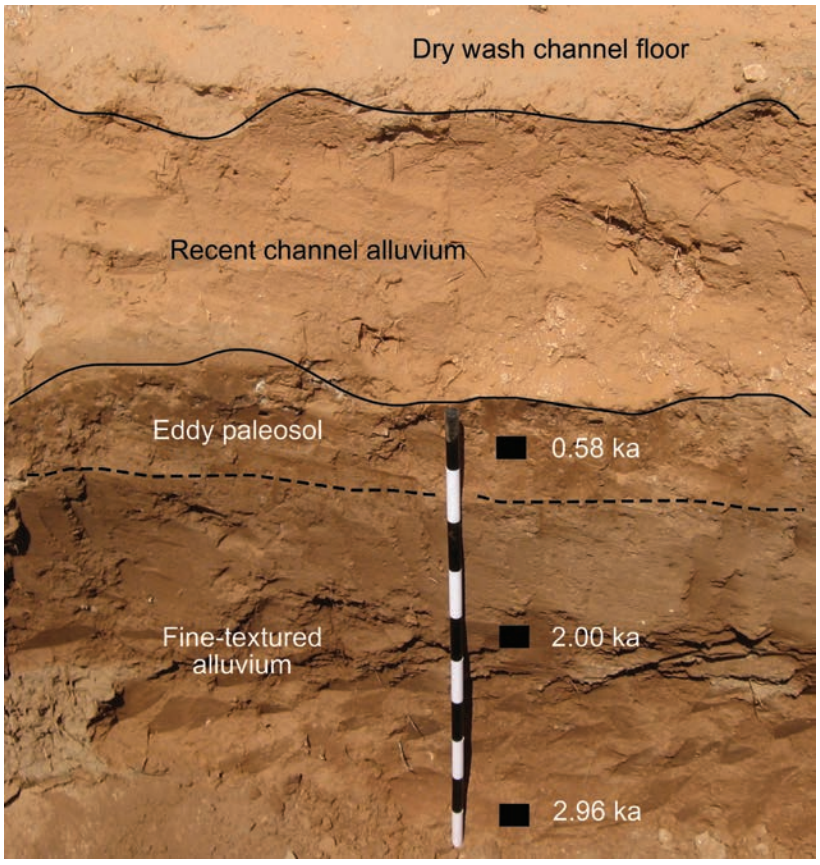

Figure 10.3. Late Holocene fine-textured alluvium exposed by trenching below the floor of a dry wash (Loc. 10); AMS radiocarbon ages in cal yr BP; recent channel alluvium is fine to medium sand; a pollen record came from this exposure (Ch. 13); four species of terrestrial snails were recovered from this dated alluvium. The Eddy paleosol and associated alluvium is buried by 0.5 m of recent channel sands of the wash; 1-m scale.

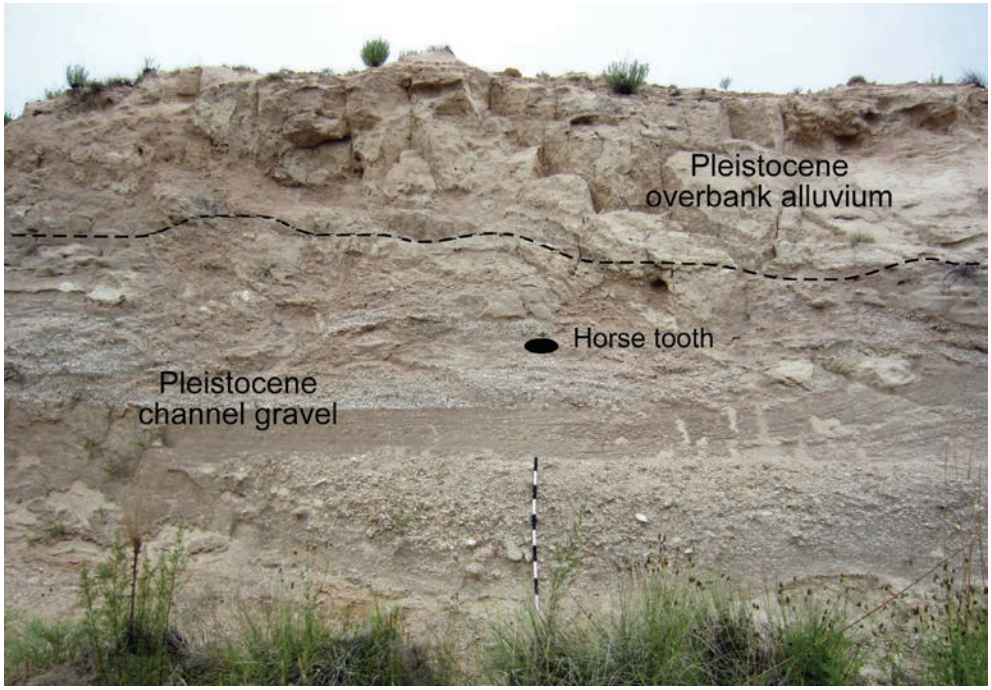

Figure 10.4. Pleistocene alluvium exposed in the bank of Red Bluff Draw, Loc. 32 (Hall, 2016); bone fragments occur in the gravel, including a tooth of *Equus* sp. (Loc. 32; Hall, 2016); 1-m scale.

Figure 10.5. Horse tooth (*Equus* sp.) from late Pleistocene alluvium, Red Bluff Draw, Loc. 32; photographed in the field (Hall, 2016).

The upper 2.0 meters is fine-textured light brown clayey silt with an absence of gravel. Small cross-beds occur in the lower half of the unit. A gypsum crust occurs at the top of the deposit. The gypsum crust is resistant to erosion and can be observed in gullies that are eroded into the terrace. The gypsum crust was also noted at the base of a trench excavated into the terrace (Fig. 10.6), where it is overlain by 1.5 meters of fine-textured Holocene alluvium. Evaporite rocks (halite, anhydrite, gypsum) of the Castile, Salado, and Rustler formations (Permian) occur in the Red Bluff Draw drainage basin; the gypsum content of the Pleistocene and Holocene alluvium is derived from these formations.

Holocene alluvium along the draw is generally thin and not everywhere present. The Holocene alluvium at Loc. 32 is approximately 1.5 meters thick and mantles the Pleistocene gravel. It is a brown clayey silt that is massive without bedding and without soil development. Sand has a low presence in the alluvium, only 7 to 29%, with silt and clay making up the remainder. The overall texture of the alluvium is coarsening-upwards as indicated by an increase in sand and decrease in clay content upwards in the measured section (Fig. 10.6). The sand grains have carbonate coats. The carbonate content ranges from 14 to 27%, increasing with depth and paralleling the increase in clay content. As observed in alluvium and eolian deposits, carbonate and clay content generally co-vary.

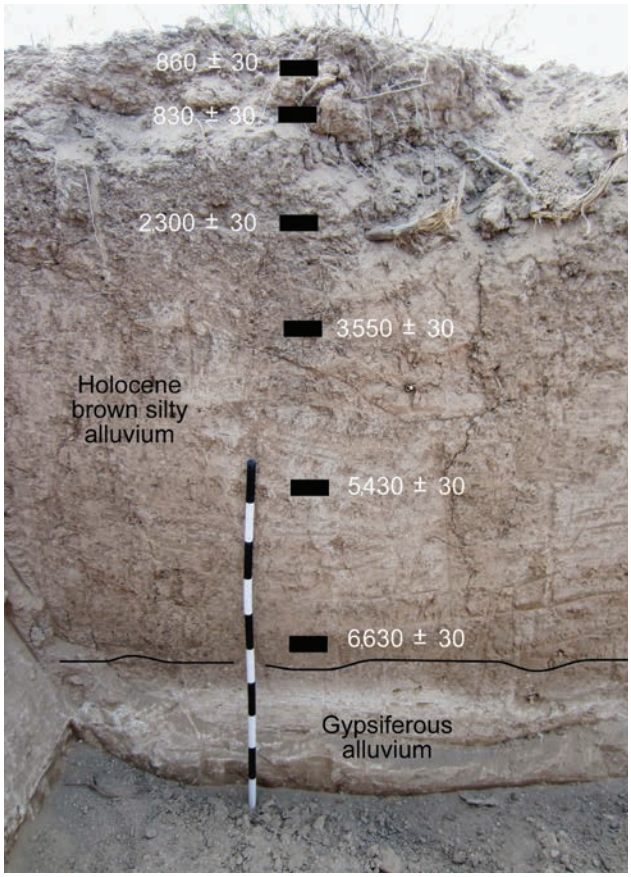

Figure 10.6. Massive to weakly bedded silty alluvium, mid- to late Holocene, Red Bluff Draw; the gypsiferous bed is late Pleistocene; the upper 30 cm at this exposure may be colluvial (Loc. 32; Hall, 2016); 1-m scale.

Seven bulk sediment samples from the entire thickness of the deposit at Loc. 32 were AMS radiocarbon dated, the ages ranging from 6,630 ± 30 to 830 ± 30 ^{14}C years BP. The mid-and late Holocene alluvium rests directly on late Pleistocene terrace deposits. The Early Holocene period appears to be missing from the local alluvial record.

Silt in Alluvium, Colluvium, and Sheet Sand

Silt is a strong component of local alluvium and colluvium west of the Pecos River in southwest New Mexico. A study of the surface geology southeast of Carlsbad documented a widespread late Holocene colluvial deposit across the area 40 to 60 cm thick with 35–50% silt and 20–40% clay, the remainder mostly very fine sand. Two AMS radiocarbon ages from the upper level of the colluvium, 20 to 30 cm depth, are 2,340 ± 40 and 1,940 ± 40 ^{14}C years BP (Hall, 2008).

In a broader study of the Azotea Mesa area west of Carlsbad, about 10% of the mapped area consists of colluvium and slope-wash deposits that are uniformly massive silt, clay, and very fine sand, averaging 44%, 24%, and 25%, respectively. The silt that makes up prominent hillslope and colluvial deposits west of Carlsbad may be derived by eolian deflation of the playa deposits in the Salt Basin located 30 to 60 miles southwest of these study areas (Hall, S.A., in Altschul et al., 2005, p. 80). Silt-bearing dust from the basin is wind-transported and deposited on limestone surfaces where it is washed by rainfall events, accumulating in slope-wash colluvium and carried into local streams where it is eventually deposited as silty alluvium.

Modern influx of atmospheric dust is well documented in the Southwest (Gile et al., 1981, p. 63; Lee and Tchakerian, 1995; Reheis et al., 2002; Reheis, 2006; Kavouras et al., 2007). The presence of measurable amounts of atmospheric silt in regional paleosols has also been documented (Holliday, 1988; Muhs and Benedict, 2002; Hall and Periman, 2007, p. 463–465).

Although an elevated silt content of eolian deposits in the Mescalero Sands has not been found, the late Pleistocene horizons that are OSL-dated 44.8 and 24.0 to 14.5 ka of the Bolson sand sheet northeast of El Paso, Texas, have consistently higher percentages of silt than occurring in early and middle Holocene eolian sand (Hall et al., 2010, p. 1962). The timing of the silt zone suggests that the southern path of the jet stream across the U.S. Southwest during the Middle- and Late-Wisconsinan (Kutzbach and Webb, 1993) may have been responsible for greater amounts of atmospheric silt entrained, transported, and deposited in the region.

The exception where silt is prominent on the Mescalero Plain is with late Pleistocene caliche of the Mescalero paleosol. It was sampled at six places in northern Eddy County. The silt content varied from 1.4 to 54%, averaging 21%. The Ogallala Formation and Caprock also have a high silt content. The Caprock silt ranges from 9 to 41%, averaging 24%. The eolian sand of the Ogallala Formation has 7 to 16% silt, averaging 11%. Late Holocene alluvium coming off of the Caprock escarpment has as much as 13% silt. Late Holocene alluvium in a small drainage in the western area of the plain (Loc. 10) has 20 to 48% silt. Even though these sources are present in the region, silt particles are not a significant component of the Mescalero Sands.

Colluvium on Hillslopes

Colluvium is defined as "a general term applied to any loose, heterogeneous, and incoherent mass of soil material and/or rock fragments deposited by rainwash, sheetwash, or slow continuous downslope creep, usually collecting at the base of gentle slopes or hillsides" (Neuendorf et al., 2005, p. 128). Colluvium occurs on all hillslopes in the Mescalero Plain. Most commonly it is a mix of eolian sand and small caliche gravel that has been moved by slopewash and has accumulated down slope (Fig. 10.7). Some colluvial deposits may have a fluvial component where runoff is concentrated in rills and small gullies, depositing sand and caliche pebbles in small temporary channels. The channels may become buried in thick colluvium (Fig. 10.8). The colluvial deposits that we have studied appear to be mostly middle to late Holocene in age and, in some cases, incorporate buried archaeology (Simpson, 2010).

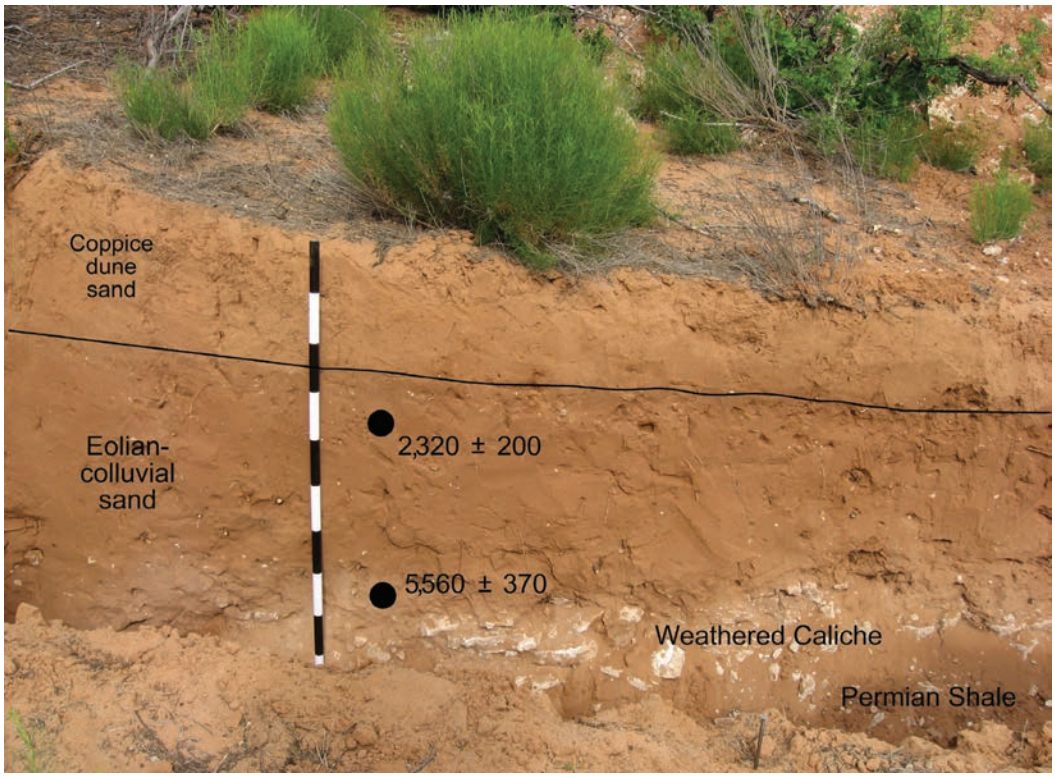

Figure 10.7. OSL dated colluvium on a low-gradient hillslope at Loc. 10; weathered caliche of the Mescalero paleosol developed on Permian red beds (Rustler Formation); 1-m scale.

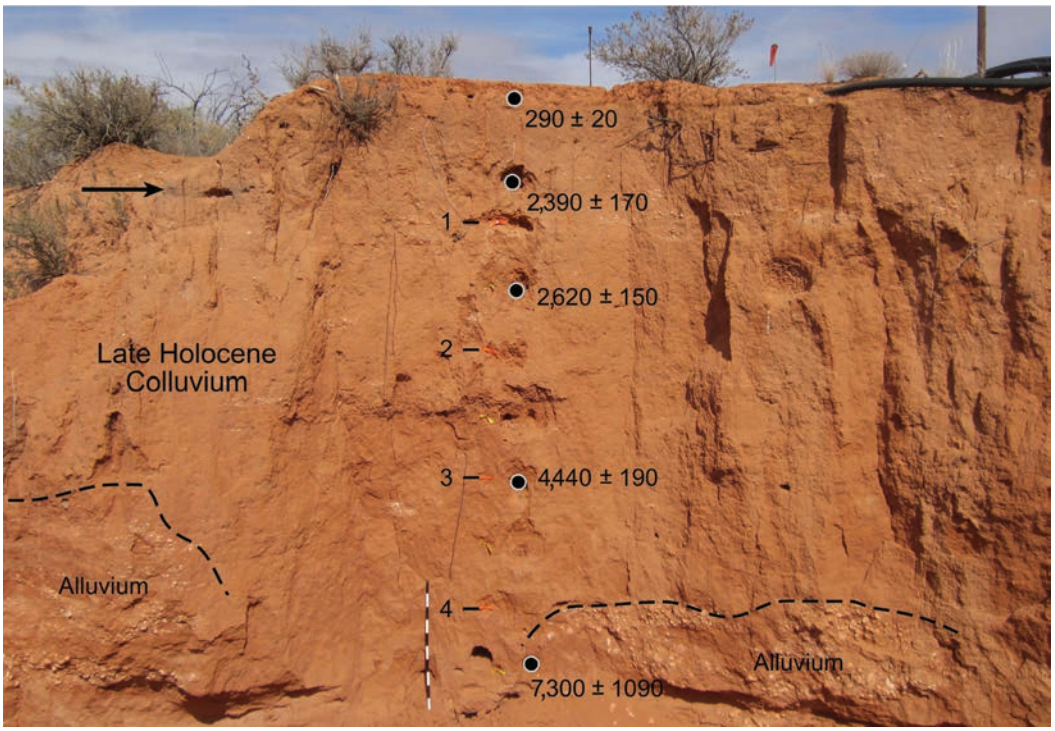

Figure 10.8. OSL dated 5 m of late Holocene colluvium with lower alluvial facies, east slope of Cedar Lake basin at Loc. 28; 1-m scale; numbers are meters below the modern ground surface; arrow in upper left points to a buried prehistoric feature with charcoal.

XI. SPRINGS, PONDS, PLAYA LAKES, DEPRESSIONS

During the Late Wisconsin and the last glacial maximum 26.5 to 20–19 ka (Clark at el., 2009), the regional climate was cool and wet. Water tables were high, playa lakes were full, springs were active, and streams were flowing.

Spring, wet meadow, and pond deposits on the Mescalero Plain are not unusual, especially along the eastern margin of the plain near the edge of the Ogallala Formation (Fig. 11.1). During the Late Wisconsin, about 35 to 15 ka, the cool wet glacial-age climate charged the Ogallala aquifer beneath the High Plains surface. The resulting high water table led to numerous active springs along the western outcrop of the Ogallala where the aquifer dewatered. The flow from these springs promoted wet meadow environments and filled small depressions with water, forming a number of ponds across the Mescalero Plain. A systematic study of these deposits has not been conducted, although a few observations can be summarized.

Glacial-Age Spring at Square Lake Road

Several areas of springs and related lacustrine deposits occur west of the Caprock escarpment. One of them is a 40- to 80-cm-thick deposit of carbonate-coated sand with small carbonate nodules and many land and freshwater snail shells. It is buried by two m of alluvium and eolian sand and exposed in an arroyo cutbank along Square Lake Road (Loc. 40; loc. 14 in Hall, 2002a). Well-preserved shells with nacreous (pearly) luster were AMS radiocarbon dated 18,900 ± 100 ^{14}C years BP (22,760 cal yr BP), corresponding to the last glacial maximum (Fig. 11.2).

Figure 11.1. Olive-colored lacustrine deposits along unnamed stream just west of Caprock Road near Loc. 3 (loc. 11, Hall, 2002a); these deposits have not been dated but contain isolated mammalian bone fragments and shells of land and aquatic snails; late Holocene alluvium on the left in this view; sediment data Appendix C, Table C-34, loc. 11.

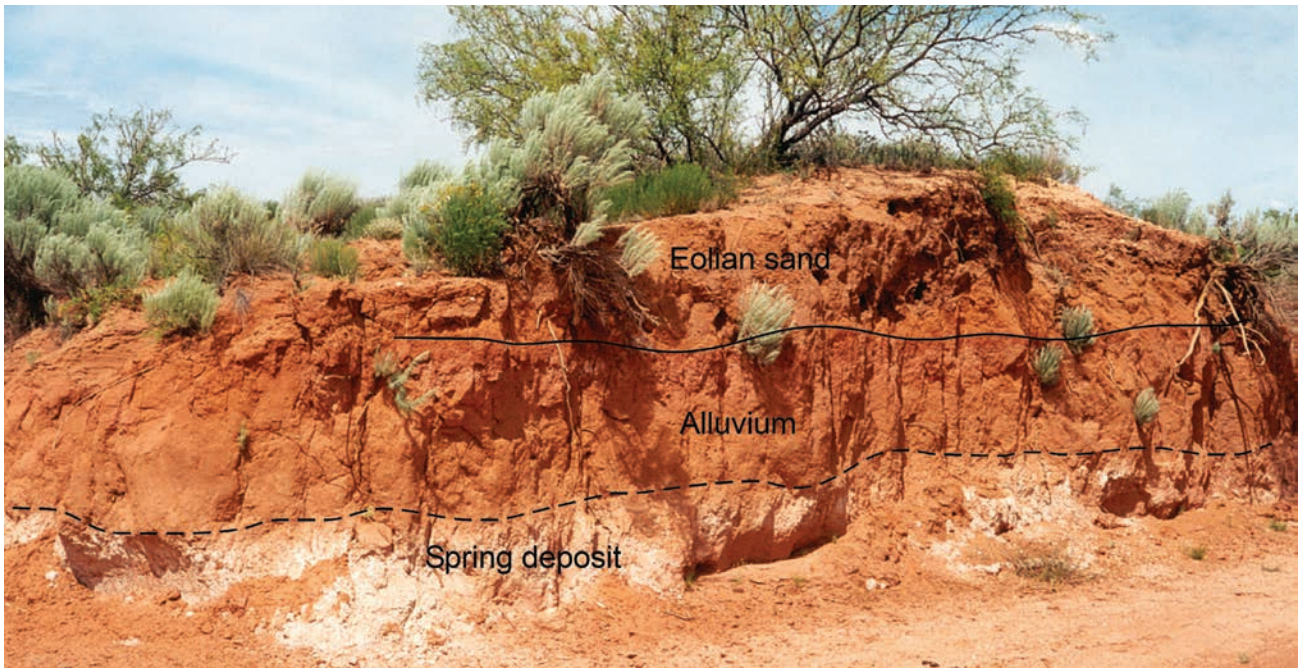

Figure 11.2. Glacial-age spring deposit exposed at base of arroyo cutbank at Square Lake Road crossing; snail shells are AMS dated 18,900 ± 100 ^{14}C years BP (22,760 cal yr BP) (Loc. 40; loc. 14 in Hall, 2002a,b).

Glacial-Age Pond at Locality 24

A lacustrine deposit was accidently discovered at the base of a deep trench at Loc. 24; there was no hint of its presence prior to backhoe work. The sandy clay has a wet color of light greenish gray but dries to a pinkish gray, losing its greenish hue. The deposit is 48 cm thick and is overlain by late Holocene eolian sand and parabolic dunes. It contains shells of terrestrial and freshwater snail as well as ostracodes; however, it is barren of pollen. The deposit is OSL dated 20,200 ± 1100 years, indicating a late full-glacial age (Hall and Goble, 2015a; Fig. 11.3). Auguring near the trench revealed the presence of lacustrine deposits at 65 cm depth. The excavation of pipeline trenches in the vicinity has also revealed additional lacustrine deposits, probably representing a single large lake as much as 1 mile in width.

Glacial-Age Spring West of Nash Draw

Trenching at Loc. 22 revealed a thick sequence of eolian sands dated from late Pleistocene to late Holocene in age. At the base of one trench is a 15-cm thick bed of light yellowish brown (5YR 6/4) eolian sand resting directly on caliche of the Mescalero paleosol. The sand grains exhibit thick carbonate coats with 9% carbonate, unusually high for local eolian sand sequences. Shells of snails or ostracodes were not present. The calcareous sand is interpreted as related to a nearby seep or spring; a spring head was not found during trenching. The OSL age of the sand is 21,600 ± 1,000 years, indicating a temporal correlation with the full-glacial Late Wisconsinan.

Playa Lakes

A number of playa lakes occur in southeastern New Mexico. However, except for a few observations on the geomorphology of dunes and soils related to archaeology, very little is known about the late Quaternary geology of the playas or their basins.

Laguna Plata

A geomorphic study of a site on the western shoreline of Laguna Plata (Loc. 38) concluded that the visible prehistoric artifacts were concentrated on the eroded surface of a Pleistocene alluvial fan. Intact artifacts and features were thought to be preserved nearby in a late Holocene fan deposit. A road cut exposure and cores from along the shoreline show that lacustrine sediments, probably late Pleistocene in age, occur topographically above the modern playa, indicating a considerable amount of deflation post-Pleistocene (Brown, 2010).

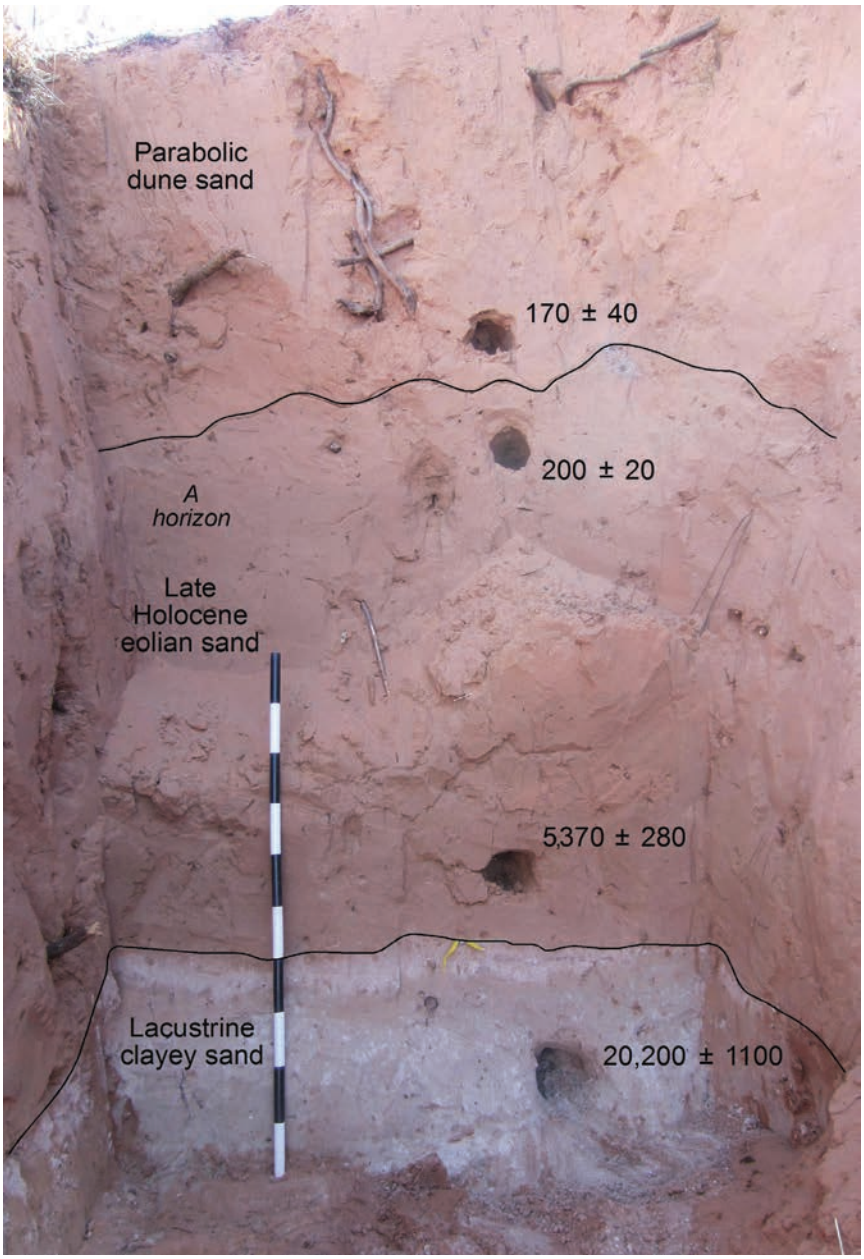

Figure 11.3. A deep cut in parabolic dune sand, exposing a late full-glacial age lacustrine deposit containing terrestrial and freshwater snails (Loc. 24). Late Holocene eolian sand overlies the pond deposit. A weak soil A horizon occurs at the top of the late Holocene sand. The contact horizon of the sheet sand with the overlying parabolic dune is an erosional surface. An additional OSL age from the late Holocene sand in an adjacent trench is 2,340 ± 450 years. Another basal age for parabolic dune sand in an adjacent trench is 160 ± 40 years. Loc. 24 is in the area of Los Medaños and may contain elements of that stratigraphy (see Chapter 4).

Eolian Sands from Beach Deposits

Eolian sands that are derived from Laguna Plata beach deposits (Loc. 6) have been discovered 1.8 miles east of the playa. The 1.15-m thick sand is light reddish brown (7.5YR 6/3-4) and is much lighter in color than the other eolian sand units (Fig. 11.4). Sand grains lack iron or humate staining, giving the deposit its whitish color. The sands are OSL dated 20,900 ± 1,100 to 11,900 ± 700 years, indicating that the shoreline deposits were available for deflation after the peak of the last glacial maximum (26.5 ka to 20–19 ka) to the end of the Younger Dryas (11.7 ka) and the beginning of the Holocene. This is the first documented example on the Mescalero Plain where local sheet sands have been derived from playa shoreline deposits.

OSL dating of lunette dunes associated with large playas on the Southern High Plains of Texas showed dune development during the period 16 ka to 11 ka, similar to the Laguna Plata-related record. Lunette dunes were also forming there during the arid middle Holocene (Rich, 2013).

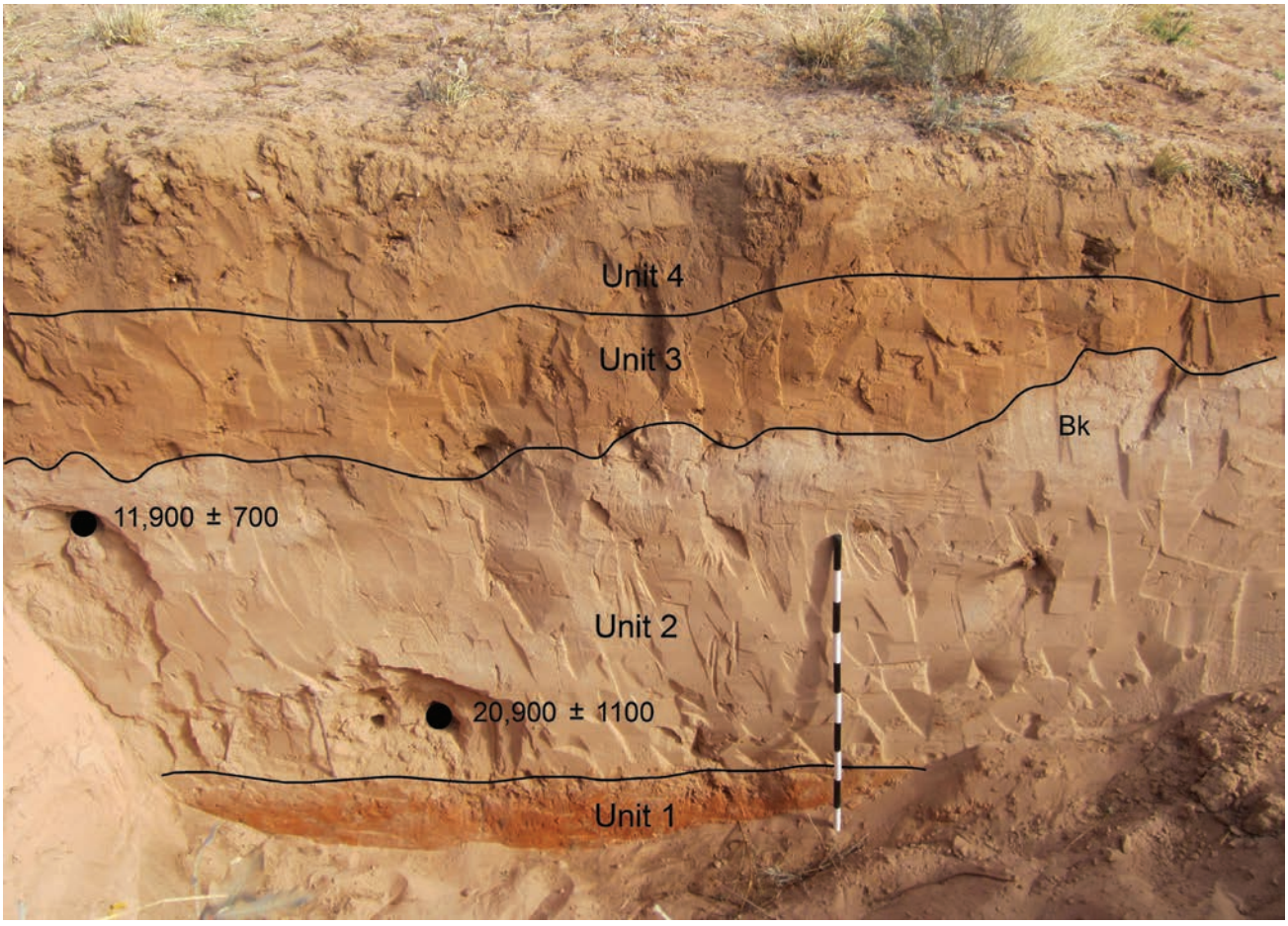

Figure 11.4. Whitish eolian sand (Unit 2) at Loc. 6 derived from deflated beach and shoreline deposits of Laguna Plata; this site is 2.9 km (1.8 miles) east of Laguna Plata; the whitish sand is OSL dated 20.9 to 11.9 ka, latest Pleistocene. Unit 1 is the Lower eolian sand unit (here OSL dated 58.5 ka); Unit 3 is Holocene eolian sand (OSL, 9.3 to est. 3 ka); Unit 4 is Cover sand (OSL dated 230 ± 80 years, A.D. 1784); from Hall and Goble, 2015a; 1-m scale.

XII. ARCHAEOLOGICAL GEOLOGY

Most of the geologic studies of prehistoric sites on the Mescalero Plain have focused on the stratigraphic position of sites within the context of deposition and erosion of local geological deposits. We have inspected and studied dozens of sites in the course of the past 19 years, nearly all of them associated with eolian sands on the Mescalero sand sheet. Summaries of the prehistoric archaeology of southeastern New Mexico have been written by Sebastian and Larralde (1989), Katz and Katz (2001), Ingbar et al. (2005), Hogan (2006), and Railey (2016); Montgomery (2018) presents an important review for all of eastern New Mexico and adjacent West Texas. For nomenclature and chronology of the regional archaeological sequence, we are following the recent synthesis by Railey (2016; Table 12.1).

A predominant universal characteristic of archaeological sites in the region is an absence of bedding or layering in the eolian sediments that contain artifacts and features. Distinctive cultural beds or horizons in the massive sheet sands are absent. Site occupation surfaces are not preserved. If a site footprint is present, any occupation surface

Table 12.1. Prehistoric archaeology of southeastern New Mexico (from Railey, 2016)

Tradition	Time Interval		Number of sites*	Notes
	A.D. - B.C.	Calendar Years BP		
Post-Formative	A.D. 1450 – 1885	500 – 65 BP	17	Ceramics absent or poorly known; bison hunting, side-notched arrow points; abandonment of earlier villages
Late Formative	A.D. 1100 – 1450	850 – 500 BP	3272	Appearance of distinctive decorated ceramics and after A.D. 1300 exotic SW ceramics; village-like sites; hunter-gatherer "farmers"
Early Formative (84% of all sites are Formative)	A.D. 500 – 1100 (site ^{14}C dates peak at A.D. 775)	1450 – 850 BP	1898	Appearance of a few (not many) ceramics and bow and arrow with small strongly shouldered, corner-notched or stemmed points; only a few house remains found; absence of maize and farming; abundant cooking pits
Late Archaic	1800 B.C. – A.D. 500	3750 – 1450 BP	660	Wetter climate than before; increased number of sites; numerous pits at sites; absence of farming; atlatl use; bison hunting
Middle Archaic	3200 B.C. – 1800 B.C.	5150 – 3750 BP	162	End of Altithermal aridity ca. 4500 BP; earliest rock middens
Early Archaic	6000 B.C. – 3200 B.C.	7950 – 5150 BP	110	Beginning of Altithermal aridity ca. 7000 BP; sites near water
Missing sites	7000 B.C. – 6000 B.C.	8950 – 7950 BP	0	Paleoindian/Archaic gap in regional record, noted by others
Late Paleoindian (Plano)	9800 B.C. – 7000 B.C.	11,750 – 8950 BP	29	Early Holocene warming, drying; unfluted lanceolate points; bison hunting
Paleoindian (Folsom/ Midland)	10,800 B.C. – 9800 B.C.	12,750 – 11,750 BP	27	Cooler, wetter climate of Younger Dryas (12.9 to 11.7 ka); fluted lanceolate points, hunted *Bison antiquus*
Paleoindian (Clovis)	11,500 B.C. – 10,800 B.C.	13,450 – 12,750 BP	7	Fluted lanceolate points, hunted extinct fauna; pre-Younger Dryas

* 6,182 sites located in the region of the Carlsbad Field Office, Bureau of Land Management

may have been erased by disturbance. Overall, it is generally impossible to physically correlate sediments or features within a site. Because of the uncertainties regarding internal stratigraphy of sites, we have elected for the most part to concentrate our investigations on deposits beyond site boundaries, avoiding culturally disturbed areas whenever possible. Ideally, geologic studies both on and off site will reveal the degree of cultural disturbance of the natural stratigraphy. A summary of the geologic occurrence of prehistoric sites on the Mescalero Plain is presented in Table 12.2.

Geographic Distribution of Prehistoric Sites through Time

Jim Railey (2016, p. 57-67) presents remarkable trends in the radiocarbon dates from sites in southeastern New Mexico and bordering Texas counties. He compiled site dates from three sub-regions: (i) the Mescalero Plain, (ii) the Pecos River Corridor defined as a 10-km (6-mi.) buffer on each side of the river, and (iii) the Mountain Slope, the eastern slope of the Sacramento-Guadalupe mountains. A fourth sub-region, the Llano Estacado, with only 4 sites with 13 radiocarbon dates was not included in the analysis.

Most of the sites are located in the Mescalero Plain (Fig. 12.1). A few sites in that area are Early Archaic and Middle Archaic, and more are Late Archaic (Fig. 12.2), briefly peaking about 720 B.C. (2,670 cal yr BP). After a decline, the number of sites mushrooms in late Late Archaic time and into the Early Formative, climaxing about A.D. 775 (1,175 cal yr BP). This trend also occurs in the Pecos River Corridor. The boom in Early Formative population is likely a response to moister conditions during the Late Holocene that resulted in greater abundance of surface water and plant and animal resources across the Mescalero Plain.

Table 12.2. Geology of archaeological sites on the Mescalero sand sheet (see Table 12.1)

Archaeology*	Geology	Paleoenvironments
Post-Formative (since 500 BP)	Sites associated with upper part of Eddy paleosol, Loco Hills paleosol, sand deposits in parabolic, cover, and coppice dunes	Severe erosion of sand sheet past 300 years, beginning ca. A.D. 1700; all Formative and some late Late Archaic sites are impacted
Late Formative (850 – 500 BP)	84% of all sites are Formative; peak radiocarbon dates ca. A.D. 775 (1175 BP); 76% of all sites correlate with the Eddy paleosol (2000 to 300 BP); Sites occur in upper levels of Eddy paleosol; sites on Upper eolian sand (Episode III)	Onset of warm-dry conditions of Medieval Warm Period, 1050 to 650 BP; short-term shift in site location from Mescalero Plain to Pecos River and mountain slope areas
Early Formative (1450 – 850 BP)	Sites occur in Eddy paleosol; sites on surface of Upper eolian sand (Episode III)	Large number of sites coincides with late Holocene wetter climate
Late Archaic (3750 – 1450 BP)	Sites occur in lower part of Eddy paleosol, upper part of Episode IV and V eolian sands; sites on old surface of Upper eolian sand unit (episode III)	Beginning ca. 4500 BP period of cooler-wetter climate after Altithermal aridity; sand sheet accumulation continued until ca. 2 ka when Episode IV and V eolian deposition ended and Eddy A horizon topsoil began to form across sand sheet
Middle Archaic (5150 – 3750 BP)	Sites occur on old surface of Upper eolian sand unit (episode III), or buried at the base of episode V sands, or buried in episode IV sands	Altithermal period of extreme aridity, hot and dry climate; continuing deposition of sand sheet
Early Archaic (7950 – 5150 BP)	All of these sites are buried in Upper eolian sand unit (episode III) or near the base of episode IV sands	Southwest climate dry and entering Altithermal period of extreme aridity 7000 to 4500 BP; continuing eolian sand deposition
Missing sites (8950 – 7950 BP)	Sites could be buried in lower Upper unit or lower Holocene unit (episodes III, IV)	Paleoindian/Archaic gap in regional prehistoric record, noted by others
Late Paleoindian (Plano) (11,750 – 8950 BP)	Surface sites occur along Pecos River, on Caprock plain, and at pluvial lakes; sites can be buried in Upper eolian sand unit (episode III) or possibly in lower part of Holocene sand (episode IV); sites may also occur on eroded surface of Lower or Middle sand (episodes I, II) or on bedrock; overall, Paleoindian remains are few and sparse	Coming out of the Younger Dryas and late Pleistocene cool-wet climates; Early Holocene climate cooler-wetter than today but warming and drying by ca. 7000 B.C., trending towards Middle Holocene aridity
Paleoindian (Folsom, Midland) (12,750 – 11,750 BP)		Folsom spans most of the Younger Dryas (12.9 to 11.7 ka)
Paleoindian (Clovis) (13,450 – 12,750 BP)		Clovis is largely a pre-Younger Dryas, pre-black mat environment (Haynes, 2008)

* from Railey, 2016

After the Early Formative peak, however, the number of radiocarbon dates from sites dramatically turns down. The decline corresponds to the onset of the warmer and dryer conditions of the Medieval Warm Period ca. A.D. 900 (1,050 cal yr BP) that persisted 400 years until about A.D. 1300 (650 cal yr BP) (Lamb, 1965; Cook et al., 2004; Hall 2018). The warmer climate likely resulted in the drying of some local surface waters and diminished plant and animal resources on the plain.

During the decline of sites on the Mescalero Plain during the warm period, sites persisted along the Pecos River and became more abundant at higher elevation in the Mountain Slope area during early Late Formative time (Fig. 12.1). After about A.D. 1200 (750 cal yr BP), however, all three sub-regions experienced a decline in population. Regardless, the increase in site numbers along the river and on the mountain slopes during the early warm-dry period is an important discovery, and a challenge to current and future researchers to investigate further.

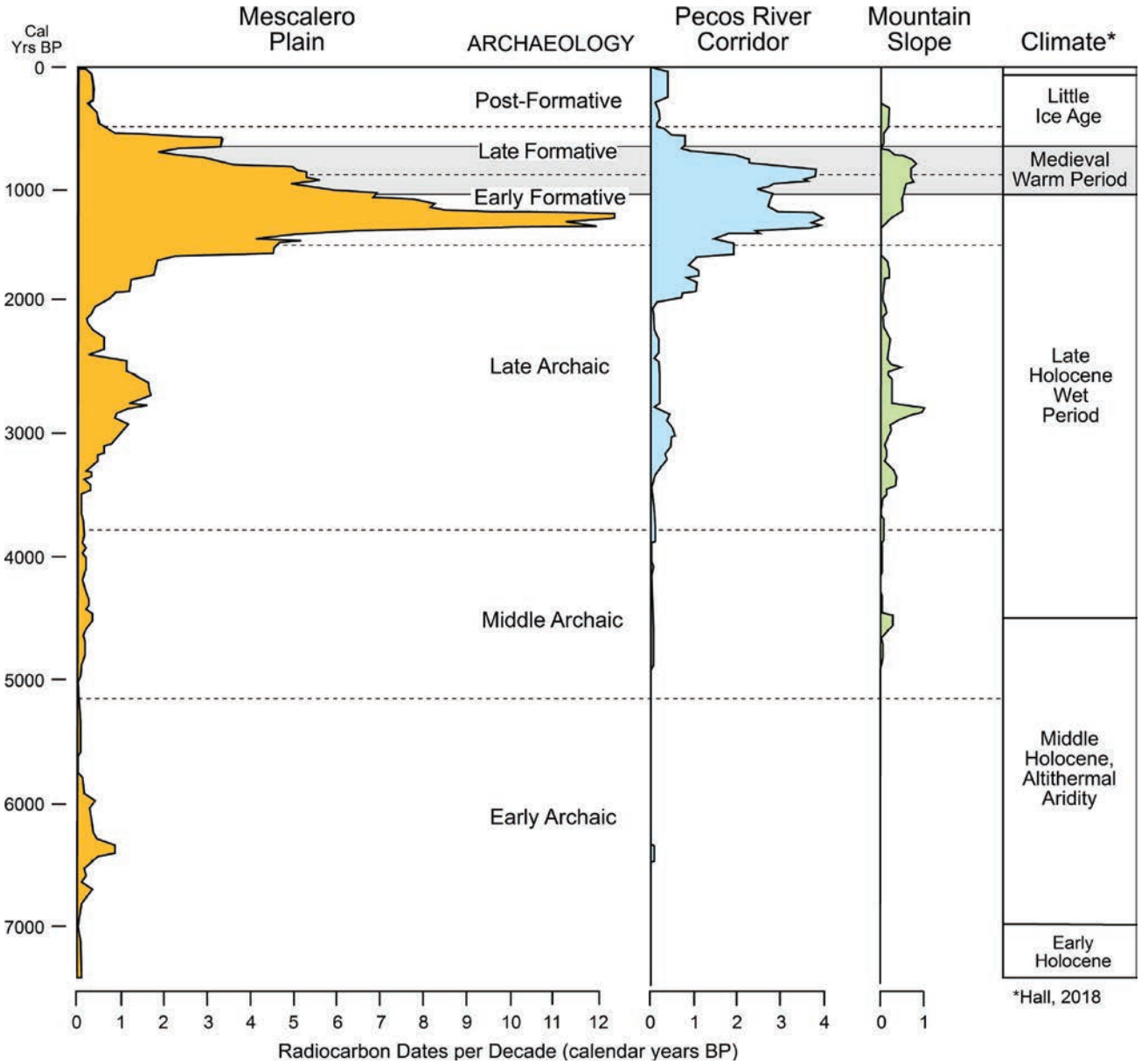

Figure 12.1. Age-frequency distribution of radiocarbon dated features from prehistoric archaeological sites, Carlsbad Field Office area, Bureau of Land Management, southeastern New Mexico; the total number of radiocarbon dates is 1,175: Mescalero Plain, 841; Pecos River Corridor, 340; Mountain Slope, 94; the diagram is modified from Railey (2016, p. 59, figure 4.5); see Railey (2016, p. 57–67) for a map of the sites from which the radiocarbon dates were obtained and for further discussion of the data.

The reader may note the apparent discrepancy between the number of Early and Late Formative sites and the distribution of dated features (Table 12.1 and Fig. 12.1). The peak in dates occurs in the Early Formative, but the greater number of recorded sites is Late Formative. Railey (2016, p. 61, 62) discusses the issue:

This can be explained by ceramic trends that influence archaeologists' identifications of Formative components in the region. Specifically, whereas undecorated brown wares occur in both Formative periods, most painted and other decorated wares are restricted to the Late Formative. Thus, when both plain brown wares and decorated (and/or white ware) sherds are found during survey, investigators tend to assign one of the component types that fall in the Late Formative period. These factors have tended to inflate the number of identified Late Formative components relative to Early Formative ones. Also,… Early Formative people in the present-day CFO [Carlsbad Field Office] region probably did not have as many ceramic vessels as at least some of their Late Formative successors did, and this may also have worked to depress the number of Early Formative components recognized and identified during survey and even excavations.

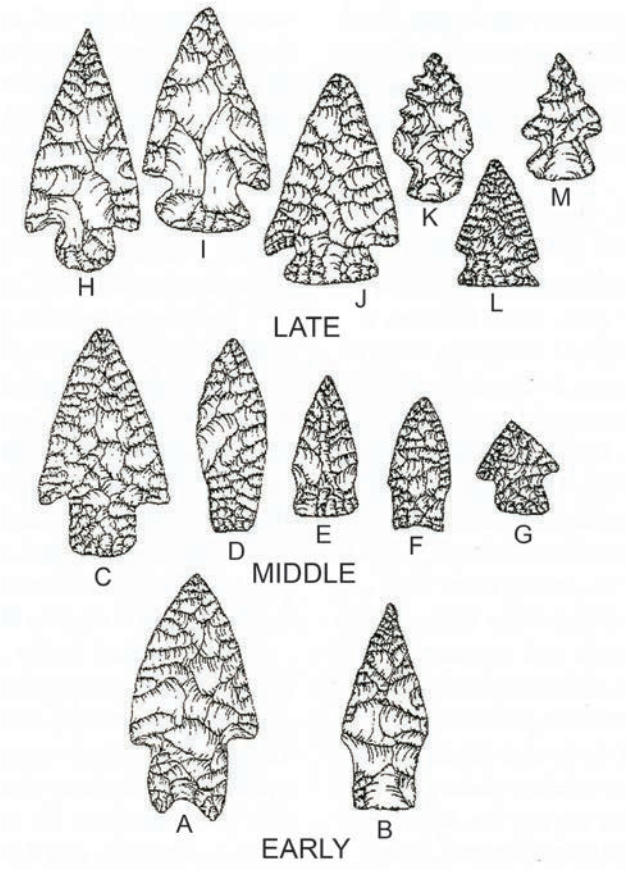

Figure 12.2. Archaic projectile points from the region: (*A*) Pedernales; (*B*) Travis; (*C*) Bulverde; (*D*) Pandale; (*E*) Trinity; (*F*) Darl; (*G*) Ellis; (*H*) Palmillas; (*I*) Williams; (*J*) Marcos; (*K*) Maljamar; (*L*) Ensor; (*M*) Carlsbad (from Montgomery, 2018, p. 160).

Site Preservation and Sedimentation Rates

Most prehistoric sites in the region are associated with the Eddy paleosol; as pointed out earlier, 76% of the dated features at sites in the Mescalero Plain correlate with the Eddy. The cumulic paleosol is 15 to 50 cm thick, although variable, and has accumulated at an average rate of 0.41 mm per year. (The sedimentation rate of sheet sands across the plain is generally less than 0.20 mm per year). Given a site that has formed on a prehistoric surface of the Eddy paleosol, the site would be buried by only 4.1 mm of eolian sand after a period of 10 years. After a century, the site would be buried by 41 mm of sand. We propose that low rates of sedimentation set the stage for a number of consequences concerning site formation and preservation on the sand sheet. A low-rate site will be susceptible to a number of processes:

- natural and cultural disturbance of the sand associated with the site occupation
- obliteration of any surface of occupation
- stratigraphic intermingling of artifacts and features from different occupations
- fine-scale deflation and sheet erosion of the site, potentially more than once
- shallow sites at risk to coarse-scale deflation beginning about 300 years ago; eroded artifacts concentrated on blowout floors and scoured surfaces between coppice dunes (Figs. 12.3, 12.4)

Overall, slow sedimentation rates lead to poor preservation of prehistoric sites with high susceptibility to disturbance, mixing of artifacts, and erosion.

Buried Sites

We conclude that almost all sites on the Mescalero Plain are or have been buried in the Eddy paleosol or associated eolian sands, although many occur at a shallower depth. Considering the OSL age of the Eddy paleosol and associated sands, the only opportunity for a prehistoric site to form at a surface *without* becoming buried is after A.D. 1700 in the Post-Formative period. This suggests that all prehistoric sites that have formed pre-A.D. 1700 have the potential to be buried, even if by only a thin layer of sand. After A.D. 1700, the sand sheet and associated shallow sites were severely eroded.

The older the site, however, the deeper it can be buried. For example, given a Late Archaic site with an age of A.D. 200 and the Eddy paleosol sedimentation rate of 0.41 mm per year, the site could be buried at a depth of 61 cm, given uniform sediment accumulation for 1,500 years.

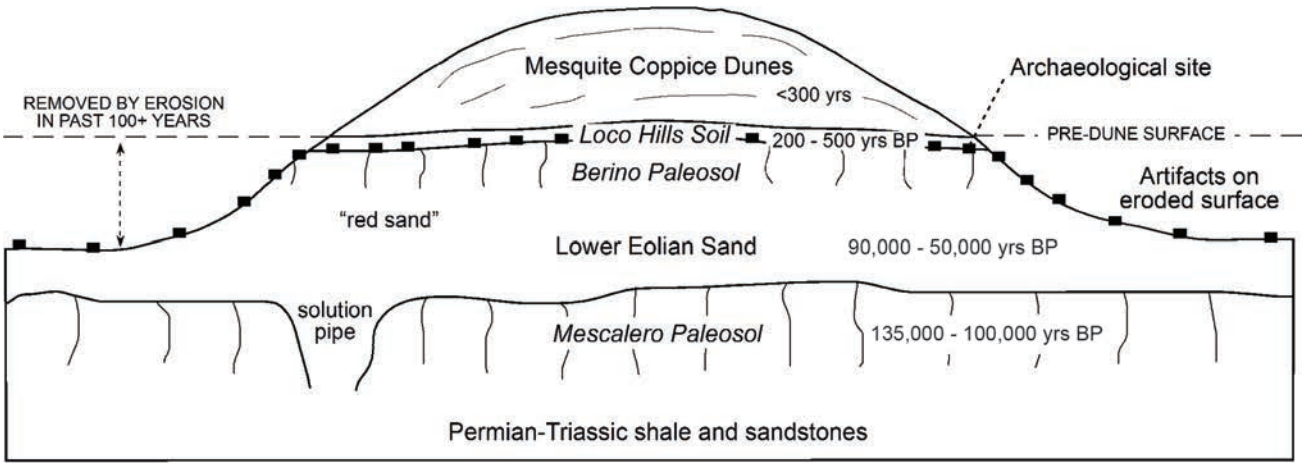

Figure 12.3. Deflated prehistoric sites and associated coppice dunes, Loco Hills area, Eddy County; sites were probably eroded before coppice dune formed; continued erosion left the initially eroded site on a pedestal beneath the mesquite-protected coppice dune (modified from Hall and Goble, 2008, 2019).

Figure 12.4. Deflated archaeological site, Loco Hills area, northern Eddy County; artifacts occur beneath the coppice dunes although the site may have been eroded before the dunes formed; photograph July 3, 2001.

However, looking at pre-Eddy paleosol sand deposits where the sedimentation rates are significantly lower, early sites are not necessarily buried deeply. In a case at Loc. 8, a late Paleoindian stone feature with an interpolated age of 10.6 ka was buried in the Upper sand unit at 58 cm depth below the modern ground surface (Fig. 3.10). The sedimentation rate of the eolian sand at that specific locality was 0.080 mm per year (Table 5.1).

If we could look back to A.D. 1500, we would see an undulating sand sheet covered by a thick topsoil with a dense grassland and some areas with shinnery oak vegetation. Stone features from recent prehistoric sites may protrude above the soil. Earlier sites would be buried in the topsoil or in the underlying sands. Dunes and their blowouts and scoured surfaces were not present at that time.

All of this changed about 300 years ago. The only reason that sites are visible in the field today is because of the almost universal deflation and erosion that has occurred across the Mescalero Plain in the past 300 years.

Buried-Site Potential

In the past few years, we have noted two criteria that can indicate the likely age and thickness of subsurface eolian sands that could be related to archaeology: dune geomorphology and vegetation (Table 12.3). The following observations on the surficial geology and vegetation may indicate subsurface conditions and potential for buried prehistoric sites:

- Areas without dunes indicate an absence of sand and no sand deposits. Thus, sites of all ages in these areas occur at the surface and are not buried.
- Coppice dunes can indicate a couple of situations. The subsurface sand is Pleistocene where all sites are at the surface, or the subsurface is Holocene, generally less than 1 meter thick, where sites can be buried. Secondary rules in this case: red sand is Pleistocene; if not red, it is Holocene.
- Parabolic dunes, small or large, indicate that the underlying sand is thick (greater than 1 meter) and it is late Holocene in age. In all cases, buried-site potential is high.
- Mesquite can occur almost anywhere. It is present in areas without eolian sand with zero buried site potential, or it is present on thin sands, less than 1 meter thick, with positive buried site potential.
- Shinnery oak is a valuable indicator of thick (greater than 1 meter) late Holocene-age eolian sand. It is nearly always found associated with parabolic dunes. Buried site potential is high.

Buried-Site Potential Maps

Buried-site potential maps are valuable resources for general cultural resource management. It is helpful in planning to have some indication that a specific land use project may or may not have the potential to encounter subsurface archaeology. The most useful buried-site potential map will contain information on the (1) age of the subsurface sedimentary deposits and (2) thickness of subsurface deposits that are the right age to potentially contain archaeology. The known age for the subsurface deposits is the most important criterion in constructing a map; without the age, thickness is moot. Without good ages for the subsurface deposits, a buried-site potential map is at best only an estimate.

Table 12.3. Geomorphic and vegetation indicators of thickness and age of subsurface deposits and their buried-site potential in southeastern New Mexico

Depth-Thickness of Holocene Eolian Sand	Dune Geomorphology and Geology	Vegetation	Buried Sites
0 cm	No dunes; no Holocene eolian sand; Pleistocene red sand; bare ground; exposed caliche	Varied; mesquite, creosote bush, grasses	No; sites of all ages at the present-day surface
<100 cm	Coppice dunes; Pleistocene or Holocene sand	Mesquite	Yes; sites exposed between coppice dunes
>100 cm	Parabolic dunes; Late Holocene sand	Shinnery oak	Yes; sites exposed in blowouts

Note: modified from Hall and Goble, 2016g, 2019.

The presence and thickness of eolian sand deposits vary tremendously on the Mescalero Plain. As noted before, one can stand on caliche of the Mescalero paleosol in one place and, within a distance of a few hundred feet, walk up to parabolic dunes that rise four meters above the caliche. The variability of the surface geology is a challenge to the field mapper. However, even with an accurate buried-site potential map in hand, "it is not a substitute for fieldwork by an experienced practitioner" (Hall, 2006, p. 2-17).

Three different types of buried-site potential maps (or geoarchaeological maps, or archaeological geologic maps) have been produced in recent years and are briefly discussed below.

Geoarchaeological Map of Southeastern New Mexico, PUMP III —A surficial geologic map with units applied to archaeology was produced by the New Mexico Pump III project (Ingbar et al., 2005). The mapped area was eight 7.5-minute quadrangles around Loco Hills, northern Eddy County, an area of about 1295 km² (500 square miles). The surficial geology was drawn on the 7.5-minute topographic maps using black-and-white and color infrared stereo aerial photographs. The map units were defined by the fieldwork previously completed in the area and published in Hall (2002a). The final map was included in the Pump III report with the caption "Geomorphology of the Loco Hills study area" (Ingbar et al., 2005, p. 53). The map was redrafted and published in Hall and Goble (2006, 2008). It was reproduced, with excavated archaeological sites added, for the Second Workshop on Archaeological Geology (Hall and Boggess, 2013, p. 28) (Fig. 12.5).

A shortcoming of PUMP III map is that, at the time, only two principal eolian units were known, the Lower and Upper sands. Subsequently, an additional late Pleistocene and two Holocene eolian sand units were discovered and documented in southern Eddy County (episodes II, IV and V). Expanded OSL dating has also provided a fresh view of the chronology of the sand sheet, including ages for parabolic and coppice dunes and cover sand.

Geoarchaeological Map of Southeastern New Mexico (2006)—The entire southeastern corner of New Mexico was mapped in 2006, a total of nine counties and an area of 79,904 km² (30,851 square miles) included in Hogan's (2006) regional research design. Because fieldwork for such a large area was out of the question at the time, the geoarchaeologic map was based on an unpublished draft map tentatively called "Surficial Geologic Map of New Mexico" at a scale of 1:500,000 (generously provided by the New Mexico Bureau of Geology and Mineral Resources). The southeastern New Mexico project area had 66 surficial map units. The ages of the 66 map units were estimated and applied to archaeology, resulting in five geoarchaeologic map units that were related to buried-site potential.

However, the accuracy of the geoarchaeologic map is questionable. The primary weakness of the map is that it was based on the draft surficial geologic map. Remarkably, none of the 66 surficial units in the draft map had actually been dated. Many of the units were based on soils. In retrospect, the surficial geologic map was a poor choice as a base for the buried-site potential map.

Model of Buried-Site Potential—For the development of a region-wide archaeological sensitivity model, three buried-site potential maps were produced for all of southern New Mexico, using the State Soil Geographic dataset of 742 soil series along with Natural Resources Conservation Service soil descriptions (Heilen et al., 2013). The soils were categorized into five map units based on estimated ages for the soils, the five units ranging from very high to very low buried site potential.

A built-in error in using soil descriptions as an index to the age of surficial deposits is that soil ages are at best only relative, not absolute. The bottom line is that soil-based criteria do not provide archaeologically relevant ages for subsurface deposits, especially within the Holocene.

Buried-Site Potential Maps: Conclusion—Three different methods have been applied to the production of buried-site potential maps: (1) direct mapping, (2) surficial geology, and (3) soils. From these choices, we conclude that direct mapping of known, well-dated deposits produces the only promising buried-site potential maps.

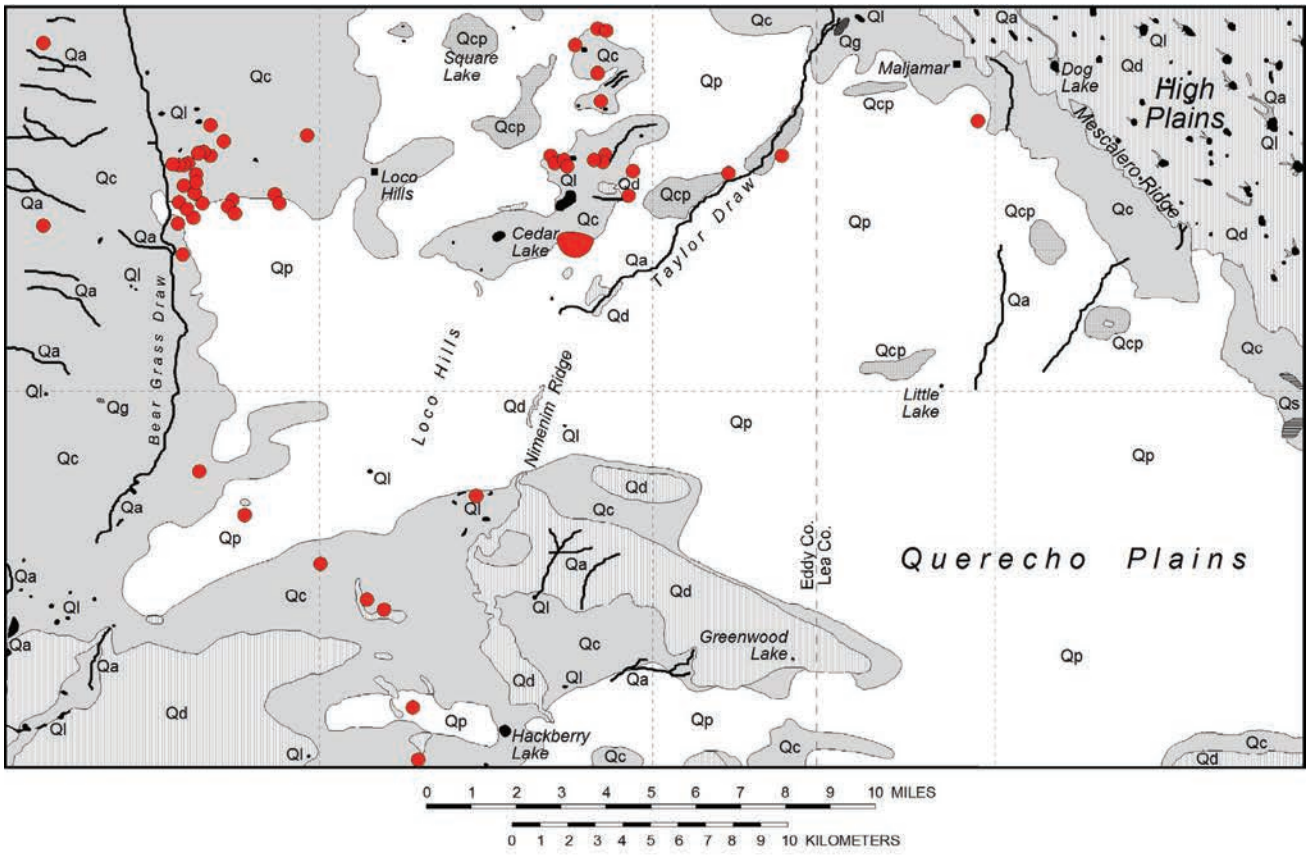

Archaeological Geologic Map of the Mescalero Sands Area, Southeastern New Mexico

by Stephen A. Hall

Excavated sites (Railey, Rissetto, Bandy, 2009)

Qc — **Coppice dunes (Historic)**; developed on Lower eolian sand and Berino paleosol (late Pleistocene); coppice dunes also developed on alluvial-colluvial sediments (late Pleistocene to Holocene) west of and adjacent to the High Plains escarpment (Mescalero Ridge); archaeological sites have high surface visibility and may be deflated and exposed between dunes.

Qp — **Parabolic dunes (Historic)**; developed on Upper, Holocene, and Late Holocene eolian sands; archaeological sites have low surface visibility and may be buried in the eolian sand.

Qcp — **Coppice dunes mixed with parabolic dunes (Historic)**; developed on Upper and Holocene-Late Holocene eolian sands; archaeological sites have low surface visibility and may be buried in the eolian sand.

Ql — **Lacustrine deposits (late Holocene)**; ponded slope-wash sediments in small depressions on the sand sheet and playa lacustrine deposits on the High Plains; archaeological sites may occur along the margins and shorelines of these depressions and playas.

Qa — **Alluvium (late Holocene)**; fluvial deposits along ephemeral streams across the sand sheet partly buried by eolian sand; alluvial and colluvial deposits along draws that drain into playa lakes on the High Plains; archaeological sites may be buried in the alluvium.

Qs — **Spring, cienega, and pond deposits (= Tahoka Formation, late Pleistocene)**; contain fossil mollusks and vertebrates; deposits are generally too old to have archaeological sites, although Paleoindian sites may be located near Qs outcrops.

Qg — **Alluvial gravels (Pleistocene)**; gravel deposits occur as low terraces along the High Plains escarpment; elsewhere gravels form a stone pavement on eroded surfaces; the gravels include clasts of Ogallala Caprock calcrete, chert, quartzite, and other rock types found at prehistoric sites on the sand sheet.

Qd — **Denuded surfaces**; formed on eroded Permian and Triassic rocks in the sand sheet area; denuded surfaces include the High Plains surface formed by eroded Caprock caliche (Pliocene-Pleistocene) at the top of the Ogallala Formation (Miocene-Pliocene); eroded surfaces may have a thin Holocene soil and sediment cover less than 0.5 m thick; archaeological sites may have high surface visibility but may be disturbed by erosion.

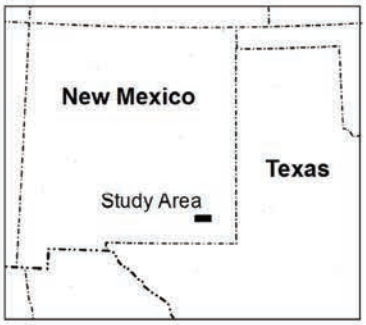

Figure 12.5. Archaeological geologic map of the Mescalero Sands area, southeastern New Mexico (modified from Hall and Goble, 2016g).

Anthrosols Versus Natural Soil A Horizons

An anthrosol is defined as "a soil that has been materially affected in its physical or chemical properties by human activities" (Neuendorf et al., 2005, p. 28). To expand on this definition, the best clues to the presence of an anthrosol are presented by Holliday (2004, p. 314):

> Anthrosols vary widely in their physical and chemical characteristics. Few traits are universal. There are several characteristics that are common or that serve as clues to soil significantly modified by human activity. The most obvious is the presence of archaeological debris within the soil—in particular, organic detritus such as bone and charcoal associated with middens. Other physical features typical of surface horizons include abrupt, smooth boundaries between horizons or layers; abrupt, laterally discontinuous layers; and dark matrix colors (low value and chroma) extending to greater-than-expected depths for natural soils…

The chemical signatures of anthrosols commonly involve organic matter and phosphorus. Anthrosols have "higher-than-expected values of organic matter relative to natural soils" (Holliday, 2004, p. 314). Holliday (2004, p. 306) also discusses phosphorus:

> All soil phosphorus derives from the weathering of phosphate minerals, especially apatite [$Ca_5(PO_4)_3(F, Cl, OH)$], in soil parent material…The phosphorus then cycles from soil to plants to animals and back to soil, or it is lost by leaching. Human activity that disrupts these cycles leads to losses or gains in phosphorus relative to the P content of the local natural soils. Most geoarchaeological research on P deals with these losses and gains. In particular, because human activity imparts so much more P to soils than is usually found naturally, and because of low solubility and relative stability and persistence of P, most archaeologically oriented P studies focus on gains in P as clues to site locations or on intrasite variability in P content as clues to site use.

In a summary of the above discussions by Holliday, and amended by us to fit the semi-arid Mescalero Plain, an anthrosol should have *all* of the following characteristics; these characteristics should be in sharp contrast compared when compared to the A horizons of the Eddy and Loco Hills paleosols (Hall and Goble, 2016g):

- presence of many archaeological materials, including abundant charcoal, throughout
- very dark color
- abrupt boundaries between layers
- thicker-deeper extent than local natural soils
- lateral extent discontinuous
- high amounts of organic matter
- high amounts of phosphorus

The only item on the above list of characteristics that we have observed and is noteworthy at various archaeological sites concerns soil thickness. A horizon thickness alone, however, is not a reliable index to the presence of an anthrosol. Whether cultural activity has resulted in a thick A horizon is difficult to ascertain. Overall, our studies of the Eddy paleosol A horizon indicate that its thickness, which can be considerable, is natural, not cultural, in origin.

Soil Phosphorus

We investigated the total phosphorus (P_t) content at two sites that at the time we mistakenly thought might have an anthrosol. Laboratory analyses of sediment columns from both sites showed the same P_t content throughout the site-related zone as well as the non-cultural eolian sand below. We conclude from all evidence that the one site (Loc. 9) situation was simply a site footprint with an Eddy paleosol influence, even though disturbed, and that the other site (Loc. 18) was the Eddy paleosol but without disturbance (Figs. 12.6, 12.7). In both cases, the P_t content was not significantly higher in sand where archaeological remains were present, supporting the interpretation that the dark-colored sands were not anthrosols.

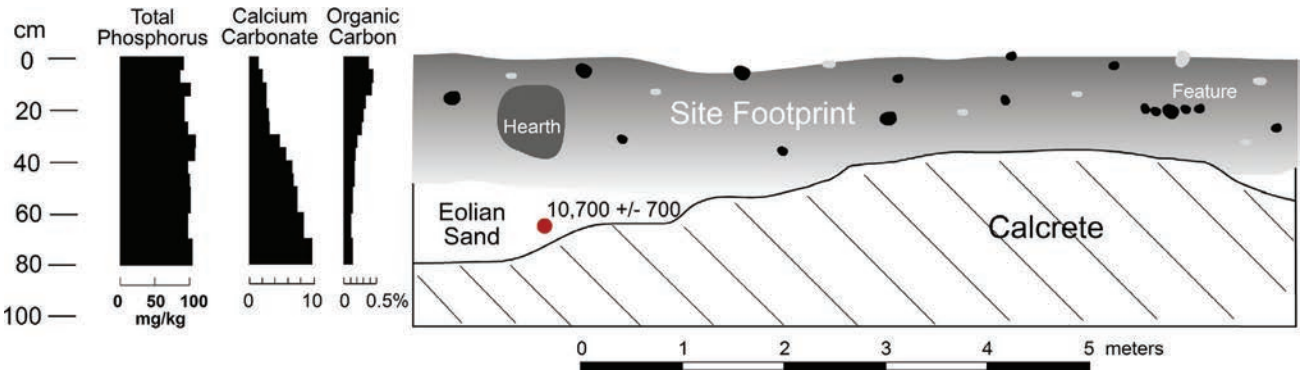

Figure 12.6. Total phosphorus and organic carbon content of the site footprint at Loc. 9, Eddy County; the mean P_t content is 98.5 ± 6.8 (1 σ) mg/kg (Milwaukee Soil Laboratory, Milwaukee, Wisconsin); photograph of the that forms the basis of the above sketch is shown in Fig. 12.9.

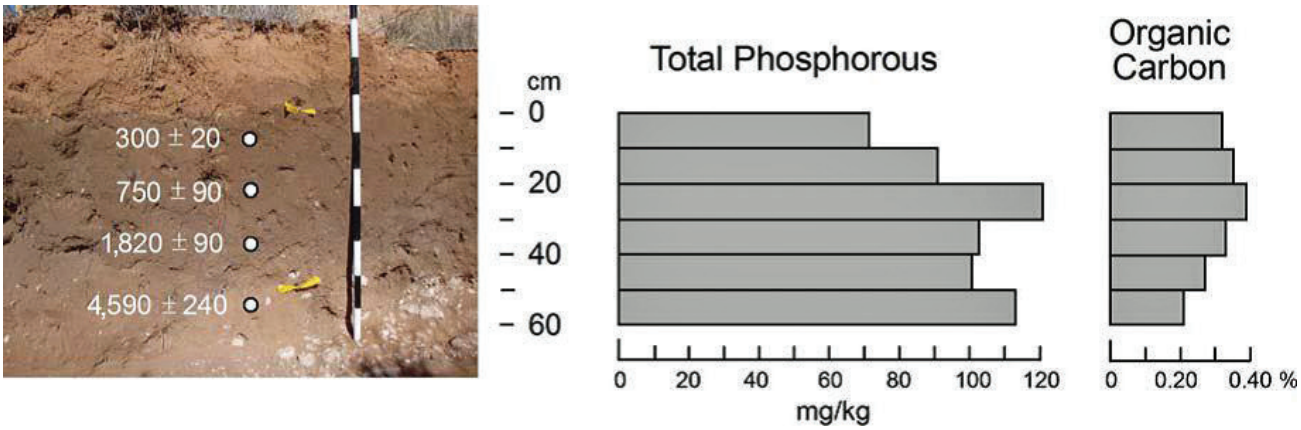

Figure 12.7. Total phosphorus and organic carbon of the Eddy paleosol at Loc. 18, Eddy County; the mean P_t content is 99.5 ± 17.6 (1 σ) mg/kg; photograph of the above in Figs. 9.4, 9.5.

Boot Hill Anthrosol

The A horizon soil at the Boot Hill site (near Loc. 37) is without question an anthrosol (Fig. 12.8). All of the seven attributes of an anthrosol, except phosphorus, which was not analyzed, are found at Boot Hill (Brown, 2011). The site is predominantly Early to Late Formative, based on ceramics and radiocarbon dates. More than 4,500 lithic artifacts and 1,620 vertebrate faunal remains were recovered during site testing; three juvenile and one adult burial were reported by previous workers at the site. As many as 450 artifacts were found in one excavation unit (1 m²).

The color of the anthrosol is very dark gray (7.5YR 3/1). It is interbedded with non-cultural sediment with sharp contacts; in one place the anthrosol and interbedded layers are 80 cm thick. The lateral extent of the anthrosol is discontinuous at the site; in some areas of the site the anthrosol is absent where it did not form. The organic matter content of the anthrosol ranges from 2.4 to 3.9% (Brown, 2011) compared with less than 0.5% from non-anthrosol A horizons in the region. The well-documented anthrosol at the Boot Hill site serves as a case study that clarifies the distinction between anthrosols and non-cultural A horizons in our semi-arid region.

Site Footprint

We define the footprint of an archaeological site as "a layer or zone of sediment in which the original physical and chemical properties have been changed by human activities" (Hall and Goble, 2016g, p. 93). During the formation of an archaeological site, the pre-site deposits are disturbed and their

sedimentologic and stratigraphic characteristics are lost (Fig. 12.9). A site footprint may include an anthrosol where a site has been strongly occupied for extended periods of time. In conjecture, once a site is abandoned, the development of a naturally occurring soil A horizon may introduce an element of complexity into the stratigraphic record, although we have not seen a clear example of this in our extensive investigations in the region.

OSL dating of site footprints has not been systematically pursued by us in the Mescalero Plain. In nearly all cases, the age of an archaeological site can be determined best by AMS radiocarbon dating of the remains of annual plants associated with cultural activity at the site. The disturbed sediment of a site footprint may yield mixed OSL ages of little value for site geochronology.

Bear Grass Draw

Four OSL samples were taken by the late geomorphologist Dr. David Kuehn, one each from a soil A horizon (the Loco Hill paleosol) that was buried by coppice dunes at four separate archaeological sites near Bear Grass Draw west of Loco Hills (Loc. 39, this bulletin). AMS radiocarbon samples from the dune-buried A horizon were also dated. The goal was to date the A horizon and to compare the results from OSL and radiocarbon dating methods. The radiocarbon ages range from 1,360 ± 40 to 890 ± 40 ^{14}C years BP, verifying the Early and Late Formative archaeology (Condon et al., 2008).

The OSL samples were analyzed by the University of Georgia laboratory and showed partial bleaching, yielding a wide range in ages that indicated sediment mixing. The maximum ages ranged from 12.8 ± 2.3 ka to 3.0 ± 0.3 ka (Condon et al., 2008). According to the accompanying stratigraphy, the soil A horizon appears to have formed on the Lower eolian sand unit that has been OSL dated 90 to 50 ka (Hall and Goble, 2006, 2012, 2016g). The OSL ages were much older than the AMS ages from the same soil A horizon, a situation to be expected especially where Pleistocene and younger sediments are mixed. The OSL and AMS data are in the Condon et al. (2008) report and are not included in this bulletin.

Figure 12.8. County road cut showing the dark-colored anthrosol at the Boot Hill site, northeast Eddy County; creosote bushes for scale; photograph February, 2016.

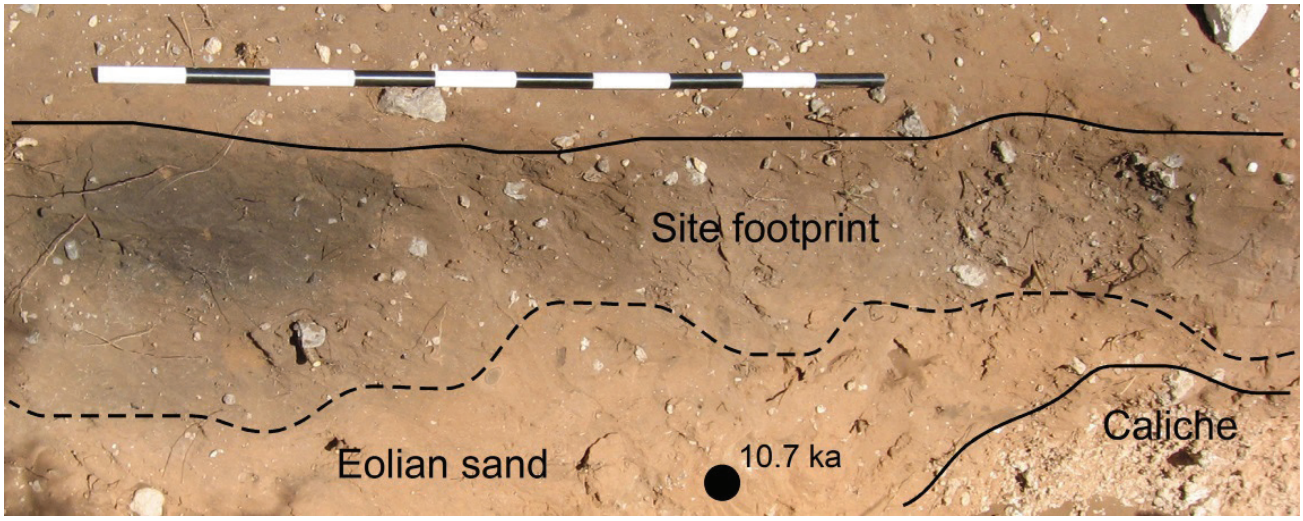

Figure 12.9. Site footprint at Loc. 9; archaeology is Late Archaic and Early Formative. The OSL age of the underlying eolian sand is 10,700 ± 700 years and correlates with the Upper eolian sand unit documented elsewhere at this site; the total phosphorus content of this section is previously shown in Fig. 12.6; 1-m scale.

Tamarisk Flat

A Paleoindian point was recovered from 18-cm depth at a site with radiocarbon ages indicating Early Archaic and Late Archaic to Formative archaeology (Loc. 29). The question concerned whether the point occurred in a pillar of Paleoindian-age sediment or if the point had been brought to the site. An OSL sample was taken at the same level as the point and dated 3,710 ± 300 years (Fig. 12.10); laboratory analysis indicates that the sediment was not mixed. Thus, it was concluded that the point had been brought to the site during post-Paleoindian time and did not represent a Paleoindian occupation (Hall and Goble, 2016a).

Calcrete at Prehistoric Sites

The dense calcrete that occurs beneath the eolian sands of the Mescalero sand sheet is susceptible to solution and may have pits and depressions at its surface that have the potential to temporarily store water for brief periods after a rainstorm, although undocumented (Fig. 12.11).

Solution Pipes in Calcrete

A solution pipe is "a vertical cylindrical hole, formed by solution and often without surface expression, that is filled with detrital matter" (Neuendorf et al., 2005, p. 613). The pipe begins as a fracture in a carbonate or gypsiferous rock. Rainwater infiltrates the soil, moves through the fracture, and slowly dissolves the rock. With the passage of time, the fracture is widened, forming the pipe, and soil and other materials fill the void.

Solution pipes are generally small in southeastern New Mexico, especially where the caliche is thin and friable. However, thick, dense calcrete occurs in some areas of the plain and has the potential for the development of comparatively large solution features (Fig. 12.12).

Mimosa Ridge

A large solution pipe with cultural significance was discovered by Monica Murrell in the floor of a trench that had been cut through eolian sand down to calcrete on Mimosa Ridge (Loc. 15) (Fig. 12.13). The width of the pipe is about 36 cm; the depth of the artifact-bearing brown sand is about 100 cm below the top edge of the pipe. The Pleistocene red sand (Middle eolian sand unit dated 24 ka at this locality) is at least 40 cm thick below the contact with brown sand and covers the base of the pipe. The pipe extends laterally at least one meter beyond the opening.

Figure 12.10. Late Holocene OSL age of sand associated with Paleoindian point at Loc. 29, Tamarisk Flat, verifying that the point was brought to the site by prehistoric occupants; 1-m scale. The site is Early Archaic and Late Archaic to Early Formative based on 14 AMS ages (Hall and Goble, 2016a).

Figure 12.11. Oblique view of an excavation revealing dense calcrete underlying the thin Eddy paleosol at Loc. 21; the surface of the calcrete has solution-formed depressions. Below the 1-m scale, the Eddy paleosol and pre-paleosol eolian sand fill a 60-cm deep depression, indicating that the depression was filling in before this site was occupied.

The artifacts recovered from the pipe include lithic debris, a ground stone fragment, a polishing stone, two sherds, and a large quantity of ochre; the site is Formative (Heilen and Merrell, 2015). Apparently, the natural Holocene-age sand fill in the pipe had been cleaned out by the site occupants. The pipe later became filled with brown sand and cultural debris. The calcrete walls of the pipe appear natural and have not been modified. The pipe is sufficiently large to accommodate a person. In reality, the pipe is a small cave. This is the only known case in the region of a solution pipe that was used for some purpose in prehistoric times.

Figure 12.12. Large solution feature in calcrete at Loc. 9 along NM 128. Upon excavation the feature was found to be circular, about 5.2 m by 5.0 m, and 0.85 m deep. It is natural in origin and does not appear to have been modified prehistorically. However, associated with the feature is a cache of calcrete cobbles (site Feature #44) that apparently were stockpiled next to the solution pipe and were buried by eolian sand (Wiseman, 2016).

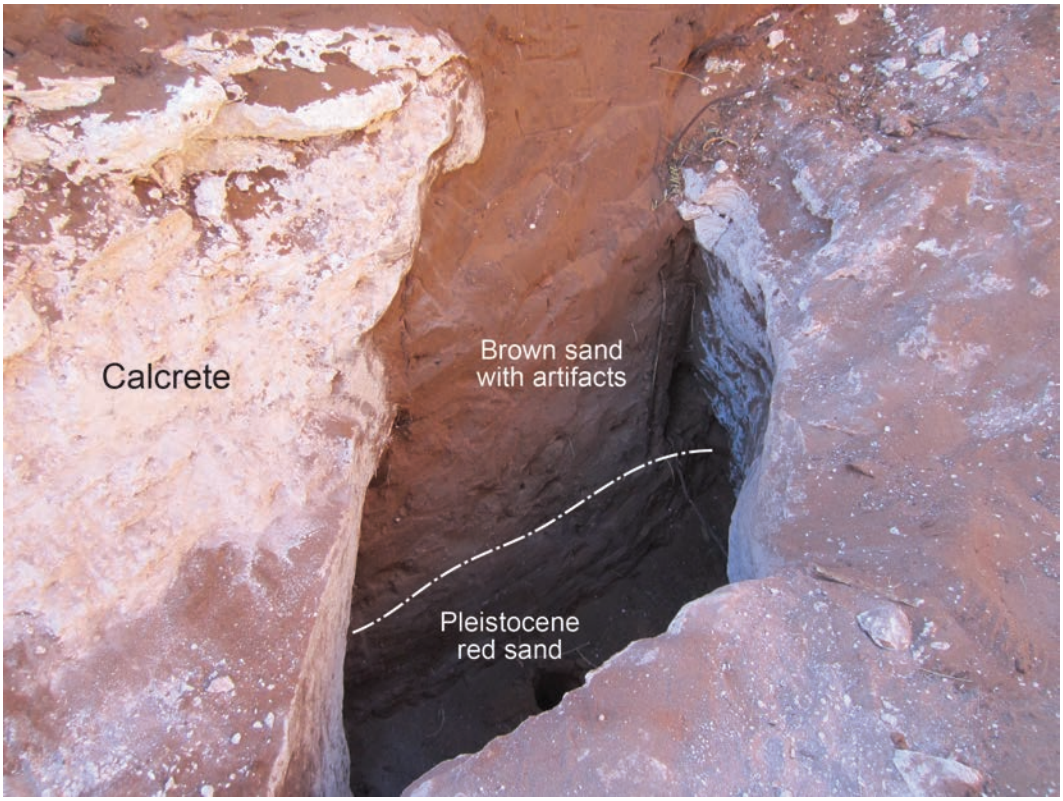

Figure 12.13. Solution pipe in calcrete on Mimosa Ridge, Eddy County, Loc. 15. The width of the pipe opening is about 36 cm. The artifact-bearing brown sand extends vertically about 100 cm and directly overlies Pleistocene-age red sand. The red sand extends an additional 40 cm to the base of the pipe. The pipe extends laterally more than 1 m to the right under the bottom edge of the opening shown in this view (Hall and Goble, 2015a).

XIII. PALEOENVIRONMENTS OF SOUTHEASTERN NEW MEXICO

Late Quaternary paleoenvironmental reconstructions fall into patterns of broad geographic regions of sub-continent scale. The paleoclimatic and paleoenvironmental history of southeastern New Mexico is the same as the rest of the American Southwest, with strong affinities to the southern Great Plains and Great Basin (Hall, 2018; Fig. 13.1; Table 13.1 of this bulletin). Broad scales of eolian geomorphic change are evident on the Mescalero Plain, although the local paleoenvironmental record is quite sparse.

Speleothems from the Carlsbad Cavern Area

A speleothem is broadly defined as any secondary mineral deposit in a cave, such as stalactites, stalagmites, and flowstone. A large complex of caves in the Carlsbad Cavern area of the Guadalupe Mountains, New Mexico and Texas, have fostered a number of speleothem studies. Most speleothems in the Southwest stopped forming at the end of the Younger Dryas when regional climate shifted from cool-wet conditions of the Pleistocene to a warm-dry Holocene climate. Nearly all of the stalactites and stalagmites one sees at Carlsbad Cavern are Pleistocene in age and are no longer forming today. Nevertheless, three records of Holocene stalagmites have been discovered and studied and are reviewed below.

Pink Panther Cave

This is the only speleothem record in the Southwest that spans the entire Holocene. The 14-cm-long sample from a stalagmite is dated 12,330 years to present and was analyzed for $\delta^{18}O$ content. Unfortunately, "the time series of $\delta^{18}O$ does not show a clear trend through the Holocene, but displays rapid variations of (a few per mil) on millennial and centennial time scales" (Asmerom et al., 2007, p. 1).

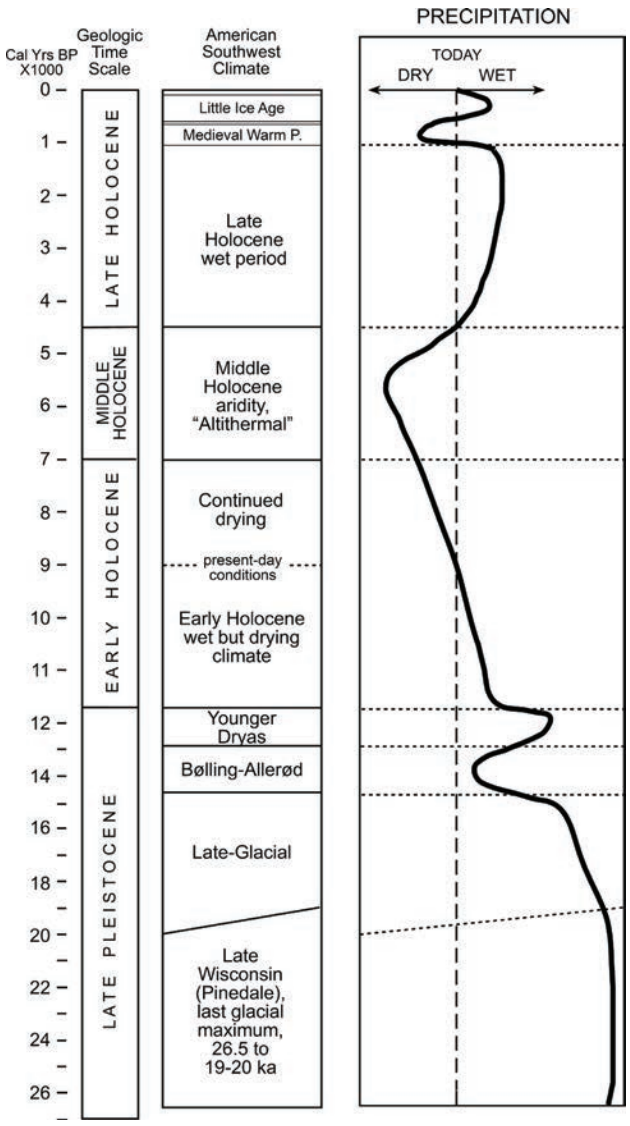

Figure 13.1. Summary paleoclimate diagram for the past 26,500 years from the American Southwest; scale change at 12 ka. The inverse relationship (not shown here) of precipitation and temperature values (cool-wet, warm-dry) follows modern-day southwestern climate and is well documented with Late Pleistocene and Middle Holocene empirical records. The diagram is modified from S.A. Hall, 2018, Paleoenvironments of the American Southwest, *in* Bradley Vierra, B.J., ed., The Archaic Southwest: Foragers in an Arid Land: Salt Lake City, University of Utah Press, p. 16-28; reproduced with permission from University of Utah Press.

Although the authors suggest a few wet and dry episodes based on peaks in the $\delta^{18}O$ record, they concede that "We…attribute the great majority of the observed variability in PP-1 [Pink Panther Cave] to be due to changes in the isotopic composition of rainfall through time" (Asmerom et al., 2007, p. 2).

A regional study in central Texas similarly concluded that cave $\delta^{18}O$ records are primarily related to sources of moisture, such as the proportion of Gulf of Mexico- or Pacific Ocean-derived moisture, and are not linked to amounts of precipitation (Wong et al., 2015). Unfortunately, in consideration of these results, the $\delta^{18}O$ record from Pink Panther Cave contains little, if any, useful paleoenvironmental information.

Hidden Cave: Mites and Stalagmites

Hidden Cave occurs about 31 km (19 mi.) southwest of Carlsbad Cavern and has yielded some interesting paleoenvironmental information. Well-preserved fossil mites were discovered in two late Holocene stalagmites in the cave (Polyak et al., 2001). The remains of twelve different genera/species of mites in the stalagmites represent a widely occurring fauna. Three of the mites are today found farther north in the United States and Canada, indicating cooler conditions at the time they lived in the cave. None of the three seem to inhabit the cave area today, although the authors admit that "little work has been done on the mite fauna in New Mexico" (Polyak et al. 2001, p. 645). Wetter conditions are supported by the presence of the speleothem itself.

Table 13.1. Summary of paleoenvironmental records from the American Southwest*

Period	Age	Paleoenvironments
Little Ice Age	A.D. 1350–1850; 600–100 cal yr BP; worldwide but with regional variability in timing and intensity	Cool and wet; speleothem growth A.D. 1560–1710; Neoglaciation in Colorado A.D. 1630–1850; channel filling and some floodplain deposition in small alluvial valleys; documented by tree-rings; does not show up in vegetation records
Medieval Warm Period[1]	A.D. 900–1300; 1050–650 cal yr BP; northern hemisphere	Warm and dry; documented by tree-rings and one speleothem record; regional arroyo cutting in alluvial valleys; does not show up in vegetation records; mixed signals for El Niño
Late Holocene wet period	4500–1000 cal yr BP	Cooler and wetter than today; aggradation of stream valleys; formation of cumulic Mollisols on floodplains and eolian sands; renewed speleothem growth; Audubon Neoglaciation in Colorado; rejuvenated springs; sagebrush steppe and pinyon pine woodland expand on Colorado Plateau; expansion of woody shrubs in deserts; increased El Niño frequency
Middle Holocene aridity	7000–4500 cal yr BP	Hot and dry; Antevs' Altithermal; pluvial lakes and alpine ponds dry up; most spring flow ceases; arroyo cutting in many valleys; previous sagebrush steppe replaced by desert grassland; soils become more alkaline; salt-tolerant shrubs invade grasslands; lunette dunes form downwind from dry playa basins; forests reach highest elevation in mountains, diminished alpine tundra, pinyon pines expand their range; El Niño frequency greatly lowered
Early Holocene	11,700–7000 cal yr BP	Rapid warming at end of Younger Dryas; begins cool and wet and becomes warm and dry; most speleothem growth ceases; sagebrush steppe diminishes in southern areas; escarpment trees die off in southern deserts; ponderosa pine and oak expand on lower montane slopes; progressive decrease in spring flow and wet meadow formation; argillic soils that formed previously across the region begin to erode with warmer climate; El Niño frequency decreases after 9 ka
Younger Dryas[2]	12,900–11,700 cal yr BP, mostly northern hemisphere	Cold and wet although less-so than full-glacial climate; peak spring-flow, wet meadow-black mat formation; glaciation in Sierra Nevada but not yet documented in SW mountains; speleothem growth; sagebrush steppe persists across plains, basins, plateaus
Bølling-Allerød Interstadial[2]	14,700–12,900 cal yr BP	Warmer and drier than full-glacial but cooler and wetter than today; speleothem growth; sagebrush steppe vegetation
Late Glacial	19-20,000–14,700 cal yr BP	Less cold; deglaciation in Northern Hemisphere beginning 20 ka to 19 ka[3]
Full Glacial, last glacial maximum[3]	26,500–19-20,000 cal yr BP, worldwide	Cold and wet; major alpine glaciation on SW peaks above 12,000 feet; river channels wide with gravel bed load; speleothem growth; argillic soil development; sagebrush steppe across plains, basins, plateaus; isolated pine-oak-juniper trees on Chihuahuan and Sonoran desert escarpments

* Reproduced and modified from Hall, 2018, p. 21; permission for the use of this table is given by the University of Utah Press and is gratefully acknowledged; (*1*) Cook et al., 2004; (*2*) Steffensen et al., 2008; (*3*) Clark et al., 2009.

All of the mites, including the three forms of paleoclimatic interest, were recovered from stalagmite F2 (#89037), which has U/Th-series ages extending from 3,135 ± 90 to 887 ± 144 years ago. One of the mites from F2 was also found in the other stalagmite F1 (#89029), dated 3,171 ± 48 to 819 ± 82 years ago. These results indicate that the climate 3,200 to 800 years ago was wetter and cooler than today, supporting other paleoenvironmental records from the Southwest and southern Great Plains (Polyak et al., 2001).

Carlsbad Cavern

Polyak and Asmerom (2001) reported a paleoclimatic history for the Southwest that they correlated with the beginning of corn and cotton agriculture and changes in settlement patterns and pueblo abandonment. They based their interpretations on thicknesses of annual growth bands in several stalagmites, especially stalagmite BC2 from Carlsbad Cavern and #89037 from Hidden Cave. Band thickness was correlated with precipitation levels: thick bands were equated with wet years, and thin bands with dry years, similar to reconstructions from tree-rings. Although they indicated that the sequence extended to ca. 4,000 years ago, the primary record from BC2 stalagmite is dated 2,796 ± 88 to 835 ± 25 years BP with additional bands dated 432 ± 13 to 236 ± 50 years BP (Polyak and Asmerom, 2001).

The Polyak and Asmerom (2001) paper has been strongly criticized (Betancourt et al., 2002). A 270-year stalagmite BC2 series (A.D. 1570–1839) was run against southwestern tree-ring records and found to have no annual or seasonal correlation whatsoever. Several possible explanations were suggested to account for the lack of correspondence between stalagmite and tree-ring records. (1) The stalagmite bands are not annual. (2) The thicknesses of bands are formed by different climate variables than seen in tree-rings. (3) The U/Th-series dates from the stalagmites are off. (4) Finally, "Groundwater travel times may impose variable time lags of years to decades between a season's worth of precipitation and speleothem deposition…" (Betancourt et al., 2002, p. 199). All of these possible explanations have merit.

Hidden Cave and Carlsbad Cavern, Revisited

Subsequently, in response to the Betancourt et al. criticism, an actively growing stalagmite was collected from Carlsbad Cavern and compared with local tree-ring and weather records for the period A.D. 1939 to 2002. Thick-thin stalagmite band width corresponded to wet-dry precipitation records better (r^2 = 0.20) than the correlation of tree-rings to precipitation (r^2 = 0.068) (Rasmussen et al., 2006), it was concluded, although the statistical correlation is weak. Tree-ring records from the Guadalupe Mountains were also compared with BC2 data back to A.D. 1700.

Encouraged by the more or less positive results from local tree-ring and weather records, band-width analyses were expanded with a new assessment of the Hidden Cave (HC1) and Carlsbad Cavern (BC2) records, including a revised chronology for BC2, which differs from the earlier paper by Polyak and Asmerom (2001) (Rasmussen et al., 2006).

The resulting paleoclimate record is somewhat uncertain, however, because the two stalagmite series do not correlate with each other. Specifically, the Hidden Cave and Carlsbad Cavern stalagmites both incorporate periods of growth and no-growth (hiatuses), but these periods do not occur at the same time in the two different sequences (Fig. 13.2). The lack of agreement calls into question whether either of the two records can be regarded as representative of local climatic history. The dissimilarity of the records is puzzling but may simply reflect differences in local groundwater conditions surrounding the two separate caves systems. Regardless of the cause, it seems clear that Carlsbad-area speleothems have yet to provide reliable, consistent evidence for late Holocene climates in this region. Also, the correlation of speleothem band width and climate, and their relationship to prehistoric cultural events, in light of the above uncertainties, appears weak.

Pollen Analysis and Vegetation Reconstruction

Pollen grains are poorly preserved in the semi-arid environment of the Mescalero Plain. Even though we know that pollen grains are abundant in the atmosphere and are dispersed by winds and deposited on the modern surface throughout all regions, once pollen grains are incorporated in dry-land sediments, they begin to deteriorate. Eventually, the grains are completely lost because of the processes of degradation, resulting in pollen-barren sediments.

Over the years, attempts to recover pollen from Holocene sediments in southeastern New Mexico have largely failed. Pollen is simply not present in the eolian deposits because of post-depositional pollen grain deterioration, a phenomenon that has been noted in other sediments throughout the region (Hall, 1995).

Only one pollen analytical record from the Mescalero Plain provides useful information on past vegetation. North of Salt Lake at Loc. 10, a trench through alluvium in a small unnamed wash revealed the presence of a thick deposit of fine-textured alluvial sediment. It was radiocarbon dated 3,100 to 500 years BP and found to contain moderately preserved pollen. Pollen analysis produced assemblages dominated by Chenopodiineae, *Ambrosia, Aster*, and Poaceae (Fig. 13.3) (Hall and Goble, 2016a). By comparison, associated modern surface pollen percentages are quite different, reflecting a shift in late historic vegetation, even though the same pollen taxa predominate. The prehistoric alluvial pollen record is similar throughout, indicating no significant trends or changes in local vegetation during the past 3,000 years.

Overall, it appears that the late Holocene vegetation of southeastern New Mexico has been shrub grassland for the period between 3.1 and 0.5 ka. We do not have pollen records from the early

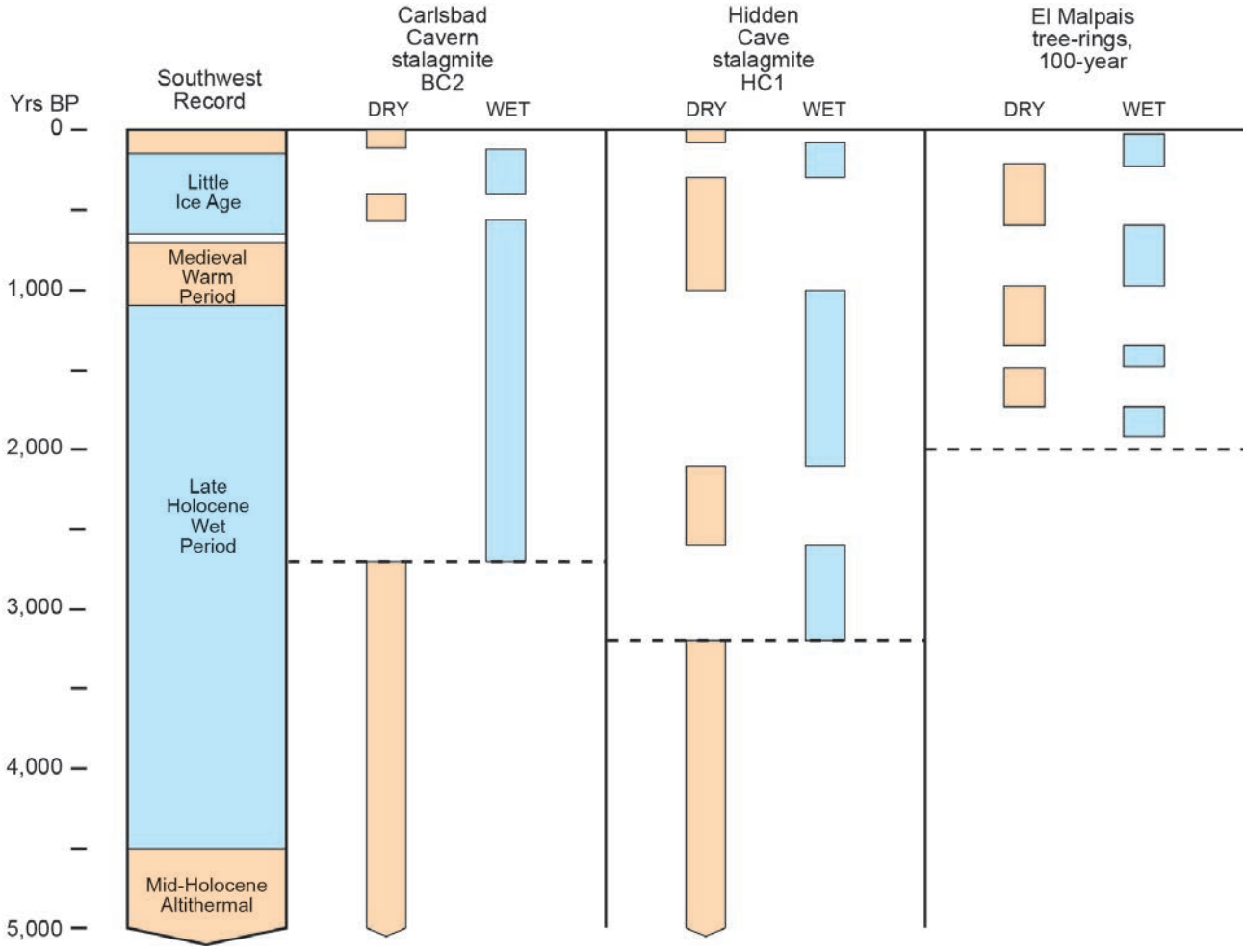

Figure 13.2. Stalagmite records from Carlsbad Cavern and Hidden Cave, Guadalupe Mountains, Eddy County, New Mexico, showing wet periods of speleothem growth (blue) and dry periods or hiatuses (yellow) in the speleothem records (Rasmussen et al., 2006). The El Malpais tree-ring record, Cibola County, New Mexico, is also shown as wet-dry periods with 100-year running averages (Grissino-Mayer, 1966). The dashed lines are as far back as the records go. Prior to 3,200 years BP at Hidden Cave and 2,700 years BP at Carlsbad Cavern, the climate was too dry for speleothem growth; the El Malpais tree-ring record ended about 2,000 years BP; the Southwest paleoclimate record is from Hall (2018).

and middle Holocene; deposits are well known, but they do not contain pollen. Glacial-age pollen records elsewhere indicate that the non-alpine Late Wisconsin vegetation in the region was sagebrush grassland (Hall and Valastro, 1995; Hall, 2001, 2005; Hall and Riskind, 2010).

Stable Carbon Isotopes

A side benefit of radiocarbon dating is the stable carbon isotope value ($\delta^{13}C$) that accompanies each date. When radiocarbon dating is applied to bulk sediment, the $\delta^{13}C$ value indicates whether the organic carbon is from a C_3- or C_4-dominated plant community; C_3 plants are woody species such as trees and shrubs, while C_4 plants are mostly grasses. Woody species have $\delta^{13}C$ values that are less (more negative) than -19.0 ‰; grasses have $\delta^{13}C$ values greater (less negative) than -19.0 ‰ (O'Leary, 1988).

Discussed elsewhere, the AMS radiocarbon dates are from soil humates that coat sand grains and specifically exclude charcoal or other solid particles in the AMS dating process. Also, the reader should note that if $\delta^{13}C$ values are to be used as an index to vegetation, the $\delta^{13}C$ content must be determined directly from the soil material itself, avoiding fractionation effects from AMS laboratory-induced sources. The AMS radiocarbon dates in our studies are by Beta Analytic, Inc.; the $\delta^{13}C$ values they provided have been measured separately by their isotope ratio mass spectrometer (IRMS) (see chapter 2).

Forty-seven $\delta^{13}C$ values from the Eddy and Loco Hills paleosols and their accompanying AMS dates are plotted below (Figs. 13.4, 13.5). The collective $\delta^{13}C$ values indicate a mix of shrub-grass and grass-shrub vegetation across the Mescalero Plain during the past 2,000 years.

However, at least one case study with four data points denotes a trend in local conditions across the region. Locality 35 at the eastern edge of the Mescalero Plains is characterized by high $\delta^{13}C$ (low negative) values indicating grass-dominated vegetation. After 1300 A.D., however, $\delta^{13}C$ values indicate greater amounts of shrubs. Another situation occurs at Locality 31 in southern Lea County where low $\delta^{13}C$ (high negative) values indicate shrub-dominated vegetation. With younger ages, the trend in $\delta^{13}C$ values indicates an increased dominance of local shrubs in the already shrubby landscape.

Two cases of alluvial records, localities 10 and 32, have high $\delta^{13}C$ values, indicating grass-dominated vegetation (Fig. 13.5). Locality 32, west of the Pecos River along Red Bluff Draw, shows continuing grassy vegetation from 7.52 to 0.74 ka. Carbon isotopes from the Eddy paleosol along Owl Draw (Loc. 34) also indicate grass-dominated vegetation during the past 1,000 years (Fig. 13.4).

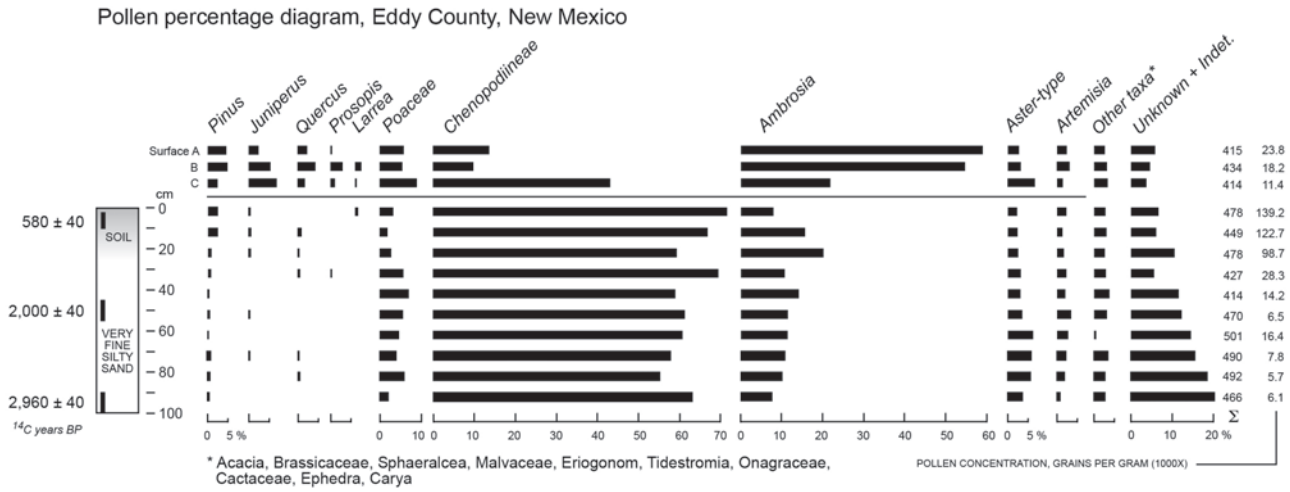

Figure 13.3. Pollen diagram from fine-textured alluvium at Loc. 10 dated about 3,100 to 500 years BP (pollen analysis by S.A. Hall; modified from Hall and Goble, 2016a). The steady decline in pollen concentration and the increase in the unknown-indeterminate category with greater depth are products of greater deterioration and loss of pollen grains with increasing depth (and time) in the sediment column.

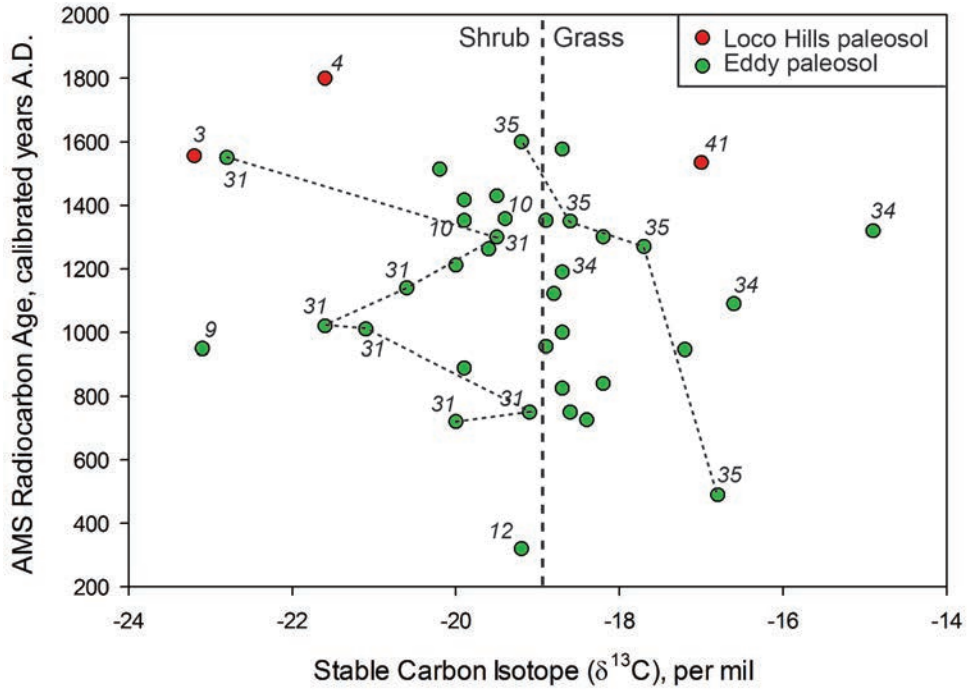

Figure 13.4. Stable carbon isotope values from the A horizons of the Eddy paleosol (35 values) and Loco Hills paleosol (3 values); some values have localities listed; the dashed lines connect 2 particular sample records (31 and 35); Fig. 9.11 is a map with study localities of the Eddy and Loco Hills paleosols; data from Appendix B.

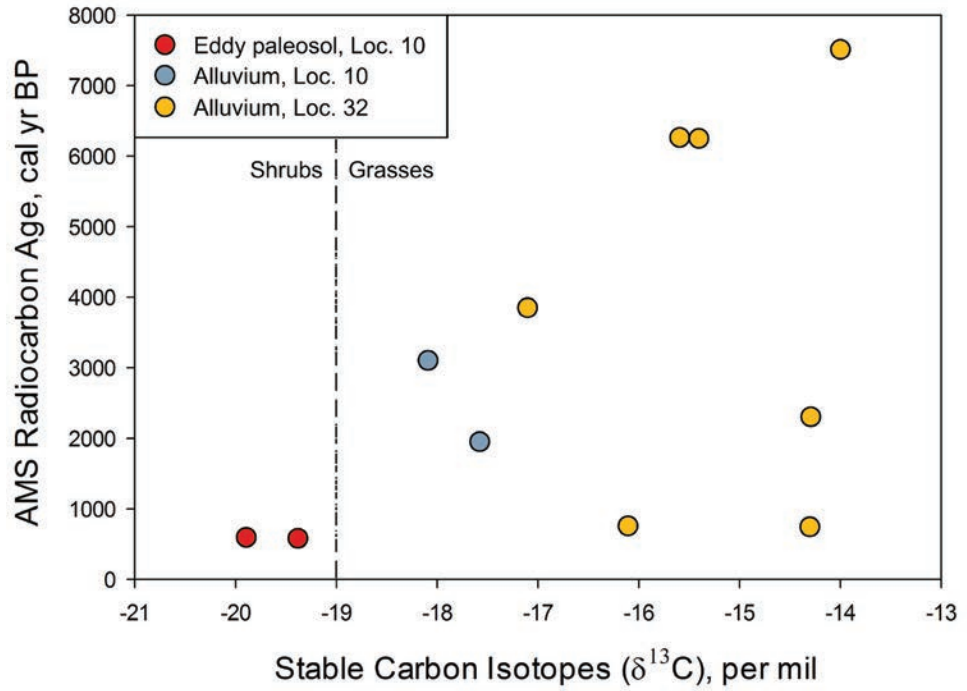

Figure 13.5. Stable carbon isotope values from alluvium (7.52 to 0.74 ka) and associated Eddy paleosol (0.60 and 0.59 ka), Locs. 10 and 32; all values represent grass-dominated vegetation (> -19.0 ‰) prior to shift to shrub-dominated vegetation by 600 cal yr BP in the Eddy paleosol; data from Appendix B.

The alluvial $\delta^{13}C$ record at Locality 10 along Highway 128 north of Salt Basin indicates grass-dominated vegetation at 3.11 and 1.96 ka (Fig. 13.5). In the same stratigraphic section, carbon isotopes from the Eddy paleosol indicate shrubby vegetation, 0.60 and 0.59 ka. The possible trend from grass- to shrub-dominated vegetation may be a shift only in local plant communities instead of a region-wide change.

Molluscan Faunas from the Mescalero Plain

In a broad view, two separate faunas of fossil mollusks occur in southeastern New Mexico. One is late Pleistocene in age and reflects the cool, wet climate of the times. Although undated, a possible Late Wisconsinan fauna of eighteen species of terrestrial and freshwater snails and pill clams has been described from Nash Draw (Ashbaugh and Metcalf, 1986). Remains of *Equus* and *Camelops* also occur with the mollusks (Table 13.2). Shells from another locality with a late Pleistocene fauna (Loc. 40) have been AMS dated 18,900 ± 100 ^{14}C years BP (22,760 cal yr BP) (Table 13.2).

At the end of the Pleistocene, the climate became warmer and drier, resulting in a die-off of the local Wisconsinan mollusks. They were replaced by a small, modest fauna of at least four terrestrial snails that are adapted to the semi-arid conditions across the Mescalero Plain during the Holocene (Tables 13.2, 13.3, Fig. 13.6). This fauna has been found in late Holocene alluvium in three separate studies in the region (Locs. 10, 26, 28) that includes the Pecos River. Overall, the fauna may represent the slightly cooler-wetter conditions during late Holocene time, although these species are not abundant in the modern environment of today.

Paleoenvironmental Summary

While the paleoclimatic record from the American Southwest applies to southeastern New Mexico, the paleoenvironmental information derived directly from the Mescalero Plain is meager. The few existing records are summarized below.

- The vegetation has been a mixed grassland and shrub-grassland during the past 3,000 years, as indicated by pollen analysis.
- Carbon isotopes from the Eddy paleosol and alluvium indicate a mixed grass-shrub and shrub-grass vegetation across the Mescalero Plains during the Holocene. Some case studies suggest a shift to greater amounts of shrubs in the local vegetation during the latest Holocene.
- Carbon isotopes from alluvium and the Eddy paleosol west of the Pecos River indicate the continued presence of a grass-dominated vegetation in that region since 7.52 ka.
- A land snail fauna from late Holocene alluvium is composed of four species that is typical of the semi-arid region. However, greater abundance of the snails in the past may indicate slightly less arid environmental conditions than found today.
- Alternating wet and dry periods characterize the Hidden Cave and Carlsbad Cavern speleothem records during the past 3,200 years. However, the records from the two different caves do not match each other.
- Fossil mites in a Carlsbad Cavern-area speleothem may indicate cooler conditions during the late Holocene; the occurrence of the speleothem itself indicates a wet climate.

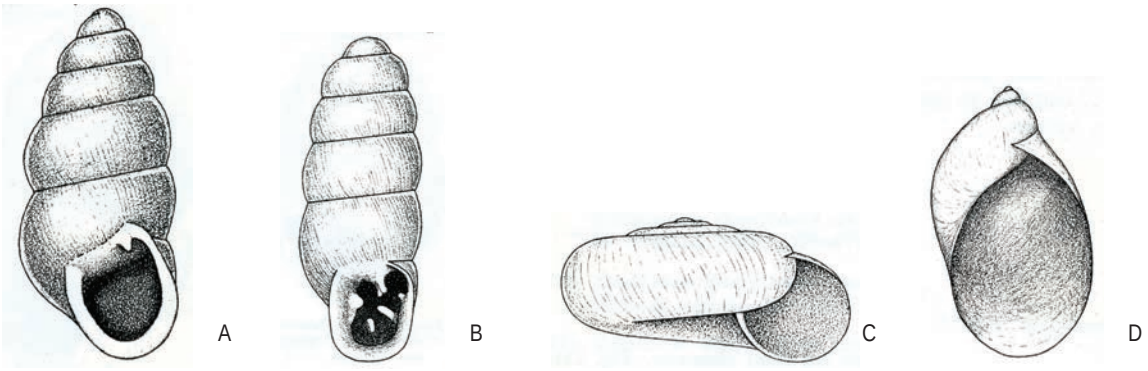

Figure 13.6. Snail species from late Holocene alluvial deposits in southeastern New Mexico: A, *Pupoides albilabris* (length 4.2–5 mm); B, *Gastrocopta pellucida* (length 1.7–2.6 mm); C, *Hawaiia minuscula* (width 2–2.8 mm); D, *Succinia ovalis* (length 6–26 mm); from Burch (1962).

Table 13.2. Late Quaternary molluscan faunas reported from the Mescalero Plain, New Mexico

Species	Late Pleistocene			Late Holocene alluvium, Locs. 10,26,28
	Nash Draw fauna (Ashbaugh and Metcalf, 1986)	Loc. 11 (Hall, 2002a)	Loc. 40* (loc. 14 in Hall, 2002a)	
AQUATIC				
Pisidium casertanum	x			
Pisidium compressum	x			
Bakerilymnaea dalli			x	
Fossaria modicella	x	x	x	
Fossaria parva	x			
Gyraulus circumstriatus			x	
Lymnaea caperata	x			
Lymnaea sp.			x	
Physa virgata	x			
TERRESTRIAL				
Carychium exiguum		x		
Deroceras leave		x	x	
Gastrocopta cristata	x			
Gastrocopta pellucida	x			x
Gastrocopta pentodon	x			
Gastrocopta sp.		x	x	
Hawaiia minuscula	x	x	x	x
Pupilla blandi	x		x	
Pupilla muscorum		x	x	
Pupoides albilabris	x			x
Succineids, spp. indet.	x	x	x	x
Vallonia cyclophorella	x			
Vallonia gracilocosta	x	x	x	
Vallonia parvula	x			
Vertigo milium	x	x	x	
Vertigo ovata	x			
Vertigo sp.		x	x	

* Shells AMS dated 18,900 ± 100 ^{14}C yrs BP (22,760 cal yr BP)

Table 13.3. Late Holocene land snail fauna from the Mescalero Plain, New Mexico

Species	Habitat
Pupoides albilabris	It is common and widespread in southern and eastern New Mexico and is found at low elevations in the northern Chihuahuan Desert (*1*); also found in dry sagebrush grasslands (*2*); one of the more common pupillids in Texas (*3*).
Gastrocopta pellucida	The synthesis of *G. pellucida* with *G. p. hordeacella* is followed (*1*). This is one of the more common land snails at low elevations in southern New Mexico and Texas in the northern Chihuahuan Desert (*1*, *3*). It is found under large stones (*1*) and dry sandy places (*4*). Shells are common in late Holocene alluvium in the Pecos and Rio Grande drainages of southern New Mexico (*1*).
Hawaiia minuscula	This is a common snail in New Mexico at low elevations on dry floodplains (*1*) and on bare ground (*4*). It is found widely across the continent in lowland and upland habitats (*2*).
Family Succineidae	"The identification of succineids is notoriously difficult because the shells of many species are similar, even those of different genera" (*1, p. 47*). Sometimes, two or more different species may be present based on shell differences, although they are seldom referred to genus or species.

References: 1, Metcalf and Smartt, 1997; 2, Leonard, 1959; 3, Cheatum and Fullington, 1973; 4, Hubricht, 1985

XIV. SUMMARY AND CONCLUSIONS

A chart summarizing the geology and archaeology of the eolian sands of the Mescalero Plain is given in Figure 14.1. An outline of the late Quaternary geology and paleoenvironments is presented in Table 14.1.

Our investigations during the past nineteen years have focused on the Mescalero Plain of southeastern New Mexico, an area of about 10,630 km² (4,100 square miles). The various surficial geology deposits, especially eolian sand that makes up the Mescalero Sands, have been dated by 177 OSL and 54 AMS radiocarbon ages. The Mescalero sand sheet is one of the better dated eolian landscapes in the Southwest-Southern Great Plains region.

Eolian Stratigraphy

The Mescalero sand sheet formed during the past 90 ka and is made up of deposits from six separate episodes of eolian activity, two during the Pleistocene and four during the Holocene. The earliest is the Lower eolian sand unit, deposited between 90 ka to 50 ka, representing episode I. The sand is capped by the non-calcic, argillic Berino paleosol. After a period of stability that persisted for 17,000 years, the sand sheet became active and the Middle eolian sand unit was deposited 33 ka to 20 ka, representing episode II. It is capped by an argillic Bt paleosol. The deposit accumulated during the full-glacial conditions of the late Pleistocene. During the Pleistocene-Holocene transition, two episodes of eolian activity were initiated. The Upper eolian sand unit was deposited from about 18 ka to 5 ka, ending in the middle Holocene, representing episode III. The sand is capped by a cambric Bw soil horizon. The episode IV sand was deposited throughout most of the Holocene from about 12 ka to 2 ka and is referred to as the Holocene eolian sand unit. It is commonly mantled by the unrelated Eddy paleosol. About the time that accumulation of the Upper eolian sands was ending, the deposition of the Late Holocene eolian sand unit was beginning. It accumulated from about 6 ka to 2 ka, representing episode V. It is mantled by the unrelated Eddy and the Loco Hills paleosol.

Beginning 2,000 years ago, the sand sheet stabilized and the cumulic Eddy paleosol A horizon began forming across the landscape. These events are related to the wetter late Holocene regional climate. About three-fourths of all of the prehistoric sites on the Mescalero Plains were occupied during this time. About 300 years ago, by A.D. 1700, the sand sheet became active again. Parabolic and coppice dune fields were established across the plain. Cover sand was deposited where dunes are absent. The earliest parabolic and coppice dune sands are directly dated as having formed in the early or mid-1700s. The dunes continued to form into the twentieth century, and some are probably active today.

Other Patterns of Eolian Sand Deposition

Not all eolian sand deposits fall into the six episodes of eolian activity. One locality (# 29) has sands that were deposited continuously from about 50 ka to 5 ka. Sands were also deposited continuously from about 35 ka to 5 ka at two other places (Locs. 25, 27). All three sequences of sand accumulation ended by about 5 ka, similar to the timing of the end of deposition of the Upper eolian sand unit (episode III). Another unique pattern of eolian sand deposition occurs in Los Medaños area, where a fine-grained sand bed is dated about 2 ka. The sand bed rests on a thin bed of very fine-grained sand dated about 4.5 ka to 4.0 ka.

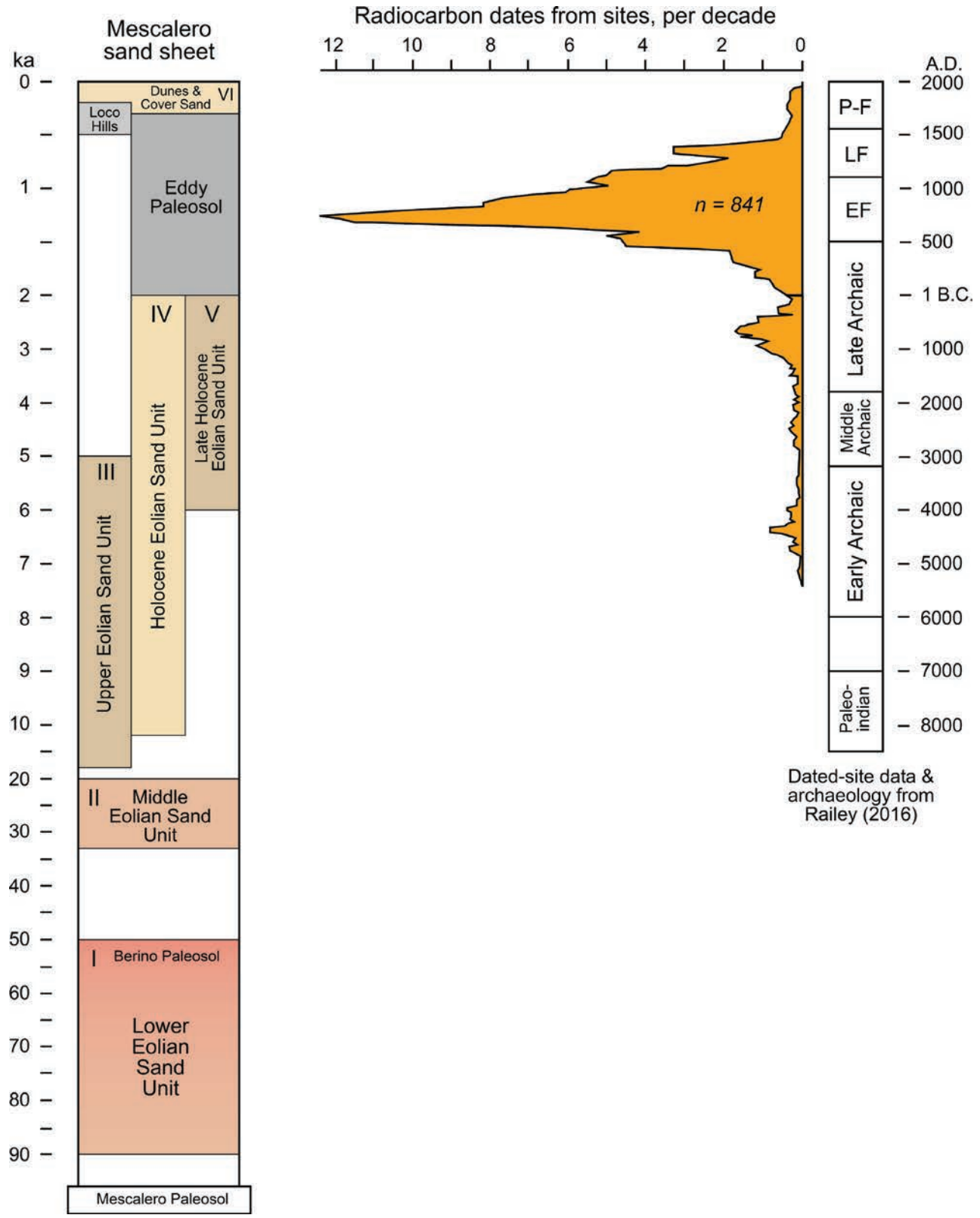

Figure 14.1. Summary of eolian stratigraphy, paleosols, and age-frequency of radiocarbon dates from archaeological sites, Mescalero Plain, southeastern New Mexico (modified from Hall and Goble, 2016g, 2019). Shown here, the chronology of the eolian sand units, including the dune sand, is based on OSL dating; the chronology of the Eddy paleosol is provided by OSL dating; the age of the Loco Hills paleosol is based on OSL and AMS radiocarbon dating. The archeological periods and the age frequency of 841 radiocarbon dates from archaeological sites in the Mescalero Plain are from Railey (2016); P-F = Post-Formative; LF = Late Formative; EF = Early Formative. Time scale changes at 10 ka and 2 ka.

Table 14.1. Summary of late Quaternary geology and paleoenvironments of Mescalero Sands, southeastern New Mexico

Time	Geology	Paleoenvironments
Late 19th and 20th centuries	Expansion of mesquite, continued eolian activity, more coppice dunes	Post-Little Ice Age warm climate, lowering of water table, ranching-farming; general shift to semi-arid shrubland
300 BP (A.D. 1700)	Beginning Episode VI, deflation of sand sheet; parabolic, coppice dunes and cover sands; end of Eddy paleosol development	Slightly cooler-wetter; Little Ice Age glaciers in Colorado A.D. 1630-1850; Carlsbad speleothem growth A.D. 1600-1900; maximum of Little Ice Age ca. A.D. 1700
500 to 200 BP	Formation of Loco Hills A horizon paleosol, ending by 200 BP	
1050 to 650 BP	Cumulic Eddy paleosol continued forming until 300 BP	Medieval Warm Period; gradual shift from grass to shrub-dominance in the local vegetation
1000 BP	Major changes in SW stratigraphic and geomorphology records; no big changes seen on the sand sheet or Eddy paleosol	Significant shift from wet to dry conditions, downcutting in alluvial valleys
2000 to 300 BP	Formation of Eddy paleosol, ended by ca. 300 years ago	Eddy began forming during wet period; desert grasslands thrive
2000 BP	Approximate end of Episode IV and V eolian activity; sand sheet stabilized; beginning of Eddy A horizon soil development	Onset of coolest-wettest interval of late Holocene climate; Audubon Neoglaciation in Colorado ca. 1800 to 1000 BP; cumulic Mollisols on river floodplains 2500 to 1000 BP
4500 to 1000 BP	Ongoing Episode IV and V eolian activity	Period of wetter-cooler climate, post-Altithermal
5000 BP	Beginning of Episode V eolian activity; end of Episode III sand deposition	Shift to less arid climate; Episode IV eolian activity was not interrupted or altered by the Altithermal interval of arid climate
7000 to 4500 BP	Ongoing Episode III and IV eolian activity	Antevs' Altithermal; arid, hot and dry climate
12,000 to 7000 BP	Beginning of Episode IV, continuing Episode III	End of Pleistocene-Younger Dryas cool-wet period, shift to Early Holocene warm-dry climate
18 ka	Beginning of Episode III eolian sand deposition in some places	Late glacial climate, still significantly wetter and cooler than today
20 ka	Beginning erosion of Middle eolian sand; Bt soil development	Cool-wet climate
33-20 ka	Deposition of Episode II Middle eolian sand; springs, ponds	Full-glacial cold-wet climate; Late Wisconsin glaciation
50 ka	End of deposition of Episode I eolian sand; beginning of erosion of sand and Berino paleosol development	Mid-Wisconsin, less cool-less wet
90 ka	Beginning deposition of Episode I eolian sand; first eolian sand on sand sheet	Moderate climate
100 to 90 ka	Erosion of Mescalero paleosol	Shift to less arid climate
135 to 100 ka	Formation of Mescalero paleosol	Sangamon Interglaciation; climate more arid than Holocene

Sedimentation Rates

Based on OSL dating, the five separate sheet sands dated 90 ka to 2 ka (excluding Eddy paleosol cap) have net rates of sedimentation ranging from 0.053 to 0.228 mm per year, averaging 0.110 mm per year (not counting the unusually thick locality of the Upper sand with a sedimentation rate of 0.896 mm per year). The Lower, Middle, Upper, Holocene, and Late Holocene sheet sands have average accumulation rates of 0.063, 0.053, 0.086, 0.107, and 0.228 mm per year, respectively. In sharp contrast, parabolic and coppice dunes have orders of magnitude greater sedimentation rates of 6.85 and 18.3 mm per year, respectively. The sedimentation rates of the Mescalero sand sheet are similar to the rates that we found at the Bolson and Strauss sand sheets near El Paso and Las Cruces, although in comparison the accumulation of the Late Holocene sheet sand is atypically high. The increased rate of sediment accumulation into the Holocene may be related to greater amounts of sand availability at the sources. OSL dating of the cumulic Eddy paleosol (post-Holocene and post-Late Holocene sheet sand) indicate that it accumulated at an average rate of 0.41 mm per year.

Sedimentology of the Mescalero Sands

We have compositional and grain-size information on 642 sediment samples. Nearly all of the eolian deposits from the Mescalero Sands are predominantly fine-grained quartz sand (0.25 to 0.125 mm; Wentworth scale). Looking at representative samples from the six episodes of eolian activity, four of the suites of samples are fine- to medium-grained sand, and two are fine- to very fine-grained sand. The finest-textured suite of samples is from episode I, the Lower eolian sand, the first eolian sand body deposited in the Mescalero Sands with the highest amounts of very fine sand; it also has the greatest variability. The coarsest-textured suite of samples is from parabolic dunes with the highest percentage of medium sand and the lowest percentage of very fine sand; the dunes originate from local sheet sand, and finer particles are carried away.

Bioturbation of the Mescalero Sands by rodents is minimal and by carnivores such as coyotes and badgers is rare. However, bioturbation of eolian sands by cicada insects appears to be universal on the Mescalero Plain. Whether actual disturbance at a locality is moderate or severe is difficult to judge. As cicada nymphs burrow in the subsurface, they backfill with the same sediment. As a result, their burrow fills are often invisible in the sand.

Chemical Signatures of Sand Deposits

All sand deposits contain different amounts of potassium oxide (K_2O), uranium (U), and thorium (Th), determined in our studies during OSL dating. Radioactive ^{40}K is found in potassium oxide (K_2O). The different amounts of these radioelements give the sand at a locality a unique signature. The amount of radioelements in a sand sample largely determines the dose rate which in turn produces the OSL age for that sample (this is explained in more detail in chapter 2).

The chemical signatures of the Mescalero sand sheet are wide ranging, while the signatures of the Bolson and Strauss sand sheets are narrow. Accordingly, the Mescalero sheet is more complex.

We have found that every locality exhibits a reduction in the amount of radioelements, along with a reduced dose rate, with the passage of time. This suggests that sand grains are subjected to a continual loss of radioelements by mineral grain abrasion and fracturing during eolian transport. Once grains are deposited, they are taken out of the cycle. However, once re-entrained, they are back in the rework cycle, resulting in further loss of radioelements. The cycle of deposition and reworking and redeposition can extend for 20,000 years or more and is ongoing today. One of the reasons this process operates is because of the low amount of available sand in sand-source reservoirs. As a consequence, sand grains tend to be recycled from an earlier deposit to a later deposit.

A change in the chemistry of some sand sources occurred sometime between 31.4 ka and 20.7 ka, during the Late Wisconsin; an increase in K_2O content by 34% was observed at one locality (Loc. 16) and by other amounts at three other sites. We interpret the shift in chemistry as an influx of new fluvial sand to the sand source reservoirs: the wetter climate facilitated the rejuvenation of local streams. The new sand may have been picked up by the wind from stream beds or fresh cutbanks as a result of increased discharge.

We conclude that the sand sources for eolian activity are many, but that the reservoir of available sand is limited. Considering the geomorphology of the plain, the sand sources are predominantly the small streams that flow from the Caprock escarpment of the Ogallala Formation across the plain towards the Pecos River (first suggested by Bachman, 1976). Today the streams are ephemeral and discontinuous, ending in the sand sheet. With wetter conditions, the streams may have been seasonal to permanent, depending upon the amount of local precipitation and spring flow from the Ogallala aquifer.

Mescalero, Bolson, and Strauss Sand Sheets: A Brief Comparison

The diversity of the chemical signatures of the six eolian sand units that make up the Mescalero Sands indicates a heterogeneous history of sand sheet development. The complexity of the sheet is due to its large size and the influence of multiple stream sand sources in different parts of the Mescalero Plain. In contrast, the Bolson and Strauss sand sheets are much less variable, indicating comparatively simple geology.

The eolian sheet sands of the Mescalero have originated from small streams that flowed across the Mescalero Plain. The other two sand sheets each have but a single source of sand: the Bolson sands are derived from the Rio Grande downstream from El Paso, Texas, and the Strauss sands are derived from pluvial Lake Palomas in northern Chihuahua, Mexico.

As mentioned previously, the Bolson and Strauss sand sheets both ended accumulation of new sand in response to the supply of sand shutting down, the Bolson at 5 ka and the Strauss at 15 ka. Subsequently, the pre-5 ka sand of the Bolson and the pre-15 ka sand of the Strauss were cannibalized, resulting in recycled sand forming eolian deposits across these sand sheets during the Holocene; the recycled sand was especially common on the Strauss sand sheet.

The accumulation of the Upper sand (episode III) of the Mescalero also ended due to the shutting down of a source (not identified), although other eolian sands (episodes IV and V) continued to be deposited across the plain. Evidence for significant cannibalization has not been found even though the late Pleistocene eolian sheet sands (Lower and Middle units) have been eroded.

The Eddy paleosol A horizon is a prominent feature across the Mescalero Plain, but this horizon did not form on the Bolson or Strauss sand sheets. However, beginning 500 years ago, a soil A horizon developed on all three sand sheets: Loco Hills (Mescalero), McGregor (Bolson), and unnamed (Strauss). Since that time, widespread erosion scoured the sand sheets, forming coppice and parabolic dunes on the Mescalero and coppice dunes on the Bolson and Strauss. The beginning of the erosion is dated A.D. 1700 on the Mescalero and since A.D. 1880 on the Strauss; this episode is not dated on the Bolson, although an OSL age of the base of a large coppice dune is 80 ± 10 years (A.D. 1926) (Hall et al., 2010).

Paleosols

Four named paleosols occur on the Mescalero sand sheet: Mescalero, Berino, Eddy, and Loco Hills. An unnamed argillic Bt horizon and an unnamed cambic Bw horizon are also present.

The Mescalero paleosol is a caliche-calcrete with stage III–IV carbonate morphology that formed on Permian-Triassic red beds and the Pleistocene Gatuña Formation across the Mescalero Plain. In some places, the upper Btk horizon is preserved. In most areas, the Mescalero sand sheet occurs directly on eroded caliche of the paleosol. Based on OSL dating, the Mescalero paleosol formed about 135 ka to 100 ka during the Sangamon Interglaciation and Marine Isotope Stage 5, a period of greater aridity than the Holocene.

The Berino paleosol is a formally named pedostratigraphic unit (Hall and Goble, 2012) that caps the Lower eolian sand. The paleosol is a noncalcic, argillic Aridisol Bt horizon with a maximum of 25% clay and 0.86% iron. It formed during a period of 17,000 to 32,000 years, depending on the age of the overlying sand at different localities.

An unnamed noncalcic, argillic Bt horizon caps the Middle eolian sand unit that has up to 17% clay and 1.0% iron. This horizon formed during the late Pleistocene last-glacial maximum until it was buried by Holocene sand. An unnamed noncalcic, cambic Bw horizon caps the Upper eolian sand unit. The accumulation of the Upper sand ended by 5 ka; the Bw horizon formed since that time. A weak calcic Bk horizon commonly accompanies

the Bw and occurs below 40 to 50 cm depth, where calcium carbonate content increases to 7%, a stage I carbonate morphology.

The Eddy paleosol is a cumulic Mollisol A horizon that formed on late Holocene eolian sand, alluvium, and colluvium across the Mescalero Plain. Cumulic soil A horizons develop for the most part with grass-dominated vegetation where grasses capture and hold wind-transported sands. Cumulic soils are less likely to form in small shrub-dominated vegetation. The Eddy is about 15 to 40 cm thick with up to 0.48% organic carbon, forming an A horizon topsoil. The Eddy topsoil is a cumulic A horizon that was built up by accumulation of wind-deposited sand and dust in grassland vegetation during a 1,700-year period between 2,000 and 300 years ago (A.D. 1 to 1700), based on OSL dating of the topsoil sand. The cumulic A horizon topsoil of the Eddy paleosol has a sedimentation rate from 0.130 to 0.612 mm per year, averaging 0.41 mm per year. The development of the Eddy paleosol horizon ended when deflation of the sand sheet was initiated about 300 years ago.

The occurrence of the Eddy paleosol is everywhere at the surface of the sand sheet; it is not buried by eolian sand except where recent parabolic and coppice dunes are present. The paleosol is commonly masked at the surface by recent cover sands. Where associated with Holocene alluvium and colluvium, this horizon is buried at shallow depths in those deposits. The Eddy paleosol formed during the Late Archaic and Formative archaeological periods. Most of the prehistoric sites on the Mescalero Plain occur in the Eddy paleosol; 78% of the 841 radiocarbon dates from all of the sites on the plain have a temporal correlation with the Eddy horizon.

The Loco Hills paleosol is a thin cumulic soil A horizon and is common in the northern part of Eddy County. It formed between 500 and 200 years ago, during a period of 300 years. This paleosol is generally found beneath coppice dunes where it has been protected from recent erosion; it was also observed beneath a parabolic dune.

Alluvial Geology

Holocene alluvium has not been a central point of our investigations across the plain. However, a few studies have shown that alluvium can incorporate paleoenvironmental information, such as terrestrial and freshwater snails and pollen, which is not forthcoming from eolian sands. Alluvium can also contain archaeology. Studies of Holocene alluvial geology may provide information on whether the small streams across the plain could have served as water resources to prehistoric populations.

West of the Mescalero Plain, a late Holocene alluvial terrace occurs 6 m above the modern floodplain of the Pecos River; the upper 1.2 m of the alluvium is OSL dated 6.64 and 3.25 ka. The terrace probably formed at 1 ka when many regional stream valleys were incised. A Late Formative site occurs on the terrace surface, consistent with the age of the alluvium and terrace development. Remarkably, this is the first case in New Mexico where Pecos River alluvium has been directly dated.

West of the Pecos River, sequences of Holocene alluvium containing prehistoric sites overlie thick deposits of Pleistocene gravel that can incorporate vertebrate fossils. The Eddy paleosol has been found in the upper levels of the Holocene alluvium.

Colluvial deposits occur on hillslopes along stream valleys, along topographic escarpments, and at the margins of large basins. The deposits are middle to late Holocene in age and contain archaeology.

Springs, Ponds, Playa Lakes

During the Late Wisconsin, the climate in southeastern New Mexico was cool and wet; the last glacial maximum occurred 26.5 ka to 20–19 ka (Clark et al., 2009). Water tables were high, playa lakes were full, springs were active, and streams were flowing. A spring deposit in an arroyo cut bank with many species of terrestrial and freshwater snail shells is AMS-dated 22,760 cal yr BP. Elsewhere, a pond deposit buried by 1.1 m of late Holocene eolian sand has snail and ostracod shells and was OSL-dated at 20.2 ka.

Although glacial-age playas in the region have yet to be systematically researched, we encountered playa-derived deposits in one study. Whitish eolian sand, devoid of mineral coats on sand grains, was derived from glacial-age beach deposits of Laguna Plata. The whitish sand occurs 2.9 km (1.8 miles) east (downwind) of the playa and was OSL-dated 20.9 ka to 11.9 ka. The sand was deposited during the period from the end of the full-glacial maximum and to the end of the Pleistocene.

Glacial-age deposits on the Mescalero Plain are not uncommon. How long high water tables, springs, and ponds may have persisted after the last glaciation when climate warmed, and whether these water resources were used by Paleoindian or Early Archaic populations, remain open questions.

Archaeological Geology

Most Late Archaic and Formative sites on the Mescalero Plain occur in the Eddy paleosol; 78% of the 841 dated archaeological features correlate with the Eddy paleosol that formed A.D. 1 to 1700, based on OSL and AMS radiocarbon dating. Almost all sites on the Mescalero Plain are buried in the Eddy paleosol or associated eolian sands, and many sites occur at shallow depth.

Site Preservation and Burial

The Eddy paleosol is a cumulic soil A horizon that built up slowly, averaging 0.41 mm per year. Eolian sheet sands accumulated even more slowly at less than 0.20 mm per year. Slow sedimentation rates lead to high susceptibility to disturbance, mixing, and erosion, resulting in poor preservation of prehistoric sites. During a period of 50 years, an abandoned site could be buried by as little as 2 cm of eolian sand, providing ample opportunity for a site to be disturbed and cultural materials to become mixed. The only opportunity for a prehistoric site to form at a surface without becoming buried is after A.D. 1700. All sites that formed before that time have the potential to be buried, even if by only a few millimeters of sand.

Exceptions to the above lie in a few areas on the western edge of the sand sheet where the Upper eolian sand unit is present and the Eddy paleosol is absent; in these cases, the surface is 5,000 years old and Middle Archaic and younger sites will occur unburied at the surface.

Site Erosion

If we could look back just prior to A.D. 1700, we would see an undulating sand sheet covered by a thick topsoil with a dense grassland and, where the sand is thick, shinnery oak vegetation. Stone features from recent prehistoric sites may protrude above the soil. Earlier sites would be buried in the topsoil or in the underlying sands. Dunes and their blowouts and scoured surfaces that dominate the landscape today would be absent.

All of this changed about 300 years ago. The principal agent of site visibility today is the almost universal deflation and erosion that has occurred across the Mescalero Plain in the past 300 years. Today, sites in the field appear to be complicated. This is because a portion of a site is buried and obscured by dunes, while another part of the site is eroded with once-buried artifacts and features now exposed and concentrated on scoured, deflated surfaces. The presence of dunes also does not guarantee that intact archaeology will be found beneath the dunes; local erosion of a site may have occurred before the dunes formed.

Anthrosols

Anthrosols seldom occur at prehistoric sites across the plain. Seven criteria for identifying the presence of an anthrosol are: (1) presence of many archaeological materials including abundant charcoal throughout; (2) very dark color; (3) abrupt boundaries between layers; (4) thicker-deeper extent of dark layers than local natural soils; (5) lateral extent discontinuous; (6) high amounts of organic matter; and (7) high amounts of phosphorus. All of these criteria together define an anthrosol. The anthrosol characteristics are in contrast with the A horizons of the Eddy and Loco Hills paleosols. Only one site, the Boot Hill site, which we did not study, appears to have an anthrosol. The soil at all of the sites that we studied is the Eddy paleosol.

Site Footprint

The footprint of an archaeological site is a layer or zone of sediment in which the physical and chemical properties have been affected by human activities. During the formation of an archaeological site, the pre-site deposits are disturbed and lose their sedimentologic and stratigraphic properties. A site footprint is a weak candidate for optical dating or paleoenvironmental study.

Buried Site Potential

Even though most sites are buried, buried site potential is not uniform across the plain. Buried site potential can be evaluated in the field by two criteria: dune geomorphology and vegetation. Parabolic dunes and shinnery oak indicate the presence late Holocene sand that is generally greater than one meter in thickness, having a high potential for buried archaeology.

Mesquite coppice dunes can indicate either the presence of thin layer of Holocene sand or the presence of the Upper sand (early Holocene) or Lower sand (Pleistocene), which have a lower (but not zero) potential for buried archaeology. The absence of dunes altogether may indicate the absence of eolian deposits; in this situation, sites of all ages can occur at the surface.

Buried-site potential maps have been produced from three sources of information: direct mapping, surficial geology, and soils. Direct mapping of known, well-dated deposits produces more reliable buried-site potential maps. However, for questions regarding locality-specific land use, a reliable map is not a substitute for field inspection by an experienced practitioner.

Paleoenvironments of Southeastern New Mexico

The paleoclimatic and paleoenvironmental history of southeastern New Mexico is the same as that of the broader American Southwest, with strong affinities to the southern Great Plains and the Great Basin.

The specific paleoenvironmental records from southeastern New Mexico, however, are sparse and add little about past climatic conditions overall. Two late Holocene speleothem records from the Carlsbad Cavern area do not match each other, giving conflicting information on past conditions. Pollen analysis indicates that the late Holocene vegetation of the western Mescalero Plain was a shrub-grassland; the record is dated 3.1 ka to 0.5 ka. Stable carbon isotope data from the past 2,000 years indicate a mix of C_3 and C_4 plant communities across the plain. Some local trends suggest a possible shift to an increase in shrubs in the vegetation during the latest Holocene. Carbon isotope data indicate the presence of grass-dominated vegetation west of the Pecos River during the past 6,000 years.

However, some important links between climate, geology, and archaeology have emerged in our investigations. The late Holocene was characterized by a comparatively cool and wet climate, the coolest and wettest since the end of the Pleistocene. The development of the Eddy paleosol beginning 2.0 ka was a response to the wetter climate and the presence of grassland vegetation; the sand sheet was stabilized by the grassland vegetation and Eddy topsoil. We speculate that local springs and streams may have had some discharge, at least seasonal. The human population of the plain had expanded in numbers during this time; three-fourths of all dated prehistoric features fall into the time span of the Eddy paleosol. The prehistoric population may have peaked on the plain about A.D. 775 in the Early Formative period. It is reasonable to conclude that the wet conditions and associated flora and fauna made the area attractive for human habitation.

ACKNOWLEDGEMENTS

Our investigations began in December 2000, and we express deep gratitude to many individuals who have helped out over the years and along the way. We thank Glenna Dean, Stephen Fosberg, Jan Biella, Tiffany Sullivan-Owens, Michael McGee, Rose Marie Havel, Doug Melton, the late Don Clifton, Hewitt Jeter, Bruce Boeke, Martin Stein, Doug Boggess, Kenneth Brown, Chris Anderson, Robert Dello-Russo, Jim Railey, Bill Whitehead, Sean Simpson, Gerry Raymond, Patrick Hogan, Mark Sale, Darden Hood, Chuck Wheeler, Matthew Bandy, Eric Ingbar, Chris Parrish, Bonnie Newman, Reg Wiseman, Robert Heckman, Monica Murrell, Richard Kettler, and Dennis Powers. We especially appreciate the support and assistance of the Carlsbad Field Office of the Bureau of Land Management throughout our investigations. We are very grateful for the support of many institutions and firms, including Lone Mountain Archaeological Services, the Office of Archaeological Studies, Ecosystem Management, Inc., the Office of Contract Archeology, Western Cultural Resource Management, Inc., Gnomon, Inc., Mesa Field Services, Statistical Research Inc., Taschek Environmental Consulting, TRC Environmental, and SWCA Environmental Consultants. We thank Jim Railey for providing archaeological information and editorial comments on an earlier edition. We especially thank Mary Jo Schabel of the Milwaukee Soil Laboratory for her dedication, providing high-resolution particle size and chemical measurements; Energy Laboratories, Inc., Billings, Montana; and A&L Great Lakes Laboratories, Fort Wayne, Indiana. We thank Shari Kelley, Tammy Rittenour, and Trevor Kludt for valuable reviews and suggestions. We thank the University of Utah Press for permission to reproduce materials from *The Archaic Southwest: Foragers in an Arid Land*.

REFERENCES CITED

Adamiec, G., and Aitken, M., 1998, Dose-rate conversion factors: Update: Ancient TL, v. 16, p. 37–50.

Aitken, M.J., 1998, Introduction to Optical Dating, The Dating of Quaternary Sediments by the Use of Photon-Stimulated Luminescence: Oxford, Oxford University Press, 267 p.

Albertson, F.W., and Weaver, J.E., 1942, History of the native vegetation of western Kansas during seven years of continuous drought: Ecological Monographs, v. 12(1), p. 23–51.

Altschul, J.H., Sebastian, L., Rohe, C.M., Hayden, W.E., Hall, S.A., 2005, Results and discussion: The Azotea Mesa study area, Chapter 6, *in* Ingbar, E., Sebastian, L., Altschul, J., Hopkins, M., Eckerle, W., Robinson, P., Judson Finley, J., Hall, S., Hayden, W., Rohe, C.M., Seaman, T., Taddie, S., and Thompson, S., 2005, Adaptive Management and Planning Models for Cultural Resources in Oil and Gas Fields in New Mexico and Wyoming: Carson City, Gnomon, Inc., p. 77–109. (PUMP III project)

Ashbaugh, K.M., and Metcalf, A.L., 1986, Fossil molluscan faunas from four spring-related deposits in the northern Chihuahuan Desert, Southern New Mexico and western-most Texas: New Mexico Bureau of Mines and Mineral Resources Circular 200, 25 p.

Asmerom, Y., Polyak, V., Burns, S., and Rassmussen, J., 2007, Solar forcing of Holocene climate: new insights from a speleothem record, southwestern United States: Geology, v. 35, p. 1–4.

Auclair, M., Lamothe, M., and Huot, S., 2003, Measurement of anomalous fading for feldspar IRSL using SAR: Radiation Measurements, v. 37, p. 487–492.

Bachman, G.O., 1976, Cenozoic deposits of southeastern New Mexico and an outline of the history of evaporite dissolution: Journal of Research of the U. S. Geological Survey, v. 4, no. 2, p. 135–149.

Bachman, G.O., 1980, Regional geology and Cenozoic history of Pecos region, southeastern New Mexico: U.S. Geological Survey Open-File Report 80-1099, 116 p., map in 12 over-size sheets, scale 1:250,000 and 1:125,000.

Bachman, G.O., 1981, Geology of Nash Draw, Eddy County, New Mexico: U.S. Geological Survey Open-File Report 81-31, 10 p.

Bachman, G.O., 1984, Regional geology of the Ochoan evaporites, northern part of Delaware Basin: New Mexico Bureau of Mines & Mineral Resources Circular 184, 22 p., 3 fig. in pocket.

Bagnold, R.A., 1954, The Physics of Blown Sand and Desert Dunes: London, Methuen & Co. Ltd., 266 p.

Bailey, R.M., and Arnold, L.J., 2006, Statistical modeling of single grain quartz De distributions and an assessment of procedures for estimating burial dose: Quaternary Science Reviews, v. 25, p. 2475–2502.

Ballarini, M., Wallinga, J., Wintle, A.G. and Bos, A.J.J., 2007, A modified SAR protocol for optical dating of individual grains from young quartz samples: Radiation Measurements, v. 42, p. 360–-369.

Barnes, V.E., 1976, Geologic Atlas of Texas, Hobbs Sheet: Bureau of Economic Geology, The University of Texas at Austin, Austin, 1 sheet, scale 1:250,000.

Betancourt, J.L., Grissino-Mayer, H.D., Salzer, M.W., and Swetnam, T.W., 2002, A test of "annual resolution" in stalagmites using tree rings: Quaternary Research, v. 58, p. 197–199.

Beuselinck, L., Govers, G., Poesen, J., Degraer, G., and Froyen, L., 1998, Grain-size analysis by laser diffractometry: Comparison with the sieve-pipette method: Catena, v. 32, p. 193–208.

Birkeland, P.W., 1999, Soils and Geomorphology (3rd edition): New York, Oxford University Press, 430 p.

Brown, K.L. (ed.), 2010, The Laguna Plata Site Revisited: Current Testing and Analysis of New and Existing Assemblages at LA 5148, Lea County, New Mexico: TRC Environmental, Inc., TRC Report 174673-C-01, Albuquerque, (Loc. 38)

Brown, M.E. (ed.), 2011, The Boot Hill Site (LA 32229): An Oasis in the Desert, Eddy County, New Mexico: TRC Environmental, Inc., TRC Report No. 174675-C-01, Albuquerque. (Loc. 37)

Burch, J.B., 1962, How to Know the Eastern Land Snails: Dubuque, Wm. C. Brown Co. Publishers, 214 p.

Buurman, P., Pape, T., Reijneveld, J.A., de Jong, F., and van Gelder, E., 2001, Laser-diffraction and pipette-method grain sizing of Dutch sediments: Correlations for fine fractions of marine, fluvial, and loess samples: Geologie en Mijnbouw, v. 80, no. 2, p. 49–57.

Buylaert, J.P., Murray, A.S., Thomsen, K.J., and Jain, M., 2009, Testing the potential of an elevated temperature IRSL signal from K-feldspar: Radiation Measurements, v. 44, p. 560–565.

Campbell, J.R., 2003, Limitations in the laser particle sizing of soils, *in* Roach, I.C., ed., Advances in Regolith: Proceedings of the CRC LEME Regional Regolith Symposia, 2003: Cooperative Research Centre, Landscape Environments and Mineral Exploration (CRC LEME), Australia, p. 38–42.

Cheatum, E.P., and Fullington, R.W., 1973, The Recent and Pleistocene Members of the Pupillidae and Urocoptidae (Gastrocopta) in Texas: Dallas Museum of Natural History, The Aquatic and Land Mollusca of Texas, Bulletin I, Part 2, 67 p.

Chugg, J.C., Anderson, G.W., King, D.L., and Jones, L.H., 1971, Soil Survey of Eddy Area, New Mexico: U.S. Department of Agriculture, Soil Conservation Service, 82 p., 151 aerial maps.

Clark, P.U., Clague, J.J., Curry, B.B., Dreimanis, A., Hicock, S.R., Miller, G.H., Berger, G.W., Eyles, N., Lamothe, M., Miller, B.B., Mott, R.J., Oldale, R.N., Stea, R.R., Thorleifson, L.H., and Vinvent, J.-S., 1993, Initiation and development of the Laurentinde and Cordilleran ice sheets following the last interglaciation: Quaternary Science Reviews, v. 12, p. 79-114.

Clark, P.U., Dyke, A.S., Shakun, J.D., Carlson, .E., Clark, J., Wohlfarth, B., Mitrovica, J.X., Hostetler, S.W., and McCabe, A.M., 2009, The last glacial maximum: Science, v. 325, p. 710–714.

Condon, P.C., Kuehn, D.D., Scott-Cummings, L., Maria Hroncich, M., Ponce, L.M., Konulainen, N., and Hermann, W., 2008, Archaeological Testing and Data Recovery Recommendations for 16 Prehistoric Sites, Bear Grass Draw, Eddy County, New Mexico: El Paso, TRC Environmental. (Loc. 39)

Cook, E.R., Woodhouse, C.A., Eakin, C.M., Meko, D.M., and Stahle, D.W., 2004, Long-term aridity changes in the western United States: Science, v. 306, p. 1015–1018.

Cunningham, A.C. and Wallinga, J., 2010, Selection of integration time intervals for quartz OSL decay curves: Quaternary Geochronology, v. 5, p. 657–666.

Dane, C.H., and Bachman, G.O., 1965, Geologic Map of New Mexico: U. S. Geological Survey, 2 sheets, scale 1:500,000.

Darton, N.H., 1928, "Red Beds" and associated formations in New Mexico, with an outline of the geology of the state: U.S. Geological Survey Bulletin 794, 372 p.

Di Stefano, C., Ferro, V., and Mirabile, S., 2010, Comparison between grain-size analyses using laser diffraction and sedimentation methods: Biosystems Engineering, v. 106, p. 205–215.

Durcan, J.A. and Duller, G.A.T., 2011, The fast ratio: A rapid measure for testing the dominance of the fast component in the initial OSL signal from quartz: Radiation Measurements, v. 46, p. 1065–1072.

Eddy, J.A., 1976, The Maunder Minimum: Science, v. 192, p. 1189–1202.

Eshel, G., Levy, G.J., Mingelgrin, U., and Singer, M.J., 2004, Critical evaluation of the use of laser diffraction for particle-size distribution analysis: Soil Science Society of America Journal, v. 68, p. 736–743.

Folk, R.L., 1968, Petrology of Sedimentary Rocks: Austin, Hemphill's, 170 p.

Friedman, G.M., and Sanders, J.E., 1978, Principles of Sedimentology: New York, John Wiley and Sons, 792 p.

Frye, J.C., and Leonard, A.B., 1957, Studies of Cenozoic geology along eastern margin of Texas High Plains, Armstrong to Howard counties: Bureau of Economic Geology, University of Texas at Austin, Report of Investigations 32, 62 p.

Galbraith, R.F., 2005, Statistics for Fission Track Analysis: Chapman & Hall/CRC Interdisciplinary Statistics, 240 p.

Galbraith, R.F., Roberts, R.G., Laslett, G.M., Yoshida, H. and Olley, J.M., 1999, Optical dating of single and multiple grains of quartz from Jinmium Rock Shelter, Northern Australia: Part I, Experimental design and statistical models: Archaeometry, v. 41, p. 339–364.

Gard, L.M., Jr., 1968, Geologic Studies, Project Gnome, Eddy County, New Mexico: U.S. Geological Survey Professional Paper 589, 32 p.

Gile, L.H., Hawley, J.W., and Grossman, R.B., 1981, Soils and Geomorphology in the Basin and Range Area of Southern New Mexico—Guidebook to the Desert Project: New Mexico Bureau of Mines & Mineral Resources Memoir 39, 222 p.

Green, F.E., 1961, The Monahans dune area, in Wendorf, F., ed., Paleoecology of the Llano Estacado: Fort Burgwin Research Center, No. 1, p. 22–47.

Grissino-Mayer, H.D., 1996, A 2129-year reconstruction of precipitation for northwestern New Mexico, USA, *in* Dean, J.S., Meko, D.M., and Swetnam, T.W., eds., Tree Rings, Environment, and Humanity: Department of Geosciences, University of Arizona, Tucson, Radiocarbon 1996, p. 191-204.

Guerin, G., Mercier, N., and Adamiec, G., 2011, Dose-rate conversion factors: update: Ancient TL, v. 29, p. 5–8.

Gustavson, T.G., 1996, Fluvial and Eolian Depositional Systems, Paleosols, and Paleoclimate of the Upper Cenozoic Ogallala and Blackwater Draw Formations, Southern High Plains, Texas and New Mexico: Bureau of Economic Geology, University of Texas at Austin, Report of Investigations No. 239, 62 p.

Hall, S.A., 1977, Geology and palynology of archaeological sites and associated sediments, *in* Henry, D.O., ed., The Prehistory of the Little Caney River, 1976 Field Season: Contributions in Archaeology No. 1, Laboratory of Archaeology, Univ. of Tulsa, p. 13-41.

Hall, S.A., 1990, Channel trenching and climatic change in the southern U.S. Great Plains: Geology, v. 18, p. 342-345.

Hall, S.A., 1995, Late Cenozoic palynology in the south-central United States: Cases of post-depositional pollen destruction: Palynology, v. 19, p. 85–93.

Hall, S.A., 2001, Geochronology and paleoenvironments of the glacial-age Tahoka Formation, Texas and New Mexico: New Mexico Geology, v. 23, p. 71–77.

Hall, S.A., 2002a, Field Guide to the Geoarchaeology of the Mescalero Sands, Southeastern New Mexico: Bureau of Land Management and the Historic Preservation Division, New Mexico Department of Cultural Affairs, Santa Fe, 67 p.

Hall, S.A., 2002b, Guidebook, First Geoarchaeology Field Course: Mescalero Sands, Southeastern New Mexico: Bureau of Land Management and the Historic Preservation Division, New Mexico Department of Cultural Affairs, Santa Fe, 23 p.

Hall, S.A., 2005, Ice Age vegetation and flora of New Mexico, *in* Lucas, S.G., Morgan, G.S., and Zeigler, K.E., eds., New Mexico's Ice Ages: New Mexico Museum of Natural History and Science Bulletin No. 28, p. 171-183.

Hall, S.A., 2006, Geoarchaeologic map of southeastern New Mexico, *in* Hogan, P.F., ed., Development of Southeastern New Mexico Regional Research Design and Cultural Resource Management Strategy: Office of Contract Archeology, University of New Mexico, UNM Report No. 185-849, p. 2-4 to 2-25.

Hall, S.A., 2007, Eolian cover sands and geoarchaeology of the Pierce Canyon area, Eddy Co., NewMexico, *in* Raymond, G., et al., eds., Cultural Resource Survey Report of a Class III Survey and Selective Spatial Data Analyses of 6,385 Acres on the Western Block 1 Lease in Pierce Canyon, Eddy County, New Mexico: Albuquerque, Ecosystem Management, Inc., Report No. 50708, p. 311–352. (Loc. 19)

Hall, S.A., 2008, Geomorphic context of archaeological sites along US Highway 62/180 corridor, Carlsbad, New Mexico, to Texas: Albuquerque, Taschek Environmental Consulting, 27 p.

Hall, S.A., 2010a, Geomorphology and archaeological geology of three sites at the Intrepid Potash-NM Solar Pond (updated), *in* Boggess, D.H.M., ed., (2009) Archaeological Treatment of Three Sites for Proposed Solar Ponds at the West Mine, Intrepid Potash-NM, LLC, Eddy County, New Mexico: Albuquerque, Lone Mountain Archaeological Services, Inc., Lone Mountain Report No. 1195. (Loc. 5)

Hall, S.A., 2010b, Archaeological geology of eolian sand and river gravel associated with LA 154539, Pierce Canyon Area, Eddy County, New Mexico (updated), *in* Boggess, D.H.M., ed., (2009) Testing at LA 154539 near Cedar Canyon, Eddy County, New Mexico: Albuquerque, Lone Mountain Archaeological Services, Inc., Lone Mountain Report No. 904-14. (Loc. 18)

Hall, S.A., 2010c, Geomorphology of LA 99434 on Quahada Ridge, Eddy County, New Mexico (updated), *in* Boggess, D.H.M., ed., Data Recovery at LA 99434 on Quahada Ridge, Eddy County, New Mexico: Albuquerque, Lone Mountain Archaeological Services, Inc., Lone Mountain Report No. 904-14. (Loc. 23)

Hall, S.A., 2013, Geomorphology and optical age of eolian sand at LA 124525, Maroon Cliffs, Eddy County, New Mexico: Albuquerque, Lone Mountain Archaeological Services, Inc., 19 p. (Loc. 25)

Hall, S.A., 2016, Geology of LA 172574 at Red Bluff Draw, Eddy County, New Mexico: Albuquerque, SWCA Environmental Consultants, Inc., 16 p. (Loc. 32)

Hall, S.A., 2017a, Geology of two sites along Owl Draw, southwest Pecos Slopes, Eddy County, New Mexico: Previous reports of an anthrosol are mistaken: Albuquerque, Statistical Research, Inc., 18 p. (Loc. 34)

Hall, S.A., 2017b, Geology of LA 183250 and coppice dunes, Lea County, New Mexico: Albuquerque, SWCA Environmental Consultants, Inc., 13 p. (Loc. 35)

Hall, S.A., 2017c, Geology of LA 171861 in eolian sands, western Mescalero Plain, Eddy County, NewMexico: Albuquerque, SWCA Environmental Consultants, Inc., 15 p. (Loc. 36)

Hall, S.A., 2018, Paleoenvironments of the American Southwest, *in* Vierra, B.J., ed., The Archaic Southwest: Foragers in an Arid Land: Salt Lake City, University of Utah Press, p. 16–28.

Hall, S.A., and Boggess, D.H.M., 2013, Second Workshop: Archaeological Geology of the Permian Basin, Southeastern New Mexico: Red Rock Geological Enterprises, Santa Fe, and Lone Mountain Archaeological Services, Albuquerque, 33 p. (Locs. 7, 25)

Hall, S.A., Boutton, T.W., Lintz, C.R., and Baugh, T.G., 2012, New correlation of stable carbon isotopes with changing Late-Holocene fluvial environments in the Trinity River Basin of Texas, USA: The Holocene, v. 22, p. 541-549.

Hall, S.A., and Goble, R.J., 2006, Geomorphology, stratigraphy and luminescence age of the Mescalero Sands, southeastern New Mexico, *in* Land, L., Lueth, V.W., Raatz, W., Boston, P., Love, D.W., eds., Caves and Karst of Southeastern New Mexico: New Mexico Geological Society Guidebook 57, p. 297–310.

Hall, S.A., and Goble, R.J., 2008, Archaeological geology of the Mescalero Sands, Southeastern New Mexico: Plains Anthropologist, v. 53, no. 207, p. 279–290.

Hall, S.A., and Goble, R.J., 2011a, New optical age of the Mescalero Sand Sheet, Southeastern New Mexico: New Mexico Geology, v. 33, p. 9–16.

Hall, S.A., and Goble, R.J., 2011b, Geology and optical dating of sediments, *in* Railey, J.A., ed., Archaeology in Far Southeastern New Mexico: Albuquerque, SWCA Environmental Consultants, Report No. 2010-68, p. 309–335. (Locs. 11, 12, 13)

Hall, S.A., and Goble, R.J., 2012, Berino Paleosol, late Pleistocene argillic soil development on the Mescalero Sand Sheet in New Mexico: The Journal of Geology, v. 120, p. 333–345.

Hall, S.A., and Goble, R.J., 2014, Late Quaternary stratigraphy, optical geochronology, and associated prehistoric sites, *in* Moore, J.L., and Akins, N.J., eds., 10,000 Years of Transient Occupation in the Jornada del Muerto: Excavations at Eight Sites at the Spaceport America Facility, Sierra County, New Mexico, Volume II: Santa Fe, Office of Archaeological Studies, Museum of New Mexico, Archaeology Notes 453, p. 567–672.

Hall, S.A., and Goble, R.J., 2015a, Assessment of the potential for subsurface archaeology based on four sites in different geologic setting, Southeastern New Mexico, *in* Heilen, M., and Murrell, M.L., eds., An Assessment of Transect Recording Unit Survey and Subsurface Testing Methods at Four Sites in the Permian Basin, New Mexico: Albuquerque, Statistical Research, Inc., Technical Report 15-68, p. 435–490. (Locs. 6, 15, 24, 26)

Hall, S.A., and Goble, R.J., 2015b, Geomorphology and archaeological geology of eolian-colluvial deposits, eastern slope of Cedar Lake Basin, *in* Railey, J.A., ed., Mobile Hunter-Gatherers in the Cedar Lake Playa Depression: Archaeological Data Recovery at the Biting Ant Site Complex (LA 117293 and LA 171726) for Linn Energy's Turner "B" South Tank Battery Produced Water Release Cleanup, Eddy County, New Mexico: Albuquerque, SWCA Environmental Consultants, p. 235–251. (Loc. 28)

Hall, S.A., and Goble, R.J., 2015c, Stratigraphy and geomorphology, *in* Railey, J.A., ed., Red Tank: Archaeological Data Recovery at LA 43257 for the Zia II Natural Gas Pipeline, Eddy County, New Mexico: Albuquerque, SWCA Environmental Consultants, p. 1–16. (Loc. 14)

Hall, S.A., and Goble, R.J., 2015d, OSL age and stratigraphy of the Strauss Sand Sheet in New Mexico, USA: Geomorphology, v. 241, p. 42–54.

Hall, S.A., and Goble, R.J., 2016a, Late Quaternary geology and associated prehistoric sites, western Mescalero Plain, Eddy County, New Mexico, *in* Wiseman, R.N., ed., Prehistoric Camps along LowerNash Draw: The NM 128 Project in Eastern Eddy County, New Mexico, Vol. 2: Santa Fe, New Mexico Department of Transportation Technical Series 2015-4, and New Mexico Office of Archaeological Studies, Department of Cultural Affairs, Archaeology Notes 398, p. 597–654. (Locs. 7, 8, 9, 10, 29)

Hall, S.A., and Goble, R.J., 2016b, Geomorphology of LA 177527 in the Nash Basin, Eddy County, New Mexico, *in* Anderson, C., and Brown, K.L., eds., Data Recovery at LA 177527 for Southwestern Public Service Company's Potash Junction to Roadrunner 345 kV Transmission Line, Eddy County, New Mexico: Albuquerque, TRC Environmental, Inc., Report 202494-C-15. (Loc. 22)

Hall, S.A., and Goble, R.J., 2016c, Late Quaternary eolian sands at LA 21136, east of Rock House Crossing, Southern Eddy County, New Mexico, *in* Anderson, C., and Brown, K.L., eds., Data Recovery at LA 21136 for Southwestern Public Service Company's China Draw to Wood Draw 115 kV Transmission Line, Eddy County, New Mexico: Albuquerque, TRC Environmental, Inc., Report 222042-C-8. (Loc. 27)

Hall, S.A., and Goble, R.J., 2016d, Holocene eolian sand and A horizon soil at LA 150002, and eolian Stratigraphy and Optical Ages at LA 181312, Antelope Draw, Lea County, New Mexico, *in* Anderson, C., and Brown, K.L., eds., Data recovery at LA 150002 and LA 181312 for Southwestern Public Service Company's Ponderosa to Custer Mountain 115 kV Transmission Line, Lea County, New Mexico: TRC Albuquerque, TRC Environmental, Inc., Report 222050-C-5. (Locs. 16, 17)

Hall, S.A., and Goble, R.J., 2016e, Optical age and geomorphology of parabolic dune sands and two Archaeological Sites, Southern Eddy Co., New Mexico, *in* Railey, J.A. and Whitehead, W.T., eds., Wolf Camp: Archaeological Data Recovery at LA 147442 and LA 147528, Eddy County, New Mexico: Albuquerque, SWCA Environmental Consultants, Inc. (Loc. 20)

Hall, S.A., and Goble, R.J., 2016f, Geomorphology and A horizon soil at LA 16902 and Jo Bar Tank, southeastern Eddy County, New Mexico: Albuquerque, SWCA Environmental Consultants. (Loc. 21)

Hall, S.A., and Goble, R.J., 2016g, Quaternary and Archaeological Geology of Southeastern New Mexico: Permian Basin Research Design 2016-2026, Vol. II: Albuquerque, SWCA Environmental Consultants, Inc., and Carlsbad Field Office, Bureau of Land Management, 184 p.

Hall, S.A., and Goble, R.J., 2017, Geology of LA 182820 on the west edge of Hackberry Lake, Eddy County, New Mexico: Albuquerque, Lone Mountain Archaeological Services, Inc., 19 p. (Loc. 33)

Hall, S.A., and Goble, R.J., 2020, Middle Pleistocene IRSL age of the upper Blackwater Draw Formation, Southern High Plains, Texas and New Mexico, USA: New Mexico Geology, v. 42(1), p. 31-38.

Hall, S.A., Goble, R.J., and Jeter, H.W., 2003, Luminescence and radioisotope chronology of the Late Quaternary Mescalero Sands, southeastern New Mexico: New Mexico Geology, v. 25, p. 46.

Hall, S.A., and Kettler, R., 2019, Surficial geology of three prehistoric sites in southern Lea County, New Mexico: Farmington, WCRM Inc., 27 p. (Loc. 31)

Hall, S.A., Miller, M.R., and Goble, R.J., 2010, Geochronology of the Bolson Sand Sheet, New Mexico and Texas, and its archaeological significance: Geological Society of America Bulletin, v. 122, p. 1950–1967.

Hall, S.A., and Periman, R.A., 2007, Unusual Holocene alluvial record from Rio del Oso, Jemez Mountains, New Mexico: Paleoclimatic and archaeologic significance, *in* Kues, B.S., Kelley, S.A., and Lueth, V.W., eds., Geology of the Jemez Region II: New Mexico Geological Society Guidebook 58, p. 459-468.

Hall, S.A., and Peterson, J.A., 2013, Floodplain construction of the Rio Grande at El Paso, Texas, USA: Response to Holocene climate change: Quaternary Science Reviews, v. 65, p. 102–119.

Hall, S.A., and Riskind, D.H., 2010, Palynology, radiocarbon dating, and woodrat middens: New applications at Hueco Tanks, Trans-Pecos Texas, USA: Journal of Arid Environments, v. 74, p. 725–730.

Hall, S.A., and Rittenour, T.M., 2010, Optical dating and New Mexico prehistory, *in* Brown, E.J., Armstrong, K., Brugge, D.M., and Condie, C.J., eds., Threads, Tints, and Edification; Papers in Honor of Glenna Dean: Archaeological Society of New Mexico, No. 36, p. 101–110.

Hall, S.A., and Valastro, S., Jr., 1995, Grassland vegetation in the Southern Great Plains during the last glacial maximum: Quaternary Research, v. 44, p. 237–245.

Haynes, C.V., Jr., 2008, Younger Dryas "black mats" and the Rancholabrean termination in North America: Proceedings of the National Academy of Science of the United States of America 105(18):6520- 6525.

Heilen, M., Leckman, P.O., Byrd, A., Homburg, J.A., and Heckman, R.A., 2013, Archaeological sensitivity modeling in southern New Mexico: Automated tools and models for planning and management: Albuquerque, Statistical Research, Inc., Technical Report 11-26.

Heilen, M., and Murrell, M.L., 2015, An assessment of transect recording unit survey and subsurface testing methods at four sites in the Permian Basin, New Mexico: Albuquerque, Statistical Research, Inc., Technical Report 15-68.

Hendrickson, G.E., and Jones, R.S., 1952, Geology and Ground-Water Resources of Eddy County, New Mexico: New Mexico Bureau of Mines & Mineral Resources, Ground-Water Report 3, 169 p.

Hogan, P.F., 2006, Development of southeastern New Mexico regional research design and cultural resource management strategy: Albuquerque, Office of Contract Archeology, University of New Mexico, Report No. 185-849, 230 p.

Holliday, V.T., 1988, Genesis of a late-Holocene soil chronosequence at the Lubbock Lake archaeological site, Texas: Annals of the Association of American Geographers, v. 78, p. 594–610.

Holliday, V.T., 1997, Paleoindian Geoarchaeology of the Southern High Plains: Austin, University of Texas Press, 297 p.

Holliday, V.T., 2001, Stratigraphy and geochronology of Upper Quaternary eolian sand on the Southern High Plains of Texas and New Mexico, United States: Geological Society of America Bulletin, v. 113, p. 88–108.

Holliday, V.T., 2004, Soils in Archaeological Research: Oxford, Oxford University Press, 448 p.

Hubricht, L., 1985, The Distribution of the Native Land Mollusks of the Eastern United States: Field Museum of Natural History, Fieldiana, Zoology, New Series No. 24, 191 p.

Huffington, R.M., and Albritton, C.C., Jr., 1941, Quaternary sands on the Southern High Plains of western Texas: American Journal of Science, v. 239, no. 5, p. 325-338.

Huntley, D.J., and Lamothe, M., 2001, Ubiquity of anomalous fading in K-feldspars and the measurement and correction for it in optical dating: Canadian Journal of Earth Sciences, v. 38, p. 1093–1106.

Ingbar, E., Sebastian, L., Altschul, J., Hopkins, M., Eckerle, W., Robinson, P., Judson Finley, J., Hall, S., Hayden, W., Rohe, C.M., Seaman, T., Taddie, S., and Thompson, S., 2005, Adaptive Management and Planning Models for Cultural Resources in Oil and Gas Fields in New Mexico and Wyoming: Carson City, Gnomon, Inc., 528 p. (PUMP III project)

Jeter, H.W., 2000, Determining the ages of recent sediments using measurements of trace radioactivity: Terra et Aqua, v. 78, p. 1–11.

Johnson, D.L., 1997, Geomorphological, geoecological, geoarchaeological and surficial mapping study of McGregor Guided Missile Range, Fort Bliss, New Mexico: Plano, Geo-Marine, Inc., Miscellaneous Report of Investigations No. 157, 412 p.

Katz, S.R. and Katz, P., 2001, Prehistory of the Pecos Country, Southeastern New Mexico, *in* Katz, S.R. and Katz, P., eds., The Archaeological Record of Southern New Mexico: Sites and Sequences of Prehistory, Part III: New Mexico Historic Preservation Division, Office of Cultural Affairs, Santa Fe, NM, 162 p.

Kavouoras, I.G., Etyemezian, V., Xu, J., DuBois, D.W., Green, M., and Pitchford, M., 2007, Assessment of the local windblown component of dust in the western United States: Journal of Geophysical Research, v. 112, D08211,doi:10.1029/2006JD007832,2007, 13 p.

Kelley, V.C., 1971, Geology of the Pecos Country, Southeastern New Mexico: New Mexico Bureau of Mines & Mineral Resources Memoir 24, 78 p.

Konert, M., and Vandenberghe, J., 1997, Comparison of laser grain size analysis with pipette and sieve analysis: A solution for the underestimation of the clay fraction: Sedimentology, v. 44, p. 523–535.

Kremkau, S.H., Zeigler, K.E., and Vierra, B.J., 2013, The Geologic and Archaeological Contexts for Lithic Resource Acquisition in Southeastern New Mexico: Albuquerque, Statistical Research, Inc., Technical Report 13-39.

Kutzbach, J.E., and T. Webb III, 1993, Conceptual basis for understanding Late-Quaternary climates, *in* Wright, H.E., Jr., Kutzbach, J.E., Webb, T. III, Ruddiman, W.F., Street-Perrott, F.A., and Bartlein, P.J., eds., Global Climates since the Late Glacial Maximum: Minneapolis, University of Minnesota Press, p. 5-11.

Lamb, H.H., 1965, The early Medieval Warm Epoch and its sequel: Palaeogeography, Palaeoclimatology, Palaeoecology, v. 1, p. 13-37.

Lee, J.A., and Tchakerian, V.P., 1995, Magnitude and frequency of blowing dust on the Southern High Plains of the United States, 1947-1989: Annals of the Association of American Geographers, v. 85, p. 684-693.

Leonard, A.B., 1959, Handbook of Gastropods in Kansas: Lawrence, University of Kansas Museum of Natural History Miscellaneous Publication 20, 224 p.

Lisiecki, L.E., and Raymo, M.E., 2005, A Pliocene-Pleistocene stack of 57 globally distributed benthic $\delta^{18}O$ records: Paleoceanography, v. 20(1), PA 1003, doi:1029/2004PA001071, 2005.

Loizeau, J.-L., Arbouille, D., Santiago, S., and Vernet, J.P., 1994, Evaluation of a wide range laser diffraction grain size analyzer for use with sediments: Sedimentology, v. 41, p. 353–361.

Lucas, S.G., and Anderson, O.J., 1993, Triassic stratigraphy in southeastern New Mexico and southwestern Texas, *in* Love, D.W., Hawley, J.W., Kues, B.S., Adams, J.W., Austin, G.S., and Barker, J.M., eds., Carlsbad Region, New Mexico and West Texas: New Mexico Geological Society Guidebook 44, p. 231–235.

Luterbacher, J., 2001, The late Maunder minimum (1675-1715) climax of the "Little Ice Age" in Europe, *in* Jones, P.D., Ogilvie, A.E.J., Davies, T.D., and Briffa, K.R., eds., History and Climate, Memories of the Future: New York, Kluwer Academic/Plenum Publishers, p. 29–54.

Machenberg, M.D., 1984, Geology of Monahans Sandhills State Park, Texas: Bureau of Economic Geology, University of Texas at Austin, Guidebook 21, 39 p.

Melton, F., 1940, A tentative classification of sand dunes; Its application to dune history in the Southern High Plains: The Journal of Geology, v. 48, p. 113–174.

Metcalf, A.L., and Smartt, R.A., 1997, Land snails of New Mexico: A systematic review, *in* Metcalf, A.L., and Smartt, R.A., eds., Land Snails of New Mexico: Albuquerque, New Mexico Museum of Natural History and Science Bulletin 10, p. 1–69.

Miller, M.R., 2007, Excavations at El Arenal and other Late Archaic and Early Formative Period Sites in the Hueco Mountain Project Area of Fort Bliss, El Paso County, Texas: Directorate of Environment, Fort Bliss Garrison Command, Historic and Natural Resources Report No. 02–12, 352 p.

Montgomery, J.L., 2018, The Archaic of eastern New Mexico, *in* Vierra, B.J., ed., The Archaic Southwest: Foragers in an Arid Land: Salt Lake City, University of Utah Press, p. 156–166.

Morrison, R.B., 1967, Principles of Quaternary soil stratigraphy, *in* Morrison, R.B., and Wright, H.E., Jr. eds., Quaternary Soils: Reno, Nevada, Center for Water Resources Research, Desert Research Institute, University of Nevada, p. 1–69.

Muhs, D.R., and Holliday, V.T., 2001, Origin of late Quaternary dune fields on the Southern High Plains of Texas and New Mexico: Geological Society of America Bulletin, v. 113, p. 75-87.

Muhs, D.R., and Benedict, J.B., 2006, Eolian additions to late Quaternary alpine soils, Indian Peaks Wilderness Area, Colorado Front Range: Arctic, Antarctic, and Alpine Research, v. 38, p. 120-130.

Munsell Color, 2009, Munsell Soil-Color Charts (revised): Grand Rapids, Munsell Color.

Murray, A.S., and Funder, S., 2003, Optically stimulated luminescence dating of a Danish Eemian coastal marine deposit: a test of accuracy: Quaternary Science Reviews, v. 22, p. 1177–1183.

Murray, A.S., and Wintle, A.G., 2000, Luminescence dating of quartz using an improved single-aliquot regenerative-dose protocol: Radiation Measurements, v. 32, p. 57–73.

Murray, A.S., and Wintle, A.G., 2003, The single aliquot regenerative dose protocol: Potential for improvements in reliability: Radiation Measurements, v. 37, p. 377–381.

Murray, A.S., Wintle, A.G., and Wallinga, J., 2002, Dose estimation using quartz OSL in the non-linear region of the growth curve: Radiation Protection Dosimetry, v. 101, p. 371–374.

Neuendorf, K.K.E., Mehl, J.P. Jr., and Jackson, J.A., eds., 2005, Glossary of Geology (5th edition): Washington, D.C., American Geological Institute, 779 p.

New Mexico Bureau of Geology and Mineral Resources, 2003, Geologic Map of New Mexico: New Mexico Bureau of Geology and Mineral Resources, 2 sheets, 1:500,000.

Nicholson, A., Jr. and Clebsch, A., Jr., 1961, Geology and Ground-Water Conditions in Southern Lea County, New Mexico: State Bureau of Mines and Mineral Resources, Ground-Water Report 6, 123 p.

North American Commission on Stratigraphic Nomenclature, 1983, North American stratigraphic code: American Association of Petroleum Geologists Bulletin, v. 67, no. 5, p. 841–875.

North American Commission on Stratigraphic Nomenclature, 2005, North American stratigraphic code: American Association of Petroleum Geologists Bulletin, v. 89, no. 11, p. 1547–1591.

O'Leary, M.H., 1988, Carbon isotopes in photosynthesis: BioScience, v. 38, no. 5, p. 328–336.

Pederson, J.L., and Dehler, C.M., 2004a, Preliminary Geologic Map of the Loving 7.5-Minute Quadrangle: New Mexico Bureau of Geology and Mineral Resources OF-GM 077 (draft), 1 sheet, 1:24,000.

Pederson, J.L., and Dehler, C.M., 2004b, Geologic Map of the Loving Quadrangle, Eddy County, New Mexico: New Mexico Bureau of Geology and Mineral Resources OF-GM 077, 6 p.

Peterson, R.S., and Boyd, C.S, 1998, Ecology and management of sand shinnery communities: A literature review: U.S. Department of Agriculture, Forest Service, General Technical Report RMRS-GTR-16, 44 p.

Polyak, V.J., and Asmerom, Y., 2001, Late Holocene climate and cultural changes in the southwestern United States: Science, v. 294, p. 148–151.

Polyak, V.J., Cokendolpher, J.C., Norton, R.A., and Asmerom, Y., 2001, Wetter and cooler Late Holocene climate in the southwestern United States from mites preserved in stalagmites: Geology, v. 29, p. 643–646.

Powers, D.W., and Holt, R.M., 1993, The upper Cenozoic Gatuña Formation of southeastern New Mexico, *in* Love, D.W., Hawley, J.W., Kues, B.S., Adams, J.W., Austin, G.S., and Barker, J.M., eds., Carlsbad Region, New Mexico and West Texas: New Mexico Geological Society Guidebook 44, p. 271–282.

Prescott, J.R. and Hutton, J.T., 1994, Cosmic ray contributions to dose rates for luminescence and ESR dating: Large depths and long-term time variations: Radiation Measurements, v. 23, p. 497–500.

Railey, J.A., 2016, Archaeology and Native American Cultural Resources: Permian Basin Research Design 2016-2026, Vol. I: Albuquerque, SWCA Environmental Consultants, Inc., and Carlsbad Field Office, Bureau of Land Management, 545 p.

Railey, J.A., Rissetto, J., and Bandy, M.S., 2009, Synthesis of excavation data for the Permian Basin mitigation program: Carlsbad Field Office, Bureau of Land Management; Albuquerque, SWCA Environmental Consultants.

Rasmussen, J.B.T., Polyak, V.J., and Asmerom, Y., 2006, Evidence for Pacific-modulated precipitation variability during the Late Holocene from the southwestern USA: Geophysical Research Letters, v. 33, L08701, doi:10.1029/2006GL025714.

Reeves, C.C., Jr., 1976, Quaternary stratigraphy and geologic history of the southern High Plains, Texas and New Mexico, *in* Mahaney, W.C., ed., Quaternary Stratigraphy of North America: Stroudsburg, PA, Dowden, Hutchinson, and Ross, Inc., p. 213–234.

Reheis, M.C., 2006, A 16-year record of eolian dust in southern Nevada and California, USA: Controls on dust generation and accumulation: Journal of Arid Environments, v. 67, p. 487-520.

Reheis, M.C., Budahn, J.R., Lamothe, P.J., 2002, Geochemical evidence for diversity of dust sources in the southwestern United States: Geochim. Cosmochim. Acta, v. 66, p. 1569–1587.

Reimer P.J., Bard, E., Bayliss, A., Beck, J.W., Blackwell, P.G., Bronk, R.C., Buck, C.E., Cheng, H., Edwards, R.L., Friedrich, M., Grootes, P.M., Guilderseon, T.P., Haflidason, H., Hajdas, I., Hatté, C., Heaton, T.J., Hogg, A.G., Hughen, K.A., Kaiser, K.F., Kromewr, B., Manning, S.W., Niu, M., Reimer, R.W., Richards, D.A., Scott, E.M., Southon, J.R., Turney, C.S.M., and van der Plicht, J., 2013, IntCal13 and marine13 radiocarbon age calibration curves 0-50,000 years cal BP: Radiocarbon, v. 55, no. 4, p. 1869–1887.

Rich, J., 2013, A 250,000-year record of lunette dune accumulation of the Southern High Plains, USA and implications for past climates: Quaternary Science Reviews, v. 62, p. 1–20.

Rich, J., and Stokes, S., 2011, A 200,000-year record of Late Quaternary eolian sedimentation on the Southern High Plains and nearby Pecos River Valley, USA: Aeolian Research, v. 2, p. 221–240.

Rodnight, H., 2008, How many equivalent dose values are needed to obtain a reproducible distribution? Ancient TL, v. 26, p. 3–9.

Rosholt, J.N., and McKinney, C.R., 1980, Uranium trend dating of surficial deposits and gypsum spring deposit near WIPP site, New Mexico, Part II, *in* Szabo, B.J., Gottschall, W.C., Rosholt, J.N., and McKinney, Uranium Series Disequilibrium Investigations Related to the WIPP Site, New Mexico: U.S. Geological Survey Open-File Report 80-879, p. 7–20.

Ruhe, R.V., 1965, Quaternary paleopedology, *in* Wright, H.E., Jr., and Frey, D.G., eds, The Quaternary of the United States: Princeton, Princeton University Press, p. 755–764.

Sebastian, L. and Larralde, S., 1989, Living on the Land: 11,000 Years of Human Adaptation in Southeastern New Mexico: New Mexico Bureau of Land Management, Cultural Resource Series No. 6, 174 p.

Šibrava, V., Bowen, D.Q., and Richmond, G.M., eds., 1986, Quaternary Glaciations in the Northern Hemisphere; Report of the International Geological Correlation Programme, Project 24 (International Union of Geological Sciences and UNESCO): Quaternary Science Reviews, v. 5, nos. 2/3, 514 p.

Simpson, S., 2010, A Data Recovery of Seven Archaeological Sites at the Tony Federal Wells: Carlsbad, Mesa Field Service Report No. 893, 472 p.

Soil Science Society of America, 1997, Glossary of Soil Science Terms: Madison, Soil Science Society of America, 134 p.

Steffensen, J.P., Andersen, K.K., Bigler, M., Clausen, H.B., Dahl-Jensen, D., Fischer, H., Goto-Azuma, K., Hansson, M., Johnsen, S.J., Jean Jouzel, J., Masson-Delmotte, V., Popp, T., Rasmussen, S.O., Röthlisberger, R., Ruth, U., Stauffer, B., Siggaard-Andersen, M.-L., Sveinbjörnsdóttir, A.E., Svensson, A., White, J.W.C., 2008, High-resolution Greenland ice core data show abrupt climate change happens in few years: Science, v. 321 (1 Aug 2008), p. 680-684.

Telford, R.J., Heegaard, E., and Birks, H.J.B., 2004, The intercept is a poor estimate of a calibrated radiocarbon age: The Holocene, v. 14, p. 296–298.

Thiel, C., Buylaert, J.-P., Murray, A., Terhorst, B., Hofer, I., Tsukamoto, S., and Frechen, M., 2011, Luminescence dating of the Stratzing loess profile (Austria)—Testing the potential of an elevated temperature post-IR IRSL protocol: Quaternary International, v. 234, p. 23–31.

Turner, M.T., Cox, D.N., Mickelson, B.C., Roath, A.J., and Wilson, C.D., 1974, Soil Survey of Lea County, New Mexico: U.S. Department of Agriculture, Soil Conservation Service, 89 p., 169 sheets.

Valentine, K.W.G., and Dalrymple, J.B., 1976, Quaternary buried paleosols: A critical review: Quaternary Research, v. 6, p. 209–222.

Vine, J.D., 1963, Surface geology of the Nash Draw Quadrangle, Eddy County, New Mexico: U.S. Geological Survey Bulletin 1141-B, 46 p.

Weaver, J.E., and Albertson, F.W., 1956, Grasslands of the Great Plains, Their Nature and Use: Lincoln, Johnsen Publishing Co., 395 p.

Wendorf, F., Krieger, A.D., and Albritton, C.C., 1955, The Midland Discovery, A Report on the Pleistocene Human Remains from Midland, Texas: Austin, University of Texas Press, 139 p.

Wentworth, C.K., 1922, A scale of grade and class terms for clastic sediments: Journal of Geology, v. 30, p. 377–392.

Wintle, A.G. and Murray, A.S., 2006, A review of quartz optically stimulated luminescence characteristics and their relevance in single-aliquot regeneration dating protocols: Radiation Measurements, v. 41, p. 369–391.

Wiseman, R.N., ed., 2016, Prehistoric Camps along Lower Nash Draw: The NM 128 Project in Eastern Eddy County, New Mexico, Vol. 1 and 2: Santa Fe, New Mexico Department of Cultural Affairs, Office of Archaeological Studies, Archaeology Notes 398, and New Mexico Department of Transportation Technical Series 2015-4, 1047 p. (Loc. 7, 8, 9, 10, 29)

Wong, C.I., Banner, J.L., and Musgrove, M., 2015, Holocene climate variability in Texas, USA: An integration of existing paleoclimate data and modeling with a new, high-resolution speleothem record: Quaternary Science Reviews, v. 127, p. 155–173.

APPENDIX A.
OSL DATES AND LABORATORY DATA

The OSL samples were processed by Dr. Ronald J. Goble at the University of Nebraska, Lincoln; Dr. Richard Kettler, University of Nebraska, Lincoln, did the OSL samples from Loc. 31. The geographic coordinates of sample localities are listed in Table 1.3.

Table A-1. Locality 1; loc. 1 in Hall, 2002a, b; Hall and Goble, 2006, 2008, 2012; revised ages in Hall and Goble, 2011a; samples collected 2001

UNL No.	Burial Depth (m)	H_2O (%)	K_2O (%)	U (ppm)	Th (ppm)	Cosmic (Gy)	Dose Rate (Gy/ka)	D_e (Gy)	No. Aliquots	Age (ka)
Lower eolian sand unit; type section of Berino paleosol										
248	1.60	2.5	0.71	0.6	2.2	0.21	1.06 ± 0.06	86.4 ± 2.0	39	81.2 ± 5.70
247	2.80	2.7	0.76	0.5	2.0	0.18	1.03 ± 0.06	93.8 ± 2.6	42	90.7 ± 6.70

Table A-2. Locality 2; loc. 8 in Hall, 2002a, b; Hall and Goble, 2006, 2008; revised ages in Hall and Goble, 2011a; samples collected 2001

UNL No.	Burial Depth (m)	H_2O (%)	K_2O (%)	U (ppm)	Th (ppm)	Cosmic (Gy)	Dose Rate (Gy/ka)	D_e (Gy)	No. Aliquots	Age (ka)
Upper eolian sand unit with clay bands										
250	1.35	2.7	0.59	0.4	1.0	0.21	0.84 ± 0.05	4.90 ± 0.06	55	5.82 ± 0.41
249	4.55	2.9	0.73	0.6	1.8	0.14	0.98 ± 0.06	9.23 ± 0.17	53	9.39 ± 0.67

Table A-3. Locality 4; loc. 13 in Hall, 2002a, b; Hall, Goble, and Jeter, 2003; Hall and Goble, 2016g; samples collected 2001

UNL No.	Burial Depth (m)	H_2O (%)	K_2O (%)	U (ppm)	Th (ppm)	Cosmic (Gy)	Dose Rate (Gy/ka)	D_e (Gy)	No. Aliquots	Age (ka)
Coppice dune; associated cesium-137 and radiocarbon age										
361	0.24	3.5	0.95	0.7	2.8	0.25	1.35 ± 0.08	0.123 ± 0.005	116	0.091 ± 0.007
Single Aliquot Minimum Age Model (Galbraith et al., 1999)								0.093 ± 0.011		0.070 ± 0.010
Single Grain Minimum Age Model (Galbraith et al., 1999)								0.111 ± 0.009	276	0.082 ± 0.009
360	0.84	0.8	1.0	0.7	2.8	0.23	1.41 ± 0.08	0.151 ± 0.004	78	0.107 ± 0.008

Table A-4. Locality 5; Hall, 2010a; Hall and Goble, 2011a; samples collected 2009

UNL No.	Burial Depth (m)	H_2O (%)	K_2O (%)	U (ppm)	Th (ppm)	Cosmic (Gy)	Dose Rate (Gy/ka)	D_e (Gy)	No. Aliquots	Age (ka)
Post-Upper eolian sand unit										
2623	0.23	0.3	0.78 ± 0.03	1.33 ± 0.05	3.07 ± 0.20	0.25	1.43 ± 0.06	2.04 ± 0.16	48	1.43 ± 0.13
Minimum Age Model (Galbraith et al., 1999)								0.89 ± 0.04		0.62 ± 0.04
Upper eolian sand unit										
2622	0.55	0.4	0.69 ± 0.03	1.29 ± 0.05	2.77 ± 0.20	0.24	1.31 ± 0.05	9.38 ± 0.23	45	7.18 ± 0.32
2621	0.89	0.4	0.71 ± 0.03	0.99 ± 0.04	2.54 ± 0.20	0.22	1.22 ± 0.05	17.0 ± 0.40	48	13.9 ± 0.60
2620	1.27	0.6	0.83 ± 0.03	1.21 ± 0.05	3.07 ± 0.20	0.21	1.40 ± 0.05	24.0 ± 0.50	47	17.3 ± 0.70
Lower eolian sand unit										
2625	2.08	0.6	0.76 ± 0.04	1.55 ± 0.06	3.43 ± 0.24	0.19	1.43 ± 0.05	87.2 ± 2.70	42	61.1 ± 3.00
2624	2.68	0.5	0.54 ± 0.03	1.22 ± 0.05	2.33 ± 0.19	0.18	1.07 ± 0.04	93.3 ± 2.70	38	87.0 ± 4.20

Table A-5. Locality 6; Hall and Goble, 2015a; samples collected 2014

UNL No.	Burial Depth (m)	H_2O (%)	K_2O (%)	U (ppm)	Th (ppm)	Cosmic (Gy)	Dose Rate (Gy/ka)	D_e (Gy)	No. Aliquots	Age (ka)
White eolian sand unit derived from playa shoreline deposits										
3954	1.86	3.6	0.55 ± 0.04	0.72 ± 0.09	1.95 ± 0.21	0.20	0.94 ± 0.05	19.57 ± 0.40	51	20.9 ± 1.1
3955	0.97	4.7	0.47 ± 0.04	0.81 ± 0.09	2.25 ± 0.26	0.22	0.92 ± 0.05	11.03 ± 0.25	53	11.9 ± 0.7
Holocene eolian sand										
3956	1.48	3.5	0.58 ± 0.04	0.79 ± 0.09	2.23 ± 0.22	0.21	1.01 ± 0.05	9.38 ± 0.32	52	9.32 ± 0.55
Eolian cover sand										
3957	0.43	4.1	0.60 ± 0.04	1.01 ± 0.10	2.68 ± 0.26	0.24	1.13 ± 0.05	0.56 ± 0.04	58	0.50 ± 0.04
Minimum Age Model (Galbraith et al., 1999)								0.26 ± 0.08		0.23 ± 0.08
Lower eolian sand unit										
3958	2.23	10.0	0.97 ± 0.04	0.99 ± 0.09	4.16 ± 0.27	0.19	1.38 ± 0.06	80.52 ± 1.90	60	58.5 ± 2.9

Table A-6. Locality 7; Hall and Goble, 2016a; revised ages in Hall and Goble, 2012; samples collected 2007

UNL No.	Burial Depth (m)	H_2O (%)	K_2O (%)	U (ppm)	Th (ppm)	Cosmic (Gy)	Dose Rate (Gy/ka)	D_e (Gy)	No. Aliquots	Age (ka)
Lower eolian sand unit										
1995	1.67	2.3	1.04	0.7	3.9	0.20	1.47 ± 0.07	86.59 ± 2.15	50	59.1 ± 3.5
1996	1.36	0.7	1.01	0.7	3.8	0.21	1.47 ± 0.08	76.89 ± 2.07	51	52.2 ± 3.1
Early Late Holocene eolian sand										
1997	1.09	1.3	0.75	0.5	2.4	0.22	1.12 ± 0.05	4.76 ± 0.02	50	4.26 ± 0.24
Los Medaños eolian sand										
1998	0.62	0.2	0.69	0.5	2.1	0.23	1.07 ± 0.05	2.33 ± 0.02	50	2.18 ± 0.12
1999	0.26	0.9	0.57	0.4	1.6	0.24	0.91 ± 0.05	1.92 ± 0.03	51	2.11 ± 0.13

Table A-7. Locality 8; Hall and Goble, 2016a; samples collected 2007

UNL No.	Burial Depth (m)	H_2O (%)	K_2O (%)	U (ppm)	Th (ppm)	Cosmic (Gy)	Dose Rate (Gy/ka)	D_e (Gy)	No. Aliquots	Age (ka)
Upper eolian sand unit										
1980	0.78	1.8	1.01	0.9	4.5	0.22	1.56 ± 0.07	19.86 ± 1.00	21	12.75 ± 0.94
1981	0.39	0.6	1.00	0.8	4.0	0.23	1.52 ± 0.07	13.61 ± 0.36	26	8.94 ± 0.53
1982	0.16	0.7	0.94	0.8	3.5	0.24	1.44 ± 0.07	7.20 ± 0.37	25	4.99 ± 0.37
Site footprint										
1983	0.35	0.4	0.90	0.7	3.1	0.24	1.37 ± 0.06	5.72 ± 0.35	23	4.19 ± 0.34

Table A-8. Locality 9; Hall and Goble, 2016a; samples collected 2007

UNL No.	Burial Depth (m)	H_2O (%)	K_2O (%)	U (ppm)	Th (ppm)	Cosmic (Gy)	Dose Rate (Gy/ka)	D_e (Gy)	No. Aliquots	Age (ka)
Eolian sand below site footprint										
1984	0.66	0.9	0.89	0.8	3.2	0.23	1.37 ± 0.06	14.66 ± 0.64	22	10.7 ± 0.7
Upper eolian sand unit										
1985	1.00	0.6	0.87	0.7	2.7	0.22	1.29 ± 0.06	15.31 ± 0.45	20	11.9 ± 0.7
1986	0.64	0.9	0.90	0.6	2.7	0.23	1.30 ± 0.06	11.97 ± 0.23	26	9.23 ± 0.53
1987	0.35	2.3	0.92	0.7	2.9	0.24	1.33 ± 0.06	8.00 ± 0.05	24	6.00 ± 0.32

Table A-9. Locality 10; Hall and Goble, 2016a; samples collected 2007

UNL No.	Burial Depth (m)	H_2O (%)	K_2O (%)	U (ppm)	Th (ppm)	Cosmic (Gy)	Dose Rate (Gy/ka)	D_e (Gy)	No. Aliquots	Age (ka)
Slope-wash colluvium										
1988	0.44	0.4	0.89	0.5	2.2	0.23	1.24 ± 0.06	6.90 ± 0.28	25	5.56 ± 0.37
1989	0.12	0.4	0.78	0.7	2.8	0.24	1.25 ± 0.06	2.91 ± 0.20	29	2.32 ± 0.20

Table A-10. Locality 11; Hall and Goble, 2011b; samples collected 2008

UNL No.	Burial Depth (m)	H_2O (%)	K_2O (%)	U (ppm)	Th (ppm)	Cosmic (Gy)	Dose Rate (Gy/ka)	D_e (Gy)	No. Aliquots	Age (ka)
Trench 9										
Unit 3, alluvium overlying Holocene eolian sand and Eddy paleosol										
2328	0.12	0.2	0.58	0.94	2.25	0.25	1.11 ± 0.05	0.21 ± 0.04	55	0.19 ± 0.03‡
2327	0.56	0.3	0.90	1.09	2.91	0.23	1.44 ± 0.06	0.22 ± 0.02	60	0.15 ± 0.02‡
Unit 2, eolian sand with Eddy paleosol, paired with AMS										
2326	0.76	0.3	0.94	1.06	2.98	0.23	1.47 ± 0.06	2.69 ± 0.02	36	1.83 ± 0.09
Holocene eolian sand										
2329	1.25	0.3	0.90	1.08	3.00	0.21	1.43 ± 0.06	11.96 ± 0.34	44	8.38 ± 0.48
2330	1.72	0.3	1.03	1.05	3.14	0.20	1.52 ± 0.06	18.14 ± 0.34	44	11.9 ± 0.60
Trench 8										
Unit 1, Late Pleistocene eolian sand underlying Holocene sand										
2332	2.11	2.6	1.03	1.22	3.52	0.21	1.56 ± 0.06	30.89 ± 0.93	46	19.8 ± 1.10
2331	3.14	0.4	0.91	1.16	3.01	0.18	1.42 ± 0.06	55.24 ± 1.85	35	38.8 ± 2.30

Ages with ‡ symbol are calculated by Minimum Age Model; Galbraith et al., 1999

Table A-11. Locality 12; Hall and Goble, 2011b; samples collected 2008

UNL No.	Burial Depth (m)	H_2O (%)	K_2O (%)	U (ppm)	Th (ppm)	Cosmic (Gy)	Dose Rate (Gy/ka)	D_e (Gy)	No. Aliquots	Age (ka)
Trench 1										
Unit 2A, Holocene eolian sand with Eddy paleosol upper 20 cm; lower age equivalent to Upper eolian sand unit										
2320	0.10	0.4	0.80	0.98	2.75	0.25	1.34 ± 0.06	4.91 ± 0.17	38	3.67 ± 0.22
2319	0.62	0.3	0.74	0.89	2.34	0.23	1.22 ± 0.05	8.01 ± 0.20	39	6.55 ± 0.38
2318	1.16	0.2	0.73	0.91	2.43	0.22	1.22 ± 0.05	9.22 ± 0.24	56	7.58 ± 0.44
2317	1.74	0.3	0.86	1.01	2.76	0.20	1.35 ± 0.06	12.45 ± 0.06	39	9.19 ± 0.46
Unit 1, Late Pleistocene eolian sand underlying Holocene sand; age equivalent to Middle eolian sand unit										
2316	2.42	0.4	0.97	1.35	3.60	0.18	1.58 ± 0.06	36.89 ± 0.85	47	23.4 ± 1.3
Trench 6										
Unit 3, alluvium overlying eolian sand and Eddy paleosol										
2323	0.10	0.3	0.93	0.95	2.51	0.25	1.42 ± 0.06	0.22 ± 0.02	55	0.15 ± 0.01‡
2322	0.26	0.4	0.56	0.81	1.90	0.24	1.03 ± 0.05	0.22 ± 0.02	50	0.21 ± 0.02‡
Unit 2B, Holocene eolian sand with Eddy paleosol, paired with AMS										
2321	0.44	0.5	0.98	1.04	3.00	0.24	1.51 ± 0.06	1.80 ± 0.07	44	1.20 ± 0.08
2325	0.88	0.4	0.95	1.11	2.95	0.22	1.49 ± 0.06	2.93 ± 0.14	45	1.97 ± 0.13
Eolian sand beneath Eddy paleosol, late Holocene										
2324	1.07	0.4	1.08	1.29	3.31	0.22	1.66 ± 0.06	4.20 ± 0.18	41	2.53 ± 0.16

Ages with ‡ symbol are calculated by Minimum Age Model; Galbraith et al., 1999

Table A-12. Locality 13; Hall and Goble, 2011b; samples collected 2008

UNL No.	Burial Depth (m)	H_2O (%)	K_2O (%)	U (ppm)	Th (ppm)	Cosmic (Gy)	Dose Rate (Gy/ka)	D_e (Gy)	No. Aliquots	Age (ka)
Cover sand										
2333	0.15	2.8	0.67	0.51	1.76	0.25	1.02 ± 0.05	0.14 ± 0.04	50	0.14 ± 0.04‡
Los Medaños sand										
2334	1.12	0.1	0.82	0.72	2.15	0.22	1.22 ± 0.05	2.32 ± 0.02	40	1.90 ± 0.10
Late Holocene eolian sand										
2335	1.69	0.2	0.93	0.93	2.77	0.20	1.39 ± 0.06	6.21 ± 0.14	48	4.48 ± 0.24

Ages with ‡ symbol are calculated by Minimum Age Model; Galbraith et al., 1999

Table A-13. Locality 14; Hall and Goble, 2015b; samples collected 2014

UNL No.	Burial Depth (m)	H_2O (%)	K_2O (%)	U (ppm)	Th (ppm)	Cosmic (Gy)	Dose Rate (Gy/ka)	D_e (Gy)	No. Aliquots	Age (ka)
Eddy paleosol, BHT-1										
3976	0.15	0.6	0.72 ± 0.04	0.74 ± 0.10	3.06 ± 0.25	0.25	1.25 ± 0.06	2.52 ± 0.12	55	2.02 ± 0.13
Minimum Age Model (Galbraith et al., 1999)								1.12 ± 0.15		0.90 ± 0.13
3977	0.21	0.5	0.67 ± 0.04	0.68 ± 0.10	2.96 ± 0.27	0.25	1.19 ± 0.06	2.75 ± 0.14	50	2.32 ± 0.16
Minimum Age Model (Galbraith et al., 1999)								1.62 ± 0.02		1.36 ± 0.07
Holocene eolian sand , BHT-1										
3978	0.49	0.8	0.69 ± 0.04	0.87 ± 0.10	2.94 ± 0.29	0.24	1.23 ± 0.06	5.57 ± 0.17	53	4.54 ± 0.25
3979	0.62	1.5	0.73 ± 0.04	0.96 ± 0.10	3.09 ± 0.27	0.24	1.28 ± 0.06	8.59 ± 0.30	52	6.71 ± 0.38
3980	0.80	0.7	0.75 ± 0.04	1.17 ± 0.10	3.39 ± 0.29	0.23	1.38 ± 0.06	12.88 ± 0.50	52	9.34 ± 0.55
3981	0.91	0.7	0.80 ± 0.04	1.11 ± 0.10	3.54 ± 0.28	0.23	1.41 ± 0.06	13.21 ± 0.46	60	9.34 ± 0.52
Holocene eolian sand, BHT-2										
3982	0.59	1.0	0.87 ± 0.04	1.08 ± 0.10	3.10 ± 0.30	0.24	1.43 ± 0.06	3.95 ± 0.11	58	2.76 ± 0.14
3983	1.10	1.4	0.92 ± 0.05	1.06 ± 0.10	3.64 ± 0.31	0.22	1.49 ± 0.06	12.67 ± 0.38	58	8.51 ± 0.49

Table A-14. Locality 15; Hall and Goble, 2015a; samples collected 2014

UNL No.	Burial Depth (m)	H_2O (%)	K_2O (%)	U (ppm)	Th (ppm)	Cosmic (Gy)	Dose Rate (Gy/ka)	D_e (Gy)	No. Aliquots	Age (ka)
Holocene eolian sand										
3962	0.94	3.4	0.89 ± 0.05	0.78 ± 0.10	3.23 ± 0.30	0.22	1.33 ± 0.06	15.32 ± 0.62	50	11.5 ± 0.7
Eddy paleosol										
3963	0.40	3.6	0.85 ± 0.04	1.01 ± 0.10	2.87 ± 0.28	0.24	1.34 ± 0.06	1.90 ± 0.16	52	1.42 ± 0.13
Minimum Age Model (Galbraith et al., 1999)								0.91 ± 0.05		0.68 ± 0.05
Coppice dune sand										
3964	0.20	1.4	0.74 ± 0.04	0.93 ± 0.10	2.27 ± 0.26	0.25	1.24 ± 0.06	0.39 ± 0.05	51	0.31 ± 0.04
Minimum Age Model (Galbraith et al., 1999)								0.21 ± 0.04		0.17 ± 0.03
Middle eolian sand										
3965	1.22	11.8	1.21 ± 0.05	1.22 ± 0.11	4.77 ± 0.30	0.21	1.64 ± 0.07	39.27 ± 1.09	52	24.0 ± 1.2

Table A-15. Locality 16; Hall and Goble, 2016d; samples collected 2015

UNL No.	Burial Depth (m)	H_2O (%)	K_2O (%)	U (ppm)	Th (ppm)	Cosmic (Gy)	Dose Rate (Gy/ka)	D_e (Gy)	No. Aliquots	Age (ka)
Lower eolian sand unit										
4115	3.23	2.1	1.16 ± 0.04	0.96 ± 0.07	3.25 ± 0.23	0.16	1.56 ± 0.06	>136 ± 5	15	>87 ± 5
4116	2.61	3.8	0.73 ± 0.03	0.84 ± 0.07	3.35 ± 0.23	0.18	1.18 ± 0.05	90.3 ± 1.7	55	76.4 ± 3.4
Middle eolian sand unit										
4117	2.20	1.1	0.64 ± 0.03	0.69 ± 0.07	2.58 ± 0.20	0.19	1.06 ± 0.04	33.4 ± 0.8	58	31.4 ± 1.5
4118	1.63	2.9	0.86 ± 0.03	1.09 ± 0.08	3.30 ± 0.21	0.20	1.37 ± 0.05	28.5 ± 0.6	59	20.7 ± 0.9
Holocene eolian sand unit										
4119	1.24	1.0	0.72 ± 0.03	0.91 ± 0.07	2.73 ± 0.19	0.21	1.22 ± 0.05	9.86 ± 0.33	53	8.06 ± 0.41
4120	0.77	1.0	0.64 ± 0.03	0.69 ± 0.06	1.97 ± 0.18	0.23	1.06 ± 0.04	4.15 ± 0.13	58	3.91 ± 0.20
Eddy paleosol sand										
4121	0.56	0.8	0.63 ± 0.03	0.66 ± 0.06	2.13 ± 0.20	0.23	1.06 ± 0.04	1.64 ± 0.10	52	1.54 ± 0.11
Minimum Age Model (Galbraith et al., 1999)								1.18 ± 0.21		1.11 ± 0.21
4122	0.42	1.1	0.55 ± 0.02	0.60 ± 0.06	1.82 ± 0.18	0.24	0.96 ± 0.04	1.05 ± 0.08	55	1.09 ± 0.10
Minimum Age Model (Galbraith et al., 1999)								0.73 ± 0.05		0.76 ± 0.07
Parabolic dune sand										
4123	0.14	0.7	0.49 ± 0.02	0.64 ± 0.06	1.73 ± 0.17	0.25	0.93 ± 0.04	0.17 ± 0.02	57	0.19 ± 0.02
Minimum Age Model (Galbraith et al., 1999)								0.11 ± 0.01		0.12 ± 0.01

Table A-16. Locality 17; Hall and Goble, 2016d; samples collected 2015

UNL No.	Burial Depth (m)	H_2O (%)	K_2O (%)	U (ppm)	Th (ppm)	Cosmic (Gy)	Dose Rate (Gy/ka)	D_e (Gy)	No. Aliquots	Age (ka)
Holocene eolian sand										
4104	1.17	3.0	0.39 ± 0.03	0.53 ± 0.07	1.67 ± 0.19	0.21	0.77 ± 0.04	5.99 ± 0.13	59	7.83 ± 0.42
4105	0.81	2.2	0.38 ± 0.03	0.54 ± 0.06	1.45 ± 0.18	0.22	0.76 ± 0.04	4.55 ± 0.14	54	6.00 ± 0.43
4106	0.43	2.3	0.32 ± 0.02	0.48 ± 0.06	1.52 ± 0.16	0.24	0.72 ± 0.04	3.04 ± 0.11	50	4.26 ± 0.33
4107	0.10	2.8	0.34 ± 0.03	0.45 ± 0.06	1.28 ± 0.17	0.25	0.71 ± 0.04	1.49 ± 0.09	57	2.09 ± 0.19
Parabolic dune sand										
4108	0.80	5.6	0.29 ± 0.02	0.46 ± 0.06	1.05 ± 0.17	0.22	0.61 ± 0.03	0.36 ± 0.05	56	0.58 ± 0.08
Minimum Age Model (Galbraith et al., 1999)								0.14 ± 0.04		0.23 ± 0.07
4109	0.51	5.8	0.31 ± 0.02	0.39 ± 0.05	1.26 ± 0.15	0.23	0.63 ± 0.03	0.42 ± 0.07	56	0.66 ± 0.12
Minimum Age Model (Galbraith et al., 1999)								0.28 ± 0.04		0.44 ± 0.07
4110	0.13	6.7	0.36 ± 0.03	0.56 ± 0.06	1.36 ± 0.18	0.25	0.73 ± 0.04	0.14 ± 0.02	59	0.19 ± 0.03
Minimum Age Model (Galbraith et al., 1999)								0.070 ± 0.01		0.10 ± 0.014
Eddy paleosol, depression facies, paired with AMS										
4111	1.45	10.5	0.41 ± 0.03	0.68 ± 0.07	1.56 ± 0.19	0.21	0.74 ± 0.04	1.53 ± 0.09	55	2.07 ± 0.16
Minimum Age Model (Galbraith et al., 1999)								0.92 ± 0.08		1.24 ± 0.13
4112	1.05	4.7	0.34 ± 0.03	0.46 ± 0.06	1.40 ± 0.17	0.22	0.68 ± 0.03	0.85 ± 0.05	54	1.25 ± 0.10
4113	0.71	3.6	0.30 ± 0.02	0.46 ± 0.06	1.57 ± 0.16	0.23	0.68 ± 0.03	0.74 ± 0.05	55	1.09 ± 0.09
Minimum Age Model (Galbraith et al., 1999)								0.53 ± 0.01		0.79 ± 0.04
4114	0.46	6.4	0.30 ± 0.02	0.45 ± 0.06	1.31 ± 0.18	0.24	0.64 ± 0.04	0.63 ± 0.06	56	0.97 ± 0.10
Minimum Age Model (Galbraith et al., 1999)								0.40 ± 0.04		0.62 ± 0.07

Table A-17. Locality 18; Hall, 2010b; samples collected 2008

UNL No.	Burial Depth (m)	H_2O (%)	K_2O (%)	U (ppm)	Th (ppm)	Cosmic (Gy)	Dose Rate (Gy/ka)	D_e (Gy)	No. Aliquots	Age (ka)
Trench 4										
Eddy paleosol, depth measured from top of paleosol										
2615	0.07	0.3	0.83 ± 0.04	1.47 ± 0.05	2.63 ± 0.21	0.25	1.47 ± 0.06	1.02 ± 0.05	53	0.69 ± 0.05
Minimum Age Model (Galbraith et al., 1999)								0.44 ± 0.03		0.30 ± 0.02
2614	0.22	2.7	0.86 ± 0.04	1.65 ± 0.07	2.64 ± 0.23	0.24	1.49 ± 0.06	1.85 ± 0.10	64	1.24 ± 0.09
Minimum Age Model (Galbraith et al., 1999)								1.13 ± 0.13		0.75 ± 0.09
2613	0.37	0.6	0.90 ± 0.03	1.70 ± 0.07	2.80 ± 0.22	0.24	1.58 ± 0.06	2.88 ± 0.10	59	1.82 ± 0.09
Eolian-colluvial sand underlying Eddy paleosol										
2612	0.54	0.5	0.93 ± 0.04	1.92 ± 0.07	2.78 ± 0.22	0.23	1.66 ± 0.06	7.61 ± 0.28	41	4.59 ± 0.24
Trench 1										
Eolian-colluvial sand on hillslope										
2609	0.20	0.8	1.04 ± 0.04	2.12 ± 0.08	3.78 ± 0.25	0.24	1.86 ± 0.07	2.78 ± 0.15	47	1.49 ± 0.10
Trench 2										
Eolian-colluvial sand on hillslope										
2610	0.26	0.8	1.05 ± 0.04	1.91 ± 0.07	3.29 ± 0.23	0.24	1.79 ± 0.07	3.97 ± 0.18	44	2.22 ± 0.13
Trench 3										
Eolian-colluvial sand on hillslope										
2611	0.25	0.6	0.93 ± 0.04	1.56 ± 0.06	3.12 ± 0.22	0.24	1.60 ± 0.06	1.98 ± 0.11	54	1.24 ± 0.08
Minimum Age Model (Galbraith et al., 1999)								0.98 ± 0.04		0.61 ± 0.04

Table A-18. Locality 19; Pierce Canyon area; Hall, 2007; samples collected 2006

UNL No.	Burial Depth (m)	H_2O (%)	K_2O (%)	U (ppm)	Th (ppm)	Cosmic (Gy)	Dose Rate (Gy/ka)	D_e (Gy)	No. Aliquots	Age (ka)
Trench 1, unit 1, gray calcic eolian sand, Middle Pleistocene, Gatuña Formation										
1614	1.63	6.1	0.73	1.7	2.3	0.20	1.29 ± 0.05	218.60 ± 12.01	20	169.8 ± 12.7
1615	1.08	6.3	0.81	0.8	2.7	0.22	1.18 ± 0.05	194.40 ± 11.44	20	164.7 ± 13.0
Trench 1, unit 2, overlying eolian sand unit, Late Pleistocene equivalent to Lower sand unit										
1616	0.66	4.8	0.77	0.9	3.1	0.23	1.23 ± 0.05	72.4 ± 4.37	20	58.69 ± 4.68
Trench 14, unit 4, Early Holocene eolian sand										
1617	0.84	2.4	0.84	0.6	2.4	0.22	1.22 ± 0.05	13.92 ± 0.44	40	11.42 ± 0.69
Trench 9, unit 4, Middle Holocene eolian sand										
1618	0.86	0.5	0.88	1.2	2.7	0.22	1.42 ± 0.06	9.37 ± 0.33	23	6.58 ± 0.40
Trench 5, unit 3, Late Pleistocene eolian sand, equivalent to Middle sand unit										
1619	1.36	4.5	0.95	1.2	4.4	0.21	1.52 ± 0.06	40.49 ± 1.11	22	26.66 ± 1.54
Trench 5, unit 4, Pleistocene-Holocene eolian sand										
1620	1.10	0.8	0.78	0.8	3.1	0.22	1.27 ± 0.06	23.26 ± 1.33	21	18.38 ± 1.42
1621	0.32	1.8	1.29	1.0	2.8	0.24	1.71 ± 0.07	5.44 ± 0.44	18	3.18 ± 0.30

Table A-19. Locality 20; Hall and Goble, 2015c; samples collected 2014

UNL No.	Burial Depth (m)	H_2O (%)	K_2O (%)	U (ppm)	Th (ppm)	Cosmic (Gy)	Dose Rate (Gy/ka)	D_e (Gy)	No. Aliquots	Age (ka)
Site A										
Holocene eolian sand unit										
3923	1.05	3.2	0.90 ± 0.04	0.80 ± 0.10	3.43 ± 0.29	0.22	1.36 ± 0.06	10.77 ± 0.20	52	7.90 ± 0.38
3931	1.40	3.3	0.88 ± 0.05	1.01 ± 0.11	2.93 ± 0.28	0.21	1.35 ± 0.06	15.28 ± 0.03	48	11.3 ± 0.6
Site B										
Parabolic dune sand										
3930	0.27	5.0	0.73 ± 0.04	0.77 ± 0.10	2.77 ± 0.24	0.24	1.17 ± 0.05	0.30 ± 0.05	51	0.25 ± 0.04
Minimum Age Model (Galbraith et al., 1999)								0.25 ± 0.04		0.22 ± 0.04
3929	0.78	2.5	0.66 ± 0.04	0.75 ± 0.09	2.24 ± 0.22	0.23	1.09 ± 0.05	0.53 ± 0.04	58	0.49 ± 0.04
Minimum Age Model (Galbraith et al., 1999)								0.30 ± 0.02		0.28 ± 0.02
Eddy paleosol										
3927	1.28	2.7	0.69 ± 0.04	0.81 ± 0.10	2.27 ± 0.27	0.21	1.11 ± 0.05	1.50 ± 0.08	55	1.35 ± 0.10
Minimum Age Model (Galbraith et al., 1999)								1.17 ± 0.06		1.06 ± 0.07
3928	1.77	2.7	0.81 ± 0.04	0.72 ± 0.10	2.85 ± 0.24	0.20	1.22 ± 0.06	2.26 ± 0.08	51	1.86 ± 0.11
Holocene eolian sand unit										
3926	2.25	3.1	0.77 ± 0.04	0.89 ± 0.10	2.88 ± 0.29	0.19	1.21 ± 0.06	4.11 ± 0.09	51	3.39 ± 0.17
3925	2.77	3.0	0.84 ± 0.04	0.85 ± 0.09	2.95 ± 0.27	0.17	1.26 ± 0.06	12.18 ± 0.36	53	9.71 ± 0.52
Middle eolian sand unit										
3924	3.07	10.7	1.40 ± 0.05	1.41 ± 0.12	5.96 ± 0.37	0.17	1.88 ± 0.08	40.79 ± 0.87	53	21.7 ± 1.0

Table A-20. Locality 21; Hall and Goble, 2016f; OSL dates were not determined although the preliminary laboratory measurements were carried out.

UNL No.	Burial depth (m)	H_2O (%)	K_2O (%)	U (ppm)	Th (ppm)
Trench 1, parabolic dune sand					
4172	0.43	1.9	0.77 ± 0.03	0.65 ± 0.07	2.05 ± 0.19
4173	0.16	1.5	0.87 ± 0.03	0.85 ± 0.07	2.33 ± 0.21
Trench 1, Holocene eolian sand, Unit 3					
4174	0.61	2.9	0.84 ± 0.03	0.72 ± 0.07	1.98 ± 0.19
4175	1.05	1.4	0.80 ± 0.03	0.67 ± 0.07	2.07 ± 0.20
4176	1.47	1.0	0.84 ± 0.03	0.56 ± 0.06	2.30 ± 0.20
Trench 1, Pleistocene eolian sand, Unit 2b					
4177	1.87	1.6	0.88 ± 0.03	0.74 ± 0.07	2.30 ± 0.21
Trench 1, Pleistocene eolian sand, Unit 2a					
4178	2.35	1.1	0.81 ± 0.03	0.59 ± 0.06	2.08 ± 0.20
4179	2.69	1.6	1.02 ± 0.03	0.83 ± 0.07	2.90 ± 0.22
Trench 6, Pleistocene eolian sand, Unit 2					
4180	0.60	6.3	1.14 ± 0.04	1.22 ± 0.08	4.81 ± 0.25
Trench 2, Holocene eolian sand and Eddy paleosol†, Unit 3					
4181	0.40†	5.7	0.89 ± 0.03	0.84 ± 0.07	3.22 ± 0.21
4182	0.21†	5.6	0.93 ± 0.03	0.99 ± 0.08	3.11 ± 0.24
4183	0.66†	5.2	0.88 ± 0.03	0.88 ± 0.07	2.76 ± 0.21
4184	0.93	4.9	0.84 ± 0.03	0.71 ± 0.07	2.56 ± 0.20
4185	1.20	4.8	0.85 ± 0.03	0.73 ± 0.07	2.24 ± 0.20
Trench 2, Middle eolian sand, Unit 1					
4186	1.35	13.8	1.07 ± 0.03	1.20 ± 0.09	4.34 ± 0.28
Trench 8, base of Pleistocene sand fill in solution pipe, Unit 2					
4187	2.95	2.1	0.93 ± 0.03	0.80 ± 0.07	2.58 ± 0.20

Analyses by Dr. Ronald J. Goble, Department of Earth and Atmospheric Sciences, University of Nebraska-Lincoln.

Table A-21. Locality 22; Hall and Goble, 2016b; samples collected 2015

UNL No.	Burial Depth (m)	H_2O (%)	K_2O (%)	U (ppm)	Th (ppm)	Cosmic (Gy)	Dose Rate (Gy/ka)	D_e (Gy)	No. Aliquots	Age (ka)
Parabolic dune sand										
4066	0.35	4.7	0.70 ± 0.04	0.66 ± 0.09	2.42 ± 0.28	0.24	1.10 ± 0.05	0.34 ± 0.04	65	0.31 ± 0.04
Minimum Age Model (Galbraith et al., 1999)								0.21 ± 0.02		0.19 ± 0.02
Holocene eolian sand unit										
4067	0.88	1.4	0.76 ± 0.04	0.76 ± 0.09	2.28 ± 0.25	0.22	1.19 ± 0.05	5.01 ± 0.18	53	4.20 ± 0.24
4068	1.46	1.0	0.86 ± 0.04	0.69 ± 0.09	2.50 ± 0.28	0.21	1.26 ± 0.06	15.59 ± 0.24	51	12.4 ± 0.60
Middle eolian sand unit										
4069	2.14	3.7	0.84 ± 0.04	0.91 ± 0.10	3.58 ± 0.35	0.19	1.32 ± 0.06	34.51 ± 0.72	50	26.2 ± 1.3
4070	1.14	4.7	0.78 ± 0.03	1.00 ± 0.09	2.93 ± 0.21	0.21	1.26 ± 0.05	27.05 ± 0.53	53	21.6 ± 1.0

Table A-22. Locality 23; Hall, 2010c; samples collected 2008

UNL No.	Burial Depth (m)	H_2O (%)	K_2O (%)	U (ppm)	Th (ppm)	Cosmic (Gy)	Dose Rate (Gy/ka)	D_e (Gy)	No. Aliquots	Age (ka)
Eolian cover sand										
2619	0.10	0.2	0.67 ± 0.03	1.36 ± 0.05	2.30 ± 0.20	0.25	1.29 ± 0.05	0.25 ± 0.03	58	0.20 ± 0.03
Minimum Age Model (Galbraith et al., 1999)								0.12 ± 0.02		0.09 ± 0.02
Loco Hills paleosol										
2618	0.10	0.2	0.74 ± 0.03	1.68 ± 0.06	2.48 ± 0.21	0.25	1.44 ± 0.05	0.93 ± 0.07	48	0.64 ± 0.06
Minimum Age Model (Galbraith et al., 1999)								0.42 ± 0.02		0.29 ± 0.02
Late Holocene eolian sand										
2617	0.38	0.3	0.77 ± 0.03	1.32 ± 0.05	2.74 ± 0.20	0.24	1.38 ± 0.05	3.98 ± 0.09	56	2.88 ± 0.13
2616	0.86	0.4	0.92 ± 0.03	1.85 ± 0.06	3.26 ± 0.22	0.22	1.65 ± 0.06	7.40 ± 0.12	43	4.48 ± 0.18

Table A-23. Locality 24; Hall and Goble, 2015a; samples collected 2014

UNL No.	Burial Depth (m)	H_2O (%)	K_2O (%)	U (ppm)	Th (ppm)	Cosmic (Gy)	Dose Rate (Gy/ka)	D_e (Gy)	No. Aliquots	Age (ka)
Glacial-age pond deposit										
3966	2.29	14.3	0.70 ± 0.04	0.90 ± 0.09	3.29 ± 0.26	0.18	1.05 ± 0.05	21.15 ± 0.59	53	20.2 ± 1.1
Late Holocene eolian sand										
3967	1.91	3.3	0.81 ± 0.05	0.77 ± 0.10	3.03 ± 0.31	0.19	1.23 ± 0.06	6.63 ± 0.14	57	5.37 ± 0.28
3970	1.59	2.6	0.59 ± 0.04	0.57 ± 0.09	1.64 ± 0.25	0.20	0.92 ± 0.05	3.00 ± 0.19	51	3.25 ± 0.26
Minimum Age Model (Galbraith et al., 1999)								2.16 ± 0.41		2.34 ± 0.45
Weak A horizon										
3968	1.07	2.7	0.70 ± 0.04	0.80 ± 0.09	2.02 ± 0.25	0.22	1.11 ± 0.05	0.50 ± 0.07	59	0.45 ± 0.06
Minimum Age Model (Galbraith et al., 1999)								0.22 ± 0.02		0.20 ± 0.02
3971	0.61	2.3	0.49 ± 0.04	0.55 ± 0.08	1.99 ± 0.24	0.23	0.89 ± 0.05	0.61 ± 0.09	56	0.68 ± 0.10
Minimum Age Model (Galbraith et al., 1999)								0.16 ± 0.04		0.18 ± 0.05
Parabolic dune sand										
3969	0.83	2.6	0.64 ± 0.04	0.76 ± 0.09	2.03 ± 0.25	0.22	1.06 ± 0.05	0.49 ± 0.09	53	0.47 ± 0.09
Minimum Age Model (Galbraith et al., 1999)								0.18 ± 0.04		0.17 ± 0.04
3972	0.44	2.2	0.53 ± 0.04	0.69 ± 0.09	2.20 ± 0.23	0.24	0.99 ± 0.05	0.39 ± 0.09	51	0.39 ± 0.09
Minimum Age Model (Galbraith et al., 1999)								0.16 ± 0.04		0.16 ± 0.04

Table A-24. Locality 25; Hall, 2013; Hall and Boggess, 2013; samples collected 2012

UNL No.	Burial Depth (m)	H_2O (%)	K_2O (%)	U (ppm)	Th (ppm)	Cosmic (Gy)	Dose Rate (Gy/ka)	D_e (Gy)	No. Aliquots	Age (ka)
Eolian cover sand										
3657	0.82	1.1	1.38 ± 0.05	0.92 ± 0.10	3.04 ± 0.25	0.23	1.81 ± 0.07	0.28 ± 0.03	50	0.15 ± 0.02
Minimum Age Model (Galbraith et al., 1999)								0.27 ± 0.03		0.14 ± 0.02
Eolian sand capped by Loco Hills paleosol										
3658	1.05	1.8	1.55 ± 0.05	0.95 ± 0.10	4.10 ± 0.24	0.22	2.01 ± 0.07	1.15 ± 0.14	52	0.57 ± 0.07
Minimum Age Model (Galbraith et al., 1999)								0.59 ± 0.03		0.30 ± 0.02
3659	1.19	2.4	1.61 ± 0.05	1.16 ± 0.11	3.98 ± 0.26	0.22	2.08 ± 0.08	2.08 ± 0.20	53	1.00 ± 0.10
Minimum Age Model (Galbraith et al., 1999)								0.78 ± 0.14		0.37 ± 0.07
Late Pleistocene-Holocene eolian sand unit										
3660	1.37	2.7	1.55 ± 0.05	1.14 ± 0.11	3.78 ± 0.24	0.21	2.00 ± 0.08	12.41± 0.54	61	6.22 ± 0.36
3661	1.72	4.1	1.69 ± 0.05	1.22 ± 0.11	4.48 ± 0.27	0.20	2.14 ± 0.08	43.02 ± 1.71	57	20.1 ± 1.1
3662	2.14	6.7	1.59 ± 0.05	1.03 ± 0.11	4.01 ± 0.25	0.19	1.91 ± 0.07	62.15 ± 1.80	53	32.5 ± 1.6

Table A-25. Locality 26; Hall and Goble, 2015a; samples collected 2014

UNL No.	Burial Depth (m)	H_2O (%)	K_2O (%)	U (ppm)	Th (ppm)	Cosmic (Gy)	Dose Rate (Gy/ka)	D_e (Gy)	No. Aliquots	Age (ka)
Coppice dune on late Holocene alluvial terrace										
3959	0.64	3.1	1.16 ± 0.05	1.19 ± 0.12	3.56 ± 0.30	0.22	1.68 ± 0.07	0.49 ± 0.06	50	0.29 ± 0.04
Minimum Age Model (Galbraith et al., 1999)								0.30 ± 0.03		0.18 ± 0.02
Late Holocene alluvial terrace, Pecos River										
3960	1.06	4.8	1.39 ± 0.05	1.84 ± 0.13	4.59 ± 0.31	0.21	2.04 ± 0.08	6.64 ± 0.17	50	3.25 ± 0.15
3961	1.97	10.4	1.89 ± 0.05	2.03 ± 0.13	6.78 ± 0.38	0.19	2.45 ± 0.10	16.29 ± 0.21	50	6.64 ± 0.28

Table A-26. Locality 27; Hall and Goble, 2016c; samples collected 2015

UNL No.	Burial Depth (m)	H_2O (%)	K_2O (%)	U (ppm)	Th (ppm)	Cosmic (Gy)	Dose Rate (Gy/ka)	D_e (Gy)	No. Aliquots	Age (ka)
Lower eolian sand unit										
4133	1.09	6.0	1.07 ± 0.04	1.09 ± 0.08	3.38 ± 0.21	0.21	1.51 ± 0.06	77.1 ± 1.5	55	51.1 ± 2.2
Pleistocene-Holocene eolian sand unit, 4136 and 4137 are paired with AMS										
4134	0.81	5.1	1.01 ± 0.03	0.91 ± 0.07	2.55 ± 0.20	0.22	1.39 ± 0.06	48.7 ± 1.4	58	35.1 ± 2.0
4135	0.57	4.6	1.01 ± 0.04	0.88 ± 0.08	2.82 ± 0.21	0.23	1.42 ± 0.06	32.2 ± 1.6	60	22.7 ± 1.4
4136	0.36	4.7	1.09 ± 0.03	1.08 ± 0.08	3.02 ± 0.21	0.24	1.54 ± 0.06	15.5 ± 0.6	59	10.0 ± 0.5
4137	0.21	4.6	1.06 ± 0.03	0.92 ± 0.08	3.07 ± 0.23	0.24	1.49 ± 0.06	13.0 ± 0.7	58	8.69 ± 0.58
Minimum Age Model (Galbraith et al., 1999)								6.84 ± 0.24		4.64 ± 0.24
Eddy paleosol, paired with AMS										
4138	0.09	4.4	1.04 ± 0.03	1.07 ± 0.09	3.06 ± 0.22	0.24	1.52 ± 0.06	5.26 ± 0.34	56	3.46 ± 0.26
Minimum Age Model (Galbraith et al., 1999)								2.23 ± 0.07		1.47 ± 0.07
Coppice dune sand, 16 cm above base										
4139	0.60	1.5	0.96 ± 0.03	0.95 ± 0.07	3.40 ± 0.22	0.22	1.48 ± 0.06	0.75 ± 0.08	65	0.50 ± 0.06
Minimum Age Model (Galbraith et al., 1999)								0.40 ± 0.04		0.27 ± 0.03

Table A-27. Locality 28; Hall and Goble, 2014; samples collected 2014

UNL No.	Burial Depth (m)	H_2O (%)	K_2O (%)	U (ppm)	Th (ppm)	Cosmic (Gy)	Dose Rate (Gy/ka)	D_e (Gy)	No. Aliquots	Age (ka)
Slope wash, alluvial-colluvial deposit exposed in arroyo										
3836	0.3	3.3	0.89 ± 0.04	1.07 ± 0.11	3.31 ± 0.27	0.25	1.49 ± 0.06	0.61 ± 0.05	59	0.41 ± 0.04
Minimum Age Model (Galbraith et al., 1999)								0.43 ± 0.03		0.29 ± 0.02
3834	0.7	0.8	0.80 ± 0.04	0.87 ± 0.10	3.79 ± 0.28	0.23	1.38 ± 0.06	5.52 ± 0.30	74	4.00 ± 0.28
Minimum Age Model (Galbraith et al., 1999)								3.30 ± 0.18		2.39 ± 0.17
3835	1.5	0.8	0.80 ± 0.04	0.92 ± 0.10	3.70 ± 0.28	0.21	1.36 ± 0.06	5.60 ± 0.22	60	4.13 ± 0.24
Minimum Age Model (Galbraith et al., 1999)								3.55 ± 0.12		2.62 ± 0.15
3837	3.0	0.7	0.89 ± 0.04	1.15 ± 0.11	3.53 ± 0.28	0.17	1.44 ± 0.06	8.66 ± 0.45	56	6.01 ± 0.41
Minimum Age Model (Galbraith et al., 1999)								6.39 ± 0.12		4.44 ± 0.19
3838	4.5	1.0	0.98 ± 0.05	1.11 ± 0.11	4.44 ± 0.31	0.14	1.54 ± 0.07	22.96 ± 1.06	95	14.9 ± 0.90
Minimum Age Model (Galbraith et al., 1999)								11.25 ± 1.6		7.30 ± 1.09
Slope wash, archaeological site										
3839	0.4	1.1	1.04 ± 0.05	0.93 ± 0.10	3.54 ± 0.28	0.24	1.58 ± 0.07	0.17 ± 0.02	59	0.11 ± 0.01
Minimum Age Model (Galbraith et al., 1999)								0.12 ± 0.01		0.08 ± 0.01
3840	0.7	2.0	1.06 ± 0.05	0.97 ± 0.11	3.93 ± 0.30	0.24	1.61 ± 0.07	5.89 ± 0.36	55	3.66 ± 0.27
Minimum Age Model (Galbraith et al., 1999)								3.16 ± 0.31		1.96 ± 0.21

Table A-28. Locality 29; Hall and Goble, 2016a; samples collected 2007

UNL No.	Burial Depth (m)	H_2O (%)	K_2O (%)	U (ppm)	Th (ppm)	Cosmic (Gy)	Dose Rate (Gy/ka)	D_e (Gy)	No. Aliquots	Age (ka)
Eolian sand fill in a solution pipe										
1990	1.26	0.7	0.96	0.5	2.5	0.21	1.29 ± 0.06	63.85 ± 2.17	23	49.4 ± 3.1
1991	0.88	0.5	0.95	0.7	2.5	0.22	1.35 ± 0.06	48.36 ± 1.17	21	36.0 ± 2.1
1992	0.47	1.0	1.01	0.8	3.6	0.23	1.50 ± 0.07	34.48 ± 1.60	51	23.0 ± 1.6
Minimum Age Model (Galbraith et al., 1999)								28.69 ± 1.00		19.1 ± 1.2
1993	0.11	0.8	0.95	0.7	3.0	0.24	1.40 ± 0.06	7.96 ± 0.06	24	5.68 ± 0.31
Site footprint, associated with Paleoindian point										
1994	0.18	1.4	1.04	0.8	3.8	0.24	1.54 ± 0.07	5.69 ± 0.35	20	3.71 ± 0.30

Table A-29. Locality 30; Hall and Goble, 2016g; sample collected 2008.

UNL No.	Burial Depth (m)	H_2O (%)	K_2O (%)	U (ppm)	Th (ppm)	Cosmic (Gy)	Dose Rate (Gy/ka)	D_e (Gy)	No. Aliquots	Age (ka)
Massive sand beneath Mescalero paleosol, Gatuña Formation										
2340	2.84	1.6	0.94	0.92	2.55	0.17	1.33 ± 0.05	189.2 ± 5.5	35	143 ± 8

Table A-30. Locality 31; Hall and Kettler, 2019; samples collected 2014

UNL No.	Burial Depth (m)	H_2O (%)	K_2O (%)	U (ppm)	Th (ppm)	Cosmic (Gy)	Dose Rate (Gy/ka)	D_e (Gy)	No. Aliquots	Age (ka)
Area C, Trench 1										
Late Holocene eolian sand, pre-Eddy paleosol										
4436	1.36	0.3	0.61 ± 0.02	0.58 ± 0.06	2.52 ± 0.18	0.21	0.96 ± 0.04	3.49 ± 0.06	62	3.66 ± 0.18[d]
4437	1.13	0.2	0.71 ± 0.02	0.67 ± 0.06	2.37 ± 0.18	0.22	1.05 ± 0.05	2.29 ± 0.04	53	2.18 ± 0.10[d]
Eddy paleosol										
4438	0.95	0.2	0.57 ± 0.02	0.57 ± 0.06	1.82 ± 0.15	0.22	0.89 ± 0.04	1.26 ± 0.04	52	1.42 ± 0.06[e]
4439	0.80	0.2	0.60 ± 0.02	0.63 ± 0.06	2.12 ± 0.17	0.23	0.95 ± 0.04	0.92 ± 0.03	52	0.97 ± 0.06[e]
4440	0.55	0.2	0.57 ± 0.02	0.46 ± 0.06	1.82 ± 0.16	0.24	0.88 ± 0.04	0.45 ± 0.08	54	0.51 ± 0.09[f]
4441	0.39	0.2	0.62 ± 0.02	0.63 ± 0.06	2.24 ± 0.17	0.24	0.99 ± 0.04	0.38 ± 0.03	54	0.38 ± 0.03[g]
Coppice dune resting on Eddy paleosol sand										
4442	0.71	0.1	0.44 ± 0.02	0.50 ± 0.05	1.68 ± 0.15	0.23	0.77 ± 0.04	0.13 ± 0.01	54	0.17 ± 0.01[d]
Area A, Trench 1										
Late Holocene eolian sand, Eddy paleosol										
4443	0.42	0.2	0.55 ± 0.02	0.74 ± 0.06	2.25 ± 0.16	0.24	0.95 ± 0.04	0.72 ± 0.08	51	0.76 ± 0.09[f]
Late Holocene eolian sand										
4444	0.74	0.3	0.49 ± 0.02	0.77 ± 0.06	2.28 ± 0.14	0.23	0.91 ± 0.04	4.33 ± 0.13	50	4.78 ± 0.26[d]
Area B, Trench 1										
Late Holocene eolian sand, Eddy paleosol										
4445	0.48	0.2	0.61 ± 0.02	0.73 ± 0.06	2.33 ± 0.14	0.24	1.00 ± 0.04	1.63 ± 0.28	57	1.63 ± 0.08[d]
Area B, Trench 2										
Holocene eolian sand, Eddy paleosol										
4446	2.79	0.2	0.56 ± 0.02	0.65 ± 0.06	2.37 ± 0.14	0.17	0.89 ± 0.04	1.73 ± 0.10	55	1.95 ± 0.14[f]
4447	2.46	0.2	0.61 ± 0.02	0.56 ± 0.06	2.31 ± 0.15	0.18	0.91 ± 0.04	1.69 ± 0.04	58	1.84 ± 0.10[d]
4448	2.11	0.2	0.60 ± 0.03	0.55 ± 0.06	2.05 ± 0.14	0.19	0.89 ± 0.04	0.55 ± 0.12	54	0.62 ± 0.14[f]
Eolian cover sand										
4449	1.77	0.2	0.51 ± 0.02	0.69 ± 0.06	1.91 ± 0.12	0.20	0.85 ± 0.04	0.19 ± 0.01	54	0.22 ± 0.02[f]
Coppice dune sand										
4450	1.47	0.2	0.43 ± 0.02	0.47 ± 0.05	1.67 ± 0.12	0.21	0.73 ± 0.03	0.10 ± 0.03	53	0.14 ± 0.01[d]
4451	0.97	0.1	0.40 ± 0.02	0.40 ± 0.05	1.69 ± 0.12	0.22	0.71 ± 0.03	0.078 ± 0.038	59	0.11 ± 0.01[d]
4452	0.46	0	0.49 ± 0.02	0.44 ± 0.05	1.87 ± 0.12	0.22	0.08 ± 0.04	0.057 ± 0.027	52	0.071 ± 0.006[d]

Notes: depth of burial may include cover sand and coppice dune sand; error on D_e is 1 standard error; ages with 1 σ error; error on age includes random and systematic errors calculated in quadrature; Models: [d] CAM; [e] MAM-3; [f] LFP; [g] MAM-4

Table A-31. Locality 33; Hall and Goble, 2017; samples collected 2016

UNL No.	Burial Depth (cm)	H_2O (%)	K_2O (%)	U (ppm)	Th (ppm)	Cosmic (Gy)	Dose Rate (Gy/ka)	D_e (Gy)	No. Aliquots	Age (ka)
Holocene eolian sand, depth below top of Eddy paleosol										
4280	9	3.3	0.62 ± 0.03	0.54 ± 0.06	2.02 ± 0.16	0.23	1.00 ± 0.04	2.58 ± 0.14	57	2.59 ± 0.18
Minimum Age Model (Galbraith et al., 1999)								1.47 ± 0.08		1.48 ± 0.10[d]
Holocene eolian sand below Eddy paleosol										
4281	19	3.0	0.72 ± 0.03	0.68 ± 0.07	2.17 ± 0.16	0.23	1.12 ± 0.04	3.93 ± 0.17	57	3.51 ± 0.21
Minimum Age Model (Galbraith et al., 1999)								2.73 ± 0.17		2.44 ± 0.18[d]
4282	40	4.0	0.71 ± 0.03	0.65 ± 0.07	1.96 ± 0.16	.22	1.07 ± 0.05	8.18 ± 0.38	55	7.67 ± 0.55
Parabolic dune sand, depth below top of dune sand at trench locality										
4283	37	0.2	0.58 ± 0.03	0.45 ± 0.06	1.51 ± 0.14	0.24	0.94 ± 0.05	0.53 ± 0.07	54	0.56 ± 0.08
Minimum Age Model (Galbraith et al., 1999)								0.29 ± 0.03		0.31 ± 0.04[d]
4284	11	4.0	0.59 ± 0.03	0.46 ± 0.06	1.87 ± 0.15	0.25	0.94 ± 0.04	0.52 ± 0.06	59	0.55 ± 0.06
Minimum Age Model (Galbraith et al., 1999)								0.19 ± 0.11		0.20 ± 0.12[d]
Middle eolian sand , depth below eroded surface of red sand										
4285	17	7.0	0.84 ± 0.03	0.83 ± 0.07	3.39 ± 0.18	0.25	1.29 ± 0.05	42.1 ± 1.4	60	32.7 ± 1.7

APPENDIX B.
AMS RADIOCARBON DATES

Calibrated ages (1σ) are from IntCal 13 (Reimer et al., 2013); weighted average of probability distributions calculated from 2σ calibrated ages and rounded to nearest 10 yr (Telford et al, 2004). The geographic coordinates of the study localities are listed in Table 1.3.

Table B-1. Locality 3; unnamed stream west of Caprock Road, loc. 12 in Hall, 2002a,b

Sample Locality	Lab No., Beta-	Material Dated	Measured Radiocarbon Years BP (1σ)	$\delta^{13}C$ (‰)	Corrected Radiocarbon Age BP (1σ)	Calibrated Age (2σ) Weighted Ave. of Probability Distribution (calendar years BP)
Loco Hills paleosol						
Buried in alluvium with coppice dune above	156687	bulk sed.	300 ± 40	-23.2	330 ± 40	390

Table B-2. Locality 4; loc. 13 in Hall, 2002a,b

Sample Depth (cm)	Lab No., Beta-	Material Dated	Measured Radiocarbon Years BP (1σ)	$\delta^{13}C$ (‰)	Corrected Radiocarbon Age BP (1σ)	Calibrated Age (2σ) Weighted Ave. of Probability Distribution (calendar years BP)
Loco Hills paleosol, with OSL and cesium-137 dates						
Paleosol beneath coppice dune, buried approx. 105 cm	159213	bulk sed.	90 ± 40	-21.6	150 ± 40	150

Table B-3. Locality 9; Hall and Goble, 2016a

Sample Locality	Lab No., Beta-	Material Dated	Measured Radiocarbon Years BP (1σ)	$\delta^{13}C$ (‰)	Corrected Radiocarbon Age BP (1σ)	Calibrated Age (2σ) Weighted Ave. of Probability Distribution (calendar years BP)
Eddy paleosol						
Buried in alluvium	247593	bulk sed.	1060 ± 40	-23.1	1090 ± 40	1000
Buried in colluvium	247594	bulk sed.	1050 ± 40	-19.9	1130 ± 40	1060

Table B-4. Locality 10; Hall and Goble, 2016a

Sample Locality and Depth (cm)	Lab No., Beta-	Material Dated	Measured Radiocarbon Years BP (1σ)	$\delta^{13}C$ (‰)	Corrected Radiocarbon Age BP (1σ)	Calibrated Age (2σ) Weighted Ave. of Probability Distribution (calendar years BP)
Eddy paleosol						
Caps colluvium	247595	bulk sed.	520 ± 40	-19.9	600 ± 40	600
Eddy paleosol, caps fine-textured alluvium						
2-10 cm below top	247596	bulk sed.	490 ± 40	-19.4	580 ± 40	590
Alluvium, fine textured						
45-55 cm below top	247597	bulk sed.	1880 ± 40	-17.6	2000 ± 40	1960
90-100 cm below top	247598	bulk sed.	2850 ± 40	-18.1	2960 ± 40	3110

Table B-5. Locality 11; Hall and Goble, 2011b

Sample Locality	Lab No., Beta-	Material Dated	Measured Radiocarbon Years BP (1σ)	$\delta^{13}C$ (‰)	Corrected Radiocarbon Age BP (1σ)	Calibrated Age (2σ) Weighted Ave. of Probability Distribution (calendar years BP)
Eddy paleosol; paired with OSL						
Caps Holocene eolian sand unit	250589	bulk sed.	1170 ± 40	-18.4	1280 ± 40	1220

Table B-6. Locality 12; Hall and Goble, 2011b

Sample Locality and Depth (cm)	Lab No., Beta-	Material Dated	Measured Radiocarbon Years BP (1σ)	$\delta^{13}C$ (‰)	Corrected Radiocarbon Age BP (1σ)	Calibrated Age (2σ) Weighted Ave. of Probability Distribution (calendar years BP)
Eddy paleosol; paired with OSL						
Caps Late Holocene eolian sand unit, 44 cm	250587	bulk sediment	980 ± 40	-18.9	1080 ± 40	1000
Caps late Holocene eolian sand unit, 88 cm	250588	bulk sediment	1620 ± 40	-19.2	1720 ± 40	1630

Table B-7. Locality 17; Hall and Goble, 2016d

Sample Depth (cm)	Lab No., Beta-	Material Dated	Measured Radiocarbon Years BP (1σ)	$\delta^{13}C$ (‰)	Corrected Radiocarbon Age BP (1σ)	Calibrated Age (2σ) Weighted Ave. of Probability Distribution (calendar years BP)
Eddy paleosol; trench 1, depression-fill facies; paired with OSL						
14-18 cm	425703	bulk sed.	50 ± 30	-21.9	100 ± 30	130
39-43 cm	425702	bulk sed.	400 ± 30	-20.5	470 ± 30	520
73-77 cm	425701	bulk sed.	530 ± 30	-21.6	590 ± 30	600
113-117 cm	425700	bulk sed.	710 ± 30	-20.4	790 ± 30	700

Table B-8. Locality 21; Hall and Goble, 2016f

Sample Depth (cm)	Lab No., Beta-	Material Dated	Measured Radiocarbon Years BP (1σ)	$\delta^{13}C$ (‰)	Corrected Radiocarbon Age BP (1σ)	Calibrated Age (2σ) Weighted Ave. of Probability Distribution (calendar years BP)
West Area						
Eddy paleosol, trench 1						
13-18 cm	418210	bulk sed.	430 ± 30	-19.9	510 ± 30	530
25-30 cm	418211	bulk sed.	650 ± 30	-19.6	740 ± 30	690
Eddy paleosol, trench 2						
6-12 cm	418212	bulk sed.	590 ± 30	-18.2	700 ± 30	650
27-31 cm	418213	bulk sed.	980 ± 30	-17.2	1110 ± 30	1000
East Area						
Eddy paleosol, trench 6						
5-10 cm	431345	bulk sed.	750 ± 30	-20.0	830 ± 30	740
18-23 cm	431346	bulk sed.	1100 ± 30	-18.7	1200 ± 30	1120
Eddy paleosol, trench 2; paired with OSL						
7-11 cm	431348	bulk sed.	190 ± 30	-18.7	290 ± 30	370

Table B-9. Locality 25; Hall, 2013

Sample Depth (cm)	Lab No., Beta-	Material Dated	Measured Radiocarbon Years BP (1σ)	$\delta^{13}C$ (‰)	Corrected Radiocarbon Age BP (1σ)	Calibrated Age **(2σ)** Weighted Ave. of Probability Distribution (calendar years BP)
Base of Cover sand overlying Loco Hills paleosol; trench 4						
88-92 cm	337737	charcoal	101.0 ± 0.4 pMC*	-11.5	140 ± 30	150
Eddy paleosol at top of middle Holocene eolian sand; trench 1						
53-57 cm	337738	bulk sed.	490 ± 30	-18.9	590 ± 30	600

* pMC = percent modern carbon

Table B-10. Locality 27; Hall and Goble, 2016c

Sample Depth (cm)	Lab No., Beta-	Material Dated	Measured Radiocarbon Years BP (1σ)	$\delta^{13}C$ (‰)	Corrected Radiocarbon Age BP (1σ)	Calibrated Age **(2σ)** Weighted Ave. of Probability Distribution (calendar years BP)
Eddy paleosol; trench 2						
5-9 cm depth	430152	bulk sed.	310 ± 30	-20.2	390 ± 30	440
Eddy paleosol; trench 4; paired with OSL						
7-11 cm	430151	bulk sed.	800 ± 30	-18.8	900 ± 30	830
19-23 cm	430150	bulk sed.	930 ± 30	-18.7	1030 ± 30	950
34-38 cm	430149	bulk sed.	1150 ± 30	-18.6	1250 ± 30	1200

Table B-11. Locality 31; Hall and Kettler, 2019

Sample Depth (cm)*	Lab No., Beta-	Material Dated	Measured Radiocarbon Years BP (1σ)	$\delta^{13}C$ (‰)	Corrected Radiocarbon Age BP (1σ)	Calibrated Age **(2σ)** Weighted Ave. of Probability Distribution (calendar years BP)
Locality C, trench 1, Eddy paleosol, dates paired with OSL ages						
70-74 cm	507446	bulk sed.	1190 ± 30	-20.0	1270 ± 30	1230
55-59 cm	507447	bulk sed.	960 ± 30	-21.1	1020 ± 30	940
30-34 cm	507448	bulk sed.	810 ± 30	-20.6	880 ± 30	810
14-18 cm	507449	bulk sed.	610 ± 30	-19.5	700 ± 30	650
Locality B, trench 2, Eddy paleosol						
90-94 cm	507450	bulk sed.	1150 ± 30	-19.1	1250 ± 30	1200
57-61 cm	507451	bulk sed.	950 ± 30	-21.6	1010 ± 30	930
22-26 cm	507452	bulk sed.	300 ± 30	-22.8	340 ± 30	400
Cover sand						
13-17 cm	507453	bulk sed.	590 ± 30	-20.1	670 ± 30	620

* Measured below top of Eddy paleosol A horizon except Beta-507453 from cover sands that overlie the Eddy paleosol

Table B-12. Locality 32; Red Bluff Draw; Hall, 2016

Sample Depth (cm)*	Lab No., Beta-	Material Dated	Measured Radiocarbon Years BP (1σ)	$\delta^{13}C$ (‰)	Corrected Radiocarbon Age BP (1σ)	Calibrated Age (2σ) Weighted Ave. of Probability Distribution (calendar years BP)
Fine-textured Holocene alluvium						
5-10 cm	447646	bulk sed.	710 ± 30	-16.1	860 ± 30	760
16-21 cm	447647	bulk sed.	650 ± 30	-14.3	830 ± 30	740
43-48 cm	447648	bulk sed.	2120 ± 30	-14.3	2300 ± 30	2310
68-73 cm	447649	bulk sed.	3420 ± 30	-17.1	3550 ± 30	3840
103-108 cm	447650	bulk sed.	5270 ± 30	-15.4	5430 ± 30	6240
137-142 cm	447651	bulk sed.	6450 ± 30	-14.0	6630 ± 30	7520
Sediment adjacent to buried stone feature near base of Holocene alluvial terrace deposits						
140-145 cm below top of terrace	447652	bulk sediment	5330 ± 30	-15.6	5480 ± 30	6270

* Measured below top of terrace alluvium/colluvium

Table B-13. Locality 34; Hall, 2017a

Sample Depth (cm)*	Lab No., Beta-	Material Dated	Measured Radiocarbon Years BP (1σ)	$\delta^{13}C$ (‰)	Corrected Radiocarbon Age BP (1σ)	Calibrated Age (2σ) Weighted Ave. of Probability Distribution (calendar years BP)
Locality B, Eddy paleosol						
0-10 cm	476282	bulk sed.	790 ± 30	-16.6	930 ± 30	860
10-20 cm	476283	bulk sed.	102.14 ± 0.38 pMC§	-20.5	-5/-7 ± 30	-
10-20 cm	476284	bulk sed.	510 ± 30	-14.9	680 ± 30	630
Locality A, Eddy paleosol						
0-10 cm	476285	bulk sed.	760 ± 30	-18.7	860 ± 30	760

* Measured below top of Eddy paleosol; Beta-476283 date is modern and too young for the age of the deposit; § pMC, percent modern carbon

Table B-14. Locality 35; Hall, 2017b

Sample Depth (cm)*	Lab No., Beta-	Material Dated	Measured Radiocarbon Years BP (1σ)	$\delta^{13}C$ (‰)	Corrected Radiocarbon Age BP (1σ)	Calibrated Age (2σ) Weighted Ave. of Probability Distribution (calendar years BP)
Eddy paleosol in eolian sand						
9-13 cm	447653	bulk sed.	180 ± 30	-19.2	280 ± 30	350
16-20 cm	447654	bulk sed.	520 ± 30	-18.6	620 ± 30	600
32-36 cm	447655	bulk sed.	610 ± 30	-17.7	730 ± 30	680
48-52 cm	447656	bulk sed.	1430 ± 30	-16.8	1560 ± 30	1460

* Measured below top of Eddy paleosol A horizon

Table B-15. Locality 36; Hall, 2017c

Sample Depth (cm)*	Lab No., Beta-	Material Dated	Measured Radiocarbon Years BP (1σ)	$\delta^{13}C$ (‰)	Corrected Radiocarbon Age BP (1σ)	Calibrated Age (2σ) Weighted Ave. of Probability Distribution (calendar years BP)
Eddy paleosol A horizon, Trench 1						
5-9 cm	447644	bulk sed.	380 ± 30	-19.5	470 ± 30	520
20-24 cm	447645	bulk sed.	1070 ± 30	-18.2	1180 ± 30	1110

* Measured below top of Eddy paleosol A horizon

Table B-16. Locality 40; loc. 14 in Hall, 2002a,b

Locality, Sample Depth (cm)	Lab No., Beta-	Material Dated	Measured Radiocarbon Years BP (1σ)	$\delta^{13}C$ (‰)	Corrected Radiocarbon Age BP (1σ)	Calibrated Age (2σ) Weighted Ave. of Probability Distribution (calendar years BP)
Buried spring deposit						
Arroyo cutbank at Square Lake Road, 166-246 cm depth	156514	snail shells	18,620 ± 100	-7.7	18,900 ± 100	22,760

Table B-17. Locality 41; loc. 3 in Hall, 2002a,b

Sample locality	Lab No., Beta-	Material Dated	Measured Radiocarbon Years BP (1σ)	$\delta^{13}C$ (‰)	Corrected Radiocarbon Age BP (1σ)	Calibrated Age (2σ) Weighted Ave. of Probability Distribution (calendar years BP)
Loco Hills paleosol A horizon						
On Lower eolian sand, beneath coppice dune	160894	bulk sediment	240 ± 40	-17.0	370 ± 40	420

APPENDIX C. SEDIMENTARY DATA

The sediment size classes are from the Wentworth scale (Wentworth, 1922; Folk, 1968), and the percentages have been produced by dedicated geotechnical laboratories.

Table C-1. Locality 1; Berino Paleosol, type locality; sand pit 0.9 mi. south of US 82 on Valley Gas Rd (Eddy Co. 212), west of Loco Hills, Eddy Co., NM; loc. 1 in Hall, 2002a; loc. 100 in Hall and Goble, 2012

Sample Interval (cm depth)	Sand Percentages					Recalculated			$CaCO_3$ (%)	Fe (%)	Dry Munsell Color‡
	Very Coarse Sand (%)	Coarse Sand (%)	Medium Sand (%)	Fine Sand (%)	Very Fine Sand (%)	Sand (%)	Silt (%)	Clay <3.9 µm (%)			
Lower Eolian Sand unit with Berino Paleosol											
0-10	0.0	0.7	27.2	56.0	16.1	88	5	7	1.4	0.25	
10-20	0.0	0.6	26.7	56.6	16.1	88	3	9	1.4	0.25	
20-30	0.0	0.6	26.0	56.7	16.7	83	2	15	1.9	0.35	
30-40	0.0	0.8	26.9	56.2	16.1	82	1	17	1.9	0.36	2.5YR 4/8
40-50	0.0	0.6	26.4	57.9	15.1	85	2	13	1.6	0.28	2.5YR 4/6
50-60	0.0	0.6	25.7	57.6	16.1	86	3	11	1.8	0.32	
60-70	0.0	0.7	26.7	55.5	17.1	89	5	6	1.3	0.23	
70-80	0.0	0.5	27.9	56.4	15.2	89	3	8	1.6	0.26	
80-90	0.0	0.5	28.4	57.3	13.8	89	2	9	1.3	0.19	
90-100	0.0	0.5	28.9	57.8	12.8	90	4	6	1.1	0.18	
100-110	0.0	0.4	26.3	60.6	12.7	92	2	6	0.9	0.19	
110-120	0.0	0.3	28.2	61.0	10.5	94	2	4	0.9	0.18	
120-130	0.0	0.3	28.5	61.1	10.1	95	1	4	0.9	0.14	
130-140	0.0	0.3	26.8	61.3	11.6	94	1	5	1.0	0.12	
140-150	0.0	0.4	31.1	59.6	8.9	94	1	5	1.1	0.12	
150-160	0.0	0.5	28.2	60.2	11.1	95	1	4	1.4	0.15	2.5YR 5/8
160-170	0.0	0.4	28.4	61.5	9.7	96	1	3	1.1	0.12	
170-180	0.0	0.5	26.6	62.5	10.4	96	1	3	0.9	--	
180-190	0.0	0.4	23.5	65.2	10.9	95	1	4	1.1	--	2.5YR 5/6
190-200	0.0	0.4	22.7	71.0	5.9	97	1	2	0.9	--	2.5YR 5/6
200-210	0.0	0.6	32.4	62.9	4.1	97	1	2	0.7	--	
210-220	0.0	1.0	30.7	60.4	7.9	97	1	2	0.8	--	
220-230	0.0	0.4	30.9	57.7	11.0	96	1	3	1.0	--	
230-240	0.0	0.4	21.5	66.3	11.8	96	1	3	0.8	--	
240-250	0.0	0.3	16.6	68.4	14.7	96	1	3	0.8	--	
250-260	0.0	0.3	13.0	67.5	19.2	97	1	2	0.9	--	
260-270	0.0	0.7	15.0	58.9	25.4	95	2	3	0.9	--	
270-280	0.0	0.1	5.9	41.1	52.9	90	5	5	1.4	--	2.5YR 5/6
280-290*	0.0	0.3	10.0	45.1	44.0	89	6	5	1.9	--	
Mescalero Paleosol (exposed in backhoe trench, now filled)											
300-310	0.0	0.4	14.7	52.4	32.5	63	12	25	3.7	0.42	
310-320	0.0	0.3	13.8	54.3	31.6	59	11	30	3.9	0.41	
320-330	0.0	0.2	11.9	57.7	30.2	50	8	42	4.7	0.55	

Table C-1. Continued

Sample Interval (cm depth)	Sand Percentages					Recalculated			$CaCO_3$ (%)	Fe (%)	Dry Munsell Color‡
	Very Coarse Sand (%)	Coarse Sand (%)	Medium Sand (%)	Fine Sand (%)	Very Fine Sand (%)	Sand (%)	Silt (%)	Clay <3.9 µm (%)			
330-340	0.0	0.1	10.3	58.8	30.8	49	9	42	4.8	0.55	
340-350	0.2	0.2	10.3	59.5	29.8	47	12	41	8.3	0.50	
350-360	0.5	0.4	10.1	61.1	27.9	47	15	38	11.0	0.44	
360-370	1.0	0.6	10.0	60.0	28.4	48	16	36	12.6	0.40	
370-380	0.8	0.6	10.5	59.6	28.5	48	16	36	12.8	0.30	

Milwaukee Soil Laboratory.

* 10-cm interval (290-300 cm depth) not collected; dash (--) not analyzed; ‡ lost most of the color data

Table C-2. Locality 4; coppice dune, east side of Square Lake Road (Eddy Co. 220) just north or jct. with Mallet Road (Eddy Co. 257) or 3.6 mi. N of US 82 on Square Lake Rd, NM; dated by OSL, AMS, cesium-137, and lead-210; loc. 13 in Hall, 2002a,b

Sample No.	Depth above base of coppice dune (cm)*	Cesium-137 (^{137}Cs activity pCi/g dry)	Lead-210 (activity pCi/g dry)
E (uppermost)	87-89	0.260 ± 0.069	--
8	85-89	0.095 ± 0.028	1.9 ± 0.6
D	83-85	0.130 ± 0.055	--
C	79-81	<0.027	--
7	77-81	0.259 ± 0.050	--
B	74-76	0.092 ± 0.049	--
A	69-71	<0.038	--
6	61-65	<0.044	--
5	51-55	<0.033	--
4	38-42	<0.025	--
3	25-29	<0.017	--
2	10-14	<0.055	--
1	3-7	<0.020	1.7 ± 0.6

Analyses provided by Dr. H.W. Jeter, Mass Spec Services, Orangeburg, NY.

* Exposed face of coppice dune, where measured and sampled, had a thickness of 96 cm; the dune face is now slumped and no longer exposed.

Table C-3. Locality 5; Potash solar pond area, Eddy Co., NM; Hall and Goble 2011; Loc. 200 in Hall and Goble, 2012

Interval (cm depth)	Very Coarse Sand (%)	Coarse Sand (%)	Medium Sand (%)	Fine Sand (%)	Very Fine Sand (%)	Sand (%)	Silt (%)	Clay **<3.9 µm** (%)	OC (%)	$CaCO_3$ (%)	Dry Munsell Color
Site 1, BHT-1											
Post-Upper eolian sand (late Holocene)											
0-10	0.0	1.0	24.5	56.0	18.5	94	2	4	0.16	0.8	5YR 4/4
10-20	0.0	1.3	27.1	53.8	17.8	93	2	5	0.29	0.7	2.5YR 4/4
20-30	0.0	1.5	25.8	52.4	20.3	91	3	6	0.18	0.8	2.5YR 4/4
30-40	0.1	1.5	26.1	52.6	19.7	92	2	6	0.15	0.8	2.5YR 4/4
Upper eolian sand unit (unit 1)											
40-50	0.0	1.5	27.1	53.0	18.4	92	3	5	0.13	0.8	2.5YR 4/6
50-60	0.0	1.3	26.2	54.5	18.0	92	2	6	0.10	0.9	2.5YR 4/6
60-70	0.0	1.3	26.2	54.9	17.6	92	1	7	0.08	1.0	2.5YR 4/6
70-80	0.0	1.2	25.3	54.9	18.6	92	2	6	0.06	0.9	5YR 4/6
80-90	0.0	1.3	24.9	53.8	20.0	93	2	5	0.06	0.8	5YR 4/6
90-100	0.0	1.5	25.1	52.6	20.8	92	3	5	0.04	0.7	5YR 4/6
100-110	0.0	1.3	24.4	52.4	21.9	92	4	4	0.04	0.6	5YR 5/6
110-120	0.0	1.6	25.1	51/6	21.7	91	6	3	0.03	0.6	5YR 5/6
120-130	0.0	1.5	24.6	51.0	22.9	92	5	3	0.03	0.7	5YR 5/6
Lower eolian sand unit with Berino paleosol upper 1 m (unit 2)											
140-150*	0.0	2.0	30.7	48.1	19.2	73	4	23	0.07	3.1	2.5YR 4/8
150-160	0.0	2.5	32.9	46.4	18.2	71	4	25	0.09	3.5	2.5YR 4/6
160-170	0.0	2.4	32.8	46.4	18.4	76	4	20	0.06	2.7	2.5YR 4/6
170-180	0.0	2.3	32.4	47.0	18.3	81	4	15	0.04	1.9	2.5YR 4/6
180-190	0.0	2.4	32.2	47.4	18.0	83	5	12	0.02	1.6	2.5YR 4/8
190-200	0.0	2.4	32.5	47.8	17.3	86	4	10	0.02	1.3	2.5YR 4/8
200-210	0.0	2.5	33.9	48.1	15.5	88	4	8	0.02	1.2	2.5YR 4/6
210-220	0.0	2.4	38.2	48.4	11.0	87	5	8	0.02	1.4	2.5YR 4/8
220-230	0.0	2.5	38.8	48.3	10.4	86	5	9	0.04	1.5	2.5YR 4/8
230-240	0.1	2.6	40.9	47.8	8.6	87	5	8	0.00	1.1	2.5YR 4/6
240-250	0.0	2.4	41.4	48.7	7.5	91	3	6	0.03	1.1	2.5YR 4/6
250-260	0.0	2.1	42.4	49.4	6.1	93	2	5	0.01	0.8	2.5YR 4/6
260-270	0.0	2.3	41.4	49.5	6.8	91	3	6	0.01	0.8	5YR 5/8
Site 2											
Unit 1											
5-15	0.1	0.3	13.1	61.6	24.9	88	6	6	0.25	1.7	--
50-60	0.2	0.4	14.6	62.7	22.1	88	5	7	0.15	1.7	--
90-100	0.4	0.5	13.0	62.3	23.8	86	7	7	0.11	4.1	--
130-140	0.6	0.5	12.5	61.6	24.8	85	9	6	0.10	4.8	--
Site 3											
Loose surface sand											
---	0.0	1.9	38.7	46.7	12.7	91	5	4	0.19	0.7	--
Unit 1, Bw soil horizon											
---	0.1	0.9	31.8	51.4	15.8	88	5	7	0.26	1.2	--
Unit 2, Bt soil horizon											
---	0.1	1.1	29.8	51.4	17.6	75	7	18	0.19	2.4	--

Milwaukee Soil Laboratory

* 10-cm interval (130-140 cm depth) at unit 2/unit 1 boundary not collected

Table C-4. Locality 6; east of Laguna Plata playa lake basin, Eddy Co., NM; Hall and Goble, 2015a

Interval (cm depth)	Very Coarse Sand (%)	Coarse Sand (%)	Medium Sand (%)	Fine Sand (%)	Very Fine Sand (%)	Sand (%)	Silt (%)	Clay (%)	$CaCO_3$ (%)	OC (%)	Dry Munsell Color
Unit 3, brown eolian sand, Holocene											
30-40*	0	2.1	20.1	63.3	14.6	94	3	3	0.2	0.1	7.5YR 5/4
50-60	0	5.2	27.5	54.3	12.9	93	4	3	0.2	0.1	7.5YR 5/4
70-80	0	4.8	32.4	51.8	11.1	94	2	4	0.3	0.1	7.5YR 5/4
90-100	0	3.5	25.3	59.7	11.5	91	4	5	0.3	0.1	7.5YR 5/4
110-120	0	3.3	27.3	59.4	9.9	95	1	4	0.3	ND†	7.5YR 5/4
130-140	0	3.9	25.0	59.2	11.8	95	2	3	<0.1	ND	7.5YR 5/4
Unit 2, light colored eolian sand, derived from playa shoreline deposits											
90-100	0	3.7	23.1	60.6	12.6	93	3	4	1.8	--	7.5YR 6/4
110-120	0	3.9	22.0	60.7	13.4	95	3	2	1.4	--	5 YR 6/3
130-140	0	4.0	20.6	61.8	13.6	96	3	1	1.1	--	5YR 6/3
150-160	0	4.3	20.2	61.5	14.0	96	3	1	1.1	--	5YR 6/3
170-180	0	4.6	20.2	61.1	14.0	97	3	ND	0.6	--	5YR 6/3
Unit 1, red sand, Lower eolian sand unit											
										Fe (mg/kg)	
upper	0	3.1	16.7	67.1	13.1	76	4	20	2.0	6820	5YR 5/6
lower	0	2.3	15.2	69.4	13.0	81	5	14	0.7	6900	5YR 5/6

Energy Laboratories, Inc., Billings, Montana.

* weak A horizon

† ND, not detected at reporting limit (0.1%)

Table C-5. Locality 7; Trench 1, Los Medaños sand area, Eddy Co., NM; loc. 300 in Hall and Goble, 2012; Fig. 6.5

Interval (cm depth)	Very Coarse Sand (%)	Coarse Sand (%)	Medium Sand (%)	Fine Sand (%)	Very Fine Sand (%)	Sand (%)	Silt (%)	Clay (%)	$CaCO_3$ (%)	OC (%)	Dry Munsell Color
Parabolic dune sand											
+10-20	0.0	0.1	30.8	62.8	6.3	97	0	3	0.6	0.08	5YR 5/6
+0-10	0.0	0.1	30.0	62.2	7.7	96	1	3	0.6	0.07	5YR 5/6
Los Medaños sand											
0-10	0.0	0.5	26.2	66.9	6.4	96	0	4	0.6	0.05	5YR 5/6
10-20	0.0	0.5	27.1	65.9	6.5	97	0	3	0.6	0.03	5YR 5/8
20-30	0.0	0.1	19.6	72.0	8.3	95	2	3	0.6	0.03	5YR 5/7
30-40	0.0	0.1	22.1	69.8	8.0	97	0	3	0.6	0.03	5YR 5/7
40-50	0.0	0.1	19.8	69.5	10.6	95	0	5	0.7	0.03	5YR 5/7
50-60	0.0	0.1	16.0	67.3	16.6	96	0	4	0.8	0.03	5YR 5/8
60-70	0.0	0.1	15.2	65.9	18.8	94	2	4	0.8	0.04	5YR 5/6
70-80	0.0	0.1	14.8	65.9	19.2	95	1	4	0.8	0.03	5YR 5/6
80-90	0.0	0.1	15.2	63.4	21.3	93	2	5	0.9	0.04	5YR 4/6
90-100	0.0	0.2	17.3	63.9	18.6	93	2	5	0.9	0.05	5YR 4/6
Late Holocene eolian sand											
100-110	0.0	0.1	8.3	32.3	59.3	92	2	6	1.0	0.03	5YR 4/6
110-120	0.0	0.1	7.7	31.7	60.5	92	1	7	1.2	0.03	5YR 4/6
Lower eolian sand unit											
130-140	0.0	0.1	9.8	30.3	59.8	80	3	17	2.1	0.05	2.5YR 4/6
140-150	0.0	0.1	9.3	30.3	60.3	84	2	14	1.7	0.03	2.5YR 4/7
150-160	0.0	0.1	8.8	30.4	60.7	81	2	17	2.1	0.03	2.5YR 4/6
160-170*	0.0	0.1	9.6	30.1	60.2	73	3	24	3.3	0.05	2.5YR 4/6

Milwaukee Soil Laboratory.

* Eolian sand rests directly on caliche of the Mescalero paleosol

Table C-6. Locality 8; Trench 1, Eddy Co., NM; Hall and Goble, 2016a

Interval (cm depth)	Very Coarse Sand (%)	Coarse Sand (%)	Medium Sand (%)	Fine Sand (%)	Very Fine Sand (%)	Sand (%)	Silt (%)	Clay (%)	$CaCO_3$ (%)	OC (%)	Dry Munsell Color
Coppice dune sand											
+10-18	0.0	0.7	23.6	57.9	17.8	89	5	6	1.6	0.24	5YR 4/3
+2-10	0.0	1.3	25.5	53.1	20.1	89	5	6	1.4	0.22	5YR 4/3
Upper eolian sand unit (Unit 1 in original report)											
0-10	0.0	2.5	29.3	50.3	17.9	85	6	9	1.5	0.19	5YR 3/4
10-20	0.0	2.2	28.1	51.0	18.7	84	6	9	1.8	0.19	5YR 3/4
20-30	0.0	2.5	29.6	50.5	17.4	84	6	10	2.0	0.18	5YR 4/4
30-40	0.0	2.6	28.0	51.0	18.4	82	6	12	2.1	0.15	5YR 4/4
40-50	0.1	2.6	28.1	51.2	18.0	82	6	12	3.2	0.13	5YR 4/6
50-60	0.1	2.2	26.7	51.8	19.2	81	5	14	4.1	0.13	5YR 4/6
60-70	0.1	2.9	29.5	50.8	16.7	79	4	17	4.5	0.13	5YR 4/6
70-80*	0.3	4.3	33.4	46.5	15.5	77	6	17	6.5	0.17	5YR 4/6

Milwaukee Soil Laboratory.

* Eolian sand rests directly on caliche of the Mescalero paleosol

Table C-7a. Locality 9a; Trench 11, Eddy Co., NM; Hall and Goble, 2016a

Interval (cm depth)	Very Coarse Sand (%)	Coarse Sand (%)	Medium Sand (%)	Fine Sand (%)	Very Fine Sand (%)	Sand (%)	Silt (%)	Clay (%)	$CaCO_3$ (%)	OC (%)	Dry Munsell Color
Upper eolian sand unit (unit 1 in original report)											
0-10	0.0	0.9	20.6	58.2	20.3	89	5	6	1.4	0.18	5YR 4/4
10-20	0.0	0.8	20.7	58.8	19.7	89	5	6	1.3	0.17	5YR 4/4
20-30	0.0	0.8	20.0	58.6	20.6	90	4	6	1.1	0.14	5YR 4/6
30-40	0.0	0.8	21.2	58.0	20.0	89	5	6	1.6	0.11	5YR 4/6
40-50	0.0	0.8	20.8	57.6	20.8	89	6	5	2.8	0.13	5YR 4/6
50-60	0.3	1.1	22.1	55.2	21.3	86	8	6	5.5	0.10	5YR 5/6
60-70	0.1	1.2	22.4	55.7	20.6	86	7	7	4.7	0.09	5YR 5/6
70-80	0.1	1.1	22.6	55.7	20.5	86	7	7	5.2	0.07	5YR 5/4
80-90	0.3	1.2	23.3	55.4	19.8	86	7	7	6.2	0.06	5YR 5/5
90-100	0.2	1.1	23.5	55.3	19.9	86	7	7	6.3	0.05	5YR 5/4
100-110*	0.3	1.3	23.5	55.4	19.5	82	10	8	7.2	0.06	5YR 5/4

Milwaukee Soil Laboratory.

* Eolian sand rests directly on caliche of the Mescalero paleosol

Table C-7b. Locality 9b; sediment data, including total phosphorus, from site footprint column, Trench 10, Eddy Co., NM; Hall and Goble, 2016a

Interval (cm depth)	Total P (mg/kg)	Very Coarse Sand (%)	Coarse Sand (%)	Medium Sand (%)	Fine Sand (%)	Very Fine Sand (%)	Sand (%)	Silt (%)	Clay (%)	$CaCO_3$ (%)	OC (%)	Dry Munsell Color
Archaeological site footprint (called an anthrosol in the original report)												
0-5	90.7	0.0	0.3	11.0	29.4	59.3	92	3	5	1.3	0.37	5YR 3/3
5-10	87.0	0.0	0.3	10.4	29.4	59.9	91	3	6	2.0	0.45	5YR 3/3
10-15	102.7	0.0	0.3	10.0	29.4	60.3	91	3	6	2.6	0.42	5YR 3/3
15-20	92.2	0.0	0.3	10.3	29.4	60.0	90	4	6	2.6	0.33	5YR 3/3
20-25	90.8	0.1	0.3	10.1	29.2	60.3	89	4	7	2.9	0.30	5YR 3/3
25-30	98.5	0.0	0.4	10.2	29.1	60.3	89	4	7	3.0	0.27	5YR 3/4
30-35	109.5	0.1	0.4	10.1	28.7	60.7	87	5	8	4.6	0.20	5YR 4/4
35-40	108.0	0.1	0.4	9.6	28.5	61.4	85	6	9	5.5	0.17	5YR 5/4
40-45	97.9	0.1	0.5	9.8	28.3	61.3	85	6	9	6.5	0.15	5YR 5/4
45-50	99.8	0.1	0.5	10.1	28.0	61.3	84	6	10	6.7	0.15	5YR 5/6
Upper eolian sand unit												
50-60	102.6	0.1	0.5	9.8	28.0	61.6	83	8	9	7.2	0.12	5YR 5/6
60-70	98.4	0.2	0.7	10.7	27.6	60.8	81	9	10	8.2	0.12	5YR 5/6
70-80*	103.2	0.2	0.8	10.8	27.4	60.8	82	9	9	9.6	0.12	5YR 5/6

Milwaukee Soil Laboratory.

* Eolian sand rests directly on caliche of the Mescalero paleosol

Table C-8. Locality 10; Sediment data from late Holocene alluvial fill from small unnamed wash just east of the locality, Eddy Co., NM; Hall and Goble, 2016a

Interval (cm depth)	Very Coarse Sand (%)	Coarse Sand (%)	Medium Sand (%)	Fine Sand (%)	Very Fine Sand (%)	Sand (%)	Silt (%)	Clay (%)	$CaCO_3$ (%)	OC (%)	Dry Munsell Color
Recent alluvium overlying Eddy paleosol											
+10-20	0.4	1.2	17.2	57.2	24.0	89	7	4	4.2	0.27	5YR 4/6
+0-10	0.9	2.2	24.0	56.7	16.2	92	4	4	3.9	0.21	5YR 4/6
Eddy paleosol and late Holocene alluvium											
0-10	0.2	0.4	8.7	37.2	53.5	39	47	14	7.9	1.05	5YR 3/4
10-20	0.0	0.3	7.4	34.1	58.2	37	48	15	10.7	0.95	5YR 3/4
20-30	0.0	0.3	9.2	41.0	49.5	57	30	13	5.6	0.66	5YR 3/4
30-40	0.0	0.3	9.7	43.8	46.2	64	22	14	3.8	0.54	5YR 3/4
40-50	0.0	0.3	10.1	43.8	45.8	63	22	15	4.0	0.49	5YR 3/3
50-60	0.0	0.4	11.0	42.3	46.3	65	20	15	3.4	0.39	5YR 3/4
60-70	0.2	0.7	10.6	39.7	48.8	57	27	16	5.8	0.37	5YR 3/4
70-80	0.2	0.8	11.3	39.9	47.8	56	28	16	6.7	0.34	5YR 4/4
80-90	1.3	1.4	13.3	39.8	44.2	61	24	15	8.5	0.34	5YR 4/4
90-100	2.0	1.6	14.1	40.8	41.5	57	27	16	9.9	0.25	5YR 4/4

Milwaukee Soil Laboratory.

* Eolian sand rests directly on caliche of the Mescalero paleosol

Table C-9. Locality 11; sediment data from trenches 8 and 9, along Hwy. 128 northwest of Jal, Lea Co., NM; Hall and Goble, 2011b

Interval (cm depth)	Very Coarse Sand (%)	Coarse Sand (%)	Medium Sand (%)	Fine Sand (%)	Very Fine Sand (%)	Sand (%)	Silt (%)	Clay (%)	$CaCO_3$ (%)	OC (%)
Trench 9										
Unit 3, alluvium, laminated, overlying Eddy paleosol										
0-10	0.0	11.6	36.6	36.9	14.9	90	4	6	1.2	0.07
10-20	0.0	8.7	39.1	37.9	14.3	93	2	5	1.3	0.07
20-30	0.0	6.6	30.7	44.6	18.1	91	3	6	1.7	0.05
30-40	0.0	3.8	30.6	46.4	19.2	92	3	5	1.7	0.06
40-50	0.0	1.6	19.1	52.2	27.1	90	3	7	1.4	0.10
50-60	0.0	0.7	15.6	50.5	33.2	87	5	8	1.5	0.14
Unit 2, Holocene eolian sand with Eddy paleosol A horizon upper 25 cm										
65-70	0.0	2.9	22.4	47.6	27.1	85	7	8	1.3	0.20
70-80	0.0	2.9	22.3	47.8	27.0	86	6	8	1.3	0.19
80-90	0.0	2.8	22.0	48.2	27.0	86	6	8	1.2	0.16
90-100	0.0	2.6	20.9	48.6	27.9	85	5	10	1.2	0.14
100-110	0.0	2.4	21.2	49.3	27.1	87	4	9	1.2	0.11
110-120	0.0	2.1	19.5	49.3	29.1	87	4	9	1.2	0.08
120-130	0.0	2.2	19.5	49.0	29.3	88	4	8	1.2	0.06
130-140	0.0	2.2	19.9	48.7	29.2	88	4	8	1.4	0.06
140-150	0.0	2.2	19.9	48.7	29.2	88	3	9	1.2	0.05
150-160	0.0	2.1	19.4	48.8	29.7	87	4	9	1.2	0.04
160-170	0.0	2.5	20.5	48.4	28.6	87	4	9	1.2	0.03
170-175	0.0	3.1	22.0	47.6	26.2	86	4	10	1.3	0.04
Trench 8										
Unit 1, Late Pleistocene eolian sand										
180-190	0.0	4.3	23.3	46.2	26.2	87	4	9	1.6	0.07
190-200	0.0	4.6	22.8	45.8	26.8	85	5	10	2.9	0.07
200-210	0.0	5.0	23.9	44.8	26.3	79	9	12	5.5	0.07
210-220	0.1	6.2	25.7	43.1	24.9	79	9	12	5.5	0.05
220-230	0.0	6.4	25.7	43.0	24.9	74	12	14	4.6	0.05
230-240	0.0	6.0	25.9	43.7	24.4	77	9	14	4.1	0.06
240-250	0.0	5.3	24.2	44.7	25.8	76	10	14	4.7	0.05
250-260	0.0	5.2	23.8	45.1	25.9	78	10	12	4.9	0.05
260-270	0.0	5.7	23.3	44.9	26.1	80	12	8	4.0	0.03
270-280	0.0	5.8	22.7	44.6	26.9	83	12	5	3.3	0.03
280-290	0.0	5.8	23.7	44.7	25.8	88	9	3	2.4	0.02
290-300	0.0	5.9	24.2	44.9	25.0	89	8	3	2.4	0.02
300-310	0.0	5.4	23.6	45.3	25.7	91	7	2	1.8	0.01
310-320	0.0	5.7	23.5	44.9	25.9	91	7	2	1.5	0.01
320-330	0.0	5.4	23.8	45.4	25.4	93	5	2	1.5	0.01
330-340*	0.0	5.2	23.5	44.8	26.5	89	7	4	1.4	0.01

Milwaukee Soil Laboratory; Munsell color not determined.

* Eolian sand rests directly on caliche of stage III calcic paleosol

Table C-10a. Locality 12a, sediment data from along Hwy. 128, NW of Jal, Lea Co., NM; Hall and Goble, 2011b

Interval (cm depth)	Very Coarse Sand (%)	Coarse Sand (%)	Medium Sand (%)	Fine Sand (%)	Very Fine Sand (%)	Sand (%)	Silt (%)	Clay (%)	$CaCO_3$ (%)	OC (%)
Trench 1										
Unit 2A, Holocene eolian sand with Eddy paleosol A horizon upper 20 cm										
0-10	0.2	7.3	28.1	43.7	20.7	85	6	9	3.9	0.19
10-20	0.2	7.8	28.0	43.4	20.6	85	6	9	4.1	0.17
20-30	0.1	8.0	27.9	43.7	20.3	85	6	9	4.5	0.13
30-40	0.1	7.1	27.5	45.0	20.3	87	5	8	4.3	0.09
40-50	0.2	7.2	26.4	44.3	21.9	85	6	9	4.9	0.08
50-60	0.2	6.9	26.9	44.4	21.6	85	7	8	4.6	0.07
60-70	0.3	7.7	28.0	43.4	20.6	86	6	8	3.9	0.07
70-80	0.1	7.2	26.3	45.0	21.4	88	5	7	3.2	0.05
80-90	0.1	7.0	27.1	45.5	20.3	86	6	8	3.7	0.06
90-100	0.1	7.1	26.8	44.6	21.4	84	7	9	4.7	0.06
100-110	0.1	5.9	25.1	46.9	22.0	85	8	7	3.7	0.04
110-120	0.1	6.1	26.0	46.1	21.7	86	7	7	3.4	0.04
120-130*	0.1	6.2	26.0	47.4	20.3	87	6	7	3.5	0.06
130-140	0.1	6.1	26.2	47.8	19.8	88	6	6	3.4	0.05
140-150	0.1	6.8	26.7	45.8	20.6	85	8	7	4.6	0.05
150-160	0.2	7.7	27.0	43.7	21.4	84	9	7	5.4	0.05
160-170	0.2	8.1	27.8	43.0	20.9	84	9	7	5.0	0.04
170-180	0.2	8.3	29.1	42.5	19.9	84	9	7	4.8	0.04
180-190	0.1	8.3	28.2	42.4	21.0	83	10	7	5.0	0.04
190-200	0.2	8.1	27.3	43.0	21.4	83	10	7	5.2	0.04
Unit 1, Late Pleistocene eolian sand										
200-210	0.6	9.0	28.1	40.9	21.4	78	12	10	8.8	0.05
210-220	0.7	8.8	28.2	40.6	21.7	74	15	11	11.2	0.05
220-230	0.6	9.3	27.9	40.4	21.8	73	16	11	10.6	0.06
230-240	0.7	10.6	29.7	37.1	21.9	64	20	16	16.6	0.08
240-250	1.4	11.4	29.6	36.7	21.9	63	21	16	17.7	0.08
250-260	2.3	10.3	27.8	37.0	22.6	61	22	17	22.1	0.08
260-270†	2.0	9.9	27.9	37.8	22.4	60	23	17	22.9	0.07

Milwaukee Soil Laboratory; Munsell color not determined.

* Eolian sand rests directly on caliche of stage III calcic paleosol

† Base of sand unit not exposed

Table C-10b. Locality 12b, sediment data from along Hwy. 128, NW of Jal, Lea Co., NM; Hall and Goble, 2011b

Interval (cm depth)	Very Coarse Sand (%)	Coarse Sand (%)	Medium Sand (%)	Fine Sand (%)	Very Fine Sand (%)	Sand (%)	Silt (%)	Clay (%)	$CaCO_3$ (%)	OC (%)
Trench 6										
Unit 3, recent alluvium										
0-10	0.4	7.8	22.7	40.8	28.3	85	10	5	3.5	0.26
10-20	0.4	6.4	19.5	34.4	39.3	79	14	7	4.4	0.29
20-30	.03	9.3	33.6	40.9	15.9	92	5	3	1.9	0.10
Unit 2B, late Holocene eolian sand with Eddy paleosol upper 60 cm										
35-40	0.2	5.8	23.7	44.4	25.9	80	11	9	3.4	0.35
40-50	.03	6.2	23.7	43.9	25.9	77	13	10	4.8	0.44
50-60	0.5	6.1	22.7	43.9	26.8	77	12	11	6.0	0.47
60-70	0.6	6.0	22.8	43.7	26.9	76	13	11	6.7	0.48
70-80	0.3	5.6	21.0	44.4	28.7	77	13	10	7.0	0.45
80-90	0.4	5.8	21.5	44.1	28.2	77	13	10	7.2	0.38
90-100	0.2	5.5	21.3	44.4	28.6	79	13	8	5.7	0.28
100-110*	0.5	4.8	17.8	42.4	34.5	76	14	10	7.9	0.26

Milwaukee Soil Laboratory; Munsell color not determined.

* Sample 5 cm above Triassic bedrock; no caliche

Table C-11. Locality 13, sediment data from Los Medaños sand area along Hwy. 128, eastern Eddy Co., NM; Hall and Goble, 2011b

Interval (cm depth)	Very Coarse Sand (%)	Coarse Sand (%)	Medium Sand (%)	Fine Sand (%)	Very Fine Sand (%)	Sand (%)	Silt (%)	Clay (%)	$CaCO_3$ (%)	OC (%)
Cover sand										
0-10	0.0	0.1	17.5	62.8	19.6	93	4	3	0.4	0.13
10-20	0.0	0.1	22.4	61.8	15.7	95	3	2	0.4	0.10
20-30	0.0	0.1	20.3	63.4	16.2	94	3	3	0.5	0.09
Los Medaños sand unit										
30-40	0.0	0.1	20.5	61.5	17.9	94	4	2	0.6	0.08
40-50	0.0	0.1	22.3	59.8	17.8	95	3	2	0.6	0.10
50-60	0.0	0.2	24.0	58.9	16.9	95	3	2	0.5	0.11
60-70	0.0	0.2	23.2	59.1	17.5	94	4	2	0.6	0.11
70-80	0.0	0.2	23.0	59.6	17.2	95	2	3	0.5	0.12
80-90	0.0	0.2	19.3	59.7	20.8	94	4	2	0.5	0.12
90-100	0.0	0.1	19.0	59.5	21.4	94	4	2	0.5	0.10
100-110	0.0	0.2	19.8	58.8	21.2	94	4	2	0.6	0.08
110-120	0.0	0.2	21.0	57.7	21.1	94	4	2	0.7	0.07
120-130	0.0	0.2	20.9	56.9	22.0	94	4	2	0.6	0.07
Early Late-Holocene eolian sand										
130-140	0.1	0.2	19.5	55.1	25.1	91	6	3	1.2	0.07
140-150	0.1	0.2	19.4	53.8	26.5	89	7	4	1.6	0.08
150-160	0.1	0.3	20.0	54.0	25.6	89	7	4	2.0	0.08
160-170	0.1	0.3	19.3	52.9	27.4	87	8	5	2.9	0.07
170-180*	0.2	0.4	19.5	52.4	27.5	86	9	5	4.2	0.08

Milwaukee Soil Laboratory; Munsell color not determined.

* Base of Late Holocene eolian sand not encountered here

Table C-12. Locality 14; sediment data from eastern Eddy Co., NM; Hall and Goble, 2015c

Interval (cm)	Very Coarse Sand (%)	Coarse Sand (%)	Medium Sand (%)	Fine Sand (%)	Very Fine Sand (%)	Sand (%)	Silt (%)	Clay (%)	$CaCO_3$ (%)	OC (%)	Dry Munsell Color
Trench 1											
Eddy paleosol A horizon											
0-10	0	0.7	21.9	64.3	13.2	94	3	3	1.3	0.2	5YR 3/2
10-20	0	0.7	21.2	64.0	14.2	94	4	2	2.0	0.2	5YR 3/2
20-30	0	0.8	22.4	60.4	16.4	90	6	4	2.9	0.2	5YR 4/4
Holocene eolian sand unit											
30-40	0	0.8	21.6	61.7	15.8	92	3	5	3.8	0.2	5YR 4/4
40-50	0	0.7	22.2	39.5	37.6	91	2	7	4.3	0.2	5YR 4/4
50-60	0	1.3	22.7	46.1	29.9	88	4	8	5.5	0.2	5YR 4/4
60-70	0	1.6	22.7	52.8	22.9	88	4	8	7.4	0.2	5YR 5/4
70-80	0	3.2	24.8	53.8	18.1	86	4	10	9.5	0.2	5YR 5/4
80-90*	0	2.9	23.7	53.0	20.4	86	5	9	10.6	0.2	5YR 5/4
Trench 2, 54 ft. east of the sediment column from Trench 1											
Eddy paleosol A horizon											
0-10	0	1.3	26.0	59.2	13.5	92	3	5	0.9	0.6	5YR 3/3
10-20	0	1.1	24.1	61.9	12.8	92	3	5	1.1	0.4	5YR 3/3
20-30	0	1.0	23.9	63.0	12.1	94	2	4	0.8	0.3	5YR 3/3
Holocene eolian sand unit											
50-60	0	0.9	21.8	62.7	14.6	91	3	6	1.9	0.2	2.5YR 4/6
70-80	0	1.1	23.2	60.0	15.7	90	4	6	2.2	0.1	2.5YR 4/6
90-100	0	1.5	26.2	57.1	15.1	89	3	8	2.1	0.1	2.5YR 4/6

Energy Laboratories, Inc., Billings, Montana.

* Directly overlies weathered caliche of the Mescalero paleosol.

Table C-13. Locality 15; near top of Mimosa Ridge, Eddy Co., NM; Hall and Goble, 2015a

Interval (cm)	Very Coarse Sand (%)	Coarse Sand (%)	Medium Sand (%)	Fine Sand (%)	Very Fine Sand (%)	Sand (%)	Silt (%)	Clay (%)	$CaCO_3$ (%)	OC (%)	Dry Munsell Color
Mesquite coppice dune, cm above base											
35-45	0	0.6	12.1	71.1	16.2	93	4	3	0.3	0.3	5YR 4/4
25-35	0	0.4	10.9	72.8	15.9	95	3	2	0.3	0.4	5YR 4/4
15-25	0	0.8	16.8	68.1	14.3	95	3	2	0.2	0.3	5YR 4/4
5-15	0	2.6	24.9	60.9	11.6	96	2	2	0.1	0.2	5YR 4/4
Holocene eolian sand unit (unit 2, eolian sand unit, cm below top of unit)											
30-40*	0	2.9	24.4	60.3	12.4	95	2	3	0.2	0.2	5YR 4/6
40-50*	0	2.6	22.4	62.0	13.0	94	4	2	0.2	0.1	5YR 4/6
60-70	0	2.7	21.2	63.5	12.7	94	2	4	0.3	0.1	5YR 4/6
70-80	0	2.7	22.1	62.8	12.4	94	2	4	0.2	0.1	5YR 4/6
80-90	0	2.6	20.5	64.2	12.7	94	2	4	0.2	ND†	5YR 4/6
90-100	0	2.7	21.0	65.2	11.1	92	3	5	0.3	ND	5YR 4/6
Middle eolian sand unit (unit 1, red sand)											
										Fe (mg/kg)	
upper	0	2.8	22.0	63.1	12.2	82	5	13	0.5	4250	2.5YR 4/6
lower§	0	2.9	22.7	60.7	13.7	74	5	21	0.8	9010	2.5YR 4/6

Energy Laboratories, Inc., Billings, Montana; † ND, not detected at reporting limit (0.1%).

* A horizon

§ Directly overlies weathered caliche and Mescalero paleosol

Table C-14. Locality 16; east of Antelope Draw, NW of Jal, Lea Co., NM; Hall and Goble, 2016d

Interval (cm depth)	Very Coarse Sand (%)	Coarse Sand (%)	Medium Sand (%)	Fine Sand (%)	Very Fine Sand (%)	Sand (%)	Silt (%)	Clay (%)	$CaCO_3$ (%)	OC (%)	**Iron (Fe)** (mg/kg)	Dry Munsell Color
Trench 1												
Parabolic dune sand												
-10-20	0	3.4	25.6	58.3	12.6	94	4	2	<0.1	--*	--	5YR 5/4
Unit 3, weak A horizon in eolian sand (Eddy paleosol)												
20-30	0	1.3	17.5	62.9	18.3	91	6	3	0.1	0.1	--	5YR 4/4
35-45	0	2.0	20.6	61.5	15.9	93	5	2	<0.1	ND*	--	5YR 4/4
50-60	0	2.0	21.1	64.5	12.3	94	3	3	0.1	ND	--	5YR 4/4
Unit 3 eolian sand (Holocene eolian sand unit)												
80-90	0	1.9	19.9	63.8	14.4	92	4	4	0.1	ND	--	5YR 4/6
120-130	0	2.8	23.5	70.5	3.2	90	5	5	0.1	ND	--	5YR 4/6
Unit 2, upper soil, Bt horizon (Middle sand unit)												
150-160	0	2.6	20.9	61.5	15.1	86	6	8	0.2	--	4740	2.5YR 4/8
Unit 2 eolian sand												
180-190	0	2.7	20.7	59.1	17.5	87	7	6	0.1	--	--	5YR 5/6
210-220	0	3.1	22.4	56.8	17.6	91	5	4	0.1	--	--	5YR 5/6
Unit 1, lower soil, Bt horizon (Lower sand unit)												
230-240	0	3.1	21.7	60.9	14.3	75	6	19	0.2	--	8650	2.5YR 4/8
250-260	0	3.4	26.8	56.5	13.4	80	4	16	0.2	--	--	2.5YR 4/8
Unit 1 eolian sand												
270-280	0	3.8	25.2	62.1	9.0	86	5	9	0.2	--	--	2.5YR 4/8
300-310	0	1.8	12.6	57.7	27.9	84	9	7	0.2	--	--	5YR 5/6
330-340	0	0.3	5.0	46.3	48.4	68	21	11	0.2	--	--	5YR 5/6
Supplemental analysis by A & L Great Lake Laboratories, Fort Wayne, Indiana												
Unit 3 (35-45 & 50-60 cm)	--	--	--	--	--	--	--	--	--	0.16%	--	--

Analyses by the Energy Laboratories, Inc., Billings, Montana; dry color by S.A. Hall

* The dash (--) symbol means no measurements were made; ND, not detected at reporting limit.

Table C-15. Loc. 17; sediment data from trenches 1, 7, and 8, NW of Jal, Lea County, NM; Hall and Goble, 2016d

Interval (cm depth)	Very Coarse Sand (%)	Coarse Sand (%)	Medium Sand (%)	Fine Sand (%)	Very Fine Sand (%)	Sand (%)	Silt (%)	Clay (%)	$CaCO_3$ (%)	OC (%)	Dry Munsell Color
Trench 1											
Parabolic dune sand											
10-20	0	1.0	29.4	66.2	3.3	98	2	ND*	0.1	0.1	2.5YR 4/4
Unit 2, Eddy paleosol A horizon, depression-fill facies of the Eddy											
40-50	0	1.3	33.1	62.0	3.6	98	2	ND	0.2	0.1	5YR 4/4
60-70	0	1.0	29.1	65.8	4.1	98	2	ND	0.1	0.1	5YR 4/4
80-90	0	1.2	26.2	67.7	5.0	98	2	ND	0.1	0.1	5YR 4/4
100-110	0	1.5	26.9	67.2	4.5	97	3	ND	0.1	ND	5YR 4/4
120-130	0	1.6	26.7	66.6	5.1	98	2	ND	0.1	0.1	5YR 4/4
140-150	0	1.6	26.5	66.5	5.4	96	4	ND	0.1	0.1	5YR 4/4
Trench 7											
Parabolic dune sand											
10-20	0	0.1	16.2	80.8	2.9	96	4	ND	0.1	0.2	2.5YR 4/4
30-40	0	0.6	22.3	73.4	3.6	98	2	ND	0.1	ND	2.5YR 4/4
50-60	0	0.6	21.4	74.7	3.3	98	2	ND	<0.1	ND	2.5YR 4/6
70-80	0	1.0	30.3	66.1	2.5	98	2	ND	0.1	ND	2.5YR 5/6
Trench 8											
Unit 1, pre-Eddy paleosol, Holocene eolian sand											
10-20	0	1.3	28.3	67.5	2.9	98	2	ND	0.1	ND	2.5YR 4/6
30-40	0	1.0	27.9	67.5	3.7	97	3	ND	0.1	ND	2.5YR 4/8
50-60	0	1.0	29.7	66.3	3.1	96	4	ND	0.1	ND	2.5YR 4/8
70-80	0	1.0	25.3	70.1	3.7	96	4	ND	0.1	ND	2.5YR 4/8
90-100	0	0.7	19.2	77.0	3.1	97	3	ND	0.1	ND	2.5YR 4/8
110-120	0	0.7	17.5	77.4	4.4	94	5	1	0.1	ND	2.5YR 5/8
Supplemental OC analysis by A & L Great Lakes Laboratories, Fort Wayne, Indiana											
Unit 2, A horizon, 40-50 & 60-70 cm										0.13%	
Unit 2, A horizon, 80-90 & 100-110 cm										0.16%	
Unit 2, A horizon, 120-130 & 140-150 cm										0.16%	

Energy Laboratories, Inc., Billings, Montana.

* ND, not detected at the reporting limit (<0.1 %)

Table C-16. Loc. 18; sediment data including Total P from Pierce Canyon area, Eddy Co., NM; Hall, 2010b

Interval (cm depth)	Total P (mg/kg)	Very Coarse Sand (%)	Coarse Sand (%)	Medium Sand (%)	Fine Sand (%)	Very Fine Sand (%)	Sand (%)	Silt (%)	Clay (%)	$CaCO_3$ (%)	OC (%)	Dry Munsell Color
Trench 4												
Coppice dune sand												
+5-10	--	0.1	0.2	19.4	64.9	15.4	94	4	2	0.7	0.21	7.5YR 4/4
Eddy paleosol A horizon												
0-10	70.5	0.1	0.3	20.9	62.5	16.2	93	4	3	0.9	0.32	7.5YR 3/2
10-20	90.7	0.1	0.3	20.0	61.7	17.9	93	3	4	1.0	0.35	7.5YR 3/2
20-30	120.6	0.1	0.3	19.8	61.0	18.8	92	4	4	1.4	0.39	7.5YR 3/2
30-40	102.8	0.3	0.3	20.0	60.7	18.7	91	4	5	1.8	0.33	7.5YR 3/3
Late Holocene eolian sand												
40-50	100.2	0.2	0.3	19.9	60.0	19.6	91	4	5	2.3	0.27	7.5YR 4/3
50-60*	112.4	0.5	0.4	18.9	59.5	20.7	88	6	6	3.6	0.21	7.5YR 4/3
Trench 1, Holocene eolian sand with underlying colluvium												
20-30†	--	0.4	0.6	28.8	53.6	16.6	82	8	10	1.3	0.21	5YR 3/4
Trench 2, Holocene eolian sand with underlying colluvium												
20-30†	--	0.1	0.4	25.7	56.6	17.2	86	5	9	1.1	0.21	5YR 3/4
Trench 3, Holocene eolian sand with underlying colluvium												
20-30†	--	0.1	0.2	21.8	58.3	19.6	89	5	6	0.9	0.21	5YR 3/4

Milwaukee Soil Laboratory.

* Eolian sand rests directly on weathered caliche of the Mescalero paleosol

† Samples from same horizon as OSL dates (Appendix A, Loc. 18).

Table C-17. Loc. 19, Pierce Canyon area, 17 trenches, western Mescalero Plain, Eddy Co., NM; Hall, 2007

Interval (cm depth)	Very Coarse Sand (%)	Coarse Sand (%)	Medium Sand (%)	Fine Sand (%)	Very Fine Sand (%)	Sand (%)	Silt (%)	Clay (%)	$CaCO_3$ (%)	OC (%)	Dry Munsell Color
Trench 1											
Unit 2, eolian sand (59 ka)											
50-55	0.0	0.7	28.3	53.7	17.3	85	6	9	2.9	0.12	5YR 4/6
Unit 1, calcic eolian sand (165-170 ka)											
100-110	0.0	0.4	25.1	51.3	23.2	77	13	10	17.1	0.08	5YR 6/6
160-170	0.1	0.4	17.3	47.8	34.4	76	17	7	16.2	0.04	5YR 5/6
Trench 5											
Unit 4, yellow eolian sand (3-18 ka)											
15-20	0.0	1.4	33.2	49.2	16.2	91	4	5	1.0	0.11	5YR 3/6
80-85	0.0	1.4	29.7	50.5	18.4	91	4	5	0.9	0.04	5YR 4/6
Unit 3, red eolian sand (27 ka)											
150-155	0.0	1.5	31.8	49.5	17.1	83	2	15	1.9	0.04	2.5YR 4/8
Trench 9											
Unit 4, yellow eolian sand (7 ka)											
23-28	0.0	1.7	31.5	49.0	17.8	92	4	4	0.8	0.1	5YR 4/6
63-68	0.0	1.3	27.5	51.0	20.2	93	4	3	0.8	0.06	5YR 4/6
Trench 14											
Unit 4, yellow eolian sand (11 ka)											
45-50	0.0	0.5	21.0	64.2	14.3	92	3	5	0.9	0.07	5YR 5/6
Trench 16											
Unit 3, red eolian sand											
85-90	0.0	2.5	33.1	45.3	19.1	86	2	12	1.4	0.1	2.5YR 4/6

Milwaukee Soil Laboratory.

Table C-18. Loc. 20, Wolf Camp (South Eddy) project, Eddy Co., NM; Hall and Goble, 2016e

Interval (cm depth)	Very Coarse Sand (%)	Coarse Sand (%)	Medium Sand (%)	Fine sand (%)	Very Fine Sand (%)	Sand (%)	Silt (%)	Clay (%)	$CaCO_3$ (%)	OC (%)	Dry Munsell Color
Site A, BHT-2											
Unit 2 eolian sand, Holocene eolian sand unit											
56-66	0	2.2	26.1	52.0	19.7	93	3	4	<0.1	--	5YR 4/6
66-76	0	2.1	25.4	52.3	20.2	95	2	3	<0.1	--	5YR 4/6
76-86	0	2.1	25.5	52.6	19.8	93	2	5	<0.1	--	5YR 4/6
86-96	0	2.0	27.3	52.3	18.3	92	3	5	<0.1	--	5YR 4/6
96-106	0	2.0	26.7	51.7	19.5	94	2	4	<0.1	--	5YR 4/6
Site B, BHT-6 (upper east end)											
Unit 3, Parabolic dune sand											
0-10	0	0.4	30.6	58.7	10.3	95	3	2	<0.1	0.2	5YR 5/6
10-20	0	0.8	29.4	57.0	12.9	95	3	2	<0.1	0.1	5YR 5/6
20-30	0	0.5	24.1	61.4	14.1	94	5	1	<0.1	ND*	5YR 5/6
30-40	0	0	11.5	69.6	18.8	95	2	3	<0.1	0.1	5YR 5/6
40-50	0	0.1	19.3	67.1	13.4	95	2	3	<0.1	ND	5YR 5/6
50-60	0	0.9	37.2	52.0	9.8	96	2	2	<0.1	ND	5YR 5/6
60-70	0	1.6	38.5	50.9	8.9	94	3	3	<0.1	ND	5YR 5/6
70-80	0	1.8	32.9	55.1	10.2	95	3	2	<0.1	ND	5YR 5/6
Unit 2, Late Holocene eolian sand											
90-100	0	2.1	38.5	48.4	11.0	95	3	2	<0.1	ND	5YR 4/6
100-110	0	1.8	38.6	48.2	11.4	96	2	2	<0.1	ND	5YR 4/6
110-120	0	1.9	33.8	51.1	13.2	96	2	2	<0.1	ND	5YR 4/6
120-130	0	1.8	34.4	52.3	11.6	95	4	1	<0.1	ND	5YR 4/6
A horizon sand											
150-160	0	1.7	48.5	35.2	14.6	95	3	2	<0.1	0.1	5YR 3/3
160-170	0	1.7	32.3	51.7	14.3	93	5	2	<0.1	0.2	5YR 3/3
170-180	0	5.1	32.8	50.1	12.0	94	5	1	<0.1	0.2	5YR 3/3
Unit 2 eolian sand											
215-225	0	2.0	31.0	52.7	14.3	94	4	2	<0.1	ND	5YR 4/6
BHT-6 (west end at blowout floor)											
10-20	0	1.7	30.0	52.9	15.4	95	2	3	<0.1	--	5YR 4/6
30-40	0	1.7	26.3	55.3	16.8	96	2	2	0.5	--	5YR 4/6
50-60	0	1.9	28.7	52.6	16.8	95	3	2	<0.1	--	5YR 4/6
70-80	0	2.2	30.2	50.3	17.4	95	2	3	<0.1	--	5YR 4/6
80-90	0	2.1	29.9	51.1	16.9	93	4	3	<0.1	--	5YR 4/6
										Fe, g/kg	
90-100	0	2.1	28.7	52.2	16.9	90	6	4	<0.1	3.05	5YR 4/6
100-110	0	2.2	28.9	51.7	17.2	91	7	2	<0.1	3.27	5YR 4/6
Unit 1 eolian sand, Middle eolian sand unit											
120-130	0	0.8	14.3	57.5	27.4	68	15	17	0.3	9.39	2.5YR4/6
130-140	0	0.9	18.2	56.2	24.8	74	10	16	0.3	10.00	2.5YR4/6

Energy Laboratories, Billings, Montana; * ND, not detected at the reporting limit.

Table C-19. Locality 21, sediment data from Jo Bar West and East, southeastern Eddy Co., NM; Hall and Goble, 2016f

Interval (cm depth)	Very Coarse Sand (%)	Coarse Sand (%)	Medium Sand (%)	Fine Sand (%)	Very Fine Sand (%)	Sand (%)	Silt (%)	Clay (%)	$CaCO_3$ (%)	OC† (%)	Dry Munsell Color
JO BAR WEST											
Trench 2											
Eolian cover sand, uppermost 1 cm											
0-1	0	3.5	21.8	51.3	23.3	89	6	5	0.3	0.2	5YR 4/4
Eddy paleosol, A horizon											
1-10	0	4.8	21.6	52.6	21.0	74	12	14	2.6	0.7	7.5YR 3/4
10-20	0	5.3	20.3	53.2	21.1	65	17	18	8.7	0.7	7.5YR 4/3
20-30	0.1	6.5	20.4	51.5	21.4	67	14	19	15.8	0.7	7.5YR 4/3
JO BAR EAST											
Trench 1											
Parabolic dune sand											
3-10	0	0.2	31.6	54.8	13.4	96	4	ND*	0.2	--	5YR 4/6
20-30	0	0.5	24.4	59.0	16.1	97	3	ND	<0.1	--	5YR 4/6
30-35	0	0.4	30.0	57.4	12.2	98	2	ND	0.1	--	5YR 4/6
40-45	0	2.5	36.5	51.6	9.4	98	2	ND	0.1	--	5YR 4/6
Unit 3, eolian sand											
55-65	0	1.6	29.8	53.3	15.2	98	2	ND	0.2	0.09	2.5YR 4/4
75-85	0	1.9	30.9	55.1	12.1	96	4	ND	<0.1	--	2.5YR 4/4
100-10	0	1.1	27.9	58.3	12.7	95	5	ND	0.1	--	2.5YR 4/6
120-30	0	1.3	25.2	62.4	11.2	98	2	ND	0.2	--	2.5YR 4/6
135-40	0	1.1	27.6	58.1	13.2	97	2	1	0.2	--	2.5YR 4/6
Unit 2b, bedded eolian sand											
160-70	0	1.8	25.9	59.2	13.0	94	2	4	0.2	--	2.5YR 4/8
180-90	0	3.9	30.6	44.7	11.8	94	2	4	0.1	--	2.5YR 4/8
200-10	0	1.9	28.0	57.7	12.3	96	4	ND	<0.1	--	2.5YR 4/8
Unit 2a, massive eolian sand											
230-40	0	0.3	27.8	53.8	18.1	95	5	ND	0.1	--	2.5YR 5/6
250-60	0	0.6	21.4	53.2	24.8	96	3	1	0.1	--	2.5YR 5/6
Trench 2											
Unit 3, Eddy paleosol A horizon (15 to 60 cm depth) and underlying Holocene eolian sand											
15-20	0	1.5	35.9	47.0	15.6	94	3	3	0.2	0.14	5YR 3/3
20-30	0	2.8	30.7	51.6	14.8	94	3	3	0.1	0.19	5YR 3/3
30-40	0	1.6	34.7	49.6	14.2	94	3	3	0.2	0.16	5YR 3/3
40-50	0	1.2	34.1	51.6	13.1	94	3	3	0.1	0.13	5YR 3/4
50-60	0	1.4	35.4	49.8	13.4	94	4	2	<0.1	0.09	5YR 3/4
60-70	0	1.1	34.8	52.0	12.0	94	4	2	0.2	0.03	5YR 4/4
70-80	0	1.4	35.7	51.4	11.4	94	4	2	0.1	0.05	5YR 4/6
80-90	0	1.0	33.4	54.6	10.9	96	4	ND	0.1	0.06	5YR 4/6
90-100	0	1.5	32.4	55.7	10.3	96	3	1	<0.1	0.03	5YR 4/6
100-10	0	0.9	32.3	56.5	10.3	96	3	1	<0.1	0.03	5YR 4/6
110-20	0	2.1	32.4	55.8	9.6	95	3	2	0.1	0.05	5YR 4/6
Unit 1, Middle eolian sand unit (?)											
red sand	0	0.4	30.1	56.3	13.2	84	4	12	0.2	--	2.5YR 4/6

Table C-19. Continued

Interval (cm depth)	Very Coarse Sand (%)	Coarse Sand (%)	Medium Sand (%)	Fine Sand (%)	Very Fine Sand (%)	Sand (%)	Silt (%)	Clay (%)	$CaCO_3$ (%)	OC† (%)	Dry Munsell Color
Trench 6											
Eddy paleosol, A horizon											
5-15	0	1.7	37.5	43.1	17.6	84	8	8	0.3	0.39	5YR 3/3
Unit 2, red eolian sand											
40-50	0	2.2	34.5	49.4	13.8	78	7	15	0.4	0.36	2.5YR 3/4
Trench 8											
Unit 2, eolian sand from deep solution pipe fill in calcrete											
295	0	2.0	29.1	50.6	18.3	96	3	1	0.6	--	5YR 5/6

Energy Laboratories, Inc., Billings, Montana.

† Organic Carbon analyses by A & L Great Lake Laboratories, Fort Wayne, Indiana.

* ND, not detected at reporting limit (1.0%); dash (--), not measured.

Table C-20. Loc. 22, Lower slope of Quahada Ridge escarpment above Nash Draw, Eddy Co., NM; Hall and Goble, 2016b

Interval (cm depth)	Very Coarse Sand (%)	Coarse Sand (%)	Medium Sand (%)	Fine Sand (%)	Very Fine Sand (%)	Sand (%)	Silt (%)	Clay (%)	$CaCO_3$ (%)	OC (%)	Dry Munsell Color
GT1, deep trench, Unit 4, parabolic dune sand											
20-30	0	3.6	30.2	55.2	11.0	95	3	2	0.2	ND*	5YR 4/6
GT1, Unit 3 A horizon, Eddy paleosol											
60-70	0	2.5	26.2	57.3	14.0	95	3	2	0.1	0.1	5YR 4/4
GT1, Unit 3, Holocene sand unit											
90-100	0	2.2	25.0	57.4	15.4	94	3	3	0.1	ND	5 YR 4/6
120-130	0	2.2	23.6	60.9	13.2	95	3	2	0.1	ND	5YR 4/6
GT1, Unit 2, Middle eolian sand unit											
150-160	0	2.7	24.4	58.0	14.8	85	5	10	0.3	0.1	5YR 5/6
180-190	0	3.2	24.3	62.2	10.3	86	6	8	0.2	ND	5YR 5/6
GT1, Unit 1, Lower eolian sand unit											
222-226	0	3.2	26.9	56.8	13.2	81	3	16	0.3	--	2.5YR 4/8
GT2, shallow trench, Unit 2, Middle sand unit											
108-113	0	1.3	19.3	61.0	18.4	84	6	10	8.8	--	5YR 6/4
115-120	0	1.8	19.1	60.4	18.2	86	5	9	8.8	--	5YR 6/4

Energy Laboratories, Inc., Billings, Montana.

* ND, not detected at the reporting limit; dash (--), not measured.

Table C-21. Locality 23; Quahada Ridge, Eddy Co., NM; Hall, 2010c

Interval (cm depth)*	Very Coarse Sand (%)	Coarse Sand (%)	Medium sand (%)	Fine sand (%)	Very Fine sand (%)	Sand (%)	Silt (%)	Clay (%)	$CaCO_3$ (%)	OC (%)	Dry Munsell Color
Coppice dune sand											
+10-20	0.0	0.1	15.2	68.6	16.1	95	3	2	0.09	0.6	5YR 4/6
+0-10	0.0	0.2	13.4	67.3	19.1	97	1	2	0.09	0.7	7.5YR 4/6
Eolian sand with Loco Hills paleosol upper 20 cm											
0-10	0.0	0.1	13.7	65.4	20.8	95	3	2	0.12	0.7	5YR 4/4
10-20	0.0	0.1	14.1	64.9	20.9	95	2	3	0.12	0.7	5YR 4/4
20-30	0.0	0.1	13.6	65.5	20.2	95	3	2	0.13	0.6	5YR 4/6
30-40	0.0	0.1	12.8	65.7	21.4	95	2	3	0.11	0.7	5YR 4/6
40-50	0.0	0.1	11.2	66.4	23.3	94	3	3	0.10	0.7	5YR 4/6
50-60	0.0	0.1	10.9	65.9	23.1	94	3	3	0.10	0.8	5YR 4/6
60-70	0.0	0.1	10.9	65.5	23.5	93	3	4	0.08	0.9	5YR 4/6
70-80	0.0	0.1	10.3	65.2	24.4	92	4	4	0.09	0.9	5YR 4/6
80-90	0.0	0.1	10.0	64.1	25.8	90	5	5	0.08	0.9	5YR 4/6
90-97	0.2	0.4	11.0	60.1	28.3	84	9	7	0.11	2.8	5YR 4/6

Milwaukee Soil Laboratory.

* Measured from top of A horizon soil

Eolian sand unit rests directly on eroded surface of local calcic soil (Mescalero paleosol) at 97 cm depth.

Table C-22a. Locality 24a; sediment data from, Los Medaños parabolic dunes, Eddy Co., NM; Hall and Goble, 2015a

Interval (cm)	Very Coarse Sand (%)	Coarse Sand (%)	Medium Sand (%)	Fine Sand (%)	Very Fine Sand (%)	Sand (%)	Silt (%)	Clay (%)	$CaCO_3$ (%)	Dry Munsell Color
Unit 5, parabolic dune sand, cm above base of dune										
20-30	0	1.3	39.1	54.7	4.9	98	2	ND*	<0.1	5YR 5/6
10-20	0	2.2	40.7	52.4	4.7	98	2	ND	0.1	5YR 5/6
Unit 4, eolian sand, cm below top of this unit										
10-20	0	0.8	29.0	63.0	7.2	98	2	ND	0.9	5YR 5/6
20-30	0	0.8	31.8	60.4	7.1	96	4	ND	0.1	5YR 5/6
30-40	0	0.9	40.4	52.4	6.2	97	3	ND	0.2	5YR 5/6
40-50	0	0.9	41.3	52.2	5.7	97	3	ND	0.1	5YR 5/6
60-70	0	0.8	47.5	46.1	5.5	96	4	ND	0.1	5YR 5/6
80-90	0	0.9	35.7	57.0	6.3	97	3	ND	<0.1	5YR 5/6
100-110	0	1.1	41.5	51.4	5.9	97	3	ND	0.1	5YR 5/6

Energy Laboratories, Inc., Billings, Montana.

* ND, not detected at reporting limit (1%)

Table C-22b. Locality 24b; sediment data from Los Medaños parabolic dunes, Eddy Co., NM; Hall and Goble, 2015a

Interval (cm)	Very Coarse Sand (%)	Coarse Sand (%)	Medium Sand (%)	Fine Sand (%)	Very Fine Sand (%)	Sand (%)	Silt (%)	Clay (%)	$CaCO_3$ (%)	Dry Munsell Color
Unit 5, parabolic dune sand, cm depth										
20-30	0	2.3	31.5	57.4	8.8	97	3	ND*	0.2	5YR 4/6
40-50	0	2.9	42.6	49.6	5.0	97	3	ND	<0.1	5YR 4/6
60-70	0	1.8	40.0	53.4	4.8	97	3	ND	<0.1	5YR 5/6
80-90	0	0.6	26.1	65.4	7.9	96	4	ND	<0.1	5YR 5/6
Unit 4, eolian sand, cm above base										
90-100	0	0.9	18.4	66.5	14.2	95	5	ND	<0.1	5YR 4/6
70-80	0	2.9	25.8	57.6	13.8	96	3	1	<0.1	5YR 4/6
50-60	0	3.2	26.3	55.9	14.6	95	5	ND	<0.1	5YR 4/6
30-40	0	2.4	23.2	61.1	13.3	95	5	ND	0.2	5YR 4/6
10-20	0	2.6	21.0	59.9	16.4	92	5	3	0.4	5YR 4/4
Unit 3, lacustrine bed, cm below top										
0-10	0	2.7	22.1	58.8	16.3	82	8	10	9.1	7.5YR 7/3
10-20	0	2.3	21.1	56.6	20.0	70	16	14	19.1	7.5YR 7/3
20-30	0	2.3	21.7	54.2	21.9	75	11	14	18.5	7.5YR 7/3
Unit 2, light brown sand beneath lacustrine bed, cm below top of lacustrine bed										
55-60	0	3.3	28.5	51.2	16.9	93	3	4	17.6	7.5YR 6/3
Unit 1, reddish sand, cm below top of lacustrine bed										
80-85	0	2.4	31.4	53.2	13.0	79	5	16	1.6	5YR 5/8

Energy Laboratories, Inc., Billings, Montana; * ND, not detected at reporting limit (1%)

Table C-23. Locality 25; sediment data from Maroon Cliffs, Eddy Co., NM; Hall, 2013; Hall and Boggess, 2013

Interval (cm depth)*	Very Coarse Sand (%)	Coarse Sand (%)	Medium Sand (%)	Fine Sand (%)	Very Fine Sand (%)	Sand (%)	Silt (%)	Clay (%)	$CaCO_3$ (%)	OC (%)	Dry Munsell Color
Unit 1, mesquite coppice dune sand, laminar											
45-55	<1	<1	42	39	17	87	6	7	0.6	0.1	2.5YR 4/4
Unit 2, massive eolian sand, pre-dune; erosional disconformity											
60-70	<1	<1	18	52	26	85	9	6	0.5	0.3	2.5YR 4/4
70-80	<1	<1	34	44	21	87	9	4	0.3	0.1	2.5YR 4/4
80-90	<1	<1	24	54	21	88	7	5	0.2	0.2	2.5YR 4/4
Unit 3,'gray' eolian sand unit, with 10-cm A horizon at top; erosional unconformity											
95-100	<1	<1	22	50	25	86	7	7	0.3	0.2	2.5YR 4/4
100-110	<1	<1	26	55	22	81	12	7	0.4	0.3	2.5YR 4/4
110-120	<1	<1	25	55	21	79	10	11	0.5	0.2	2.5YR 4/4
Unit 4, 'red' eolian sand unit; Permian bedrock underlying eolian sand at 238 cm depth											
120-130	<1	<1	22	51	22	80	8	12	0.6	0.2	2.5YR 4/6
130-140	<1	<1	37	43	20	79	9	12	0.6	0.0	2.5YR 4/6
140-150	<1	<1	26	50	22	78	10	12	0.8	0.2	2.5YR 4/6
150-160	<1	<1	26	54	22	73	14	13	2.6	0.1	2.5YR 4/6
160-170	<1	<1	24	52	22	73	12	15	4.9	0.2	2.5YR 4/6
170-180	<1	<1	20	52	24	75	10	15	5.5	0.2	2.5YR 4/6
180-190	<1	<1	21	51	25	75	9	16	2.9	0.1	2.5YR 4/6
190-200	<1	<1	21	50	25	78	9	13	2.4	0.1	2.5YR 4/6
200-210	<1	<1	16	50	27	77	8	15	2.6	0.1	2.5YR 4/6
210-220	1	1	19	50	26	67	13	20	17.3	0.1	2.5YR 5/6
220-230	1	2	19	44	28	67	12	21	20.7	0.1	2.5YR 5/6

Energy Laboratories, Inc., College Station, Texas; * Measured from top of coppice dune.

Table C-24. Locality 26; coppice dune and Pecos River alluvial terrace, SE of Malaga, Eddy Co., NM; Hall and Goble, 2015a

Interval (cm depth)	Very Coarse Sand (%)	Coarse Sand (%)	Medium Sand (%)	Fine Sand (%)	Very Fine Sand (%)	Sand (%)	Silt (%)	Clay (%)	$CaCO_3$ (%)	Dry Munsell Color
Mesquite coppice dune, on terrace surface										
0-10	0	0	0.2	49.8	50.0	90	9	1	8.7	7.5YR 6/4
20-30	0	0	0.2	53.4	46.4	90	8	2	8.6	7.5YR 6/4
40-50	0	0	0.5	64.4	35.1	92	6	2	8.5	7.5YR 6/4
60-70	0	0	0.3	58.7	41.0	90	8	2	8.3	7.5YR 6/4
Alluvium, Late Holocene terrace										
90-100	0	0	0.4	58.6	41.0	90	8	2	9.0	7.5YR 6/3
110-120	0	0	0.2	36.1	63.7	80	16	4	13.7	7.5YR 6/3
130-140	0	0	0.1	42.1	57.8	56	39	5	19.3	7.5YR 6/4
150-160	0	0	0	14.1	85.9	54	35	11	23.6	7.5YR 6/4
170-180	0	0	0	9.5	90.5	50	41	9	20.2	7.5YR 6/4
190-200	0	0	0	16.7	83.3	38	53	9	22.2	7.5YR 6/4

Energy Laboratories, Inc., Billings, Montana.

Table C-25. Locality 27; east of Rock House Crossing on Pecos River, south of Malaga, Eddy Co., NM; Hall and Goble, 2016c

Interval (cm depth)	Very Coarse Sand (%)	Coarse Sand (%)	Medium Sand (%)	Fine Sand (%)	Very Fine Sand (%)	Sand (%)	Silt (%)	Clay (%)	$CaCO_3$ (%)	OC (%)	Dry Munsell Color
Trench 2											
Coppice dune sand, depth measured from dune crest 76 cm high above Unit 2											
46-56	0	1.7	26.3	49.2	22.9	91	8	1	0.4	--	7.5YR 4/4
61-71	0	3.8	31.2	46.0	19.0	92	8	ND*	0.4	--	7.5YR 4/4
Trench 4											
Unit 2 eolian sand with A/Bw horizon upper 45 cm											
5-15	0	5.2	35.7	43.2	15.9	92	4	4	0.2	--	5YR 4/3
15-25	0	4.6	36.3	43.0	16.0	92	5	3	0.3	--	5YR 4/4
25-35	0	5.2	37.1	41.0	16.6	91	6	3	0.4	--	5YR 4/4
35-45	0	5.6	36.1	42.8	15.4	92	5	3	0.5	--	5YR 4/4
Unit 2 eolian sand with weak Bk horizon											
50-60	0.1	8.9	36.2	39.8	15.0	89	7	4	1.4	--	5YR 4/6
60-70	0	5.0	34.2	44.4	16.3	90	5	5	1.6	--	5YR 5/6
75-85	0.1	4.5	32.3	45.7	17.3	91	5	4	1.2	--	5YR 5/6
Unit 1 eolian sand with 2Bk horizon											
100-110	0.2	4.1	32.0	44.7	18.9	87	7	6	1.3	--	5YR 5/6
Supplemental analysis by A & L Great Lakes Laboratories, Fort Wayne, Indiana											
Unit 2 eolian sand with A/Bw horizon upper 45 cm											
5-15	--	--	--	--	--	--	--	--	--	0.14	--
15-25	--	--	--	--	--	--	--	--	--	0.19	--
25-35	--	--	--	--	--	--	--	--	--	0.06	--
35-45	--	--	--	--	--	--	--	--	--	0.11	--

Energy Laboratories, Inc., Billings, Montana.

* ND, not detected at the reporting limit; dash (--) indicates not analyzed

Table C-26. Locality 28; from 5-meter-thick alluvial-colluvial section, east side of Cedar Lake basin, east of Loco Hills, Eddy Co., NM; Hall and Goble, 2015b

Interval (cm depth)	Very Coarse Sand (%)	Coarse Sand (%)	Medium Sand (%)	Fine Sand (%)	Very Fine Sand (%)	Sand (%)	Silt (%)	Clay (%)	$CaCO_3$ (%)	Munsell Color dry
60-70	0	1.0	14.9	66.1	18.0	91	5	4	3.5	2.5YR 5/4
100-110	0	2.4	20.2	64.6	12.9	92	4	4	3.5	2.5YR 5/4
140-150	0	1.1	16.0	65.2	17.6	87	8	5	3.9	2.5YR 4/6
200-210	0	0.4	12.4	68.3	18.9	86	8	6	3.7	2.5YR 4/6
250-260	0	0.4	11.7	62.5	25.5	87	6	7	4.3	2.5YR 4/6
300-310	0	0.1	11.0	65.2	23.7	88	5	7	3.0	2.5YR 4/6
350-360	0	0.1	7.6	61.4	30.9	85	8	7	3.6	2.5YR 4/6
400-410	0	0.4	12.1	66.1	21.4	89	6	6	3.0	2.5YR 4/6
450-460	0	0.1	5.7	59.1	35.1	77	12	11	6.4	2.5YR 4/6
Average percentages of sand, silt, clay, carbonate (excluding base sample)										
	0	0.6	13.2	64.9	21.1	88	6	6	3.6	

Energy Laboratories, Billings, Montana.

Table C-27. Locality 29; Loving Lakes project, north of Hwy. 128, Eddy Co., NM; Hall and Goble 2016a

Interval (cm depth)	Very Coarse Sand (%)	Coarse Sand (%)	Medium Sand (%)	Fine Sand (%)	Very Fine Sand (%)	Sand (%)	Silt (%)	Clay (%)	OC (%)	$CaCO_3$ (%)	Dry Munsell Color
Coppice dune sand											
+0-10	0.3	0.9	21.4	57.5	19.9	91	3	6	0.31	1.2	5YR 4/6
Eolian sand fill in solution pipe through caliche and Permian gypsum bedrock											
0-10	0.1	0.8	19.8	56.4	22.9	87	4	9	0.26	1.3	2.5YR 3/4
10-20	0.0	0.7	17.9	58.5	22.9	89	3	8	0.20	1.2	2.5YR 3/4
20-30	0.1	0.6	17.0	58.3	24.0	87	5	8	0.18	1.2	2.5YR 4/4
30-40	0.1	0.7	18.4	57.5	23.3	85	3	12	0.17	1.4	2.5YR 3/6
40-50	0.0	0.8	18.6	57.3	23.3	85	3	12	0.17	1.6	2.5YR 4/6
50-60	0.0	0.7	18.5	57.0	23.8	85	2	13	0.15	1.7	2.5YR 4/6
60-70	0.0	0.6	17.9	57.1	24.4	86	3	11	0.14	1.6	2.5YR 4/6
70-80	0.1	0.6	16.6	56.3	26.4	85	4	11	0.12	2.6	2.5YR 4/6
80-90	0.0	0.7	16.8	56.9	25.6	88	3	9	0.04	1.9	2.5YR 4/8
90-100	0.0	0.6	16.4	56.5	26.5	87	5	8	0.04	1.9	2.5YR 4/6
100-110	0.1	0.6	16.1	56.9	26.3	87	5	8	0.03	2.3	2.5YR 4/8
110-120	0.1	0.5	15.3	57.0	27.1	87	4	9	0.03	2.3	2.5YR 4/8
120-130	0.1	0.6	15.0	57.2	27.1	87	5	8	0.03	2.1	2.5YR 4/8
130-140	0.1	0.6	14.7	56.8	27.8	87	5	8	0.03	1.8	2.5YR 4/8

Milwaukee Soil Laboratory.

Table C-28. Locality 31, coppice dune field, southwest Lea Co., NM; Hall and Kettler, 2019

Interval (cm depth)	Very Coarse Sand (%)	Coarse Sand (%)	Medium Sand (%)	Fine Sand (%)	Very Fine Sand (%)	Sand (%)	Silt (%)	Clay (%)	$CaCO_3$ (%)	OC (%)	Dry Munsell Color
Area B, Trench 2											
Coppice dune sand; depth measured up from base of dune above contact with underlying paleosol A horizon											
+115-120	<0.1	<0.1	8.5	72.2	19.3	90	10	ND	0.1	--	5YR 4/4
+95-100	<0.1	<0.1	11.6	77.6	10.8	97	3	ND	0.1	0.03	5YR 4/4
+75-80	<0.1	<0.1	15.7	74.7	9.6	97	3	ND	0.1	--	5YR 4/4
+55-60	<0.1	<0.1	18.1	70.4	11.5	96	4	ND	0.1	0.03	5YR 4/6
+35-40	<0.1	<0.1	18.3	69.8	11.9	98	2	ND	0.1	--	5YR 4/6
+15-20	<0.1	<0.1	12.2	74.6	13.2	98	2	ND	0.1	0.03	5YR 4/6
Cover sands; depth measured from top of cover sand											
0-5	<0.1	<0.1	11.3	70.3	18.4	96	4	ND	0.1	0.10	5YR 4/4
10-15	<0.1	<0.1	13.9	68.0	18.0	96	4	ND	0.1	0.10	5YR 4/4
20-25	<0.1	<0.1	13.1	69.0	17.9	97	3	ND	0.2	0.13	5YR 4/4
Eddy paleosol A horizon											
30-35	<0.1	<0.1	12.8	67.8	19.4	96	4	ND	0.2	0.16	5YR 4/4
40-45	<0.1	<0.1	13.1	69.1	17.8	96	4	ND	0.1	0.16	5YR 4/4
50-55	<0.1	<0.1	13.6	67.0	19.4	96	4	ND	0.2	0.13	5YR 4/4
60-65	<0.1	<0.1	13.6	66.4	20.0	96	4	ND	0.2	0.03	5YR 4/4
70-75	<0.1	<0.1	13.4	67.5	19.1	97	3	ND	0.2	0.16	5YR 4/4
80-85	<0.1	<0.1	12.9	67.0	20.0	96	4	ND	0.3	0.16	5YR 4/4

Table C-28. Continued

Interval (cm depth)	Very Coarse Sand (%)	Coarse Sand (%)	Medium Sand (%)	Fine Sand (%)	Very Fine Sand (%)	Sand (%)	Silt (%)	Clay (%)	$CaCO_3$ (%)	OC (%)	Dry Munsell Color
90-95	<0.1	<0.1	13.4	66.9	19.7	94	6	ND	0.4	0.16	5YR 4/4
100-105	<0.1	<0.1	13.2	66.5	20.3	97	3	ND	0.3	0.16	5YR 4/4
110-115	<0.1	<0.1	12.9	64.2	22.9	94	6	ND	0.4	0.19	5YR 4/4
Area C, Trench 1											
Coppice dune sand; depth measured up from base of dune above contact with underlying paleosol A horizon											
+15-20	<0.1	0.2	19.4	68.4	12.1	96	4	ND	0.1	--	2.5YR 4/4
+5-10	<0.1	<0.1	20.8	66.4	12.8	96	4	ND	0.2	--	2.5YR 4/4
Eddy paleosol A horizon; depth measured from top of paleosol											
0-5	<0.1	<0.1	15.4	64.8	19.7	95	5	ND	0.2	0.13	5YR 3/3
10-15	<0.1	<0.1	16.4	66.0	17.7	96	4	ND	0.2	0.19	5YR 3/3
20-25	<0.1	0.3	17.0	64.9	17.9	95	5	ND	0.2	0.19	5YR 3/3
30-35	<0.1	<0.1	17.8	64.1	18.2	96	4	ND	0.1	0.16	5YR 3/3
40-45	<0.1	0.3	17.4	65.1	17.1	96	4	ND	0.1	0.23	5YR 3/3
50-55	<0.1	<0.1	18.5	63.6	17.9	96	4	ND	0.1	0.19	5YR 3/3
60-65	<0.1	0.3	18.0	63.9	17.9	93	7	ND	0.2	0.16	5YR 4/4
70-75	<0.1	<0.1	18.5	62.9	18.6	96	4	ND	0.1	0.13	5YR 4/4
Pre-paleosol sand											
80-85	<0.1	0.2	17.5	64.1	18.3	96	4	ND	0.2	0.10	5YR 4/6
90-95	<0.1	0.1	16.7	65.2	18.0	96	4	ND	0.3	0.13	5YR 4/6
100-105	<0.1	0.4	18.6	64.2	16.8	96	4	ND	0.2	0.10	5YR 4/6
110-115	<0.1	0.1	21.2	60.2	18.4	96	4	ND	0.2	0.10	5YR 4/6
Area B, Trench 1											
Coppice dune sand; depth measured up from base of dune above contact with underlying paleosol A horizon											
+15-20	<0.1	0.1	19.2	71.8	8.9	96	4	ND	0.1	--	5YR 4/6
+5-10	<0.1	<0.1	20.4	65.8	13.9	96	4	ND	0.2	--	5YR 4/6
Eddy paleosol A horizon; depth measured from top of paleosol											
0-5	<0.1	0.2	16.2	64.2	19.5	94	6	ND	0.2	0.16	5YR 4/4
10-15	<0.1	<0.1	16.1	62.5	21.4	94	6	ND	0.2	0.10	5YR 4/4
20-25	<0.1	<0.1	14.6	64.3	21.0	94	6	ND	0.2	0.10	5YR 4/4
30-35	<0.1	<0.1	13.9	68.1	17.9	94	6	ND	0.2	0.06	5YR 4/4
40-45	<0.1	<0.1	14.6	63.9	21.3	92	8	ND	0.2	0.13	5YR 4/4

Energy Laboratories, Inc., Billings, Montana; organic carbon (OC) analyses by A&L Great Lakes Laboratories, Fort Wayne, Indiana; * ND, not detected at the reporting limit; dash (--) indicates not analyzed.

Table C-29. Locality 32, south side of Red Bluff Draw, Eddy Co., NM; Hall, 2016

Interval (cm depth)	Very Coarse Sand (%)	Coarse Sand (%)	Medium Sand (%)	Fine Sand (%)	Very Fine Sand (%)	Sand (%)	Silt (%)	Clay (%)	$CaCO_3$ (%)	OC† (%)	Dry Munsell Color
0-10	<0.1	<0.1	0.4	3.5	96.1	29	59	12	13.5	--	7.5YR 5/3
20-30	<0.1	<0.1	0.2	16.1	83.7	27	49	24	14.1	0.31	7.5YR 4/3
40-50	<0.1	<0.1	<0.1	22.2	77.7	23	47	30	19.9	0.63	7.5YR 4/3
60-70	<0.1	<0.1	4.1	14.4	81.4	25	45	30	19.2	0.38	7.5YR 4/3
80-90	<0.1	<0.1	0.3	30.6	69.1	17	46	37	21.8	--	7.5YR 4/3
100-110	<0.1	<0.1	<0.1	23.1	76.8	9	50	41	27.3	--	7.5YR 5/4
120-130	<0.1	<0.1	<0.1	19.1	81.0	7	49	44	26.7	--	7.5YR 5/4

Energy Laboratories, Inc., Billings, Montana.

†Organic Carbon analyses by A & L Great Lake Laboratories, Fort Wayne, Indiana.

Table C-30. Locality 33, west side of Hackberry Lake, Eddy Co., NM; Hall and Goble, 2017

Interval (cm depth)	Very Coarse Sand (%)	Coarse Sand (%)	Medium Sand (%)	Fine Sand (%)	Very Fine Sand (%)	Sand (%)	Silt (%)	Clay (%)	$CaCO_3$ (%)	OC (%)	Dry Munsell Color
Eddy paleosol, Holocene eolian sand at Block 1, depth below top of Eddy paleosol											
5-15	<0.1	0.4	24.7	65.7	9.2	95	3	2	<0.1	0.210	5YR 5/6
Holocene eolian sand below Eddy paleosol											
15-25	<0.1	<0.1	21.6	66.6	11.7	94	2	4	0.1	0.194	5YR 4/6
25-35	<0.1	<0.1	20.3	67.0	12.7	94	2	4	0.3	--	5YR 4/6
35-45	<0.1	<0.1	18.6	66.1	15.3	90	4	6	1.9	--	5YR 4/6
Parabolic dune sand, depth from top											
10-20	<0.1	<0.1	17.4	72.2	10.4	96	2	2	<0.1	--	5YR 5/6
30-40	<0.1	<0.1	21.4	69.4	9.2	94	4	2	<0.1	--	5YR 5/6
55-65	<0.1	<0.1	19.4	71.3	9.3	95	3	2	<0.1	--	5YR 5/6
80-90	<0.1	0.3	34.6	57.5	7.5	96	2	2	<0.1	--	5YR 5/4
Playa deposits, edge of Hackberry Lake, depth from surface; BHT-12											
20-30	<0.1	<0.1	24.9	62.5	12.6	94	2	4	0.3	--	5YR 4/6
40-50	<0.1	<0.1	27.3	62.6	10.1	94	2	4	0.1	--	5YR 4/6
60-70	<0.1	<0.1	19.7	63.3	16.9	93	3	4	0.2	--	7.5YR 5/6
100-110	<0.1	<0.1	17.1	60.6	22.3	86	7	7	3.4	--	7.5YR 5/6
130-140	<0.1	<0.1	22.2	55.0	22.7	79	9	12	12.7	--	7.5YR 6/4

Energy Laboratories, Billings, Montana; organic carbon by combustion by A&L Great Lakes Laboratories, Fort Wayne, Indiana; dash (--), not measured.

Table C-31. Locality 34; from along Owl Draw, SW Pecos Slopes, Eddy Co., NM; Hall, 2017a

Interval (cm **depth)**	Very Coarse Sand (%)	Coarse Sand (%)	Medium Sand (%)	Fine Sand (%)	Very Fine Sand (%)	Sand (%)	Silt (%)	Clay (%)	$CaCO_3$ (%)	OC (%)	Total P (%)	Dry Munsell Color
NORTH SIDE OF DRAW												
Site core area												
Eddy paleosol, A horizon												
0-10	<0.1	0.1	1.9	17.0	81.0	46	40	14	14.8	0.86	0.043	7.5YR 5/2
10-20	<0.1	<0.1	4.4	30.2	65.4	42	43	15	13.9	0.92	0.044	7.5YR 5/3
Pre-soil A horizon												
20-30	<0.1	<0.1	5.5	29.1	65.4	32	63	5	19.3	--	--	7.5YR 5/3
30-40	<0.1	<0.1	5.7	35.1	59.2	33	58	9	21.0	--	--	7.5YR 5/4
Off-site area												
Eddy paleosol, A horizon												
0-10	<0.1	<0.1	0.3	1.9	97.7	24	60	16	9.3	2.03	0.072	7.5YR 4/2
10-20	<0.1	<0.1	0.1	7.2	92.6	22	57	21	11.6	1.30	0.065	7.5YR 4/2
Pre-soil A horizon												
20-30	<0.1	<0.1	4.5	15.9	79.6	24	54	22	12.5	--	--	7.5YR 4/3
30-40	<0.1	<0.1	0.2	27.3	72.5	27	47	26	12.2	--	--	7.5YR 4/3
SOUTH SIDE OF DRAW												
Site core area												
Eddy paleosol, A horizon												
0-10	<0.1	<0.1	0.6	10.3	89.1	37	47	16	14.5	1.68	0.054	7.5YR 4/2
Pre-soil A horizon												
20-30	<0.1	<0.1	33.3	30.6	36.1	16	49	35	17.3	--	--	7.5YR 5/4
30-40	<0.1	<0.1	25.1	30.2	44.7	16	47	37	17.9	--	--	7.5YR 4/4

Energy Laboratories, Billings, Montana; organic carbon and total phosphorus by A&L Great Lakes Laboratories, Fort Wayne, Indiana; dash (--), not measured.

Table C-32. Locality 35; eastern edge of Mescalero Plain, Lea Co., NM; Hall, 2017b

Interval (cm depth)	Very Coarse Sand (%)	Coarse Sand (%)	Medium Sand (%)	Fine Sand (%)	Very Fine Sand (%)	Sand (%)	Silt (%)	Clay (%)	$CaCO_3$ (%)	OC† (%)	Dry Munsell Color
Coppice dune sand											
upper	<0.1	<0.1	1.3	70.0	28.7	93	3	4	0.1	--	5YR 4/4
lower	<0.1	0.2	3.4	73.2	23.2	94	2	4	0.1	--	5YR 4/4
Eolian sand with Eddy paleosol											
5-15	<0.1	0.4	4.4	71.3	23.8	93	5	2	0.1	0.28	5YR 4/4
15-25	<0.1	0.3	4.7	71.0	23.9	92	5	3	0.1	0.28	5YR 4/4
25-35	<0.1	0.5	4.9	69.9	24.6	93	4	3	0.1	0.28	5YR 4/4
35-45	<0.1	0.4	5.1	69.4	25.1	91	3	6	0.1	0.25	5YR 4/4
45-55	<0.1	0.6	4.7	71.8	22.8	90	2	8	0.1	0.22	5YR 4/4
Red eolian sand											
60-70	<0.1	0.5	5.2	71.7	22.5	84	5	11	0.6	--	5YR 4/4
70-80	<0.1	1.0	6.2	64.0	28.8	71	12	17	7.7	--	5YR 5/6
80-90	<0.1	0.7	7.7	60.6	30.9	65	14	21	10.1	--	5YR 5/6
Red sand unit											
95-105	<0.1	0.9	8.8	64.3	26.0	71	11	18	6.4	--	2.5YR 4/6

Analyses by the Energy Laboratories, Inc., Billings, Montana; percentages by weight

† Organic Carbon analyses by A & L Great Lake Laboratories, Fort Wayne, Indiana

Table C-33. Locality 36; high alluvial terrace surface, east side of Pecos River, north of Loving, Eddy Co., NM; Hall, 2017c

Interval (cm depth)	Very Coarse Sand (%)	Coarse Sand (%)	Medium Sand (%)	Fine Sand (%)	Very Fine Sand (%)	Sand (%)	Silt (%)	Clay (%)	$CaCO_3$ (%)	OC† (%)	Dry Munsell Color
Coppice dune sand											
upper	<0.1	5.0	36.3	44.0	14.7	96	2	2	0.6	--	7.5YR 5/4
lower	<0.1	4.0	33.7	44.8	17.5	94	4	2	0.6	--	7.5YR 5/4
Eolian sand with Eddy paleosol											
0-10	<0.1	2.6	20.8	47.7	28.9	88	6	6	2.2	0.34	7.5YR 5/4
10-20	<0.1	2.8	21.5	47.0	28.6	88	6	6	3.7	0.34	7.5YR 5/4
20-30	0.1	2.9	20.4	47.1	29.5	84	8	8	6.7	--	7.5YR 5/3
30-40	0.1	2.6	19.8	46.8	30.7	84	8	8	8.7	--	7.5YR 5/3
Red eolian sand area											
Loose surface cover sand											
surface	0.5	6.2	26.5	41.8	25.0	88	6	6	0.5	--	7.5YR 5/4
Red sand unit											
shallow	0.1	4.3	24.1	46.8	24.7	80	8	12	0.3	--	5YR 4/4

Energy Laboratories, Inc., Billings, Montana; † Organic carbon analyses by A & L Great Lake Laboratories, Fort Wayne, Indiana

Table C-34. Miscellaneous sediment samples from the Mescalero Plain in northern Eddy County (p. 35–36 in Hall, 2002a). Original Locality numbers are given along with newly assigned Locality numbers, where appropriate.

Sample locality, depth (cm)	Sand Percentages					Recalculated			$CaCO_3$ %	OC %	Dry Munsell Color
	Very Coarse Sand	Coarse Sand	Medium Sand	Fine Sand	Very Fine Sand	Sand	Silt	Clay			
Ogallala Formation, Caprock, measured from top of calcrete											
85	11.2	18.7	18.9	25.6	25.6	64.3	21.5	14.2	89.5	-	-
200	0.6	1.9	7.6	59.5	30.0	87.3	9.3	3.3	86.9	-	-
270	0.9	14.8	10.7	17.4	56.3	44.2	40.8	15.0	80.6	-	-
Ogallala Formation, below Caprock, samples from escarpment along Caprock Road											
350	2.6	1.9	11.2	58.2	26.1	81.8	16.0	2.2	14.6	0.3	5YR 7/3
550	0.8	0.6	13.4	59.2	26.0	88.2	10.2	1.6	5.3	0.3	5YR 7/3
800	0.1	0.1	11.2	64.1	24.5	88.2	7.3	2.1	3.3	0.3	5YR 7/3
Locality 1, Valley Gas Road sand pit (Loc. 1, Fig. 3.1, this Bulletin)											
80 cm depth	0	0.9	31.1	55.2	12.7	82.8	3.4	13.8	0.3	-	2.5YR 4/8
200	0	0.6	26.5	61.1	11.8	91.1	3.2	5.7	1.3	-	2.5YR 5/8
320	0	0.7	15.5	62.7	21.2	94.2	2.0	3.8	0.5	-	5YR 5/8
370, caliche	0.5	0.8	11.4	53.2	34.2	35.5	20.6	43.9	17.9	-	-
Locality 2, Valley Gas Road soil pit											
Coppice dune	0	0.3	20.7	61.5	17.5	90.9	3.0	6.1	0.9	-	-
10, Loco Hills A hor.	0	1.5	28.2	52.9	17.4	92.7	4.2	3.1	0.3	0.30	5YR 4/4
60, below soil	0	0.8	26.2	60.8	12.2	90.2	3.1	6.7	0	-	2.5YR 5/8
130	0	1.2	28.1	56.4	14.3	77.1	4.7	18.2	0.3	-	2.5YR 4/8
Locality 3, Old Loco Road soil pit (Loc. 41, this Bulletin)											
Coppice dune	0	0.8	19.1	60.2	19.9	90.4	3.2	6.4	0.1	-	5YR 5/5
10, Loco Hills A hor.	0.1	1.2	19.2	56.3	23.2	82.0	7.8	10.3	0.4	0.75	5YR 4/4
40, below soil	0	2.2	22.0	54.5	21.5	72.6	6.9	20.5	0.1	-	2.5YR 4/8
80	0	1.8	20.5	55.9	21.8	70.9	9.6	19.5	0.8	-	2.5YR 4/8
110, caliche	29.6	18.9	19.4	21.3	10.8	81.9	10.2	7.9	63.8	-	-
Locality 4, F Lane soil pit											
50	0	0.2	14.9	61.7	23.1	94.2	2.2	3.6	0	-	5YR 5/6
180	0	0.4	15.3	62.0	22.3	80.4	3.7	15.9	0.5	-	2.5YR 4/8
240, caliche	33.2	18.7	15.0	21.1	12.0	79.0	10.6	10.3	63.5	-	-
Locality 5, Hagerman Cutoff caliche pit											
caliche	9.0	12.5	15.5	37.9	25.1	48.4	27.0	24.7	51.6	-	-
Locality 8, Booger Langston Road eolian and lacustrine deposits (Loc. 2, Fig. 3.8, this Bulletin)											
100, parabolic dune	0	0	14.9	78.9	6.2	98.2	0.2	1.6	0.1	-	5YR 6/6
170, Loco Hills A hor.	0	0	13.6	77.8	8.6	98.1	0.4	1.5	0.3	0.15	5YR 6/6
250	0	0	15.6	72.3	12.1	96.8	1.2	2.0	0.3	-	5YR 6/6
400, clay bands	0	0	14.8	74.8	10.4	92.9	0.5	6.6	0.7	-	5YR 5/8
400, sand	0	0	13.0	70.0	17.0	96.9	0.6	2.5	0.1	-	5YR 6/6
500	0	0	12.9	65.5	21.6	96.1	1.2	2.7	0.2	-	5YR 6/6
600, pond	2.0	5.3	16.0	53.9	22.8	63.2	25.3	11.5	36.3	-	-
Locality 9, Square Lake Road caliche pit											
Caliche	8.1	12.8	17.9	36.0	25.2	23.2	54.5	22.3	55.3	-	-

Table C-34. Continued

Sample locality, depth (cm)	Sand Percentages					Recalculated			$CaCO_3$ %	OC %	Dry Munsell Color
	Very Coarse Sand	Coarse Sand	Medium Sand	Fine Sand	Very Fine Sand	Sand	Silt	Clay			
Locality 10, Square Lake Road soil pit											
30, Loco Hills A hor.	0	0.5	20.9	68.8	9.8	96.2	1.8	2.0	0.2	0.29	5YR 5/6
50, below soil	0	0.4	17.1	70.3	12.3	94.2	2.3	3.5	0.3	0.29	5YR 5/8
110	0	0.1	10.9	59.4	29.6	29.6	22.8	49.6	0	-	2.5YR 4/6
Locality 11, Caprock Road, lacustrine deposits (Fig. 11.1, this Bulletin)											
Pond deposits	0.1	0.1	8.0	65.0	26.8	85.1	9.8	5.0	0.3	-	-
Locality 12, west of Caprock Road, alluvium with dated Loco Hills paleosol (Loc. 3, Fig. 9.10, this Bulletin)											
30, coppice dune	0	0.1	16.0	68.3	15.6	94.4	2.7	2.9	1.0	-	10YR 6/4
70	0	10.2	16.2	66.0	17.5	94.4	3.1	2.5	2.1	-	10YR 6/4
90, Loco Hills A hor.	0	0.1	9.4	59.9	30.6	82.2	11.3	6.5	1.7	0.93	10YR 4/3
150	0.4	0.5	9.8	61.8	27.5	73.3	13.7	13.0	9.9	-	7.5YR 5/4
Locality 14, Square Lake Road, spring deposit (Loc. 40, Fig. 11.2, this Bulletin)											
40	0	0	4.5	64.1	31.3	94.4	1.1	4.5	0.6	-	2.5YR 5/8
120	0	0.1	12.2	64.2	23.4	80.7	7.7	11.6	1.5	-	2.5YR 5/6
185, spring	0.3	0.5	10.5	66.0	22.7	84.6	5.7	9.7	7.9	-	-
Locality 15, Shugart Road sand pit											
40, Loco Hills A hor.	0	0.1	13.7	64.2	22.0	95.6	2.0	2.5	0	0.30	5YR 5/6
125, below soil	0	0	12.9	71.0	16.0	94.3	0.9	4.7	0.8	-	2.5YR 4/8
350	0	0.1	12.4	67.5	20.0	95.7	1.6	2.8	1.3	-	5YR 6/6
Locality 16, Caliche paleosol east of Ishee Lake, Eddy-Chaves Co. line											
Caliche	8.2	9.9	18.0	46.9	17.0	93.5	1.4	5.1	69.4	-	-

Analyses by Milwaukee Soil Laboratory, Milwaukee, WI; particle size from Wentworth scale; organic carbon determined by Walkley-Black method; carbonate determined by Chittick method; numbers are percentages.

"0" = measured but zero percent; "-" = not measured or determined.

Page intentionally left blank.

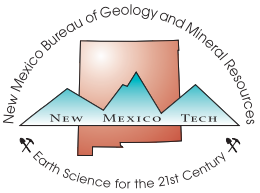

New Mexico Bureau of Geology and Mineral Resources
A Research Division of New Mexico Institute of Mining and Technology
geoinfo.nmt.edu
801 Leroy Place
Socorro, NM 87801
(575) 835-5490